

**FABRICATION AND CHARACTERIZATION OF  
POLYPHENYLSULFONE-BASED MEMBRANES  
WITH NANOCOMPOSITE ADDITIVES FOR  
WATER PURIFICATION APPLICATION**

Thesis

Submitted in partial fulfilment of the requirements for the degree of  
DOCTOR OF PHILOSOPHY

by

M CHANDRA SHEKHAR NAYAK



DEPARTMENT OF CHEMISTRY

NATIONAL INSTITUTE OF TECHNOLOGY KARNATAKA

SURATHKAL, MANGALORE – 575 025

JANUARY, 2019



## DECLARATION

I hereby *declare* that the thesis entitled “**Fabrication and characterization of polyphenylsulfone-based membranes with nanocomposite additives for water purification application**” which is being submitted to the National Institute of Technology Karnataka, Surathkal in partial fulfillment of the requirements for award of the degree of *Doctor of Philosophy* is a *bonafied report of the research work carried out by me*. The material contained in this thesis has not been submitted to any University or Institution for the award of any degree.

M CHANDRA SHEKHAR NAYAK

Reg. No. 155124CY15F03

Department of Chemistry

Place: NITK, Surathkal,

Date:





## **CERTIFICATE**

This is to certify that the thesis entitled “**Fabrication and characterization of polyphenylsulfone-based membranes with nanocomposite additives for water purification application**” submitted by **M Chandra Shekhar Nayak (Reg. No: 155124CY15F03)** as the record of the research work carried out by him is *accepted* as the Research Thesis submission in partial fulfillment of the requirements for the award of degree of *Doctor of Philosophy*.

**Prof. Dr. Arun M. Isloor**  
**Research Guide**

**Chairman- DRPC**



## ACKNOWLEDGEMENTS

I would like to express my deep sense of gratitude to my research supervisor, Professor Dr. Arun M. Isloor, Department of Chemistry, NITK, Surathkal for giving me an opportunity to pursue my research work under his guidance. Without his supervision and determination, this thesis would not have been possible.

I acknowledge to NITK, Surathkal for providing the fellowship and financial support necessary for the completion of my doctoral research work.

My sincere thanks to my RPAC members, Prof. Dr. Arkal Vittal Hegde, Department of Applied Mechanics and Hydraulics and Dr. Saikatdutta, Assistant Professor, Department of Chemistry, for their timely assessment and evaluation of my research progress. Their valuable inputs at various stages of my work have contributed immensely in giving the final shape to my research work.

I am very thankful to the present Head of the Department, Prof. D. Krishna Bhat, and former Head of the Department, Prof. B. Ramachandra Bhat for providing the administrative facilities and infrastructure. I am also thankful to Prof. A. Chitharanjan Hegde, Prof. A. Nithyananda Shetty, Prof. A. Vasudeva Adhikari, Dr. D. Udayakumar, Dr. Darshak R. Trivedi, Dr. Sib Sankar Mal, Dr. Beneesh P.B., Dr. Debashree Chakraborty for their motivation and support.

I would like to convey my thankfulness to Prof. K. Narayan Prabhu, Prof. Rajendra Udupa, and Prof. Uday Bhat of Department of Metallurgical and Materials Engineering, NITK for allowing me to avail the instrumentation facility whenever required. I am thankful to Dr. Hari Mahalingam, Dr. Ashraf Ali, Dr. Keyur Raval and Dr. B Raj Mohan Department of Chemical Engineering for extending the instrumental facilities. I also thank Prof. Manjunath Pattabi, Department of Material Science and Dr. Murari, Scientific Officer, DST-PURSE, Mangalore University for extending the instrumentation facility. I am thankful to Prof. Dr. Balakrishna Prabhu, Department of Chemical Engineering, Manipal Institute of technology, Manipal to extend the instrumentation facility and kind support. I am very thankful to Prof. Ahmed Fauzi Ismail, Advanced Membrane Technology Centre (AMTEC), Universiti Teknologi Malaysia for the providing opportunity me to conduct research work in his laboratory. Special thanks to Dr. Zulhairun Abd. Karim, Dr. Lau Woie Jye, Dr. Mohd. Hafiz Dzarfan B. Othman and Dr. Noorhaniza AMTEC, Universiti Teknologi Malaysia for permitting me to avail the laboratory facilities and assistance in Malaysia.

I truthfully appreciate the support extended by my research group at NITK, including Dr. Seema S. Shenvi, Dr. Valeen Rashmi Pereira, Dr. Harikrishna Nandam, Dr. Raghavendra Hebbar, Dr. Irfana Moideen K, Mr. Syed Ibrahim, Miss. Nikhila, Miss. Panchami, Mr. Sathyanarayan and Mr. Mithun Kumar. I am thankful to all my friends at NITK, for making my stay during research days a fun-filled and memorable one.

I am thankful to the non-teaching staff, Mrs. Shamila Nandini, Mrs. Deepa, Mrs. Sharmila, Mr. Pradeep, Mr. Prashanth, Mr. Harish, Mr. Santosh, Mr. Ashok, Mr. Gopal and Ms. Rashmi for their timely cooperation with laboratory and analysis work.

I am highly indebted to my beloved parents M. Yenkya Nayak & M. Jangilamma, brothers, sister-in-laws, and uncles, Nephew Mr. Chandra Kanth, Mr. Yashaswin, Niece Miss. Chaitanya Laxmi, Miss. Padmavathi and Miss. Divyasree for their cooperation, encouragement, support, love and affection.

A big thank to my wife, G. Swathi Devi and family for their support and love on me. It was because of strong support of my family, that I am able to complete my PhD work. Finally, I extend my gratitude to all those who have contributed directly or indirectly towards the completion of my Ph.D. work.

Thank you.

**M CHANDRA SHEKHAR NAYAK**

## ABSTRACT

Nowadays, membrane separation processes are become as prestigious over other methods towards water purification, due to the low energy consumption and easy to accessible operational conditions. Polyphenylsulfone (PPSU) based membranes are most widely using water purification membrane processes due to its chemical stability, thermal stability, and better mechanical properties. But, one of the major drawback of this polymer is hydrophobicity. In current research, focused to enhance the hydrophilicity as well as the separation efficacy of PPSU membranes with the incorporation of various inorganic hydrophilic nanoparticles.

In present work, PPSU based flat-sheet and hollow fiber membranes fabricated with the incorporation of various nanoparticles such as, BiOCl-AC, MWCNTs, ZSM-5, SnO<sub>2</sub> and Al<sub>2</sub>O<sub>3</sub>-AAC *via* phase inversion process. The fabricated membranes morphological changes were studied with scanning electron microscopy and atomic force microscopy techniques. The permeability and separation efficacy of membranes was assessed with water, proteins, dyes, heavy metal solutions and different oil/water samples using dead-end and cross-flow filter units.

The PPSU membrane with 2 wt. % BiOCl-AC additive exhibited superior performance towards oil/water separation, above 80 % for diesel fuel and above 90 % for crude oil. The PZ-3 type hollow fiber membrane (0.4 wt. % ZSM-5) showed dye rejection performance of 90.81 % for Reactive Black-5 and 82.84 % for Reactive Orange-16. The PCNT-3 membrane (0.3 wt. % MWCNTs) revealed maximum heavy metal ions removal efficacy of 98.13 % for Pb<sup>2+</sup>, 76.12 % for Hg<sup>2+</sup> and 72.92 % for Cd<sup>2+</sup> ions, respectively. SnO<sub>2</sub> NPs (0.4 wt. %) incorporated hollow fiber membranes (PS-3) were successful in rejection of Reactive Black-5 (RB-5) and Reactive Orange-16 (RO-16) dyes up to 94.44 % and 73.09 % from aqueous solutions. PPSU with alumina doped acid treated activated charcoal incorporated membrane (PA-3) (1 wt. %) displayed above 90 % rejection with BSA and egg albumin (EA) proteins, above 80 % and 70 % rejection with Pb<sup>2+</sup> and Cd<sup>2+</sup> heavy metals, and in oil-water separation exhibited above 94 % and 87 % rejection with bio-diesel and kerosene oils, respectively.

**Key words:** Polyphenylsulfone, nanoparticles, permeability, anti-fouling, proteins, dye and heavy metals rejection, Oil-water emulsion separation.



# CONTENTS

CHAPTER 1	PAGE NO.
<b>INTRODUCTION.....</b>	<b>1</b>
1.1 WORLDWIDE SCENARIO OF WATER.....	3
1.2 MEMBRANE HISTORY.....	5
1.3 DEFINATION AND BASIC TERMINOLOGY IN MEMBRANES.....	6
1.3.1 Basic terms in membrane science.....	7
1.4 MEMBRANE CLASSIFICATIONS.....	8
1.4.1 Classification based on membrane morphology.....	8
1.4.2 Classification based on driving force.....	10
1.4.2.1 Pressure driven membrane processes.....	11
1.4.3 Classification based on configuration.....	13
1.5 MERITS AND DEMERITS OF MEMBRANE PROCESSES.....	15
1.6 MEMBRANE MATERIALS.....	16
1.6.1 Polyphenylsulfone as a membrane material.....	17
1.6.2 Importance of nanoadditives in polymeric membranes.....	18
1.7 MEMBRANE PREPARATIONS AND FILTRATION METHODS.....	19
1.7.1 MEMBRANE PREPARATION METHODS.....	19
1.7.2 MEMBRANE FILTRATION METHODS.....	21
1.8 MEMBRANE TECHNOLOGY APPLICATONS.....	22
1.9 LITERATURE SURVEY.....	23
1.10 SCOPE OF THE WORK.....	29
1.11 OBJECTIVES.....	30

## **CHAPTER 2**

### **PREPARATION AND CHARACTERIZATION OF PPSU MEMBRANES WITH BiOCl NANOWAFERS LOADED ON ACTIVATED CHARCOAL FOR OIL IN WATER SEPARATION.....31**

#### **2.1 INTRODUCTION.....33**

#### **2.2 EXPERIMENTAL.....39**

##### **2.2.1 Materials.....39**

##### **2.2.2 Nanoparticles synthesis procedure.....40**

##### **2.2.3 Preparation of BiOCl-AC incorporated PPSU membranes.....40**

##### **2.2.4 CHARACTERIZATION.....41**

##### **2.2.4.1 Characterization of BiOCl nanowafers by FTIR.....41**

##### **2.2.4.2 SEM and EDS of BiOCl nanowafers and membranes.....41**

##### **2.2.4.3 Water Contact Angle (WCA) of membranes.....41**

##### **2.2.4.4 Pure water flux (PWF).....42**

##### **2.2.4.5 Antifouling study of membranes.....42**

##### **2.2.4.6 Water uptake.....43**

##### **2.2.4.7 Membrane Porosity.....43**

##### **2.2.4.8 Procedure for oily water separation.....43**

#### **2.3 RESULTS AND DISCUSSION.....44**

##### **2.3.1 FTIR result.....44**

##### **2.3.2 SEM results.....45**

##### **2.3.3 EDS analysis.....46**

##### **2.3.4 Contact angle.....47**

##### **2.3.5 Pure water flux.....48**



2.3.6 Antifouling study.....	48
2.3.7 Porosity and water uptake.....	49
2.3.8 Oil in water rejection study.....	50
2.4. CONCLUSIONS .....	51
<b>CHAPTER 3</b>	
<b>FABRICATION OF NOVEL PPSU/ZSM-5 ULTRAFILTRATION HOLLOW FIBER MEMBRANES FOR SEPARATION OF PROTEINS AND HAZARDOUS REACTIVE DYES.....</b>	
<b>53</b>	
3.1 INTRODUCTION.....	55
3.1.1 Hollow fiber membranes.....	64
3.2 EXPERIMENTAL.....	65
3.2.1 Materials.....	65
3.2.2 Preparation of zeolite ZSM-5 hollow fiber (HF) membranes.....	65
3.2.3 Membrane Characterization .....	67
3.2.3.1 Scanning Electron Microscopy.....	67
3.2.3.2 Water contact angle analysis.....	67
3.2.3.3 Water uptake .....	67
3.2.3.4 Porosity.....	68
3.2.3.5 Water permeability.....	68
3.2.3.6 Antifouling ability.....	68
3.2.4 Procedure for proteins and hazardous dyes rejection.....	69
3.3 RESULTS AND DISCUSSION.....	70
3.3.1 Contact angle.....	70
3.3.2 Membranes morphology.....	70
3.3.3 Pure water flux (PWF).....	73

3.3.4 Antifouling study.....	73
3.3.5 Water uptake and porosity.....	74
3.3.6 Rejection performance of membranes.....	75
3.3.6.1 Proteins rejection.....	75
3.3.6.2 Dye rejection.....	76
3.4 CONCLUSIONS.....	77

## **CHAPTER 4**

### **EFFECTS OF MULTIWALLED CARBON NANOTUBE ON NOVEL POLYPHENYLSULFONE COMPOSITE ULTRAFILTRATION MEMBRANES FOR THE EFFECTIVE REMOVAL OF LEAD, MERCURY AND CADMIUM FROM THE AQUEOUS SOLUTIONS.....79**

4.1 INTRODUCTION.....	81
4.2 EXPERIMENTAL.....	88
4.2.1 Materials.....	88
4.2.2 PPSU/MWCNT membrane compositions.....	88
4.2.3 Characterization techniques.....	89
4.2.3.1 Scanning electron microscope (SEM).....	89
4.2.3.2 Atomic force microscope (AFM).....	89
4.2.4 Rejection study of toxic heavy metal ions.....	89
4.3. RESULTS AND DISCUSSION.....	90
4.3.1 Contact angle (CA).....	90
4.3.2 Porosity and water uptake.....	91
4.3.3 Membrane morphology.....	92
4.3.3.1 Scanning electron microscopy analysis.....	92
4.3.3.2 Atomic force microscopic results.....	94

4.3.4 Pure water flux.....	95
4.3.5 Antifouling results.....	96
4.3.6 Heavy metal ions rejection results .....	97
4.4 CONCLUSIONS.....	100
<b>CHAPTER 5</b>	
<b>NOVEL PPSU/ NANO TINOXIDE MIXED MATRIX ULTRAFILTRATION HOLLOW FIBER MEMBRANES WITH ENHANCED ANTIFOULING PROPERTY AND TOXIC DYES REMOVAL.....</b>	
5.1 INTRODUCTION.....	103
5.2 EXPERIMENTAL.....	111
5.2.1 Materials.....	111
5.2.2 Fabrication of PPSU/SnO <sub>2</sub> mixed matrix hollow fiber membranes.....	111
5.2.3 CHARACTERIZATION.....	112
5.2.3.1 Molecular weight cut-off (MWCO) experiment.....	113
5.2.4 Dyes rejection experimental methodology.....	113
5.3 RESULTS AND DISCUSSION.....	114
5.3.1 Membrane morphological results.....	114
5.3.1.1 SEM morphology.....	114
5.3.1.2 Atomic force microscopy results.....	116
5.3.2 Contact angle.....	117
5.3.3 Water uptake and porosity.....	118
5.3.4 Molecular weight cut-off (MWCO) results.....	119
5.3.5 Pure water flux.....	120
5.3.6 Antifouling study.....	121
5.3.7 Dye rejection and dye flux performance of membranes.....	122

5.4 CONCLUSIONS .....	123
-----------------------	-----

## **CHAPTER 6**

<b>NOVEL PPSU/ NANO ALUMINIUM TRIOXIDE DOPED ACID TREATED ACTIVATED CHARCOAL INCORPORATED MIXED MATRIX MEMBRANES FOR EFFICIENT REMOVAL OF PROTEINS, HEAVY METALS, AND OIL-WATER EMULSION SEPARATION.....</b>	<b>125</b>
--	------------

6.1 INTRODUCTION.....	127
-----------------------	-----

6.2 EXPERIMENTAL.....	137
-----------------------	-----

6.2.1 Materials.....	137
----------------------	-----

6.2.2 Al <sub>2</sub> O <sub>3</sub> -AAC mix preparation.....	137
--	-----

6.2.2.1 Acid treatment of activated charcoal (AAC).....	137
---	-----

6.2.2.2 Doping process of Al <sub>2</sub> O <sub>3</sub> NPs on AAC.....	138
--	-----

6.2.3 Fabrication of PPSU/ Al <sub>2</sub> O <sub>3</sub> -AAC mixed matrix membranes.....	138
--	-----

6.2.4 CHARACTERIZATION.....	139
-----------------------------	-----

6.2.5 Membranes rejection experimentations.....	139
---	-----

6.2.5.1 Proteins rejection study.....	139
---------------------------------------	-----

6.2.5.2 Heavy metals rejection study.....	140
---	-----

6.2.5.3 Oil-water emulsion separation study.....	140
--	-----

6.3 RESULTS AND DISCUSSION.....	141
---------------------------------	-----

6.3.1 Morphological results.....	141
----------------------------------	-----

6.3.1.1 FESEM results of alumina and EDS analysis of Al <sub>2</sub> O <sub>3</sub> -AAC.....	141
---	-----

6.3.1.2 SEM results of the Al <sub>2</sub> O <sub>3</sub> -AAC incorporated PPSU membranes.....	142
---	-----

6.3.1.3 SEM-EDS analysis of PA-3 membrane.....	144
--	-----

6.3.1.4 AFM-membrane surface roughness effects.....	144
---	-----

6.3.2 Contact angle (CA) results.....	145
---------------------------------------	-----

6.3.3 Membrane water uptake and porosity results.....	145
6.3.4 MWCO results.....	146
6.3.5 Water permeability results of membranes.....	147
6.3.6 Anti-fouling performance of membranes.....	148
6.3.7 Rejection results.....	149
6.3.7.1 Proteins rejection performance of membranes.....	149
6.3.7.2 Heavy metals rejection performance of membranes.....	150
6.3.7.3 Oil-water separation studies.....	152
6.4 CONCLUSIONS.....	153
<b>CHAPTER 7 SUMMARY AND CONCLUSIONS.....</b>	<b>155</b>
7.1 SUMMARY.....	157
7.2 CONCLUSIONS.....	161
REFERENCES.....	163
LIST OF PUBLICATIONS.....	193
LIST OF CONFERENCES ATTENDED.....	195
BIO DATA	



## LIST OF FIGURES

	PAGE NO.
<b>Figure 1.1</b> Pi-chart of distribution of water on earth surface.....	3
<b>Figure 1.2</b> Predicted water scarcity and stress in 2025.....	4
<b>Figure 1.3</b> Schematic illustration of membrane filtration process.....	6
<b>Figure 1.4</b> Fouling formation on membrane surface.....	8
<b>Figure 1.5</b> (a) Surface, (b) cross sectional morphology of symmetric membranes.....	9
<b>Figure 1.6</b> Cross sectional morphology of asymmetric membranes.....	9
<b>Figure 1.7</b> Schematic illustrations of integral asymmetric (a) and TFC membrane (b)....	10
<b>Figure 1.8</b> Schematic representations of different membrane processes (A) Gas separation (B) Pervaporation (C) Dialysis (D) Electro dialysis (E) Forward Osmosis (F) Membrane distillation.....	11
<b>Figure 1.9</b> Pressure driven membrane processes.....	12
<b>Figure 1.10</b> Digital photograph of lab prepared flat-sheet membrane.....	13
<b>Figure 1.11</b> Schematic illustration of flat-sheet membrane preparation <i>via</i> phase inversion method.....	13
<b>Figure 1.12</b> Schematic representations of plate and frame module, and spiral wound Modules.....	14
<b>Figure 1.13</b> Hollow fiber configurations.....	14
<b>Figure 1.14</b> Schematic representation of hollow fiber membrane fabrication.....	15
<b>Figure 1.15</b> Structures of some commonly used polymers in membrane preparations....	16
<b>Figure 1.16</b> Chemical structure of Polyphenylsulfone (PPSU) polymer.....	17
<b>Figure 1.17</b> Graphical representation of Phase inversion technique.....	20
<b>Figure 1.18</b> Asymmetric membrane structure.....	21
<b>Figure 1.19</b> Graphical representation of Dead-end and Cross-flow filtration methods....	21

<b>Figure 1.20</b> SEM micrographs of PESF foams, at different foaming temperatures (a) at 140 °C, (b) 200 °C, at different foaming times (c) at 15 seconds (d) at 120 seconds.....	24
<b>Figure 1.21</b> SEM micrographs of microcellular foams prepared from S-PSF (Na)/PBI, S-PPSF (Na)/ PBI.....	25
<b>Figure 1.22</b> Water uptake in equilibrium at 50 °C: comparison between phosphonated and sulfonated membranes.....	25
<b>Figure 1.23</b> Laboratory setup - Apparatus of gas permeation.....	26
<b>Figure 1.24</b> (a) the time-dependent permeate flux of the PPSU/PEI blend membranes, (b) HA adsorption amounts on the PPSU/PEI blend membranes.....	26
<b>Figure 1.25</b> Water fluxes and BSA rejections of the SPPSU membranes.....	27
<b>Figure 1.26</b> Antibacterial activity of PPSU/TiO <sub>2</sub> nanocomposites against E. coli (a), and S. aureus (b), Solid and dashed bars correspond to experiments performed without and with irradiation, respectively.....	28
<b>Figure 1.27</b> SEM cross-sectional images of PPSU UF membranes with different pore forming additives (A) PVP (B) PEG.....	28
<b>Figure 1.28</b> Schematic illustration of nanocomposite membrane surface and protein molecules interactions.....	29
<b>Figure 2.1</b> (a) SEM image of BiOCl crystals and (b) Fluorescence effects: BiOCl with visible light and BiOCl without light.....	35
<b>Figure 2.2</b> Possible pathway for the oxidized MWCNT surface with acid mixture.....	35
<b>Figure 2.3</b> Synthesis of G-PANCMI.....	36
<b>Figure 2.4</b> (a) Lab-scale filtration setup, (b) Schematic illustrating the adsorption affinity between the MNPs and the adsorbents.....	37
<b>Figure 2.5</b> Schematic description of thermo-responsive characteristics of the membrane and separation for water/oil emulsions.....	37
<b>Figure 2.6</b> SEM images of membranes (inset) contact angles of (a) Plane, (b) MMM-1 and (c) MMM-3 membranes.....	38
<b>Figure 2.7</b> SEM micrographs of synthesized charcoal activated with (a) H <sub>3</sub> PO <sub>4</sub> , (b) ZnCl <sub>2</sub> , and (c) FeSO <sub>4</sub> · 7H <sub>2</sub> O.....	39



<b>Figure 2.8</b> Schematic diagram of oil in water separation through Cross flow UF system.....	44
<b>Figure 2.9</b> FTIR spectrum of BiOCl nano wafers.....	45
<b>Figure 2.10</b> (a) is the SEM result of BiOCl nanowafers outlook image and (b) is the SEM image of magnified BiOCl nanowafers.....	46
<b>Figure 2.11</b> SEM images of M-0 (A), M-1 (B), M-2 (C), M-3 (D).....	46
<b>Figure 2.12</b> (a) SEM image of M-2 membrane surface, (b) EDS analysis of modified M-2 membrane.....	47
<b>Figure 2.13</b> Contact angle results of PPSU membranes.....	47
<b>Figure 2.14</b> Time dependent pure water flux of membranes.....	48
<b>Figure 2.15</b> (a) Flux V/s time for membranes at 0.2 MPa under three conditions: water flux for 20 min; 0.8 g L <sup>-1</sup> BSA Protein solution flux for 20 min; and water flux for 20 min after thoroughly washing with distilled water, (b) FRR & anti-fouling behavior of membranes.....	49
<b>Figure 2.16</b> Porosity and water uptake results of membranes.....	50
<b>Figure 2.17</b> Oil in water separation results of membranes with diesel fuel and crude oil...51	51
<b>Figure 3.1</b> (a) Effect of pH on the decolorization percentages of IC on Mn/ZSM-5, (b) Effect of photocatalyst content of Mn/ZSM-5 on the decolorization of IC.....	56
<b>Figure 3.2</b> Percentage of the decomposition of dyes by in situ-supported titania–zeolite...57	57
<b>Figure 3.3</b> SEM Cross-sectional micrographs of: (a) PSF/PI (50/50) 10 wt% ZSM-5 and (b) PSF/PI (50/50) 20 wt% ZSM-5.....	58
<b>Figure 3.4</b> Schematic depiction of the formation of GO/PEI gels, (A) GO and (B) amine-rich PEI were combined to give (C) GO/PEI hydrogels. (D & E) Gelation pictures.....	59
<b>Figure 3.5</b> SEM images of (a) NVZI/ZSM and (b) NVZI/SuZSM.....	60
<b>Figure 3.6</b> The percent of adsorption and photo degradation of MB from initial concentrations of 20 mg/L with different photocatalysts.....	60

<b>Figure 3.7</b> Apparatus for adsorption of MO on PVA/PDADMAC/ZSM-5 membrane.....	61
<b>Figure 3.8</b> Effect of the ZSM-5 concentration on the PV performance.....	62
<b>Figure 3.9</b> Crystal structure of zeolite (3-D view) (a) tetrahedral interconnected cages (b).....	63
<b>Figure 3.10</b> Schematic representation of hollow fiber membrane fabrication unit.....	67
<b>Figure 3.11</b> Schematic diagram for the rejection of proteins, dyes through HF membranes.....	69
<b>Figure 3.12</b> Contact angle results of membranes.....	70
<b>Figure 3.13</b> Magnified FESEM image of ZSM-5 crystals.....	71
<b>Figure 3.14</b> (a) SEM cross sectional outlook image of HF membrane, and remain are the magnified images of membranes without additive (PZ-0) and with ZSM-5 additives (PZ-1, PZ-2 and PZ-3).....	72
<b>Figure 3.15</b> (a) FESEM surface appearance of PZ-3 membrane, (b) EDS result of revised PZ-3 membrane.....	72
<b>Figure 3.16</b> Time dependent PWF performance of membranes.....	73
<b>Figure 3.17</b> (a) Flux V/s time for membranes at 0.3 MPa under three conditions: water flux; BSA Protein flux; and water flux after thoroughly washing with water, (b) FRR and anti-fouling results of membranes.....	74
<b>Figure 3.18</b> water uptake and porosity results of membranes.....	75
<b>Figure 3.19</b> Proteins rejection results of membranes.....	76
<b>Figure 3.20</b> (a) Dyes rejection performance of membranes, (b) time dependent dye flux result of PZ-3 membrane.....	77
<b>Figure 3.21</b> the digital images of (a) RB-5, (c) RO-16 dyes rejection results with membranes and (b & d) are the outlook images of membrane adaptors after rejection.....	77
<b>Figure 4.1</b> Comparisons of H <sub>2</sub> /CH <sub>4</sub> (a), CO <sub>2</sub> /CH <sub>4</sub> (b) selectivity of PBNPI doped membranes earlier and afterwards the addition of MWCNTs/PBNPI.....	83

<b>Figure 4.2</b> Adsorption performance of selected metal ions, (a) wastewater and (b) Red Sea water.....	83
<b>Figure 4.3</b> FESEM micrographs of CNT/PSf composite membranes.....	84
<b>Figure 4.4</b> Adsorption of Pb (II) onto MWCNTs/ThO <sub>2</sub> nanocomposite.....	84
<b>Figure 4.5</b> (a) Heavy metals removal efficiency of membranes, (b) Schematic illustration of PEI complexation mechanism with metal ion.....	85
<b>Figure 4.6</b> (a) TEM image of PES/Pb(II)-imprinted-MWNTs, and SEM results of membranes (b) 0%, (c) 1%, (d) 2%.....	86
<b>Figure 4.7</b> Reaction between MWCNTs-COOH and APTMS.....	86
<b>Figure 4.8</b> Synthesis of MWCNT/ PANI.....	87
<b>Figure 4.9</b> Graphical illustration of heavy metal ions rejection by lab scale dead-end filter setup.....	90
<b>Figure 4.10</b> Contact angle results of membranes.....	91
<b>Figure 4.11</b> Porosity and water uptake outcomes of membranes.....	92
<b>Figure 4.12</b> SEM outlook (A), and magnified images of MWCNTs (B).....	93
<b>Figure 4.13</b> Cross sectional SEM images of PPSU/MWCNT membranes.....	94
<b>Figure 4.14</b> 3D AFM analysis images of membranes.....	95
<b>Figure 4.15</b> (A) Top surface digital photograph of prepared membranes, (B) PWF of membranes.....	96
<b>Figure 4.16</b> (a) Flux V/s time for membranes at 0.3 MPa under three conditions: PWF; BSA flux; and PWF after systematically wash with water, (b) FRR and antifouling behavior of membranes.....	97
<b>Figure 4.17</b> Graphical representation of heavy metals complexation with PEI (a), Heavy metal ions rejection results of membranes (b).....	99
<b>Figure 4.18</b> A, C and E are the SEM-EDS analysis results of PCNT-3 membranes and B, D and F are the elemental mapping descriptions of Pb <sup>2+</sup> , Hg <sup>2+</sup> and Cd <sup>2+</sup> ions.....	100
<b>Figure 5.1</b> SnO <sub>2</sub> unit cell structure, Ben Mills-Rutile structure.....	104

<b>Figure 5.2</b> Retention coefficient (a) and permeate flux (b) of the different salts solutions as a function of the ionic strength.....	105
<b>Figure 5.3</b> Formation Process of TNT nanofibers from Mesoporous Silica.....	106
<b>Figure 5.4</b> MB photo degradation by SnO <sub>2</sub> , RGO–SnO <sub>2</sub> and P25 under UV irradiation (a) and sunlight (b).....	107
<b>Figure 5.5</b> (a) Biosynthesis of SnO <sub>2</sub> nanoparticles (b) photocatalytic degradation procedure of dyes by SnO <sub>2</sub> NPs.....	107
<b>Figure 5.6</b> Investigational data v/s expected data MLR (a), LSSVR (b).....	108
<b>Figure 5.7</b> Possible mechanism of dye degradation under SnO <sub>2</sub> photocatalyst.....	109
<b>Figure 5.8</b> (a) TEM image of SnO <sub>2</sub> NPs (8-10 nm) and (b) dye degradation mechanism.....	109
<b>Figure 5.9</b> Flux and rejection performance of the membranes.....	110
<b>Figure 5.10</b> Lab scale cross-flow filter unit and graphical representation of dye rejection mechanism.....	114
<b>Figure 5.11</b> SEM outlook image (a) and magnified image (b) of SnO <sub>2</sub> nanoparticles.....	116
<b>Figure 5.12</b> PS-3 membrane FESEM surface outlook (a) and studied EDS analysis result (b).....	116
<b>Figure 5.13</b> AFM 3-D images of membranes.....	117
<b>Figure 5.14</b> Contact angle results of membranes.....	118
<b>Figure 5.15</b> Water uptake and porosity outcomes of membranes.....	119
<b>Figure 5.16</b> MWCO results of PS-3 membrane.....	120
<b>Figure 5.17</b> Time dependent PWF result of membranes.....	120
<b>Figure 5.18</b> (a) Flux v/s time for membranes at 0.2 MPa under three conditions: water flux; BSA flux; and water flux after thoroughly wash with water, (b) FRR and anti-fouling outcomes of membranes.....	121
<b>Figure 5.19</b> A&B are the dye rejection results of membranes, D is the time dependent dye flux of PS-3 membrane, C-1 & C-2 are the outlook images of dye permeates.....	123
<b>Figure 6.1</b> Schematic design of oil-water filtration.....	128

<b>Figure 6.2</b> Water flux results (a), SEM cross-sectional micrograph (b) of membranes...	129
<b>Figure 6.3</b> Lab-scale oil-water microfiltration experimental setup.....	130
<b>Figure 6.4</b> (a) Electrospinning unit (b) Effect of initial ion concentrations on the uptake capacity of nanofibrous membranes.....	131
<b>Figure 6.5</b> SEM images of membranes (a) cross sectional, (b) top view image, and (c) Revisited Robeson plot for CO <sub>2</sub> /CH <sub>4</sub> mixtures.....	131
<b>Figure 6.6</b> Schematic illustrations of recirculation and concentrate mode operations...	132
<b>Figure 6.7</b> (a) Flow loop system, (b) Cd (II) ion interactions with the CNT-Al <sub>2</sub> O <sub>3</sub> membrane.....	133
<b>Figure 6.8</b> Schematic illustration of ACM fabrication (A), membrane thickness and pore size were controlled by regulating the addition of AC and rGO (B).....	134
<b>Figure 6.9</b> Fabrication procedure of the polymer@CNT nanohybrid membranes.....	135
<b>Figure 6.10</b> (a) Schematic image of alumina membrane, (b) Oil-water separation experimental setup.....	135
<b>Figure 6.11</b> Schematic image of lab scale dead-end filter unit for separation.....	141
<b>Figure 6.12</b> (A) Magnified FESEM image of Al <sub>2</sub> O <sub>3</sub> -NPs, (B) Outlook FESEM image of Al <sub>2</sub> O <sub>3</sub> doped AAC, (C) FESEM surface appearance Al <sub>2</sub> O <sub>3</sub> -AAC, (D & E) are EDS elemental mapping results of Al <sub>2</sub> O <sub>3</sub> -AAC.....	142
<b>Figure 6.13</b> SEM cross sectional results of membranes.....	143
<b>Figure 6.14</b> (a) FESEM surface appearance and (b) EDS result of PA-3 membrane....	144
<b>Figure 6.15</b> AFM surface roughness results of membranes.....	145
<b>Figure 6.16</b> (a) Contact angle, (b) porosity and water uptake results of membranes.....	146
<b>Figure 6.17</b> Molecular weight cut-off result of PA-3 membrane.....	147
<b>Figure 6.18</b> Water permeability results of membranes.....	147
<b>Figure 6.19</b> (a) Flux V/s time for membranes at 0.2 MPa under three conditions: J <sub>w1</sub> ; J <sub>p</sub> ; and J <sub>w2</sub> , (b) FRR and anti-fouling effects of membranes.....	148

<b>Figure 6.20</b> Proteins rejection (a), and time dependent protein flux (b) of PA-3 membrane.....	150
<b>Figure 6.21</b> Heavy metals rejection (a), and heavy metal flux of PA-3 membrane (b), elemental mapping results of Pb <sup>2+</sup> ions (c1&c2) and Cd <sup>2+</sup> ions (d1&d2).....	151
<b>Figure 6.22</b> Oil-water emulsions separation results (a) bio-diesel, and (b) kerosene, (c&d) are the feed and permeate samples outlook images.....	153
<b>Figure 7.1</b> PWF comparison results of fabricated (a) Flat-sheet and (b) HFMs.....	159
<b>Figure 7.2</b> Contact angle results of fabricated membranes.....	160
<b>Figure 7.3</b> FRR results of fabricated membranes.....	160

## LIST OF TABLES

<b>Table 1.1</b>	Classification of membranes on the basis of driving force.....	10
<b>Table 2.1</b>	Membrane compositions.....	41
<b>Table 2.2</b>	Membrane permeability studies.....	49
<b>Table 2.3</b>	Membrane properties.....	50
<b>Table 3.1</b>	HF membranes characterization techniques.....	64
<b>Table 3.2</b>	Membrane compositions.....	66
<b>Table 3.3</b>	Spinning parameters of HFMs.....	66
<b>Table 3.4</b>	Membrane permeability study.....	74
<b>Table 3.5</b>	Membrane properties.....	75
<b>Table 4.1</b>	Membrane configurations.....	88
<b>Table 4.2</b>	Membrane properties.....	91
<b>Table 4.3</b>	Surface roughness parameters of membranes.....	95
<b>Table 4.4</b>	Membrane permeability studies.....	97
<b>Table 5.1</b>	Membrane configurations.....	112
<b>Table 5.2</b>	Spinning parameters of HFMs.....	112
<b>Table 5.3</b>	Surface roughness variables of membranes.....	117
<b>Table 5.4</b>	Membrane properties.....	119
<b>Table 5.5</b>	Membrane permeability studies.....	122
<b>Table 6.1</b>	Membrane dope solutions compositions.....	138
<b>Table 6.2</b>	Surface roughness variables of membranes.....	145
<b>Table 6.3</b>	Membrane properties.....	146
<b>Table 6.4</b>	Membrane permeability results.....	149
<b>Table 7.1</b>	Membrane series.....	158





## LIST OF ABBREVIATIONS

AAC	Acid treated activated charcoal
AC	activated charcoal
ACMs	Activated carbon membranes
ADS	Ammonium dodecyl sulphate
AFM	Atomic force microscopy
Al <sub>2</sub> O <sub>3</sub>	Aluminium trioxide
APTMS	(3-aminopropyl)-trimethoxysilane
BET	Brunauer Emmett Teller analysis
BiCl <sub>3</sub>	Bismuth trichloride
BiOCl	Bismuth oxychloride
BSA	Bovine Serum Albumin
CA	Contact angle
CA	Cellulose acetate
Cd (NO <sub>3</sub> ) <sub>2</sub>	Cadmium nitrate
CeO <sub>2</sub>	Cerium dioxide
CH <sub>4</sub>	Methane
CNT	Carbon nanotubes
CO <sub>2</sub>	Carbon di oxide
COD	Chemical oxygen demand
CS	Chitosan
DB	Direct blue 71
DIPS	Diffusion induced phase separation
DLS	Dynamic light scattering

DMF	N, N dimethyl formamide
DMSO	Dimethylsulfoxide
DSC	Differential scanning calorimetry
DW	Deionized water
DY	Direct yellow 8
E. coli	Escherichia coli (Gram-negative) bacteria
EA	Egg albumin
EBT	Erichrome black T
EDX/EDS	Energy Dispersive X-ray Spectroscopy
EtOH	Ethyl alcohol
FA	Formamide
Fe <sub>2</sub> O <sub>3</sub>	Ferric oxide
FESEM	Field Emission scanning electron microscopy (FESEM)
FeSO <sub>4</sub>	Ferrous sulfate
FO	Forward Osmosis
FRR	Flux recovery ratio
FS	Flat-sheet membranes
FTIR	Fourier transform infrared spectrometer
GO	Graphene oxide
G-PANCMII	Graphene oxide grafted poly acrylonitrile co maleimide
H <sub>2</sub>	Hydrogen
H <sub>2</sub> O	Water
H <sub>2</sub> SO <sub>4</sub>	Sulphuric acid
H <sub>3</sub> PO <sub>4</sub>	Phosphoric acid

HCl	Hydrochloric acid
HFM	Hollow fiber membranes
HgCl <sub>2</sub>	Mercuric chloride
<sup>1</sup> H-NMR	Proton nuclear magnetic resonance spectroscopy
HPLC–MS	High-performance liquid chromatography–mass spectrometry
HQ	Hydroxyquinoline
HRTEM	High-resolution transmission electron microscopy
HTAC	Hexadecyl trimethyl ammonium chloride
IC	Indigo carmine dye
ID	Inner diameter
IEC	Ion exchange capacity
IGS	Innovative Gas Systems
KDa	Kilo Dalton
LCMS	Liquid chromatography–mass spectrometry
LSSVR	Least squares support vector regression model
MB	Methylene blue
MDES	Methyldiethoxysilane
MeOH	Methyl alcohol
MF	Microfiltration
MLR	Multiple linear regressions model
MMMs	Mixed matrix membranes
MnO <sub>2</sub>	Manganese oxide
MOF	Metal organic framework
MS	Membrane series
MV6B	Methyl violet 6B

MW	Molecular weight
MWCNTs	Multiwalled carbon nanotubes
MWCO	Molecular weight cut-off
N <sub>2</sub>	Nitrogen
NaOH	Sodium hydroxide
NF	Nanofiltration
NGL	Natural gas liquids
NIPS	Non-solvent induced phase separation
nm	Nano meters
NMP	N-methyl 2-pyrrolidone
NPs	Nanoparticles
NR	Neutral red
NZVI	Nanoscale zero-valent iron
OD	Outer diameter
PA	Propionic acid
PAA	Polyacrylic acid
PAI	Polyamideimide
PAN	Polyacrylonitrile
PANI	Polyaniline
Pb (NO <sub>3</sub> ) <sub>2</sub>	Lead nitrate
PBI	Polybenzimidazole
PDADMAC	Poly (diallyldimethylammonium chloride)
PDMS	Polydimethylsiloxane
PEG	Polyethylene glycol
PEI	Polyetherimide

PEI	Polyethylenimine
PESF	Polyethersulfone
PMMA	Polymethylmethacrylate
ppm	Parts per million
PPSU	Polyphenylsulfone
PSf	Polysulfone
PSMA	Poly (stearyl methacrylate)
PTFE	Polytetrafluoroethylene
PVC	Polyvinylchloride
PVDF	Polyvinylidenedifluoride
PVP	Polyvinylpyrrolidone
PWF	pure water flux
QDs	Quantum dots
RB-5	Reactive black 5
RGO	Reduced graphene oxide
RhB	Rhodamine B
RO	Reverse osmosis
RO-16	Reactive orange 16
S. aureus	Staphylococcus aureus (Gram-positive) bacteria
SDS	Sodium dodecyl sulphate
Sdv	Standard deviation
SEM	Scanning electron microscopy
SFE	Surfactant-free water-in-oil emulsions
SnO <sub>2</sub>	Tin oxide

SPES	Sulphonated polyethersulfone
S-PPSF	Sulfonated polyphenylsulfone
SSE	Surfactant-stabilized water-in-oil emulsions
TCD	Thermal conductivity detector
TEM	Transition electron microscopy
TFC	Thin film composite
TGA	Thermo gravimetric analysis
ThO <sub>2</sub>	Thorium oxide
TiO <sub>2</sub>	Titanium dioxide
TIPS	Thermally induced phase separation
TMA	Thermal mechanical analysis
TMP	Trans membrane pressure
TOC	Total organic carbon analyzer
UF	Ultrafiltration
UNEP	United national's environment programme
UTM	Universal testing machine
UV-Vis	Ultraviolet and visible spectroscopy
WCA	Water Contact Angle
Wt. %	Weight percentage
XRD/XPRD	X-ray powder diffraction
ZnCl <sub>2</sub>	Zinc chloride
ZnO	Zinc oxide
ZrO <sub>2</sub>	Zirconia
ZSM-5	Zeolite Socony Mobil-5







**CHAPTER 1**  
**INTRODUCTION**



## Abstract

*This chapter provides detailed information about the ongoing research in the field of membrane science and technology towards water purification. It mainly highlights the worldwide water crisis, membrane history, various membrane separation classifications, membrane types, membrane preparation methods, and applications of membrane technology. This chapter also includes a literature review that enlightens the usage of polyphenylsulfone as membrane material and the importance of nanomaterials in polymeric membranes towards water purification applications.*

## 1.1 WORLDWIDE SCENARIO OF WATER

Water is one of the essential sources to survey the life on earth to the ecosystem and to the human life. Water is a modest chemical complex with chemical formula  $H_2O$ . The most crucial problem today around the world is water scarcity. The Earth's surface consists of nearly 70 % water. The oceans (salt water) account for 97 % of this water, while the other 3 % is reflected freshwater. Out of this 3 % freshwater, ~68.7 % is latched in glaciers and icecaps, ~30.1 % as well groundwater, 0.9 % is in other forms and hardly 0.3 % of water can access from lakes and rivers to survive life. The below diagram Figure 1.1 can explain the water distribution percentages throughout the earth.

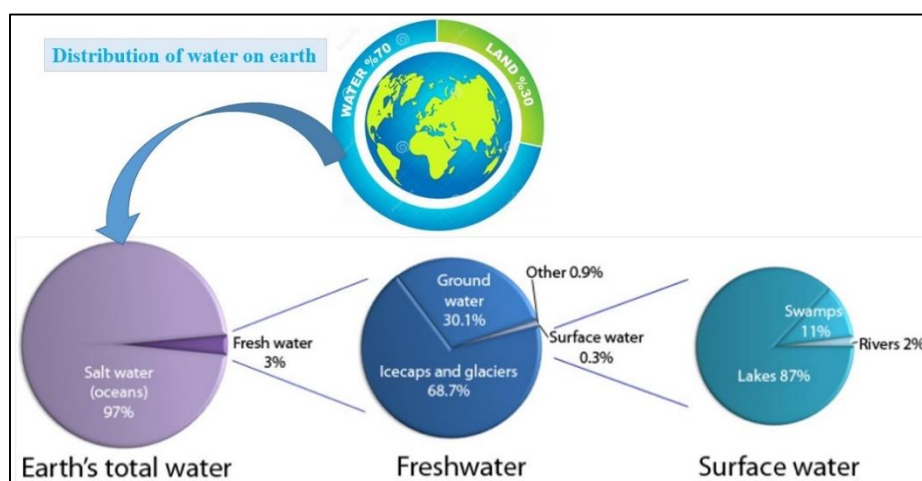


**Figure 1.1** Pi-chart of distribution of water on earth surface (Source: The University of Waikato, earth's water distribution, 2009)

The demand for water is increasing rapidly due to the world population growth that accomplishes larger difficulties of water for national, agriculture and industrial use. Both food production growth and industrial development advance the number of contaminations and waste discharges are directed towards the inside of water sources, polluting the water and creating some health difficulties. Moreover, receiver water, such as lakes, rivers, and coastal areas are polluted by large amounts of industrial, agricultural and municipal waste directly as well as indirectly through atmospheric deposition of gaseous emissions. At present, world population 7.2 billion, according to the United Nations survey reports, by 2050 it will cross 9.6 billion. Currently, according to the UNEP (United national environment programme) survey, 2006 around 1.2 billion people phasing difficulties to access the drinking water. Unsafe human activities are becoming the main reason behind the water scarcity. This water scarcity can affect the ecosystem seriously day-by-day. In the future, nearly seven billion people going to phase water scarcity difficulties. Inappropriately, water is soiling very effortlessly due to the various reasons but, it's too tough to recycle the contaminated water and it's too chargeable (Begon *et al.* 2006). The water scarcity problem going to phase throughout the world by 2025 (UNEP, 2008) elucidated in Figure 1.2.

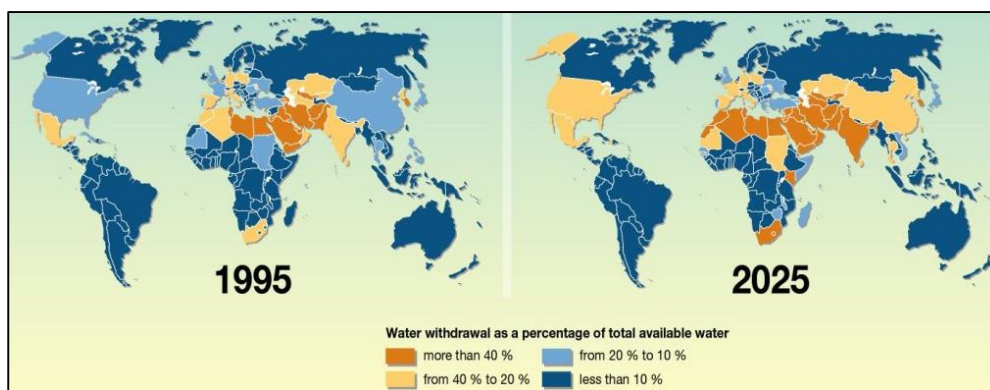


**Figure 1.2** Predicted water scarcity and stress in 2025 (Source: UNEP, 2008)

Many types of research across the globe are working very hard to overcome the water problem. Some of the other sources that have been studied to challenge the fresh water scarcity with the treatment of brackish water, wastewater and seawater into potable water. Starting in the sixties of the last century, in industrial applications

membrane processes are stage by stage slowly initiated towards the production of dirt-free water.

## 1.2 MEMBRANE HISTORY

In the recent year's availability of clean water is the biggest challenge for the common public and industries. Effectual separation processes are essential to get high-quality water, and remove toxins, components from the soiled water. To achieve these objectives, researchers have developed different techniques such as extraction, adsorption, ion-exchange method, and crystallization, precipitation, and distillation methods. In recent, these conservative separation systems accompanied personally by utilizing semipermeable membranes as separation barriers.

Jean Antoine Nollet, exposed the permeation phenomena using pig's bladder to separate water-ethanol mixture. Most likely Nollet was the first person to differentiate the relation between a semipermeable membrane and the osmotic pressure (Nollet 1748). Dutrechet accommodated the method consists, osmosis phenomenon to exemplify the movement of liquids over a permeable barrier (Dutrechet 1820). Fick synthesized semipermeable membranes artificially using nanocellulose material (Fick 1855). Practical interpretations of mass transference in semipermeable membranes were reinforced by Graham studies. Graham presented the gas separation phenomena and became the first person to introduce the dialysis procedure using membranes (Graham 1866). Traube synthesized semipermeable thin layered membranes using cupric ferrocyanide to study the transport properties of membranes in osmosis (Traube 1867). Bechold *et al.* first time prepared thin film ultrafiltration (UF) membranes by imparting filter paper in nitrocellulose in glacial acetic acid (GAA) mixture (Bechhold 1908). Donnan elucidated the concept of membrane equilibrium and membrane capability in the attendance of electrolytes (Donnan 1911). The nitrocellulose membranes equipped with diverse pore sizes and used in laboratory analytical applications to improve the effective hemodialysis function (Kolff 1944). Loeb and Sourirajan, University of California scientist, have successfully fabricated asymmetric reverse osmosis (RO) membranes with cellulose acetate (CA) polymer, to study the flux behavior and salt removal capability of membranes from seawater (Loeb and Sourirajan 1962). After the 1960's the usage of membrane technology in various

medical fields such as blood purification, drug transportations, etc. increased due to the polymeric membranes specific characteristics. During 1960 to 1980, a foremost improvement was noticed in membrane technology due to the availability of broad scope of polymeric materials and their precise properties such as polysulfone, polyacrylonitrile, polyethylene for the preparation of synthetic membranes.

The present rapid growth was observed in industrial applications with various membrane processes which cover water distillation, sea, and brackish water desalination, wastewater recovery, gas and vapor separation, hazardous industrial waste treatment, hemodialysis, protein separation, and oil in water separation.

### 1.3 DEFINITIONS AND BASIC TERMINOLOGY IN MEMBRANE SCIENCE

“Membrane is a separation barrier to pass the selective fine particles only through it, not others” (Hsieh 1996). Figure 1.3 can illustrate the schematic representation of the membrane filtration process. Due to the effect of pressure, the fine particles from feed solution can separate through the membrane is called as permeate, and limited of the particles cannot pass through the membranes, those rejected particles can call as retentate.

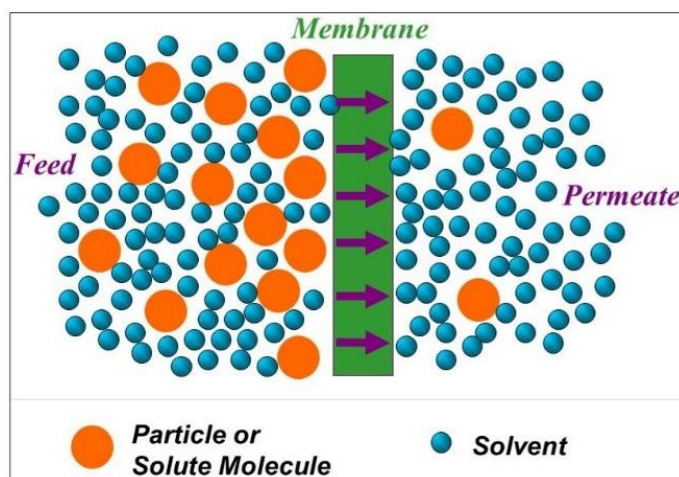


**Figure 1.3** Schematic illustration of the membrane filtration process (Source: Colorado School of mines)

### 1.3.1 BASIC TERMS IN MEMBRANE SCIENCE

**1.3.1.1 Flux:** “The amount of water passing through a unit area of the membrane per unit time” is called as flux. Eq. 1.1 can use to calculate the pure water flux (PWF) of membranes.

$$J_w = \frac{Q}{\Delta t \times A} \quad \text{Eq. (1.1)}$$

Where ‘ $J_w$ ’ is pure water flux (L/m<sup>2</sup>h), ‘ $Q$ ’ is an amount of water collected (L) in time ‘ $\Delta t$ ’ (h), ‘ $A$ ’ is membrane area (m<sup>2</sup>).

**1.3.1.2 Solute Rejection:** Selectivity assets of membranes were given in terms of rejection, and Eq. 1.2 can apply to calculate the rejection ability of membranes.

$$\% R = \left(1 - \frac{C_p}{C_f}\right) \times 100 \quad \text{Eq. (1.2)}$$

Where ‘ $C_p$ ’ and ‘ $C_f$ ’ are the solute concentrations in permeate and in the feed solution.

**1.3.1.3 Water uptake:** Water uptake is the complementary characteristic to quantify the surface wettability of membranes. Eq. 1.3 employ to calculate the water uptake ability of membranes,

$$\% \text{ Water uptake} = \left(\frac{W_w - W_d}{W_w}\right) \times 100 \quad \text{Eq. (1.3)}$$

Where ‘ $W_w$ ’ and ‘ $W_d$ ’ are wet and dry weights of membrane sample.

**1.3.1.4 Porosity:** Membrane porosity characteristics were measured according to their dry-wet weights, by gravimetric method (Eq. 1.4).

$$\% \text{ Porosity} = \left(\frac{W_1 - W_2}{A \times l \times d_w}\right) \times 100 \quad \text{Eq. (1.4)}$$

Where ‘ $W_1$ ’ weight of wet membrane, ‘ $W_2$ ’ weight of dry membrane, ‘ $A$ ’ area of membrane (m<sup>2</sup>), ‘ $l$ ’ membrane thickness (m) and ‘ $d_w$ ’ density of water (0.998 g cm<sup>-3</sup>).

**1.3.1.5 Fouling:** Fouling is a process in which the suspended particles, macromolecules, salts etc. from the feed solution are deposit on the membrane surface or within the membrane pores (Figure 1.4), can reduce the membrane performance. Due to the pores blockage phenomena in membrane separation method, it can able to

observe a lesser amount of flux compares with water flux. This fouling process can impact the irreversible permeability performance of membranes, due to this, the fouling can reduce.

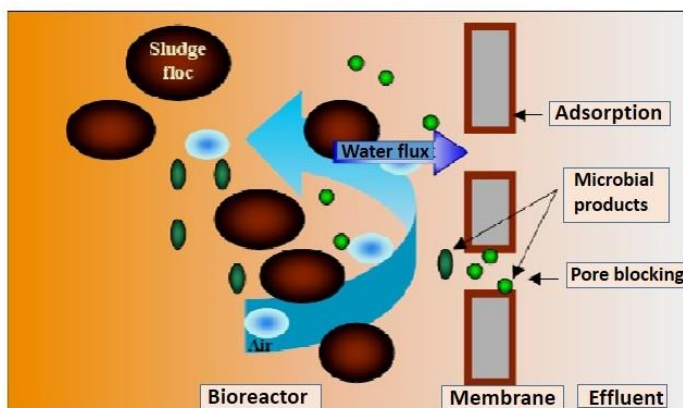


**Figure 1.4** Fouling formation on membrane surface (Source: Hoek and Elimelech 2003)

## 1.4 MEMBRANE CLASSIFICATIONS

Classification of membranes is very difficult to make, membranes are broadly classified on the basis of morphology, configuration, nature, and applications. Such as,

- (a) Organic or inorganic membranes, (b) Symmetric or asymmetric membranes,
- (c) Solid, liquid or gel membranes, (d) Porous or non-porous membranes,
- (e) Positive, negative, or neutral membranes, (f) Biological or synthetic membranes.

### 1.4.1 CLASSIFICATION BASED ON MEMBRANE MORPHOLOGY

Based on the structural morphology of membranes, the membranes are categorized into two types, they symmetric and asymmetric membranes.

**1.4.1.1 Symmetric Membrane:** In this type of membranes, one can observe the uniform pore size distribution across the membrane (Figure 1.5). These membranes can prepare by sintering or track etching methods.



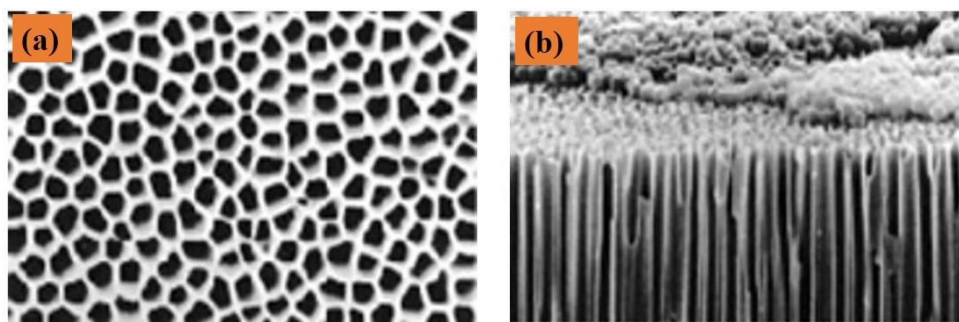


**Figure 1.5** (a) Surface, (b) cross-sectional morphology of symmetric membranes (Anopore™)

**1.4.1.2 Asymmetric Membrane:** From the cross-sectional diagram of the membrane, one can clearly notice the asymmetric structures with dense thin skin layer and porous sub-layers (Figure 1.6). Nowadays these asymmetric membranes are extensively using in different membrane separation processes. While performing the separation study, the porous sub-layer can mostly affect the separation outcomes of membranes.

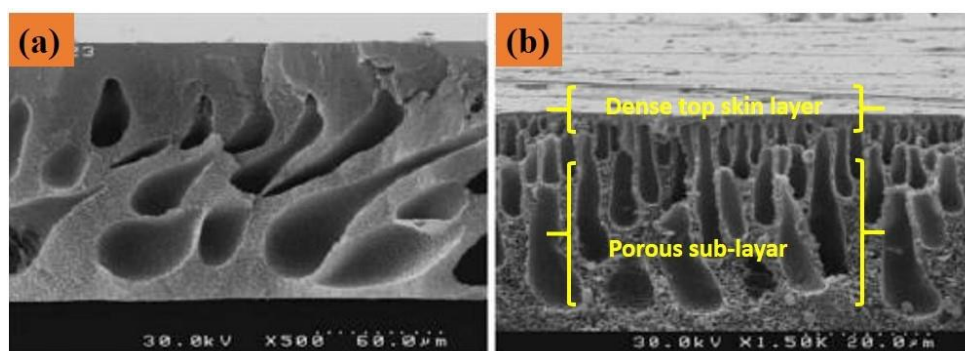


**Figure 1.6** Cross sectional morphology of asymmetric membranes (Rezaee 2015)

These asymmetric membranes further categorized two types based on the skin layer effects in the membrane separation process, they can be classified as follows:

**1.4.1.2.1 Integrally skinned asymmetric membrane:** In these type of membranes the dense top layer and the porous support are composed of the same material (Figure 1.7). These membranes can obtain by phase inversion method.

**1.4.1.2.2 Thin film composite (TFC) membrane:** In this, an ultra-thin layer of a polymer is deposited on the top of porous support (Figure 1.7). The ultra-thin layer and the porous support layers were made with different materials, which can be physically separated.

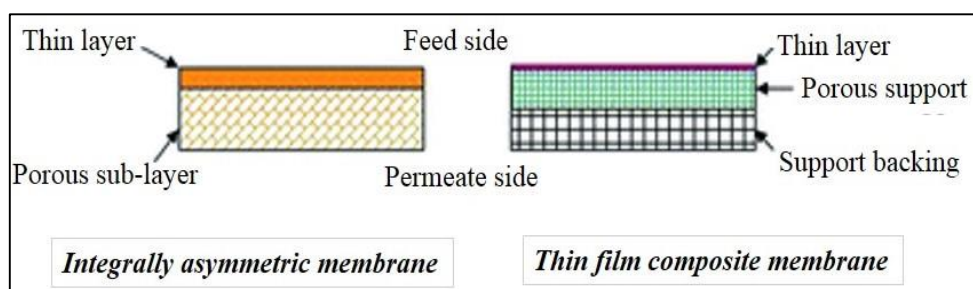


**Figure 1.7** Schematic illustrations of integral asymmetric (a) and TFC membrane (b) (Li and Wang *et al.* 2010)

#### 1.4.2 CLASSIFICATION BASED ON DRIVING FORCE

The physical and chemical properties of the membrane directive by the mechanism by which the separation of solutes is carried about. If feed holds with more than two constituent composites, then the separation is decided by the transport rate of interphase. The driving force for this transportation can be concentration gradient ( $\Delta C$ ), electrical potential gradient ( $\Delta E$ ), pressure gradient ( $\Delta P$ ) or temperature gradient ( $\Delta T$ ) (Table 1.1). Based on the driving force, membrane processes have been classified as follows.

**Table 1.1** Classification of membranes on the basis of driving force

Driving force	Membrane process
Concentration gradient ( $\Delta C$ )	Gas separation, Dialysis, Pervaporation, Forward Osmosis
Electrical potential gradient ( $\Delta E$ )	Electro dialysis, Electro deionization, Fuel cell membranes
Temperature gradient ( $\Delta T$ )	Membrane distillation
Pressure gradient ( $\Delta P$ )	Microfiltration, Ultrafiltration, Nanofiltration, Reverse osmosis

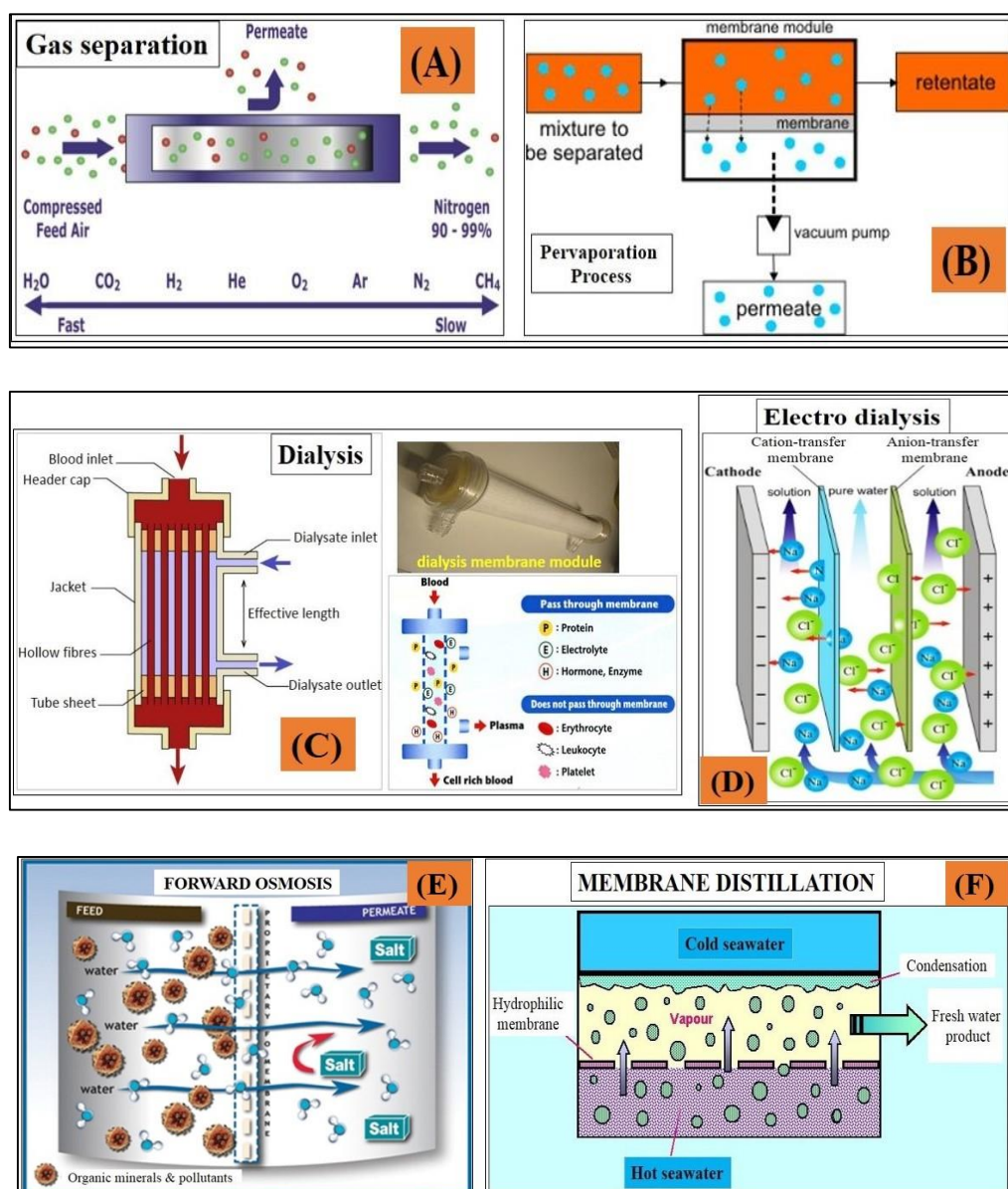


**Figure 1.8** Schematic representations of different membrane processes (A) Gas separation (@ SMC, Innovative Gas Systems (IGS)), (B) Pervaporation (@ REBEL, Sustainable management), (C) Dialysis (Yamashita *et al.* 2015), (D) Electro dialysis (@ Absun Palayesh 2010, Iran, Tehran), (E) Forward Osmosis (@ Hydrogen Technology Innovations, Albany), and (F) Membrane distillation (@ SM Cheah, 2000)

#### 1.4.2.1 PRESSURE DRIVEN MEMBRANE PROCESSES

In membrane separation processes the separation depended on the type, the charge of the membrane and the membrane pores by size exclusion principle (sieving

mechanism). In sieving mechanism, the smaller particles (particle size less than the pore size) can permit over it, and the bigger molecules cannot pass through the membrane pores easily. In non-porous membrane separations will occurs due to the selective adsorption and diffusion mechanisms.

Based on pore sizes the pressure driven membranes classified into following four types, they Microfiltration, Ultrafiltration, Nanofiltration and Reverse osmosis (Mulder 1996).

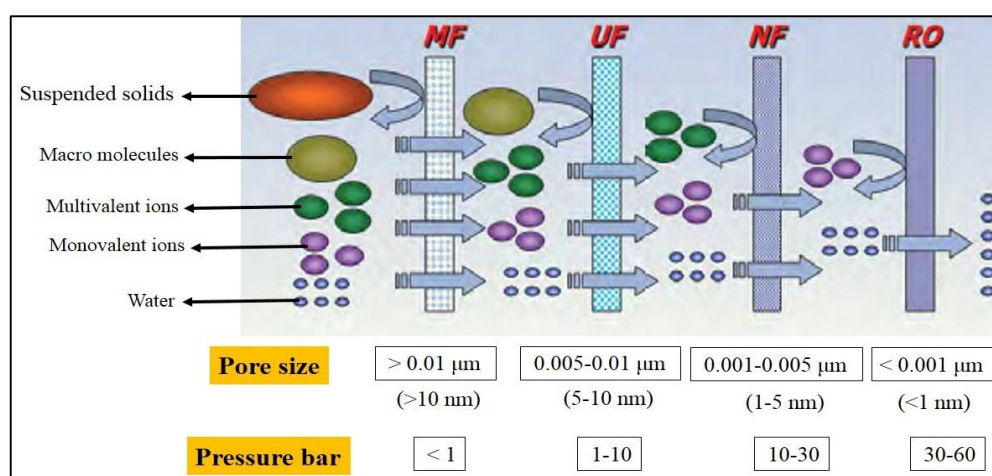


**Figure 1.9** Pressure-driven membrane processes (Source: Solute rejection model, Tzahi Y. Cath)

- i. **Microfiltration (MF):** The average pore size of these membranes is  $>0.01 \mu\text{m}$  ( $> 10 \text{ nm}$ ). At low pressure, it can operate, below 1 bar. MF membranes can able to separate the suspended solids, virus, and bacteria from the feed solution.
- ii. **Ultrafiltration (UF):** The average pore size range of these membranes is  $0.005$  to  $0.01 \mu\text{m}$  ( $5\text{-}10 \text{ nm}$ ). At  $1\text{-}10$  bar pressure, it can operatable. Membrane performance can affect by fouling, concentration polarization and with different operational conditions. UF membranes have the ability to distinct macromolecules and proteins from feed solution by sieving mechanism.
- iii. **Nanofiltration (NF):** The average pore size range of these membranes is  $0.001$  to  $0.005 \mu\text{m}$  ( $1\text{-}5 \text{ nm}$ ). At  $10\text{-}30$  bar pressure, it can operatable. These NF membranes can separate organics, multivalent ions from the feed solution.

- iv. **Reverse osmosis (RO):** The average pore size of these membranes is  $< 0.001\mu\text{m}$  ( $< 1\text{ nm}$ ). At higher pressures, it can be operated and the pressure range to the RO membranes is from 30-60 bar. These RO membranes retain organics, monovalent ions from the solutions. These RO membranes mainly used in desalination of seawater treatment. In this, the separation will go by the solution-diffusion mechanism.

### 1.4.3 CLASSIFICATION BASED ON CONFIGURATION

Based on configurations membranes categorized two types, they flat-sheet and hollow fiber membranes.

**1.4.3.1 Flat-sheet membranes:** In this type of membranes, the active layer is flat with low surface area. Most of the cases, these flat-sheet membranes fabricate by casting process via the phase inversion method. Desired geometry based on module shape, either circular or rectangular.

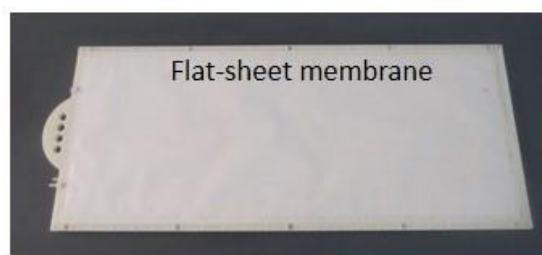


**Figure 1.10** Digital photograph of lab prepared flat-sheet membrane

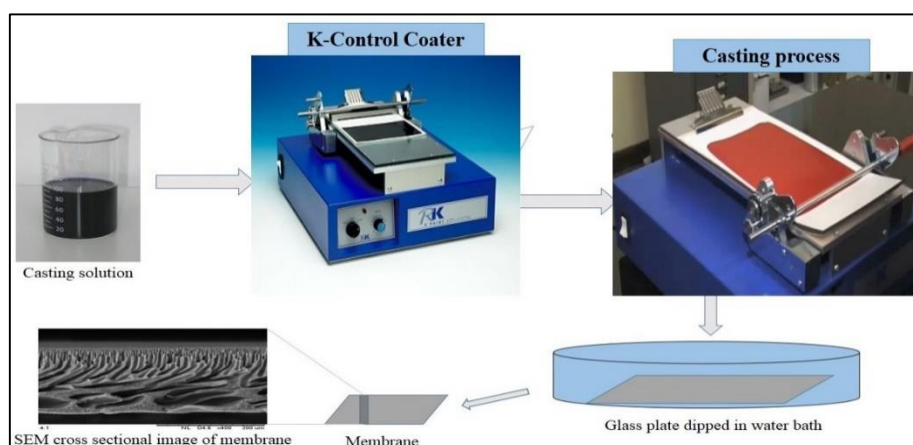


**Figure 1.11** Schematic illustration of flat-sheet membrane preparation *via* phase inversion method



These Flat-sheet membranes again divided into two types such as plate and frame module and spiral wound modules can be used in separation applications.

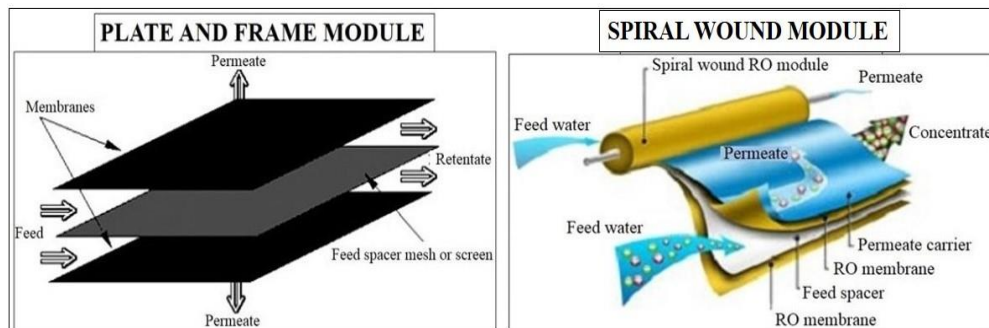


**Figure 1.12** Schematic representations of plate and frame module, and spiral wound modules (Source: Aqua research, Innovations in water technology, USA)

**1.4.3.2 Hollow fiber membranes:** In this type of membranes, the active layer is inside with high surface per volume compare with flat-sheet membranes. While performing the pressure-dependent permeability studies with HFMs, permeate can cross the outer surface and enter into the active layer and exist from fiber ends. The greatest advantage of these HFMs, it can able to fix a large number of fibers at a time in membrane modules. Due to enhancing the surface area good separation results can observable (Baker 2004).

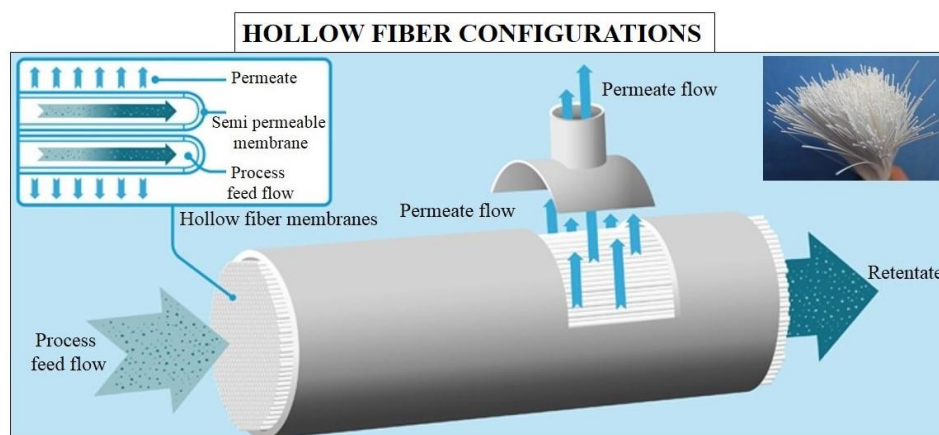


**Figure 1.13** Hollow fiber configurations (Koch Membrane Systems)

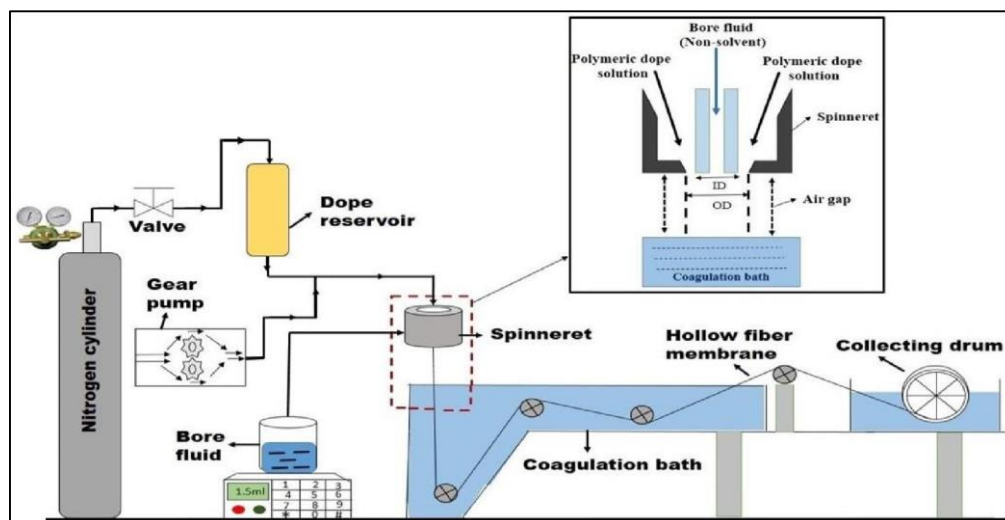


**Figure 1.14** Schematic representation of hollow fiber membrane fabrication

## 1.5 MERITS AND DEMERITS OF MEMBRANE PROCESSES

### Merits:

- Basic concept is simple and easy to understand,
- Very low energy consumption and able to operate at low temperatures,
- Simple to operate and easy to scale up,
- Membrane separation is dependable and needs minimum human intrusion during separation,
- Membrane processes can easily syndicate with other separation processes,
- No waste generation and environmentally green.

### Demerits:

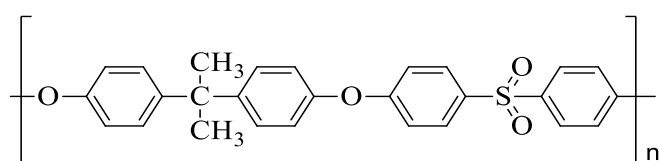
- Low membrane lifetime,
- Low selectivity,
- Sensitive to chemical attack,
- Sometimes need extreme pre-treatment due to the membrane sensitivity towards concentration polarization and fouling process,
- Membrane mechanical strength is very less, due to this it can easily be damaged under extreme operational conditions (Mulder 1996),
- Sometimes synthetic membranes cannot produce effective results.

## 1.6 MEMBRANE MATERIALS

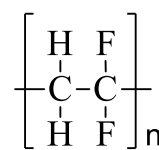
In present, the usage of different materials such as polymers, ceramics, glass materials, metals, etc., to fabricate the commercial synthetic membranes with the addition of various types of nano additives is increased (Mulder 1996). All types of polymers cannot form the membranes. Every membrane material has its own distinct properties with respect to the degree of hydrophilicity, chemical resistance, mechanical strength and flexibility. The selected polymeric material can decide the property of the membrane.

A good membrane material shows the following characteristics:

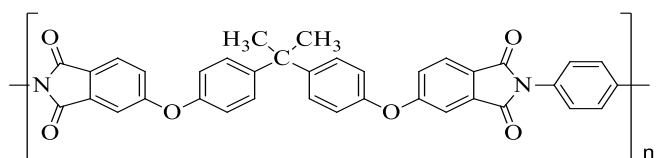
- i. Interrelated film forming ability, it is one of the main parameters to the membrane material for construction of the uniform film.
- ii. Mechanical strength assets must be high, it must be responsible for flexibility and stability to the film to stand at high operating pressures.
- iii. Glass transition temperature ( $T_g$ ) of the membrane material should be higher than that of the process temperature.
- iv. Better chemical stability.
- v. Membrane material should possess a better balance between hydrophilic and hydrophobic environs, to get the better performance results, and negligible fouling during operation.



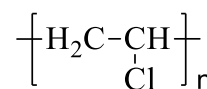
Polysulfone



Polyvinylidenedifluoride



Polyetherimide



Polyvinylchloride

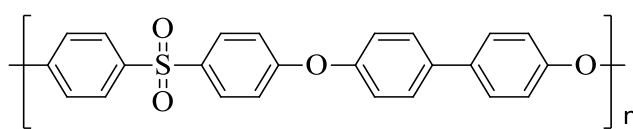
**Figure 1.15** Structures of some commonly used polymers in membrane preparations



Basically, these polymeric materials are hydrophobic in nature but disclose exceptional thermal, chemical and mechanical stabilities prerequisite for a membrane. The polymers can be mixed with different inorganic nanomaterials to enhance the membrane properties such as hydrophilicity, water uptake, porosity and permeability properties, etc.

### 1.6.1 Polyphenylsulfone as a membrane material

In current research work, Polyphenylsulfone (PPSU) choose as a principal polymeric membrane material to fabricate the flat-sheet and hollow fiber membranes with the incorporation of various inorganic nanomaterials, due to its specific properties such as chemical stability, solvent-resistance ability, better mechanical properties, hydrophobicity, high-temperature resistance, and outstanding thermal stability, etc. Polyphenylsulfone (PPSU) is generous of high-performance polymer generally containing of aromatic rings associated by sulfone (-SO<sub>2</sub>) groups. PPSU glass transition temperature (T<sub>g</sub>) is 220 °C which is greater than polysulfone (190 °C) (Darvishmanesh *et al.* 2011). With these extraordinary characteristics using polyarylsulfones in household applications, and in medical, electronics, mechanical, automotive engineering fields, food technology, and in many other applications. However, the great hydrophobic nature is one of the major drawbacks of this PPSU polymer. This hydrophobic property can influence the fouling resistance of PPSU polymer. This hydrophobic nature of PPSU polymer can reduce with the incorporation of different organic or inorganic additives and several hydrophilic agents. Currently, modified PSF and PPSU polymeric membranes are most widely used in UF, NF, and MF which play the main role in medicine, beverage processing and in drinking water treatments (Kunststoffe international 10/2011).



Polyphenylsulfone

**Figure 1.16** Chemical structure of Polyphenylsulfone (PPSU) polymer

### 1.6.2 Importance of nano-additives in polymeric membranes

At present, the industrially manufactured synthetic membranes are frequently using in various membrane separation applications. These synthetic membranes are facing most common problems, such as fouling, less flux, short mechanical strength, less hydrophilicity, etc. Among all, fouling is one of the main drawback property to the polymeric synthetic membranes. Due to the fouling behavior, the solute particles be able to deposit on the membrane surface and fewer permeability results can observable due to the pore blocking. Most of the research is going on to moderate these difficulties such as membrane surface modifications, pre-treatment methods, physical and chemical membrane cleaning methods and so on.

Membrane surface modification processes performed with several techniques such as blending, surface chemical modification, grafting, and by the incorporation of various types of organic and inorganic nanomaterials to the polymers. By surface chemical modification process membrane surface grafted with hydrophilic monomers to reduce the fouling behavior of membranes (Ng *et al.* 2013). Few of the research results displayed the properties with enhanced membrane permeability, mechanical strengths, and fouling performances with the fine addition of some of the inorganic nanoparticles to the membranes. These added nanoparticles can affects the conductivity, permeability, fouling, mechanical strength, pore morphology, surface roughness and antibacterial properties of membranes (Kim and Bruggenb 2010). Although the incorporated nanoparticles improving the performances of membranes and at same some of the disadvantages also observed. So, choosing suitable and correct nano additives for research is very challenging. In some cases, after the incorporation of nanoparticles to the polymeric solution, the resultant membranes exhibited improved hydrophilicity, water permeability, tensile strength results and other properties by the intermolecular forces among the polymeric chains and the nano-additives. The continuous enhancement of nanoparticle content in a polymeric solution will affect the performance of membranes. Sometimes the membrane thickness, pore morphology, and separation efficiency will also affect. These findings can conclude that the selection of suitable nano additive for further research is very important.

In current research work, totally five types of different inorganic nanoparticles such as BiOCl loaded activated charcoal, MWCNTs, ZSM-5 NPs, Tin oxide NPs and alumina doped acid treated activated charcoal etc., incorporated into the PPSU dope solution and fabricated several flat-sheet (FS) and hollow fiber membranes (HFM) via phase inversion method. Different filtration setups were applied to study the synthesized membranes water purification efficiency at various conditions. In additionally, Polyvinylpyrrolidone (PVP) used as a pore-forming agent to all PPSU dope solutions. Throughout the research, used N-methyl 2-pyrrolidone (NMP) as a solvent and distilled water as non-solvent.

## **1.7 MEMBRANE PREPARATIONS AND FILTRATION METHODS**

### **1.7.1 MEMBRANE PREPARATION METHODS**

Several methods were developed to fabricate the membranes. The selection of method depends on polymer assets, preferred construction of the membrane either FS or HFM and also the application of membrane (Lalia *et al.* 2013). Membrane permeability performance mainly depends on the structural morphology of membranes. Several techniques such as Sintering of pressed powder, Stretching of films, Track etching, Phase inversion, Template leaching, Coating process etc., were employed to fabricate the membranes.

#### **1.7.1.1 Phase inversion method/ Non-solvent induced phase separation (NIPS)**

Phase inversion method is one of the important and frequently used methods for the preparation of membranes. Commercially available membranes are mostly prepared by this phase inversion method. In this method, polymer alters into a controlled method from liquid to solid state (Kumar *et al.* 2013). It is a flexible technique to attain all kinds of morphologies. Phase inversion method involves in the ternary scheme, which contains at least one polymer integrant, one solvent, and a non-solvent, where the solvent and the non-solvent are immiscible. Morphology of the membranes can be controlled by the phase transition condition. The phase inversion is attained by several proceeds like solvent evaporation, thermal precipitation, vapor phase precipitation, immersion precipitation. But in membranes preparation majority

using immersion precipitation method. Most of the commercialized membranes are prepared by immersion precipitation method. In immersion precipitation method polymer solution cast on appropriate support of glass plate and then the plate dipped in a non-solvent coagulation bath for phase separation, then immediately within few seconds precipitated film forms because of the exchange of solvent and non-solvent (Figure 1.17).

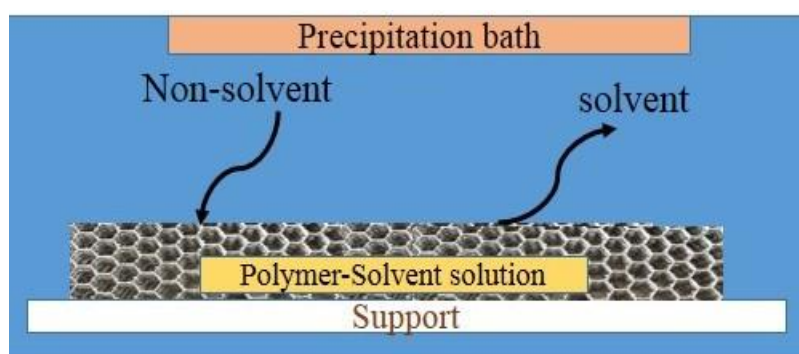


**Figure 1.17** Graphical representation of Phase inversion technique

### 1.7.1.2 Diffusion induced phase separation (DIPS) method

In the preparation of basic asymmetric membranes applied diffusion induced phase separation process. The process contains the following steps:

- The polymer dissolved in appropriate solvent ratio to form homogeneous solution contains 10-30 % of the polymer,
- Prepared solution pour on the glass plate and cast into a film,
- The film thickness range 100-500  $\mu\text{m}$ ,
- The film is quenched in non-solvent normal water.

The polymer solution separates into two phases during the quenching process.

- (a) Polymer rich solid phase - forms membrane structure,
- (b) Solvent rich liquid phase - forms liquid-filled membrane pores.

Normally the pores formed on the film surface, where precipitation arises first and fast, are much smaller than in the inner or the bottom side of the film. This will show the asymmetric membrane structure.

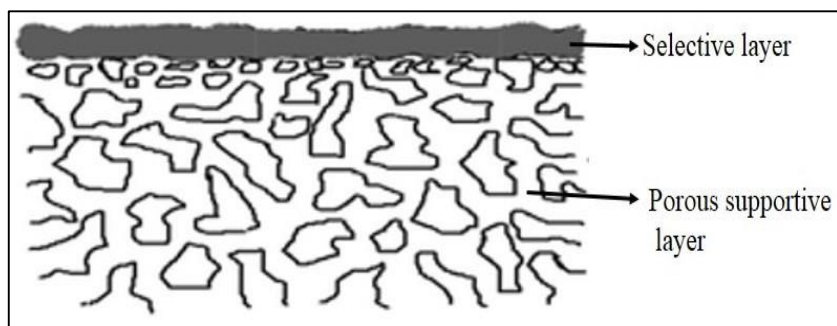


**Figure 1.18** Asymmetric membrane structure (Harold B. Tanh Jeazet *et al.* 2012)

## 1.7.2 MEMBRANE FILTRATION METHODS

Two types of filtration operations were most widely using, they are Dead-end and Cross-flow filter operations.

### 1.7.2.1 Dead-end filter operation

- Feed flow was perpendicular to the membrane.
- Membrane will go contaminate very fast, so regular cleaning is mandatory.
- If the membrane cleaning is not proper in time, unable to get good flux.

### 1.7.2.2 Cross-flow filter operation

- Feed flow along or equivalent to the membrane surface.
- Due to the continuous feed flow, the concentration polarization effect quite less and can able get good permeability results.
- Higher operational energy required for this operation.

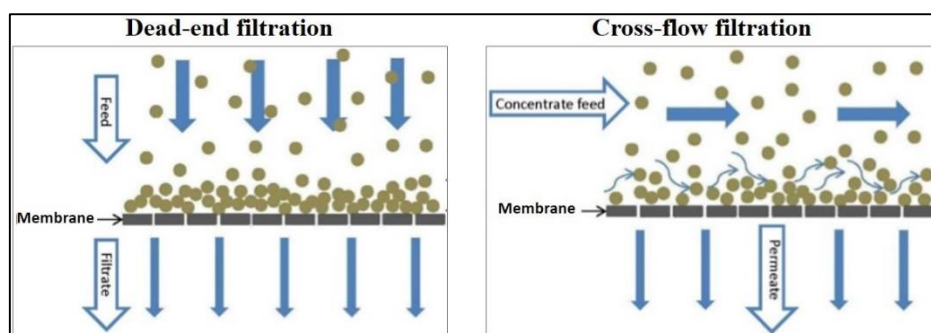


**Figure 1.19** Graphical representation of Dead-end and Cross-flow filter methods (POREX Filtration group)

## 1.8 MEMBRANE TECHNOLOGY APPLICATIONS

Membranes have wide and various applications. Today the usage of membrane technology in various industrial processes such as food and beverage, mining industries, paint, textile, dairy processing units, pharma industries, etc., increased towards removal of impurities from polluted water, to produce clean water. Pressure-driven membrane processes are selectively using in membrane technology for various separation applications. They listed below,

- RO membranes successfully applied since the 1970's for brackish water treatments, seawater desalination process. RO membranes are using in food processing units, textile, paint, pharma, paper, and pulp industries to decrease the waste generation and in wastewater treatments.
- NF membrane functions are comparable with RO membranes, these membranes can target several separations such as separate multivalent ions from aqueous solutions, color removal, pesticide deletion, in medicine to extract the amino acids and lipids from blood, etc.
- UF membranes are used in various applications such as enzymes removal from cow milk, in food industries for isolation process, removal of suspended solids, macromolecules and turbidity from industrial wastewater, and in dialysis blood purification treatments (Bowry *et al.* 2011).
- MF membranes are used to exclude the suspended particles in the range of  $> 0.01 \mu\text{m}$  from wastewater. MF membranes most widely using in pharmaceutical companies to prepare the sterile water and using in chemical, food and beverage industries for various applications.
- In electrodialysis process semi-permeable membranes can apply to separate either positive or negative ions under the influence of electricity.
- In the food and beverage industries accomplished membrane processes to treat the bottled water, it means for the removal of constituents, microorganisms, bacteria, fine-particles, and ingredients from bottled water.
- In dairy industries membranes are embraced from past few years, for the separation of casein from whey products, removal of bacteria, spores and suspended solids from milk products.

- In an industry level, it can able to find a lot of separation applications using membrane technology. Few of them are,
- Separation of enzymes, proteins, sugars and natural products.
  - Biomass removal using MF and UF membranes.
  - Organic solvents extractions using NF membranes.
  - Various types of metals removal from mining wastewater.
  - Separation of various gases such as nitrogen, hydrogen sulfate, carbon dioxide, natural gas liquids (NGL) and recovery of hydrocarbons, petrochemical wastes from oil and petroleum industries.

Considering membrane technology as a “*GREEN TECHNOLOGY*”, due to the non-involvement of chemicals in separation processes.

## **1.9 LITERATURE SURVEY**

A significant amount of research has been done in membrane science and technology for the treatment of water. Membranes will play the main role in the water purification treatments and improve the membrane separation enactment by adding the nanomaterials with membrane polymers. Nowadays sulfone-based polymers are most widely using in membrane technology for water purification applications due to their exceptional mechanical, chemical and thermal applications.

Fritzsche and research group fabricated hollow fiber membranes (HFM) from polyethersulfone and polyphenylsulfone from propionic acid: N-methyl pyrrolidone (PA/NMP) Lewis acid: base complex solvent system and from non-complexing N-methyl pyrrolidone/ formamide (FA/NMP) solvent/ nonsolvent mixture via phase inversion spinning technique, to investigate the helium/ nitrogen gas separation assets of HFMs. Characteristic analysis performed with differential scanning calorimetry (DSC) test to detect the glass transition temperatures of HFMs, oxygen plasma ablation test to determine the relative thicknesses of the effective separating layers of the two types of HFM, and morphological changes observed with SEM analysis. In conclusion, PA/NMP complexed HFMs exhibited better gas separation performance compare with FA/NMP non-complexed HFMs (Fritzsche *et al.* 1990).



High performance thermoplastic polymers polyethersulfone (PESF) and polyphenylsulfone (PPSF) were used to form the polymeric microcellular foams via two-stage batch foaming method. Water-displacement test conducted to measure the foam density and the foam size distributions, morphology properties were studied with SEM analysis. The experimental results disclosed the significant foam size enhancement was observed with the continuous increase of temperature as well as time (Sun *et al.* 2002).

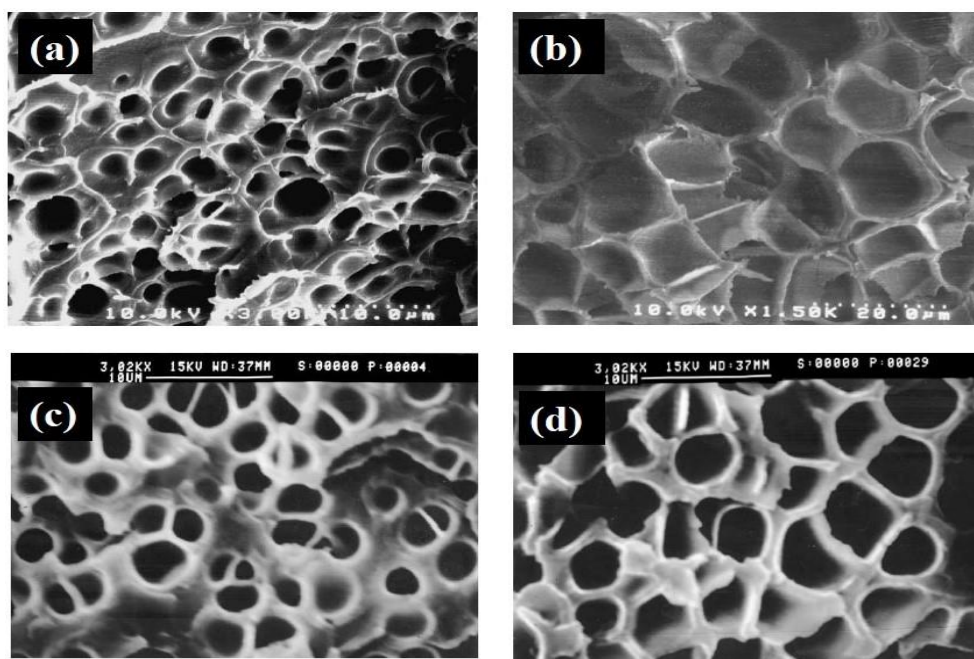


**Figure 1.20** SEM outcomes of PESF foams, at different foaming temperatures (a) at 140 °C, (b) 200 °C, at different foaming times (c) at 15 seconds (d) at 120 seconds (Sun *et al.* 2002)

Laboratory modified sulfonated polysulfone (S-PSF) and sulfonated polyphenylsulfone (S-PPSF) polymers were employed with sodium salts, obtained S-PSF(Na) and S-PPSF(Na) salts blended with polybenzimidazole (PBI), and fabricated S-PSF(Na)/PBI and S-PPSF(Na)/PBI films by casting method. The composite films were characterized by several techniques such as FTIR, TGA, DSC, TMA (thermal mechanical analysis). With TGA test observed enhanced thermal stability due to the effect of PBI. The newly formed microcellular foams morphology was observed with SEM instrument and these foams will show the better separation efficacy in membrane separations (Sun *et al.* 2004).



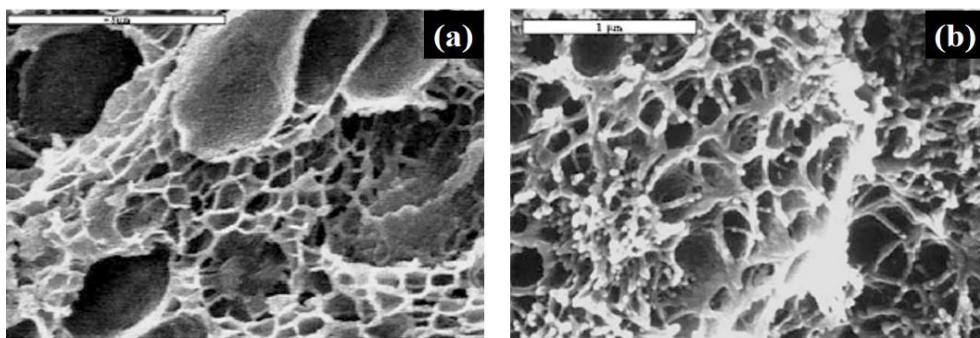


**Figure 1.21** SEM images of microcellular foams arranged from S-PSF (Na)/PBI, S-PPSF (Na)/ PBI (Sun *et al.* 2003)

Phosphonated polyphenylsulfone (P-PPSF) and sulfonated polyphenylsulfone (S-PPSF) polymeric blend membranes fabricated using N-methyl pyrrolidone (NMP) as a solvent. After the blending of phosphorous and sulfone to the PPSF, membranes assessed with  $^1\text{H-NMR}$ , TGA, water uptake process, etc. Water and ethanol permeability performance of membranes assessed, results found with S-PPSF exhibited good analysis results compare with P-PPSF (Parcero *et al.* 2006).

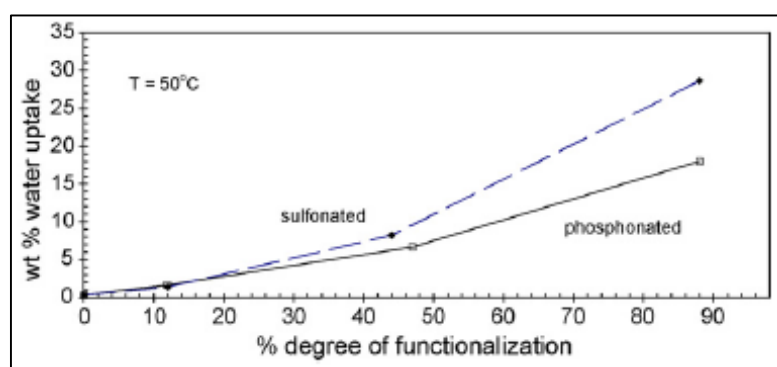


**Figure 1.22** Water uptake comparison between phosphonated and sulfonated membranes (Parcero *et al.* 2006)

Novel poly (bisphenol-A-co-4-nitro phthalic anhydride-co-1,3-phenylenediamine) (PBNPI) and polyphenylsulfone (PPSU) polymeric blend flat-sheet membranes fabricated by different wt. % via solution costing method, to examine the  $\text{H}_2$ ,  $\text{CO}_2$  and  $\text{CH}_4$  gas permeability ability of membranes. In conclusions, the membranes exhibited effective results with increasing the PPSU concentration in the polymer matrix, the gas permeability property decreased continuously as well as the gas separation ability was increased (Weng *et al.* 2008).

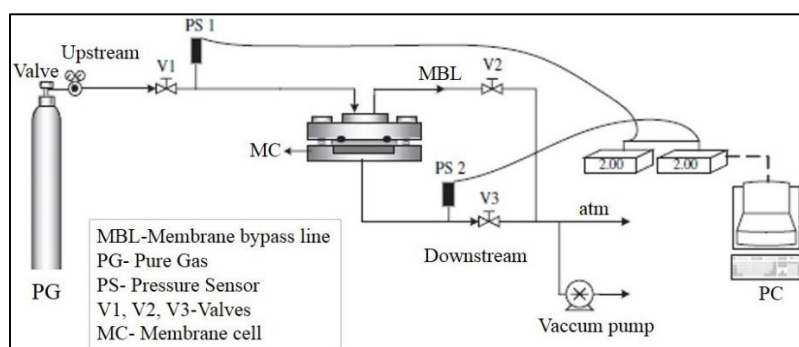


**Figure 1.23** Laboratory setup - Apparatus of gas permeation (Weng *et al.* 2008)

New method accommodated to fabricate the sulphonated polyphenylsulfone (SPPSU) and sulphonated polyethersulfone (SPES) blend polymeric membranes via annealing method using dimethylsulfoxide (DMSO) as a solvent. The fabricated cross-linked membranes characterized by FTIR, TGA, AFM, and water uptake measurements. The objectives of their work were to study the hydration and mechanical behavior, thermal stability, surface topography, surface wettability nature and ion exchange capacity (IEC) of membranes. In conclusions, the promising results were observed with all membranes (M.L. Di Vona *et al.* 2010).

Polyphenylsulfone (PPSU)/ Polyetherimide (PEI) blended mixed matrix flat-sheet membranes with different wt. % were fabricated via phase inversion process, to study the humic acid rejection efficacy from aqueous solution. Due to the effects of PVP and polyethylene glycol (PEG), the continuous pore size enhancement was observed with SEM cross-sectional studies. The permeability, fouling, and humic acid rejection efficacy properties were continuously improved from E0 to E40 type membranes (Hwang *et al.* 2011).

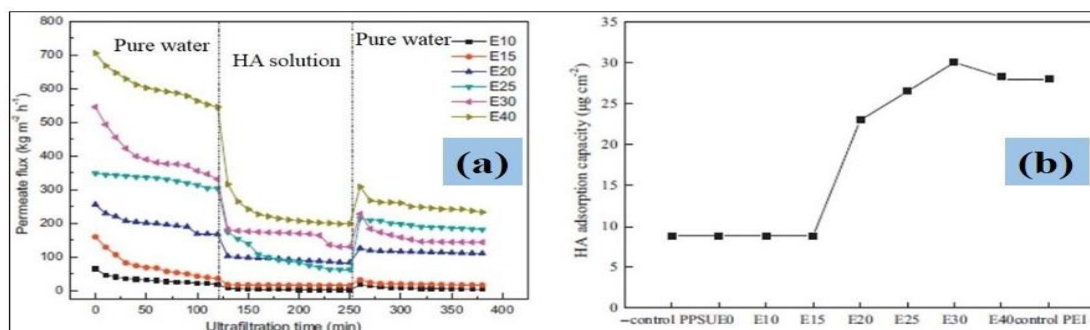


**Figure 1.24** (a) Time-dependent flux of the PPSU/PEI blend membranes, (b) HA rejection % of membranes (Hwang *et al.* 2011)

Sulfonated polyphenylsulfone (SPPSU) ultrafiltration membranes with different wt. % were prepared by direct copolymerization method via phase separation process, to study the BSA protein fouling and rejection ability. Membranes characterized by various techniques such as DSC, TGA, SEM, contact angle, etc. Dead-end filtration unit employed to study the permeability properties of membranes. In conclusion, the continuous enhancement was observed with permeability as well as with BSA rejection (Liu *et al.* 2012).

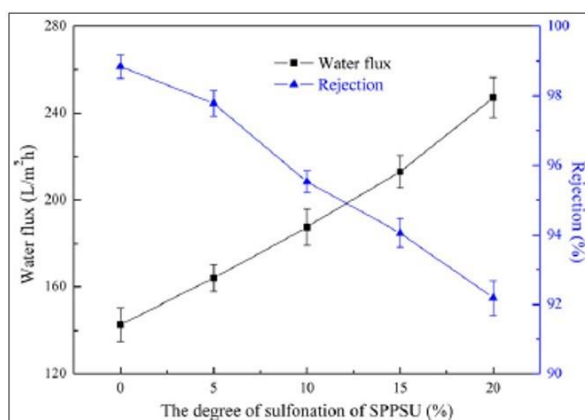


**Figure 1.25** Water fluxes and BSA rejections of the SPPSU membranes (Liu *et al.* 2012)

Titanium dioxide nanoparticles (TiO<sub>2</sub>-NPs) incorporated polyphenylsulfone (PPSU) nanocomposite membranes were fabricated via a solution casting process, to study the biocompatible assets of membranes. Two types of bacteria such as *Escherichia coli* (Gram-negative) and *Staphylococcus aureus* (Gram-positive) bacteria with and without UV irradiation selected, to investigate bactericidal effects against the microorganism from a clinical viewpoint. The final results found with continuous enhancement of antibacterial activity under UV irradiation from the plane membrane to higher additive (5 wt. %) membranes, due to the effect of additive TiO<sub>2</sub>-NPs (Diez-Pascual *et al.* 2014).

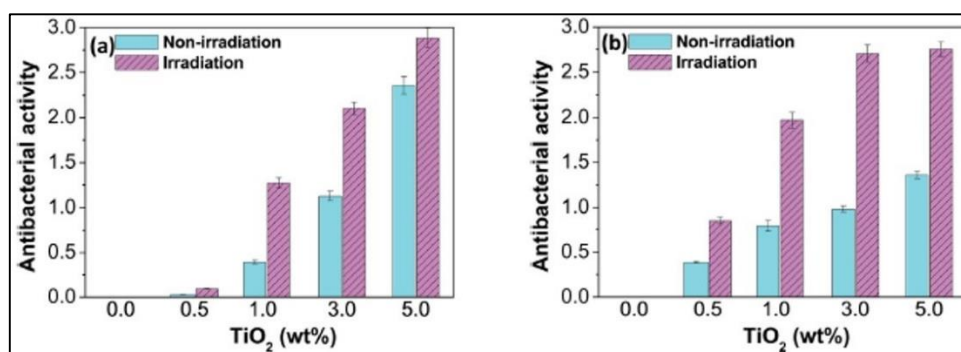


**Figure 1.26** Antibacterial activity of PPSU/TiO<sub>2</sub> nanocomposites against *E. coli* (a), and *S. aureus* (b) (Diez-Pascual *et al.* 2014)

Novel polyphenylsulfone (PPSU) nanofibrous membranes fabricated by electrospinning method with the addition of different wt. % of polyethylene glycol 400 (PEG 400) (0, 2, 5, and 10 wt. %), to study the BSA protein fouling behavior of membranes. In conclusion, the continuous enhancement was observed with water flux as well as with BSA fouling from plane membrane to higher PEG additive (10 wt %) membrane (Kiani *et al.* 2015).

Asymmetric polyphenylsulfone (PPSU) based flat-sheet UF membranes fabricated using different wt. % of pore-forming agents Polyvinylpyrrolidone (PVP) and polyethylene glycol (PEG) via non-solvent induced phase separation (NIPS) process, to study the antifouling behavior of membranes. Membrane characterizations assessed with SEM, contact angle and porosity measurements. Cross-flow filter was employed to revise the water permeability and BSA rejection ability of membranes. The PVP added membranes displayed better results compare with PEG additive membranes towards permeability as well as BSA rejection (Liu *et al.* 2016).

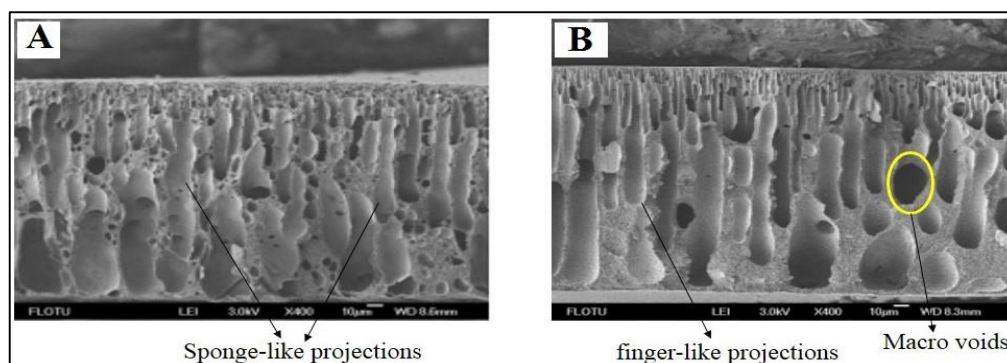


**Figure 1.27** SEM results of PPSU membranes with dissimilar pore forming additives PVP (A) PEG (B) (Liu *et al.* 2016).

Asymmetric polyphenylsulfone (PPSU) based flat-sheet membranes fabricated with the addition of different wt. % of graphene oxide (GO) (0, 0.2, 0.5 and 1.0 wt. %) nanocomposites via phase inversion process, to study the selected proteins BSA and Pepsin rejection efficacy of membranes. Membranes characterized by several techniques such as SEM, contact angle, TGA, AFM, tensile strength and porosity analysis. The membrane with 0.5 wt. % of GO exhibited enhanced permeability and good protein rejection results (Shukla *et al.* 2017).

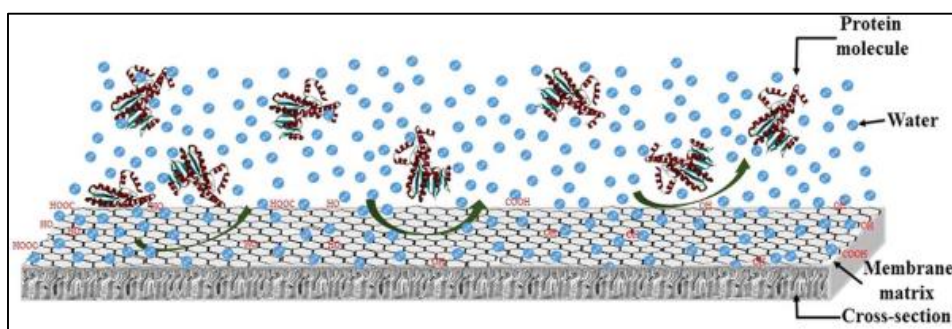


**Figure 1.28** Schematic illustration of the nanocomposite membrane surface and protein molecules interactions (Shukla *et al.* 2017)

From the above literature review reports, we can conclude that the polyphenylsulfone polymer is the good membrane material, and not that much work results are reported till. There is a large scope to fabricate different types of PPSU membranes by the addition of different organic or inorganic nanoparticles to the PPSU polymer for the removal of heavy metals from contaminated water, industrial dye, protein rejection, oil-water separation, and some other water purification applications. Keeping all these factors in mind we propose our research work.

## 1.10 SCOPE OF THE WORK

From the literature survey results, it is obvious that the sulfone-based polymers, like PSF, PPSU and PES has been extensively used as membrane material due to their outstanding mechanical, chemical and thermal applications. In present research choose, PPSU polymer choose as a principle membrane material. However, hydrophobic nature is one of the major drawbacks of this PPSU polymer. Keeping in view, research is in progress to overcome this problem by added various appropriate inorganic nanoparticles and pore-forming agents to make the perfect membrane material for water

purification applications. There is a possibility to increase the PPSU membrane properties in terms of hydrophilicity, porosity, permeation, antifouling, rejection properties by the addition of various nanomaterials as an additive to PPSU polymeric membranes in the near future.

### **1.11 OBJECTIVES**

1. To prepare neat and inorganic nano additive incorporated PPSU based ultrafiltration flat-sheet and hollow fiber membranes.
2. Characterization of the in-house prepared membranes by FESEM, SEM-EDS, AFM, contact angle, water uptake, porosity, and molecular weight cut-off study.
3. To study the in-house prepared membranes in terms of surface roughness, membrane morphology, pure water permeability, and antifouling ability.
4. Application study of in-house prepared membranes for heavy metal, industrial dye, proteins & various oil-water emulsions separation.

## **CHAPTER 2**

# **PREPARATION AND CHARACTERIZATION OF PPSU MEMBRANES WITH BiOCI NANOWAFERS LOADED ON ACTIVATED CHARCOAL FOR OIL IN WATER SEPARATION**





**Abstract**

*The laboratory prepared bismuth oxychloride nano-wafers were loaded on activated charcoal (BiOCl-AC) and used as a novel adsorbing agent for the separation of oil from water. The polyphenylsulfone (PPSU)/BiOCl-AC/polyvinylpyrrolidone (PVP) mixed matrix membranes synthesized by the phase separation process. Membrane morphology evaluated with scanning electron microscopy (SEM). Permeability nature was assessed with pure water flux (PWF) and antifouling performance with Bovine serum albumin (BSA) flux. Cross-flow filter unit was engaged to assess the oil removal efficacy of diesel fuel and crude oil. Membrane M-3 exhibited rejection results, 80 % for diesel fuel and 90.74 % for crude oil, respectively.*

**2.1 INTRODUCTION**

Especially in the oil field, an annually large volume of oily wastewater is producing from the petrochemical, paint, automobile, pharmaceutical, as well as food industries by different kinds of processes (Chakrabarty *et al.* 2008, Yusoff *et al.* 2011, Mueller *et al.* 1997 and Lin *et al.* 1998). Usually, there are three categories of oils form, they are industrial oily wastewater, stable oil in water emulsion, and unstable oil in water emulsion. The oil extraction, storage, and transportation are the major three stages where the possibility of oil pollution can occur. It can be seen as the release of contaminants or pollutants associated with the extraction of petroleum oil, diesel, and crude oil into the environment. The whole environment, especially the wetland ecosystem and thereby the aquatic organisms, have been affected badly by the development of oil field industries, due to the effects of oil pollution (Omorieg *et al.* 1997). Diesel fuel is one of the major reasons for the ever-increasing environmental pollution through global emissions from vehicles, leading to many serious health issues such as cancer, cardiovascular and respiratory problems. Due to the serious environmental pollution and global climate change issues, many diesel fleet emission control programs were started worldwide (Lloyd *et al.* 2001). The bio-accumulation of the environmentally present pollutants like crude oil, petroleum products, aromatic hydrocarbons, etc., in the food chains, can disturb the biochemical or physiological functions of many organisms leading to severe problems of carcinogenesis and

mutations. Biomarkers or biological endpoint parameters are used to measure the consequences of oil pollutants. Hegde *et al.* (2016) investigated the effect of emulsified clean operating fuel through the addition of surfactant and water into diesel fuel. Since the emulsion droplets are in micron size, it takes longer time for gravity separation. To address these, new advanced techniques such as biological methods (Ratlege *et al.* 1992), membrane-based separation procedures like reverse osmosis (Mohammadi *et al.* 2003), pervaporation (Deng *et al.* 1991), microfiltration (Ohya *et al.* 1998), ultrafiltration (Bodzek *et al.* 1992), and distillation (Gryta *et al.* 1999) have been tried. Finally, ultrafiltration was concluded as the finest method for the water distillation process.

Polyethersulfone (PES) and polyamideimide (PAI) based various temperature based microporous membranes were fabricated by the addition of different inorganic additives PVP, supportive catalysts alumina, and palladium acetate, palladium chloride via machine casting method. The main object of current research to calculate the fabricated catalytic membranes hydrogenation activity of sunflower oil. Temperature alterations can impact the membrane pore structure, performance, and the reaction development was assessed with gas chromatography. Alumina contained membranes exposed to low activity due to the catalyst lower concentrations. In the obtained results, the porous membranes revealed good permeability performance with water and oil flux, and the hydrogenation activity was also decreased with the continuous enhancement of time (Fritsch *et al.* 2006).

Bismuth oxychloride (BiOCl) nanocrystals synthesized via the simplest hydrolysis method, and the BiOCl nanocrystals employed with various characterization techniques such as TEM, SEM, BET surface area analysis, XRD etc. The aim of the current research was to study the photocatalytic degradation of toxic dye Neutral red (NR) under UV-visible light irradiation in the presence of BiOCl catalyst. High-performance liquid chromatography–mass spectrometry (HPLC–MS) was employed to assess the degradation performance of NR dye. Finally, observed 100 % chemical oxygen demand (COD) and complete degradation of NR into CO<sub>2</sub> and inorganic ions (Sarwan *et al.* 2012).

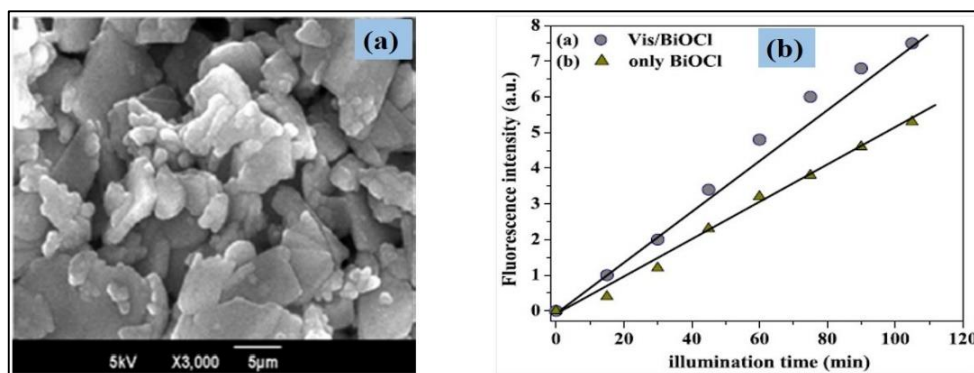


**Figure 2.1** (a) SEM image of BiOCl crystals and (b) Fluorescence effects: BiOCl with visible light and BiOCl without light (Sarwan *et al.* 2012)

The Polyvinylidenedifluoride (PVDF)/ modified multiwalled carbon nanotubes (MWCNTs) with different wt. % mixed matrix nanocomposite membranes were prepared by the phase separation process, for the filtration of petroleum refinery wastewater pollutants under photo-catalytic conditions. Titanium-dioxide ( $\text{TiO}_2$ ) nanoparticles were used as a photocatalyst in a photocatalytic reactor. 1 wt. % of oxidized MWCNTs added PVDF membranes were revealed best results towards deletion of oil wastes from wastewater (Moslehyani *et al.* 2015).

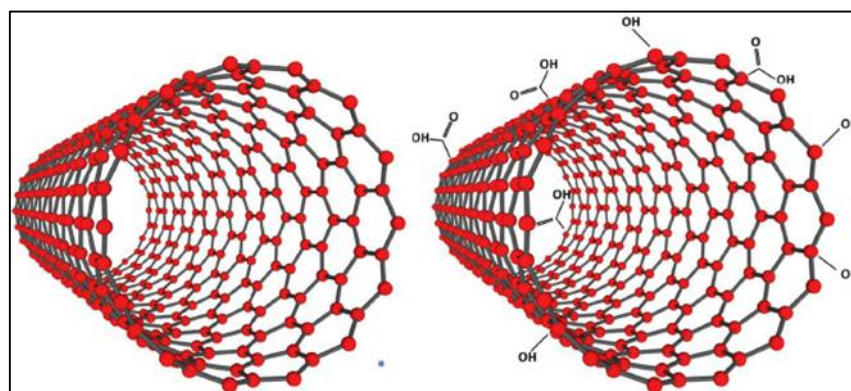


**Figure 2.2** Oxidization of MWCNTs surface with an acid mixture (Moslehyani *et al.* 2015)

Prince and group members fabricated Polyethersulfone (PES) and graphene oxide grafted polyacrylonitrile co maleimide (G-PANCMi) hollow fiber membranes, to assess the for oil-water emulsion separation efficacy of membranes. Primarily, graphene was functionalized with amine and carboxyl groups to increase the wettability

nature, after grafted with PANCMI and fabricated HF membranes by dry-wet spinning process. In results, the G-PANCMI membranes exhibited the best results as compared with PES membranes towards oil-water separation (Prince *et al.* 2016).

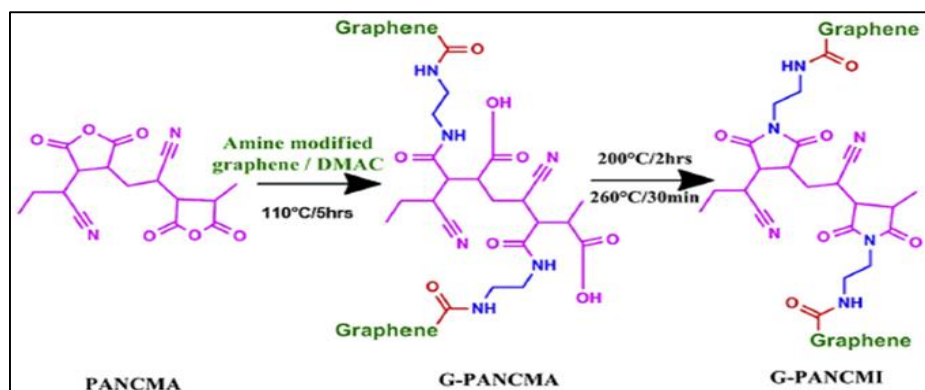


**Figure 2.3** Synthesis of G-PANCMII (Prince *et al.* 2016)

Polysulfone (PSf)/ Pebax/ functionalized multiwalled carbon nanotubes (F-MWCNTs) mixed matrix NF membranes prepared to check the oil/water separation efficacy. The different wt. % about 0.5, 1 and 2 wt. % of additive F-MWCNTs incorporated in the polymer matrix, and various techniques used in characterization such as SEM, FTIR, contact angle, tensile strength and TGA, etc., 2 wt. % membrane showed enhanced permeability results as well as with oil/water separation test (Saadati *et al.* 2016).

Nanoscale magnetic  $\text{Fe}_3\text{O}_4$  nanoparticles (MNPs) synthesized by precipitation method and was coated on carbon fabric (CF) membranes by Zhang *et al.* (2016). They have studied the adsorption efficacy towards contaminants and oils from aqueous media. Adsorption experiment was accompanied with methylene blue (MB) dye,  $\text{Cu}^{2+}$  metal ion solution and with olive oil mixed wastewater. In results, the MNPs-coated CF membranes displayed better results towards removal of contaminants from wastewater (Zhang *et al.* 2016).

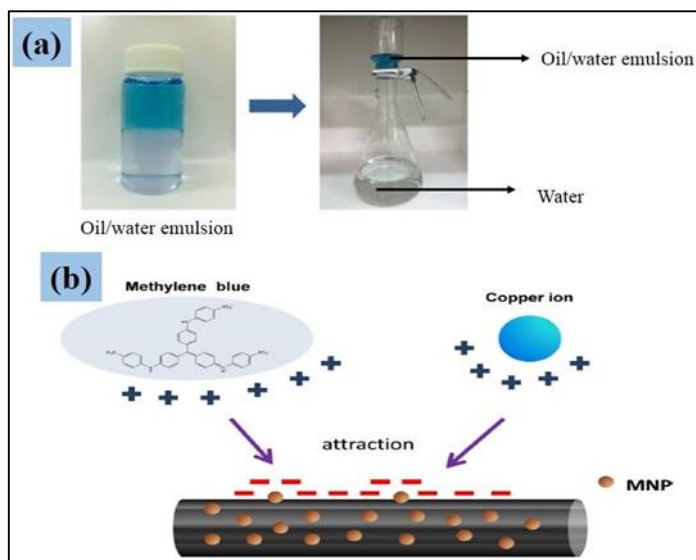


**Figure 2.4** (a) Lab-scale filtration setup, (b) Schematic illustrating the adsorption affinity between the MNPs and the adsorbents (Zhang *et al.* 2016)

Polyvinylidene fluoride (PVDF)/ poly (stearyl methacrylate) (PSMA) mixed matrix thermal responsive hydrophobic flat-sheet membranes fabricated via non-solvent induced phase inversion technique, to investigate the oil/water removal efficiency of membranes. Surfactant-free and Surfactant-stabilized water/oil emulsions were used to examine the separation efficacy of membranes. In conclusion with M-9 type membrane, the flux reached  $230 \text{ kg}\cdot\text{m}^{-2} \text{ h}^{-1}$  and the oil rejection was observed above 99 % (Yuan *et al.* 2017).

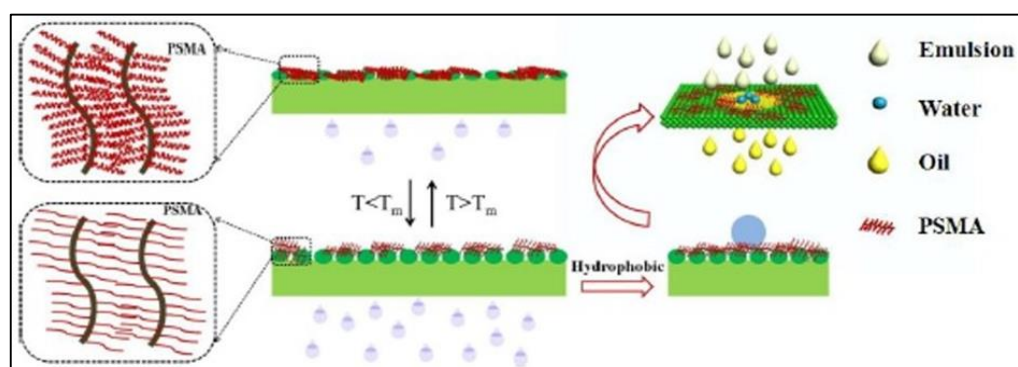


**Figure 2.5** Thermo responsive features of the membrane and oil/water separation phenomena (Yuan *et al.* 2017)

Polyethersulfone (PES)/ hydrophilic manganese oxide nanoparticles ( $\text{MnO}_2$  NPs) blended flat-sheet membranes fabricated via phase inversion method, to investigate the oil-water separation ability of membranes. Oil/water separation test was conducted with three different concentrated crude oil samples (5000, 10000 and 15000 ppm), and the results analyzed with UV-visible spectrometer. Sodium dodecyl sulfate (SDS) was added as a surfactant to stabilize the oil/water samples. In conclusion, the membrane with higher additive wt. % of  $\text{MnO}_2$  NPs (MMM-2 membrane) exhibited good results with oil separation test, about 82 % (Doraisammy *et al.* 2018).

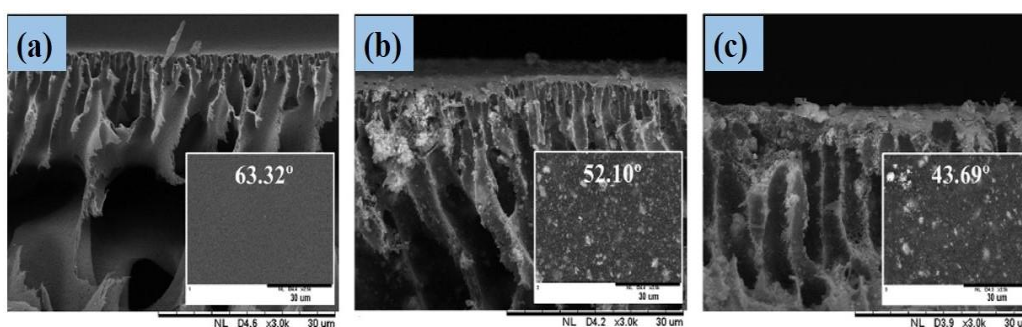


**Figure 2.6** SEM images of membranes (inset) contact angles of (a) Plane, (b) MMM-1 and (c) MMM-3 membranes (Doraisammy *et al.* 2018)

Charcoal was synthesized from saw dust chemically treated with various activating agents like phosphoric acid, zinc chloride, and ferrous sulfate heptahydrate, etc. The obtained charcoal was characterized with few techniques such as SEM, BET analyzer, FTIR, SEM-EDS, etc. The objective behind the work was to determine the oil adsorption efficacy of charcoal from crude oil/water emulsion. The main purpose of chemical treatment is to enhance the surface area on charcoal. In conclusion, charcoal treated with phosphoric acid was exhibited good results, about 98 % compared with other chemical agents (Rajak *et al.* 2018).



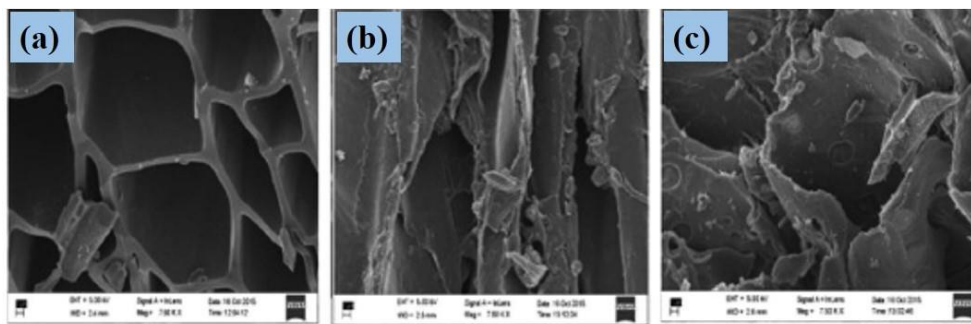


**Figure 2.7** SEM micrographs of charcoal blended with (a)  $\text{H}_3\text{PO}_4$ , (b)  $\text{ZnCl}_2$ , and (c)  $\text{FeSO}_4 \cdot 7\text{H}_2\text{O}$  (Rajak *et al.* 2018)

From the above literature survey, it's hard to find the oil/water separation reports using membrane technology. The fabrication of cost-effective PPSU/BiOCl-AC/PVP additive contained membranes for the oil/water separation were not yet reported. In the current research, fabricated various PPSU based flat-sheet membranes with the addition of different wt. % of BiOCl-AC additive. The main aim was to investigate the crude oil and diesel fuel separation efficiency of prepared membranes. The membranes were characterized with various techniques, and permeability studies performed with water flux, antifouling ability check with BSA flux. The cross-flow filter unit was employed to investigate the oil/water separation ability of membranes.

## 2.2 EXPERIMENTAL

### 2.2.1 Materials

PPSU (Radel R-5000) ( $\text{MW} \sim 50,000 \text{ g/mol}^{-1}$ ) was provided by Solvay Advanced Polymer, Belgium. Activated charcoal and N-methyl-2-pyrrolidone (NMP) were obtained from Merck India, Ltd. Bovine Serum Albumin (BSA) ( $\text{MW} \sim 69 \text{ kDa}$ ) was purchased from CDH Chemicals, India. Bismuth trichloride ( $\text{BiCl}_3$ ) procured from Spectrochem, Mumbai, India. Methyl alcohol (MeOH) and Ethyl alcohol (EtOH) were acquired from S D fine-chem Ltd. Hydrochloric acid (HCl), and Sodium hydroxide (NaOH) bought from Loba Chemie Pvt. Ltd. Ammonium dodecyl sulfate (ADS) and Polyvinylpyrrolidone (PVP) were obtained from Sigma-Aldrich Co., Bangalore, India.

## 2.2.2 Nanoparticles preparation process

### 2.2.2.1 Synthesis of BiOCl nano wafers

Synthesis procedure for BiOCl nano wafers was followed as given in the literature (Nekouei *et al.* 2017). Simple and fast precipitation scheme was engaged in the synthesis process. 0.5 g of BiCl<sub>3</sub> was added to 47 ml distilled water and added 2 ml of MeOH in HCl, for better solubility of BiCl<sub>3</sub>, continued reaction at 40 °C for 1 h. Further added 1 ml of 2 % ADS and the temperature was raised up to 70 °C. Continued the reaction up to 3 h, for the better interaction of BiOCl with ADS. Then, 8-10 drops of NaOH (1M) was added to the mixture. Afterward, washing was performed to the acquired product with water and ethanol solutions a few more times. The gained product was preserved in a hot air oven at 70 °C for 7 h. After which, performed calcination at 350 °C to the above attained BiOCl nano wafers.

### 2.2.2.2 BiOCl-NWs-loaded on activated charcoal

Above obtained BiOCl nano wafers were mixed with 10 g of activated charcoal in a beaker and sonicated up to 1 h. Afterward, the beaker was kept overnight without any disturbance as such. Next day, the settled mixture was washed several times with deionized water, and the obtained BiOCl-AC was saved in the sample container for further studies.

## 2.2.3 Preparation of BiOCl-AC incorporated PPSU membranes

PPSU/BiOCl-AC mixed UF membranes were fabricated via phase inversion process (Hebbar *et al.* 2016). The different wt. % of BiOCl-AC was added to the NMP solvent and performed sonication for 30 min for the proper dispersion of BiOCl nano wafers in NMP. Further, added 16 g PPSU, 4 g of PVP to the above solution and preserved for 50 °C, stirring was continued up to 24 h to get a clear dope solution. Again performed degasification to the above-gained solution to remove the air bubbles from dope solution. After some time, the dope solution was poured on a clean glass plate and cast using glass rod, and immediately placed in water bath for phase inversion (Kumar *et al.* 2013).



**Table 2.1** Membrane compositions

Membranes	PPSU (g)	NMP (g)	PVP (g)	BiOCl-AC (wt. %)	BiOCl-AC (g)
M-0	16	80	4	0	0
M-1	16	79.92	4	0.5	0.08
M-2	16	79.84	4	1	0.16
M-3	16	79.68	4	2	0.32

## 2.2.4 CHARACTERIZATION

### 2.2.4.1 Characterization of BiOCl nano wafers by FTIR

The laboratory synthesized BiOCl nano wafers were characterized by Fourier transform infrared spectrometer (FTIR) apparatus. KBr (potassium bromide) mixed with BiOCl nano wafers (3:1 ratio) and the pellets were analyzed with FTIR, and conserved the range at 500–4000  $\text{cm}^{-1}$  to record the spectrum.

### 2.2.4.2 SEM and EDS of BiOCl nano wafers and membranes

To inspect the structural and surface morphological properties of BiOCl nano wafers, used Zeiss Sigma Field Emission scanning electron microscopy (FESEM) instrument (Model: EVO MA18), and the presence of incorporated BiOCl nano wafers in membrane matrix was documented through SEM Energy Dispersive Spectroscopy (EDS) analysis. The membrane samples were dipped in liq.  $\text{N}_2$  for 4 min and the freezing parts of membranes were attentively cracked after the fractured samples were sputtered with gold, and then detected the cross-sectional morphologies of membranes by SEM instrument at high magnifications (Shenvi *et al.* 2015).

### 2.2.4.3 Water Contact Angle (WCA) of membranes

The surface wettability, WCA of membranes was observed by FTA-200 Dynamic contact angle analyzer instrument by the sessile droplet technique (Liu *et al.* 2013). In experimental, small pieces of the dried membrane samples were hired on the sample holder, after which the water droplets were hired on membrane sample with the help of microsyringe and then determined the WCA values. With each membrane sample, the WCA experiment conducted four times repeatedly on different sites and detailed the average values.

#### 2.2.4.4 Pure water flux (PWF)

Pure water flux (PWF) and antifouling tests were performed to assess the membrane permeability properties using a dead-end filter system, with an active membrane area of 5 cm<sup>2</sup>. After fixing the membrane in membrane holder, initially maintained 0.3 MPa TMP and preserved for compaction up to 30 min, afterward TMP was decreased to 0.2 MPa. Time-dependent PWF study was implemented and maintained 1 min time interim for each permeate collection, and the study was sustained up to 20 min. All over the study used deionized water and Eq. 2.1 employed to compute the  $J_w$  (L/m<sup>2</sup> h) result.

$$J_w = \frac{Q}{\Delta t \times A} \quad \text{Eq. (2.1)}$$

Where, ' $J_w$ ' pure water flux, ' $Q$ ' amount of water collected (L) in time ' $\Delta t$ ' (h), ' $A$ ' membrane area (m<sup>2</sup>).

#### 2.2.4.5 Antifouling study of membranes

After PWF study, BSA protein solution (800 mg/L) was used to examine the membrane antifouling conductance. BSA solution was reserved in feed tank and BSA flux operated at 0.2 MPa TMP and 1 min time interval was maintained and noted ' $J_p$ ' (L/m<sup>2</sup> h) values for each membrane and study was sustained up to 20 min. Afterward, the membranes were perfectly cleaned with distilled water to recover the water permeability. Again performed the PWF study under the same conditions as mentioned above and recorded the ' $J_{w2}$ ' (L/m<sup>2</sup> h) values. The fouling feature of membranes, flux recovery ratio (FRR) was measured by Eq. 2.2.

$$\text{FRR (\%)} = \frac{J_{w2}}{J_{w1}} \times 100 \quad \text{Eq. (2.2)}$$

The fouling impact on the membranes was further analyzed with total fouling ratio ( $R_t$ ), reversible fouling ratio ( $R_r$ ) and irreversible fouling ratio ( $R_{ir}$ ) by the following equations (Shao *et al.* 2014).

$$R_r (\%) = \frac{J_{w2} - J_p}{J_{w1}} \times 100 \quad \text{Eq. (2.3)}$$

$$R_{ir}(\%) = \frac{J_{w1} - J_{w2}}{J_{w1}} \times 100 \quad \text{Eq. (2.4)}$$

$$R_t(\%) = \frac{1 - J_p}{J_{w1}} \times 100 \quad \text{Eq. (2.5)}$$

#### 2.2.4.6 Water uptake

Water uptake aptitude is one of the major parameters to find out the membrane swelling volume. In this, the membrane samples were cut into 1 cm<sup>2</sup> size pieces and then dipped in water up to 24 h. Next day, the membrane samples wiped with tissue paper properly and noted the wet weight of membranes. Afterward, the samples placed in an oven at 50 °C up to 6 h for dry. Further, again noted the dry weight of membrane, using weighing balance (Model: SHIMADZU AU Y 220). Eq. (2.6) was used to measure the swelling volume of membranes,

$$\% \text{ Water uptake} = \left( \frac{W_w - W_d}{W_w} \right) \times 100 \quad \text{Eq. (2.6)}$$

Where 'W<sub>w</sub>' and 'W<sub>d</sub>' are the wet and dry weight of the membrane.

#### 2.2.4.7 Membrane Porosity

The porosity of membranes was determined using the gravimetric process (Zhang *et al.* 2013). Eq. (2.7) was employed to calculate the porosity of the membranes,

$$\% \text{ Porosity} = \left( \frac{W_1 - W_2}{A \times l \times d_w} \right) \times 100 \quad \text{Eq. (2.7)}$$

Where 'W<sub>1</sub>' wet membrane weight, 'W<sub>2</sub>' dry membrane weight, 'A' area of membrane (m<sup>2</sup>), 'l' the membrane thickness (m), 'd<sub>w</sub>' density of water (0.998 g cm<sup>-3</sup>).

#### 2.2.4.8 Procedure for oily water separation

Crude oil collected from TCO Marine Limited Company, Singapore and diesel fuel from Singapore Shell International Eastern Trading Company (SIETCO). Cross-flow filter unit was employed to assess the oil rejection percentages of membranes (Figure 2.8). 100 ppm concentrated oil/water samples were equipped individually by mixing oil in water and the mixture was sonicated up to 12 h at 40 °C. No, any other surfactants were added to the oil samples for stabilization. The feed solution was

transferred into the feed reservoir and membranes were fixed in membrane modules. After fixing the membranes, the permeation test was started. Primarily, membranes were preserved for compaction at 6 bar TMP for 20 min. After which, the TMP decreased up to 4 bar and continued the separation test. The oil permeates concentrations were investigated by using a UV-spectroscopy (Model: HACH, DR/5000). The absorbance was recorded at a wavelength of 196 nm to diesel fuel and 262 nm to crude oil (Huotari *et al.* 1999). Eq. 2.8 was employed to measure the oil rejection percentage of membranes,

$$\% R = \left(1 - \frac{C_p}{C_f}\right) \times 100 \quad \text{Eq. (2.8)}$$

Where ' $C_p$ ' and ' $C_f$ ' the oil concentration in permeate and feed solutions.

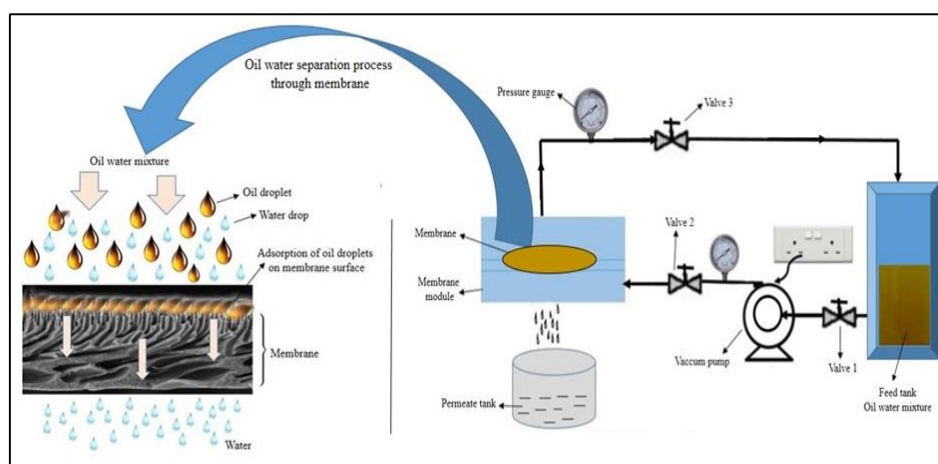


**Figure 2.8** Schematic illustration of oil/water separation over cross-flow filter unit

## 2.3 RESULTS AND DISCUSSIONS

### 2.3.1 FTIR result

The laboratory prepared BiOCl nano wafers further analyzed by FTIR spectroscopy to detect the functional groups, and the results were reported in Figure 2.9. The peak observed at  $527\text{ cm}^{-1}$  is ascribed to the characteristics Bi–O stretching vibration (Gao *et al.* 2012), and peak at  $1618\text{ cm}^{-1}$  is due to adsorbed atmospheric  $\text{CO}_2$  on the surface at the time of preparation or during the investigation. The additional peaks appearing in the spectrum at  $2922\text{ cm}^{-1}$ ,  $2852\text{ cm}^{-1}$  indicates C–H stretching

vibrations of ethanol, and the peak at  $3449\text{ cm}^{-1}$  is attributed due to the O–H group of an adsorbed water molecule.

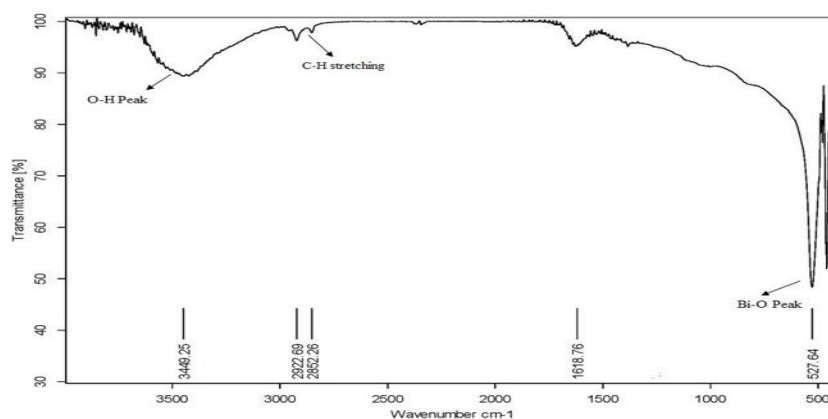


**Figure 2.9** FTIR analysis of BiOCl nano wafers

### 2.3.2 SEM results

Lab synthesized BiOCl nano wafers morphology was assessed with SEM at different magnifications (Figure 2.10). In results, observed the thickness range of BiOCl nano wafers was between 97 nm and 124 nm (Figure 2.10 (b)). The cross-sectional pore morphology of membranes was assessed by SEM. The cross-sectional images of membranes showing representative asymmetric structures with a thick top layer and bottom sub-layer have finger-like structures. With increasing the additive BiOCl-AC wt. % in membranes, the finger-like projections are enhancing progressively. Figure 2.11 reveals the cross-sectional micrographs of all membranes (A, B, C, D). The added hydrophilic PVP affects the pore morphology in membranes (Morihamma *et al.* 2014).

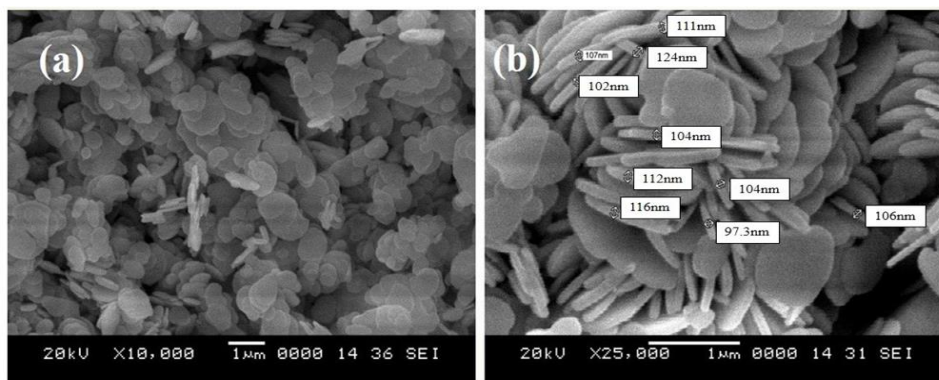


**Figure 2.10** SEM image (a), magnified SEM image (b) of BiOCl nano wafers

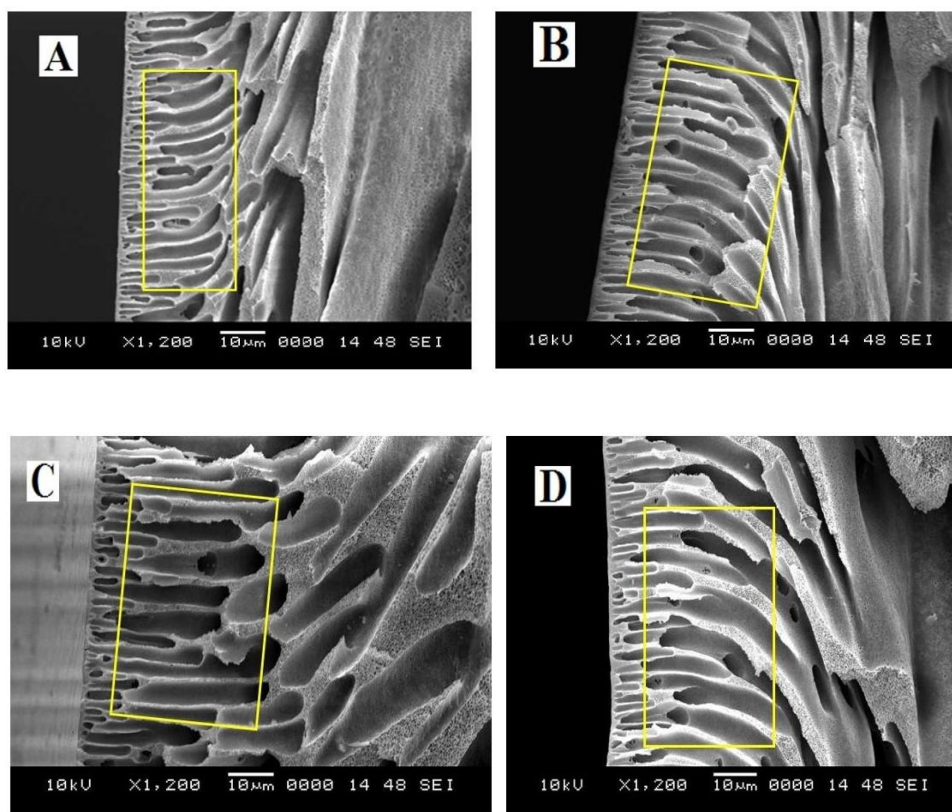


**Figure 2.11** SEM images of M-0 (A), M-1 (B), M-2 (C), M-3 (D) membranes

### 2.3.3 EDS analysis

The presence of Bi, Cl and other elements on the membrane surface was determined using EDS. Figure 2.12 discloses the EDS analysis of the M-2 membrane. From Figure 2.12 (b), it can able to observe O<sub>2</sub>, Na, and found a large amount of sulfur

elements. The added quantity of polymer PPSU is more, so in result found more sulfur elements. These results can conclude, the proper dispersion of BiOCl-AC NPs in the pay matrix.

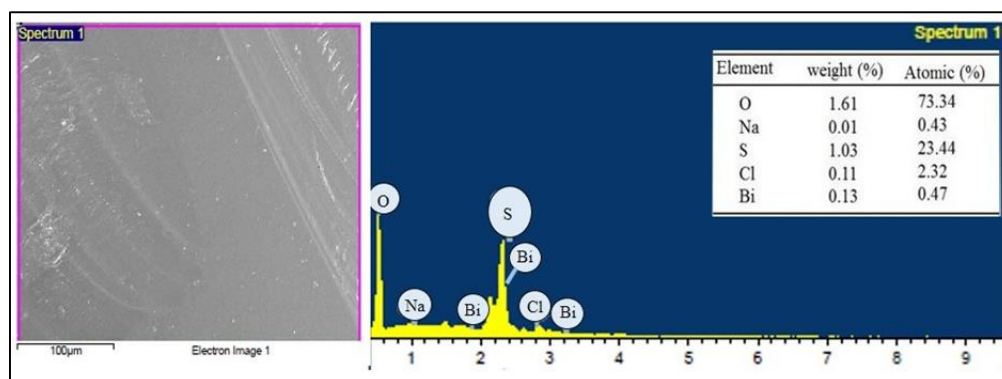


**Figure 2.12** (a) SEM surface picture of M-2 membrane surface, (b) EDS results of M-2 membrane

### 2.3.4 Contact angle (CA)

Surface wettability nature of the membrane was assessed using CA study. In general, the membrane hydrophilicity is higher while the contact angle values are smaller. Figure 2.13 discloses the information regarding CA analysis. M-0 membrane showed CA  $76.15^{\circ}$  due to the hydrophobic nature of the membrane. After the incorporation of BiOCl-AC additive into the PPSU polymer, the hydrophilic nature on the surface was increased continuously and reported in Table 2.3. With M-3 membrane the CA was decreased up to  $67.40^{\circ}$ . The reducing order of CA is: M-0 < M-1 < M-2 < M-3.

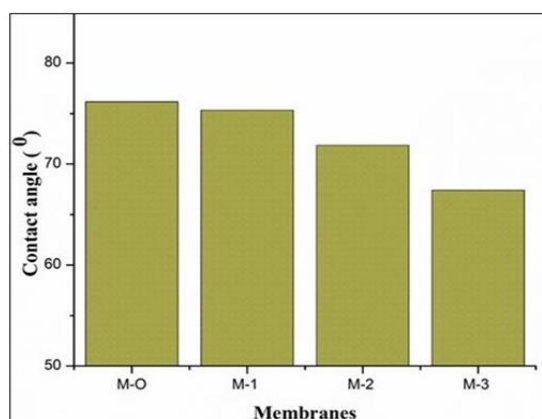


**Figure 2.13** Contact angle results of PPSU membranes



### 2.3.5 Pure water flux (PWF)

Figure 2.14 reveals the information regarding the PWF performance of membranes. From M-0 to M-3 membrane, the continuous enhancement in PWF was observed. The added additive BiOCl nano wafers can influence the pore structures and can affect the water permeability of membranes. So, in PWF result observed continuous enhancement, with increasing the BiOCl-AC wt. % in PPSU polymer. The water-soluble additive PVP also can influence the pore morphology of membranes, and these changes can be observable from Figure 2.11. Initially the PWF was  $165.94 \text{ L/m}^2 \text{ h}$  with M-0 membrane, afterwards, it reached  $465.35 \text{ L/m}^2 \text{ h}$  for M-3 membrane. In conclusion, M-3 membrane exhibited superior performance with PWF and observed water permeability four times greater than the pristine membrane.

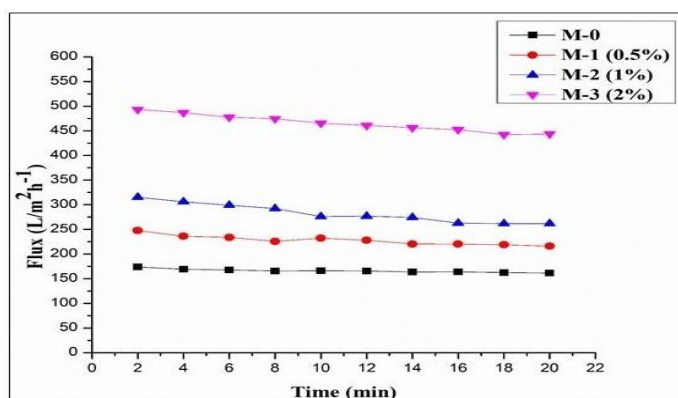


**Figure 2.14** Time-dependent pure water flux of membranes

### 2.3.6 Antifouling study

Primarily, the permeability ability of membranes observed with PWF, after that time bounded BSA flux was performed with all membranes to assess the antifouling nature of membranes. Figure 2.15 (a) reveals the information regarding antifouling behavior of all fabricated membranes. With BSA flux observed very less flux than PWF, due to the larger size effects of BSA molecules. While performing the BSA flux study, the BSA molecules can adsorb on the membrane surface because of the higher hydrophilic nature of membranes. Due to the pore blockage phenomena on the membrane surface, less flux was observed than PWF. Figure 2.15 (b) reveals the antifouling behavior of membranes. Table 2.2 displays the FRR of all membranes, and



the reversible fouling ( $R_r$ ), irreversible fouling ( $R_{ir}$ ) and total fouling ( $R_t$ ) outcomes of membranes.

**Table 2.2** Membrane permeability studies

Membrane code	Permeate flux ( $L/m^2 \cdot h$ )			Fouling performance (%)			
	$J_{w1}$	$J_p$	$J_{w2}$	FRR	$R_t$	$R_r$	$R_{ir}$
M-0	165.94	8.43	18.92	11.40	94.91	6.32	88.59
M-1	227.93	9.55	48.77	21.39	95.81	17.2	78.6
M-2	282.61	11.51	158.18	55.97	95.92	51.89	44.02
M-3	465.35	12.76	249.23	53.55	97.25	50.81	46.44

$J_{w1}$ -pure water flux;  $J_p$ - protein flux;  $J_{w2}$ -pure water flux (Membrane after cleaning);  $R_r$ -reversible fouling;  $R_{ir}$ -irreversible fouling; FRR-flux recovery ratio.

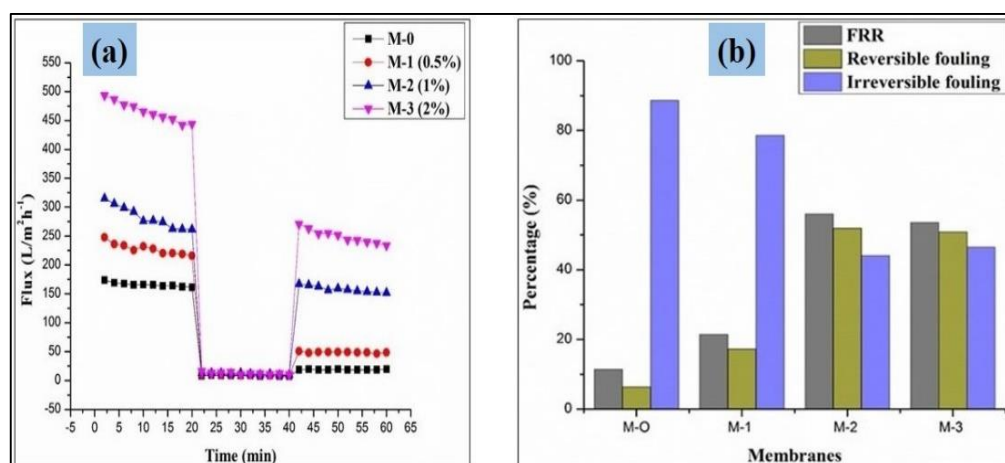


**Figure 2.15** (a) Flux V/s time for membranes at 0.2 MPa under three conditions: water flux; BSA protein flux; and water flux after carefully wash with distilled water, (b) FRR results of membranes

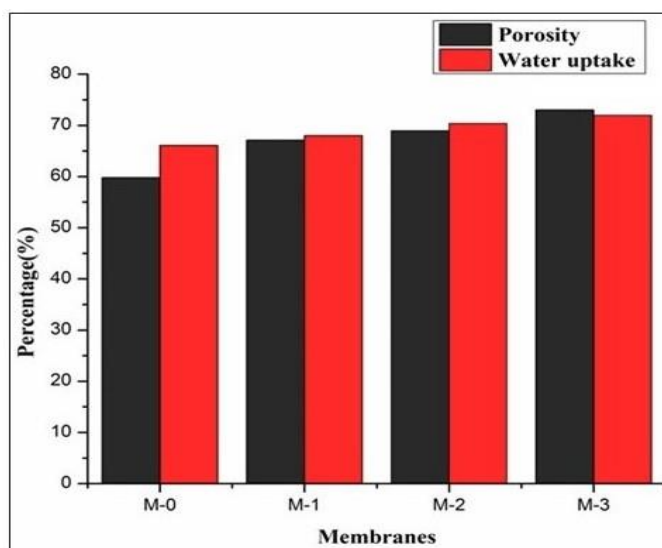
### 2.3.7 Porosity and water uptake

Figure 2.16 revealed the water uptake and porosity results of membranes. With increasing the BiOCl-AC wt. % in PPSU polymer, the porosity and water uptake behavior of membranes enhanced from M-0 to M-3 membrane continuously. This is because of the incorporated BiOCl nano wafers effect. These BiOCl nano wafers can

influence the pore sizes, so the water uptake nature of membranes improved. The enhanced porosity and water uptake results were reported in Table 2.3.

**Table 2.3** Membrane properties

Membranes	Membrane thickness ( $\mu\text{m}$ )	Water uptake (%)	Porosity (%)	Contact angle ( $^{\circ}$ )
M-0	180	66.04	59.77	76.15
M-1	156	67.97	67.09	75.32
M-2	149	70.34	68.91	71.83
M-3	138	71.94	72.99	67.40



**Figure 2.16** Porosity and water uptake results of membranes

### 2.3.8 Oil in water rejection study

The oil/water separation test was performed with the selected oil samples such as diesel fuel and crude oil by cross-flow filter unit (Figure 2.8). No other surfactants were added to stabilize the oil/water samples. The feed oil/water mixture was poured in feed tank and performed the rejection test with all membranes one by one. In results, with enhancing the additive BiOCI-AC wt. % in PPSU polymer, the improved oil rejection results were obtained with all membranes (M-0 to M-3). Among all, the M-3 membrane exhibited better results towards oil/water separation, above 80 % for diesel fuel and above 90 % for crude oil, respectively (Figure 2.17).

Normally activated charcoal is having with good adsorbing capability, and after the loading of BiOCl nano wafers on activated charcoal, the surface adsorption efficiency improved than earlier. Hence, while performing the oil/water separation experiment, the oil drops can trap on to the charcoal surface, and only the water molecules can move through the membrane pores. Hence in results got oil-free water.

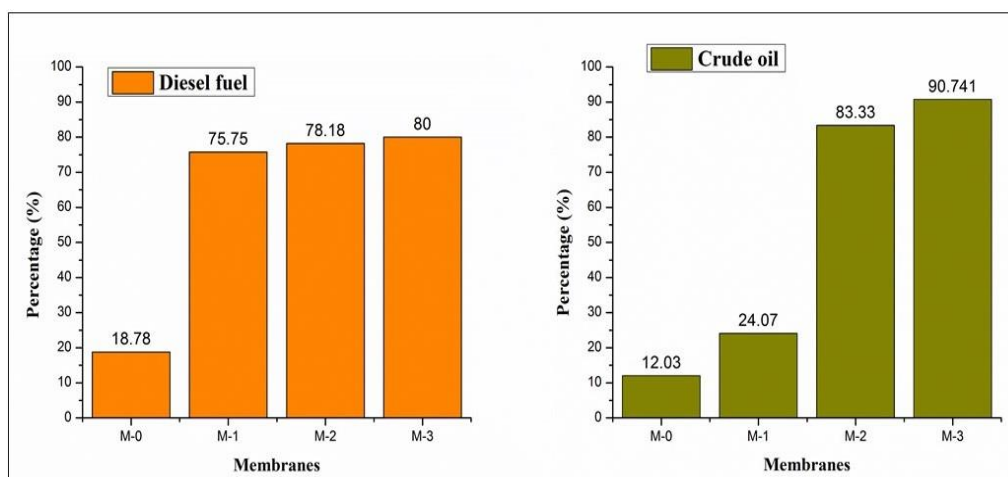


**Figure 2.17** Oil/water rejection performance of membranes

## 2.4. CONCLUSIONS

The PPSU/BiOCl-AC/PVP mixed matrix UF membranes were fabricated via phase inversion process. The fabricated membranes (M-0 to M-3) exhibited superior performance with water permeability, antifouling, as well as with oil/water separation tests. The membrane morphological changes were observed with scanning electron microscopy, and the elemental mapping analysis of M-2 membrane performed with SEM-energy dispersive spectroscopy. In conclusion, with the oil/water rejection test, M-3 membrane exhibited better results towards oil/water separation, above 80 % for diesel fuel and above 90 % for crude oil, respectively.



**CHAPTER 3**  
**FABRICATION OF NOVEL PPSU/ZSM-5**  
**ULTRAFILTRATION HOLLOW FIBER MEMBRANES**  
**FOR SEPARATION OF PROTEINS AND HAZARDOUS**  
**REACTIVE DYES**



**Abstract**

*Novel Polyphenylsulfone (PPSU)/ ZSM-5 (Zeolite Socony Mobil-5)/ Polyvinylpyrrolidone (PVP) mixed matrix hollow fiber membranes were (HFMs) fabricated via dry/wet phase separation process. The main objective of current research, to study the selected proteins such as bovine serum albumin (BSA), egg albumin (EA) and dyes Reactive black 5 (RB-5), Reactive orange 16 (RO-16) from aqueous media. Several techniques were employed to characterize the HFMs such as Field Emission scanning electron microscopy (FESEM), water uptake, porosity, contact angle, water permeability, antifouling capability as well as proteins and dyes rejection experiments. Due to the adsorbing as well as hydrophilic agent ZSM-5 effect, the proteins and dyes rejection capability of membranes enhanced continuously from PZ-0 to PZ-3 membrane. In conclusions, the PZ-3 membrane reveals the rejection results, above 100 % and 95 % for BSA and EA proteins and with dyes above 90 % and 82 % for RB-5 and RO-16, respectively.*

**3.1 INTRODUCTION**

Currently, large quantities of dye containing waste product are releasing from several industrial units such as textile, paint, cosmetic, printing, food and leather companies (Ghaedi M *et al.* 2012, Gupta V K *et al.* 2009). These dye wastes were directly entering into the environment and affecting ecological system due to their color, high chemical oxygen and low biochemical oxygen demand (Pagga *et al.* 1986). Dye removal from wastewater is very difficult due to the stability towards heat, light, and also biologically non-degradable characteristics (Dogan *et al.* 2007, Mall *et al.* 2006). In earlier, few of the techniques such as liquid-liquid extraction (Gharehbaghi *et al.* 2012), membrane filtration (Salleh *et al.* 2011, Dass *et al.* 2010), sedimentation, oxidation, and adsorption (Rekha *et al.* 2015) are reported towards dye removal from wastewater. Among the above procedures, membrane separation processes were highly used for the removal of several proteins and dye wastes from wastewater (Arockiasamy *et al.* 2013, Hebbar *et al.* 2017). Membrane technology is the most favorable process to separate dyes and proteins due to its specific features, high productivity, cost-effective, easy to handle, etc. (Xing *et al.* 2017).

Smith and group members (1995) demonstrated the fabrication of hollow fiber carbon membranes with the coating of three different types of zeolites such as ZSM-5, Silicalite-1, and mordenite in autoclave operative model, used polyacrylonitrile (PAN) as precursors. The fabricated hollow fiber composite membranes were characterized by SEM, EDX and XRD techniques. The purpose of facilitating with different zeolites to create the nucleation sites and to impregnate the hollow fiber membranes outer surface with silicon atoms. The uniform distribution of zeolites on the membrane surface and an inside of membrane walls confirmed with SEM-EDX investigations. This research mainly determines zeolites are acts as the good supportive materials to the hollow fiber carbon membranes, further separation applications (Smith *et al.* 1995).

Hydrothermally produced ZSM-5 zeolite was amended with manganese (Mn/ZSM-5), lanthanum (La/ZSM-5) and mixture of both (Mn–La/ZSM-5) by impregnation method to test the decolorization (adsorption) and mineralization effects (in the presence of UV irradiation) of indigo carmine (IC) dye from wastewater. IC (100 ppm) was chosen as a dye sample for the photocatalytic degradation study, due to its volatile property and it can found mostly in industrial wastewaters as a common pollutant. However, Mn/ZSM-5 exposed better results towards removal of IC dye (Othman *et al.* 2006).

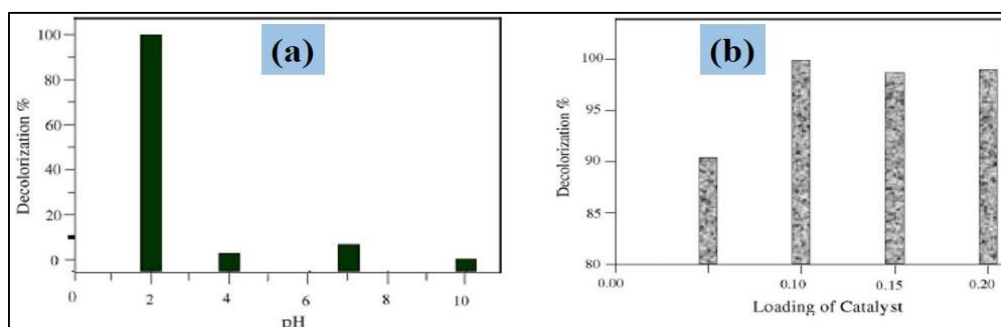


**Figure 3.1** Effect of pH (a), an effect of photocatalyst content (b) of Mn/ZSM-5 on the decolorization of IC (Othman *et al.* 2006)

Zeolites were synthesized from rice husks and supported by Titania catalysts via the impregnation of  $\text{TiCl}_4$  on to zeolites. Titania supported catalysts photodecomposition catalytic degradation activity was determined with various dyes such as methylene blue (MB), direct blue 71 (DB), direct yellow 8 (DY), etc.



Maintained standard dye concentration of 30 ppm, and these dye solutions illuminated with 0.05 g of Titania catalyst, then the decomposition of dyes results supervised with UV–visible spectroscopy (Petkowicz *et al.* 2010).

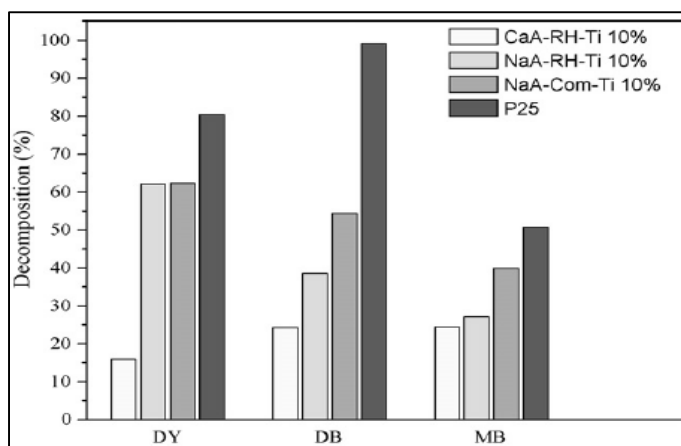


**Figure 3.2** Percentage of the decomposition of dyes by in situ-supported titania–zeolite (Petkowicz *et al.* 2010)

Polysulfone/ polyimide (PSF/PI) polymeric blend membranes prepared with the addition of different wt. % of ZSM-5 nanocrystals into the polymer matrix via a solution casting method. The purpose of the current work is to determine the membranes separation abilities of selected gases such as N<sub>2</sub>, O<sub>2</sub>, CO<sub>2</sub>, and CH<sub>4</sub>. The prepared membranes were characterized by SEM, FTIR and TGA studies. The incorporated ZSM-5 nanocrystals impact the selectivity and pore morphologies of membranes, so in results observed the superior gas permeability belongings with increasing the continuous ZSM-5 wt. % in the polymer matrix. In conclusions observed, the blend membranes with 20 wt. % of ZSM-5 nanocrystals revealed the better gas separation capability with O<sub>2</sub> compare with other gases. Even, the thermal stabilities of membranes also enhanced continuously due to the additive ZSM-5 effect in membranes (Dorosti *et al.* 2011).

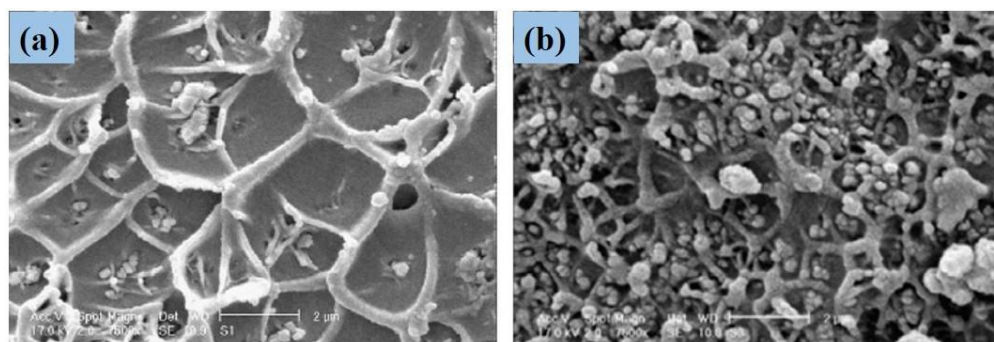


**Figure 3.3** SEM Cross-sectional micrographs of (a) PSF/PI (50/50) 10 wt. % ZSM-5 and (b) PSF/PI (50/50) 20 wt % ZSM-5 (Dorosti *et al.* 2011)

MFI zeolite membranes prepared on porous alumina hollow fibers via in-situ hydrothermal crystallization process. The objective of the current work is to study the methyl-diethoxysilane (MDES) modified membranes  $H_2/CO_2$  gas separation ability from gaseous mixture as well as the separation of p-xylene/o-xylene mixture. The permeate streams were assessed with gas chromatography furnished with a thermal conductivity detector (TCD). Sieving mechanism was involved in the separation process. Further, it was observed that the modified hollow MFI zeolite membranes were thermo-chemically stable and exhibited superior gas separation performance with  $H_2$  gas (Hong *et al.* 2013).

Graphene oxide (GO)/ polyethylenimine (PEI) mixed polymeric hydrogels were used for the deletion of methylene blue (MB) and Rhodamine B (RhB) from wastewater. GO sheets with various hydrophilic functional groups such as carboxyl, hydroxyl, and epoxides, these can form hydrogen bonds with amines or amine-containing molecules under suitable conditions. As well as the added polymer PEI also acts as a good adsorption agent and had adhesion properties. GO/PEI blend polymeric hydrogels showed best results, closely 100 % for both MB and RhB dyes rejection (Guo *et al.* 2015).

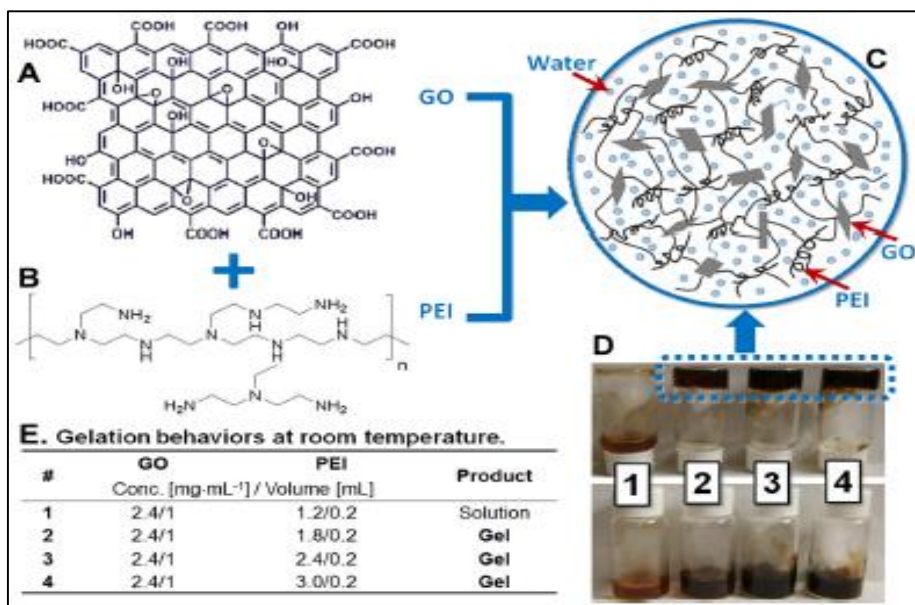


**Figure 3.4** Schematic illustration of the formation of GO/PEI gels, (A) GO and (B) amine-rich PEI were combined to give (C) GO/PEI hydrogels, (D & E) Gelation pictures (Guo *et al.* 2015)

Novel adsorbent sugar was infused into ZSM-5 zeolites (SuZSM) through carbonization process in a nitrogen environment. Nanoscale zero-valent iron (NZVI) impregnated with ZSM-5 (NVZI/ZSM) and with SuZSM (NVZI/SuZSM) adsorbents were employed to examine the methylene blue (MB) dye adsorption efficiency from aqueous solutions. The batch experiment was implemented to examine the MB dye adsorption experimentation, and the concentration variation between the feed and collected samples examined with UV-visible spectrophotometry. In conclusion, NVZI/SuZSM adsorbent exhibited effective dye adsorption outcomes, about 77 % at 300 °C. With increasing the experimental temperature the removal efficacy also increased, which reached up to 92 % at 500 °C (Hameed *et al.* 2016).

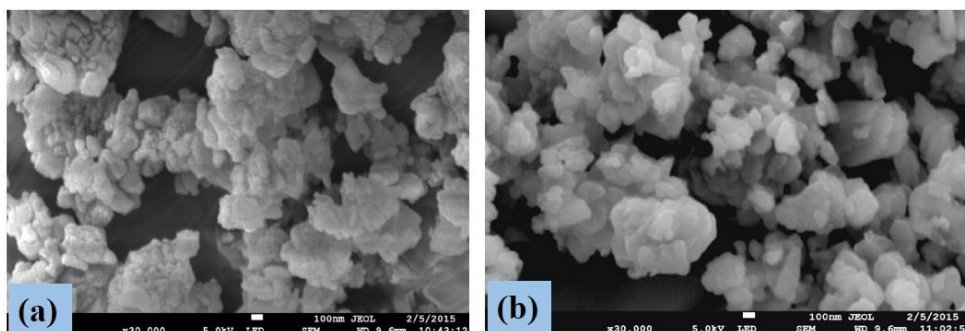


**Figure 3.5** SEM images of (a) NVZI/ZSM and (b) NVZI/SuZSM (Hameed *et al.* 2016)

Primarily, ZSM 5 nanocrystals were synthesized by natural raw materials viz., rice husk and kaolin clays. Afterward, TiO<sub>2</sub> nanoparticles (100-200 nm) incorporated ZSM5 (TiO<sub>2</sub>-zeolite) photocatalyst was synthesized by solvothermal and impregnation methods, to study the photocatalytic degradation of methylene blue (MB) dye from aqueous media. 20 ppm concentrated MB solution was prepared and the results examined with UV-Visible spectrophotometer. In the final, TiO<sub>2</sub> contained zeolites showed better MB deletion efficacy than TiO<sub>2</sub> anatase and zeolite (Setthaya *et al.* 2017).

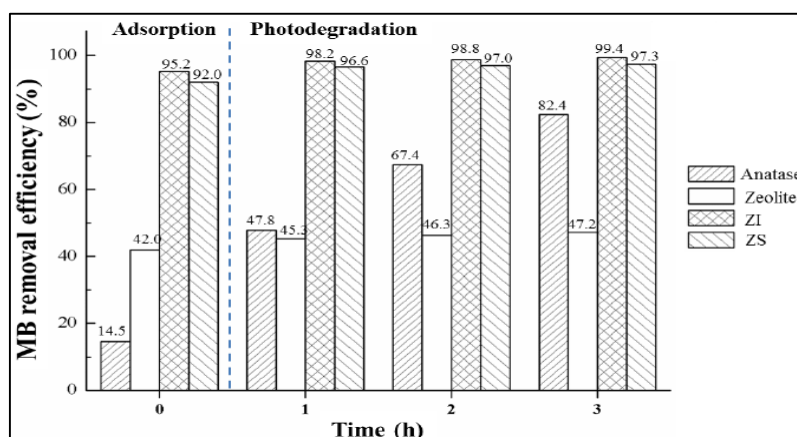


**Figure 3.6** The adsorption and photodegradation results of MB by different photocatalysts (Setthaya *et al.* 2017)

Polyvinylalcohol/ hydrophilic poly (diallyldimethylammonium chloride)/ ZSM-5 zeolite (PVA/PDADMAC/ZSM-5) mixed matrix membranes fabricated via a solution casting method. The main object of the current work is to investigate the methyl orange (MO) dye adsorption efficacy from industrial wastewater and to test the antibacterial activity of prepared membranes. The membranes were characterized by

various techniques such as SEM, XRD, TGA, UTM (universal testing machine), FTIR and water uptake measurements. The MO dye removal ability of membranes enhanced with the continuous enhancement of ZSM-5 wt. % in the polymer matrix. In results, the higher ZSM-5 wt. % contained membrane (PPZ-5) exhibited better outcome, about 95 % of MO dye adsorption and the membranes showed antibacterial features (Sabarish *et al.* 2018).

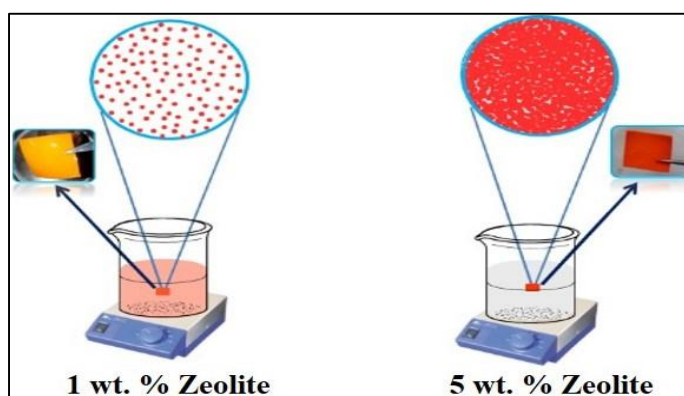


**Figure 3.7** Apparatus for adsorption of MO on PVA/PDADMAC/ZSM-5 membrane (Sabarish *et al.* 2018)

Polyvinylidene fluoride (PVDF)/ polydimethylsiloxane (PDMS) polymeric cross-linked blend HFMs fabricated with the addition of different wt. % of ZSM-5 zeolites (0 %, 10 %, 20 %, 30 %, 40 % and 50 %) to the polymer matrix via dynamic negative pressure coating process. The main object of current research is to examine the phenol recovery competence of membranes from feed mixtures through pervaporation process. Water contact angles of membranes improved with the continuous enhancement of hydrophobic ZSM-5 wt. % in membranes, it can impact the hydrophobic nature of membranes, so observed the reduced water flux. In conclusions, with phenol separation test the separation efficacy was enhanced continuously with increasing the ZSM-5 wt. % in membranes. But, the phenol permeability enhanced up to the addition of 20 wt. % of ZSM-5, after that again the phenol flux was decreased slowly (Li *et al.* 2018).

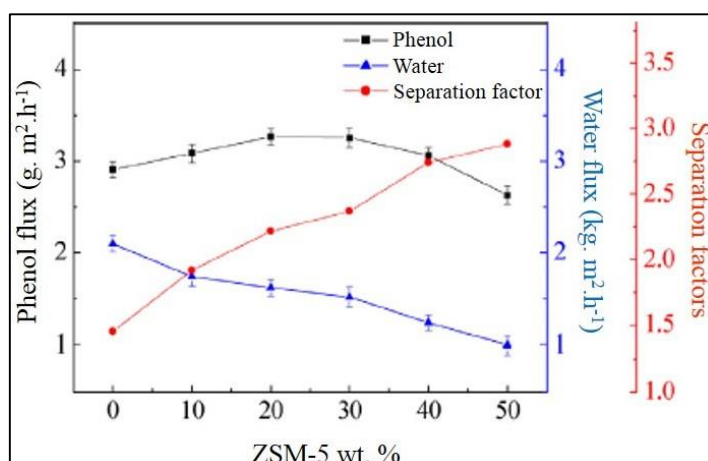


**Figure 3.8** Effect of the ZSM-5 concentration on the PV performance (Li *et al.* 2018)

Reactive Black 5 (RB-5) is azo dye, and mostly used in textile industries for the dyeing process. The dye wastes were directly entering into the water without any treatment, so the water going to contaminate and this wastewater can cause numerous health problems. Investigators computed numerous degradation processes for RB-5 dye over photocatalytic action (Kurbus *et al.* 2003), ultrasound (Voncina *et al.* 2003) methods. Reactive Orange 16 (RO-16) is a reactive dye with azo [N=N] chromophore and with sulfate ethyl sulphone groups, and mostly using in dye processing units (Cameiro *et al.* 2004).

Zeolites are the aluminosilicates with 3-D framework structures (Figure 3.9 a), and the  $[\text{AlO}_4]^{5-}$  and  $[\text{SiO}_4]^{4-}$  are connected with each other by sharing  $\text{O}_2$  atoms (Figure 3.9 b) and forms tetrahedral interconnected cages between the molecules and forms crystalline structures (Jin *et al.* 2008). Zeolites common formula is  $\text{M}_{e/2n}\text{O} \cdot \text{Al}_2\text{O}_3 \cdot x\text{SiO}_2 \cdot y\text{H}_2\text{O}$  (Roskill services, 1988). Where ‘M<sub>e</sub>’ alkaline/ alkali earth metal, ‘n’ charge of the atom, ‘x’ no. of silicones, ‘y’ no. of H<sub>2</sub>O molecules. Si and Al combine together then forms structures, and the O<sub>2</sub> will be present in corners and forms tetrahedral frames between two cages.



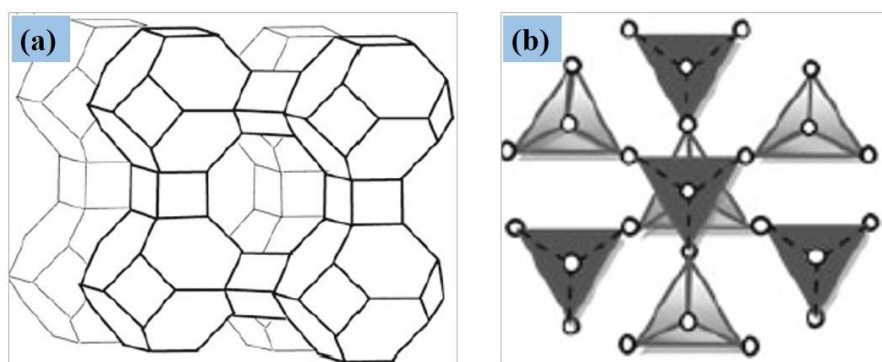
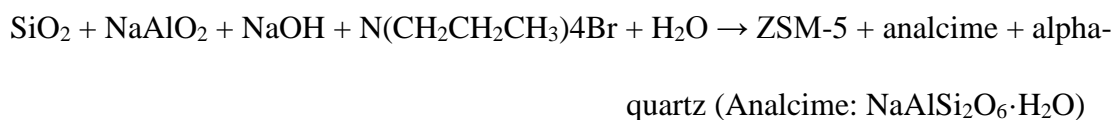


**Figure 3.9** Crystal structure of zeolite (3-D view) (a), tetrahedral interconnected cages (b) (Jha *et al.* 2016)

In zeolites, it was able to differentiate the types based on their structural frameworks and arrangement of the atom. Among that, ZSM-5 is belonged to the pentasil family (five-membered rings). ZSM-5 is a synthetic zeolite (Argauer *et al.* 1972). ZSM-5 chemical formula  $\text{Na}_n\text{Al}_n\text{Si}_{96-n}\text{O}_{192}\cdot 16\text{H}_2\text{O}$  ( $0 < n < 27$ ). Usually, ZSM-5 can synthesize in Teflon-coated autoclaves by the addition of various amounts of Al or Si contained complexes at different pressures and temperatures.



ZSM-5 has been acting as good supporting material and most widely used in catalysis reactions. ZSM-5 with Al-O-Al bonds will exhibit more hydrophilic property. Numerous reports conclude that zeolites are used as the most favorable adsorbing agent in various separation processes, municipal wastewater treatments etc., (Mumpton *et al.* 1999) because of their large surface area and high cation exchange aptitude (Ahmed *et al.* 2013, Selim *et al.* 2004). The organically functionalized zeolites can influence the surface hydrophilic or hydrophobic properties. In the current research, selected PPSU polymer as the principle polymer due to its specific features mechanical, chemical stability, and solvent resistant ability, etc.

From the earlier literature reports, it concludes that the usage of ZSM-5 in the membrane technology field is very less. These survey reports inspired us to fabricate the hollow fiber membranes with the addition of ZSM-5 to the PPSU polymer. The

main object of current research is to fabricate the hollow fiber membranes (HFMs), to examine the selected proteins and dyes removal efficiency from aqueous media. The HFMs were characterized by SEM, water uptake, porosity, and contact angle. Cross-flow filter unit was employed to assess the water permeability as well as proteins, and dyes removal efficacy of HFMs.

### 3.1.1 Hollow fiber membranes

In this chapter, fabricated various nano additive contained hollow fiber membranes to observe the proteins and dyes rejection performance from wastewater. The HF membranes fabrication procedure and spinning parameter conditions were discussed detailed in section 3.2.2. Currently, the HFMs fabrication via phase separation process becomes one of the most common methods (Verissimo *et al.* 2005). HFMs fabricated via phase separation process are specifically with appreciable surface and possess good mechanical strength. Table 3.1 reveals information regarding the membranes several characterization techniques. Several polymers such as PVDF, PES, PEI, PPSU, PSf, PEK, PAN, PDMS, PANI, etc. are employed to fabricate the HFMs.

**Table 3.1** HF membranes characterization techniques (Tylkowski *et al.* 2015)

Method	Characteristic
Gas and liquid displacement methods (GLDP), Liquid-liquid displacement porosimetry (LLDP)	Pore size distribution
Scanning electron microscopy (SEM), Transmission electron microscopy (TEM)	Top layer thickness, Surface porosity, Pore size distribution, Qualitative structure analysis
Atomic force microscopy (AFM)	Surface topography
Flux and retention measurements	Permeability, Selectivity
Molecular weight cut-off (MWCO)	Type of membrane
Gas adsorption/desorption (GAD)	Pore size distribution
SEM + X-Ray microanalysis (EDS)	Chemical analysis, Surface analysis
Infrared Spectroscopy (FT-IR, ATR)	Functional group analysis



Contact angle, water uptake measurement	Surface hydrophilic property
Brunauer–Emmett–Teller (BET)	Surface area, pore volume

Figure 3.10 can reveal the schematic representation of lab scale hollow fiber membranes fabrication unit. Hollow fibers demonstrate better permeability and exhibit the effective separation results compare with flat-sheet membranes. These membranes were more capable of fouling and difficult to clean, so pre-treatment is required to clean the hollow fiber modules. These HFMs were broadly using in various separation processes such as, gas separation (Spillman *et al.* 1989, Wang *et al.* 2002), ultrafiltration (Khulbe *et al.* 2007), desalination (Sukitpaneenit *et al.* 2012), dialysis, forward osmosis (Setiawan *et al.* 2011), wastewater treatments (Jansen *et al.* 2005), cell culture, tissue engineering, dye removal (Nayak *et al.* 2018), organic solvents separation (Son *et al.* 2011), etc.

## 3.2 EXPERIMENTAL

### 3.2.1 Materials

PPSU (Radel R-5000) was delivered by Solvay Advanced Polymer, Belgium. Zeolite ZSM-5 (CAS No.:308081-08-5) was obtained from Hangzhou Yunuo Chemical, China. 1-methyl-2-pyrrolidone EMPLURA<sup>®</sup> (M 99.13 g/mol) was supplied by Merck Millipore Corporation Ltd. Germany. Bovine serum albumin (BSA) (MW~66 kDa), albumin from chicken egg white (EA) (MW~44.3 kDa), polyvinylpyrrolidone (PVP) (~MW 36,000), and dyes Reactive Orange 16 (RO-16) and Reactive Black 5 (RB-5) were acquired from Sigma-Aldrich Co., USA.

### 3.2.2 Fabrication of PPSU/ZSM-5 mixed hollow fiber membranes

PPSU/ZSM-5/PVP mixed hollow fiber membranes fabricated via a dry/wet spinning process. Totally four types of HFMs were fabricated with the incorporation of different wt. % of ZSM-5 additive to the PPSU polymer. Primarily, an appropriate amount of ZSM-5 was added to NMP and performed sonication up to 40 min for the proper dispersion of ZSM-5 in NMP. Further, 18 g of PPSU, 2 g of PVP were added,

by maintaining temperature 70 °C and continued the stirring up to 24 h to become a clear dope solution. Afterward, performed degasification to the gained dope solution on sonicator, for the removal of air bubbles from dope. The dope compositions were clearly mentioned in Table 3.2.

The above-obtained dope compositions were individually moved over the spinneret in nitrogen pressure. Deionized water was used as bore fluid and permit through the inmost tubes of the spinneret. The spinneret parameters were stated in Table 3.3. After, the dope solution directly entered into the coagulation bath and immediately the hollow fibers will form due to the phase separation process. The fibers were collected at collecting drum by maintaining the specific drum speed. The gained fibers were placed in water for 24 h, and in the next day placed in 10 wt. % glycerol solution for post-treatment process about 24 h. Afterward, the fibers kept for air dry and used for further investigations.

**Table 3.2** Membrane configurations

Membranes	PPSU (g)	NMP (g)	PVP (g)	ZSM-5 (wt. %)	ZSM-5 (g)
PZ-0	18	80	2	0	0
PZ-1	18	79.982	2	0.1	0.018
PZ-2	18	79.964	2	0.2	0.036
PZ-3	18	79.928	2	0.4	0.072

**Table 3.3** Spinning parameters of HFMs

Parameter	Condition
Spinneret OD/ID (mm)	1.1/0.55
Dope solution	PPSU/ZSM5/PVP/NMP
Dope extrusion rate (mL/min)	3
Bore fluid	RO water
Bore flow rate (mL/min)	2.5
Air gap (cm)	5
Treatment bath	Water
Washing bath temp.	26 °C
Drum speed (rpm)	7

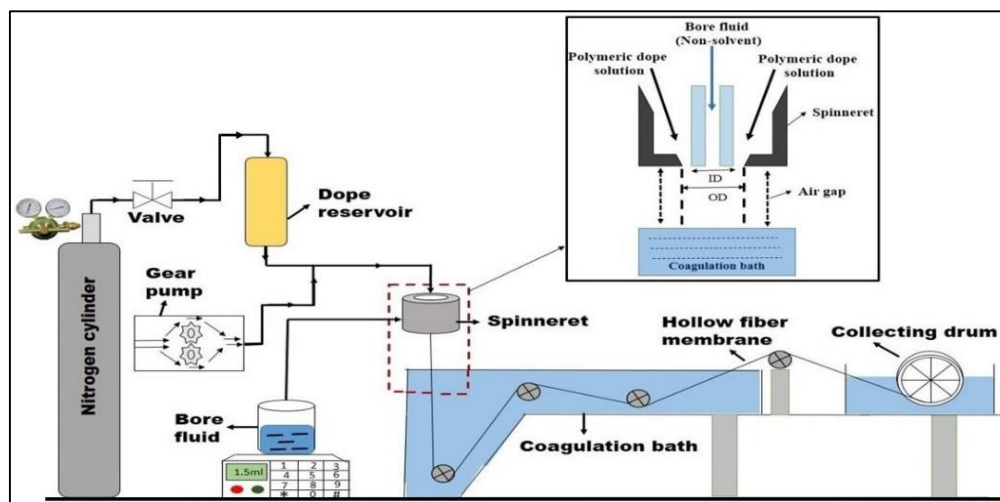


**Figure 3.10** Schematic representation of a hollow fiber membrane fabrication unit

### 3.2.3 Membrane characterizations

#### 3.2.3.1 Scanning electron microscopy

To determine the morphology of ZSM-5 crystals and the prepared HF membranes morphological changes were assessed with the SEM instrument. The sample preparation procedure for SEM study was reported as explained earlier in section 2.2.4.2 of CHAPTER 2.

#### 3.2.3.2 Water contact angle analysis

To measure the surface wettability (water contact angle) characteristics of the fabricated HF membranes was evaluated by following the procedure mentioned in section 2.2.4.3 of CHAPTER 2.

#### 3.2.3.3 Water uptake

To investigate the water uptake ability of HFMs, the membranes were cut into 3 cm<sup>2</sup> size pieces and both ends were closed with epoxy mixture (Resin: Hardener - 2:1 ratio) and kept for dry. After, the dried samples were rinsed in water for 24 hours and removed, additionally the excess water extracted with tissue and noted the wet weight of the sample. Afterthought, the sample was placed in dry in oven upto 6 h, and then recorded the dry weight of the sample (Hebbar *et al.* 2017).

$$\% \text{ Water uptake} = \left( \frac{W_w - W_d}{W_w} \right) \times 100 \quad \text{Eq. (3.1)}$$

Here, 'W<sub>w</sub>' and 'W<sub>d</sub>' are the wet and dry weights of HF membranes.

### 3.2.3.4 Porosity

To study the porosity studies of HF membranes were done by following the method mentioned in section 2.2.4.7 of CHAPTER 2.

### 3.2.3.5 Pure water permeability

Cross-flow filter unit was employed to assess the pure water permeability of fabricated HF membranes. From membrane bundle, five number of fibers were collected and maintained  $\approx 10$  cm length and potted on stainless steel holder using the epoxy mixture. After, the holder fixed with cross flow unit and continued the water permeability test. Primarily, the system was preserved for compaction at 0.5 MPa TMP, and after some time the TMP decreased to 0.3 MPa and performed the time-bound water permeability test. 2 min time gap maintained for each permeate collection, and sustained the water permeability up to 30 min (Kumar *et al.* 2013). Eq. 3.2 employed to calculate the HF membranes water flux,

$$J_{w1} = \frac{Q}{n\pi L \Delta P D_i} \quad \text{Eq. (3.2)}$$

where 'J<sub>w1</sub>' permeate flux, 'Q' volumetric flow rate (mL/min), 'n' no. of fibers, 'D<sub>i</sub>' inner diameter of HF membrane (cm), 'L' length of fiber (cm) and 'ΔP' transmembrane pressure (bar).

### 3.2.3.6 Antifouling ability

The antifouling ability of the synthesized HF membranes was tested by calculating FRR values as described in section 2.2.4.5 of CHAPTER 2. The BSA flux was measured at 0.3 MPa TMP and maintained 2 min time interval for each permeate collection.

### 3.2.4 Procedure for proteins and hazardous dyes rejection

Cross-flow filter unit was engaged to investigate the BS, EA proteins and RB-5, RO-16 dyes rejection efficiency of fabricated HF membranes. In rejection experiment, maintained the protein solutions concentration with 800 ppm and the dyes concentration was 100 ppm. The solution's pH was maintained at  $6.8 \pm 0.4$  with 0.1M HCl. The feed solutions were poured in feed tank one after one and the rejection studies were performed at 0.4 MPa TMP. Afterward, the concentration variations of feed and permeate samples were evaluated with UV-Spectrometry (Zhong *et al.* 2003 and Huotari *et al.* 1999). The maximum absorbance for protein solutions was 278 nm and for RO-16 and RB-5 dyes, the maximum absorption was observed at a wavelength of 494 nm and 598 nm, respectively. Eq. 3.3 employed to determine the rejection % of membranes,

$$\% R = \left(1 - \frac{C_p}{C_f}\right) \times 100 \quad \text{Eq. (3.3)}$$

Where  $C_p$  and  $C_f$  are the protein/dye concentrations in permeate and in the feed.

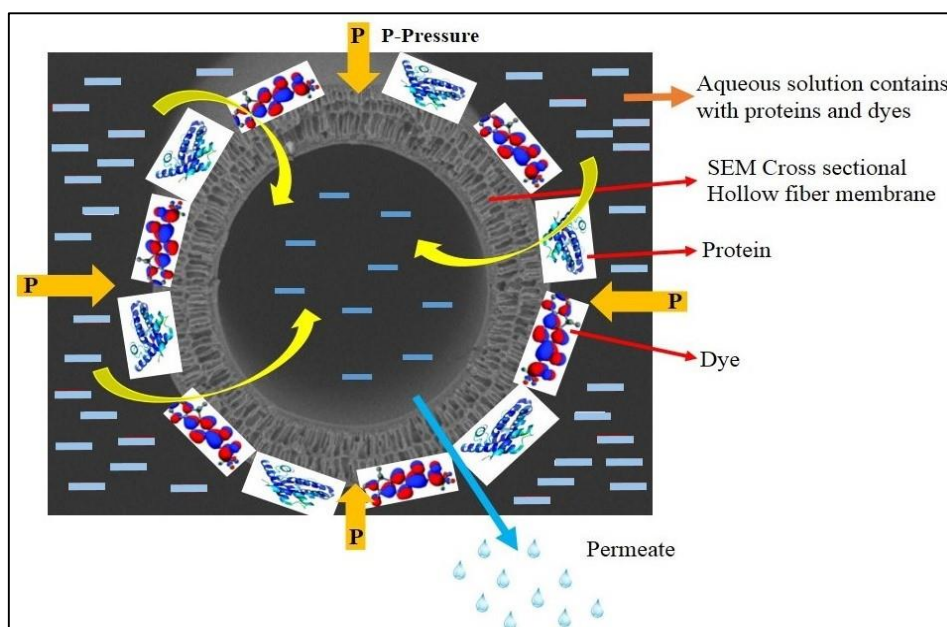


**Figure 3.11** Schematic representation of proteins and dyes separation mechanism over hollow fiber membrane

### 3.3 RESULTS AND DISCUSSION

#### 3.3.1 Contact angle (CA)

The contact angle is one of the main parameters to measure the surface hydrophilic nature of the membrane. In current research hydrophilic ZSM-5 was used as an additive to all membranes. These Zeolites with oxygen bonds (-O), and these bonds can form hydroxyl groups (-OH) by absorbing water molecules, so the surface will become hydrophilic. In conclusion, the continuous CA decrement was observed with all membranes, it means the surface hydrophilic behavior gradually increased from PZ-0 to PZ-3 membrane. The resulted CA values stated in Table 3.4.

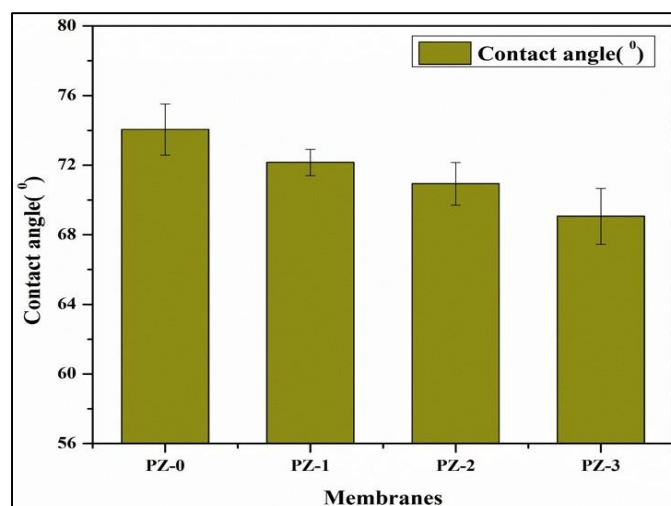
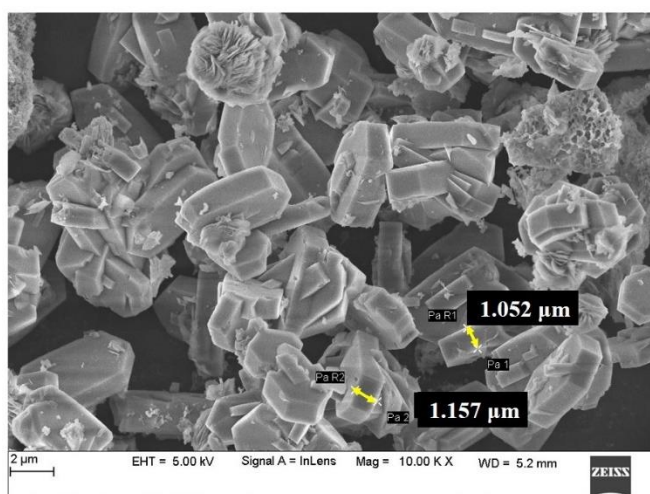


Figure 3.12 Contact angle results of membranes

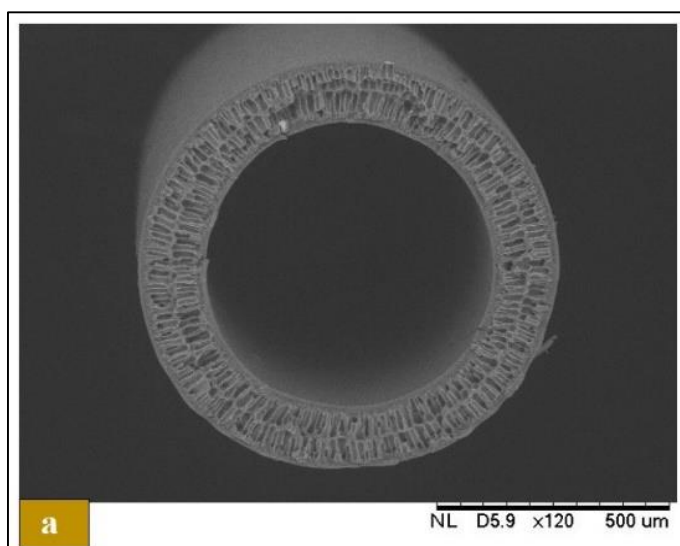
#### 3.3.2 Membranes morphology

The structural morphology of ZSM-5 crystals was assessed with FESEM and observed the thickness range was 1.052  $\mu\text{m}$  and 1.157  $\mu\text{m}$  (Figure 3.13). The fabricated HFMs cross-sectional structural changes were evaluated with SEM studies (Figure 3.14). In results, the membranes contained asymmetric structure with top skin layer and bottom sublayer with finger-like cavities, sponge-like cavities and macro voids (Verma *et al.* 2015 and Chen *et al.* 2015). With increasing the continuous wt. % of ZSM-5 additive in the polymer matrix, the effective enhanced morphological changes were observed from PZ-0 to PZ-3 membrane. In PZ-1, PZ-2 and PZ-3 membranes some of

the horizontal projections observed, these projections can impact the permeability properties of membranes, so further enhancement was observed with all membranes (Zinadini *et al.* 2014 and Wang Z *et al.* 2012). The added hydrophilic additive ZSM-5 and the water-soluble PVP, also one of the cause to enhance the water permeability as well as the rejection efficiency of membranes (Morihamma *et al.* 2014 and Nayak *et al.* 2017).



**Figure 3.13** FESEM micrograph of ZSM-5 crystals





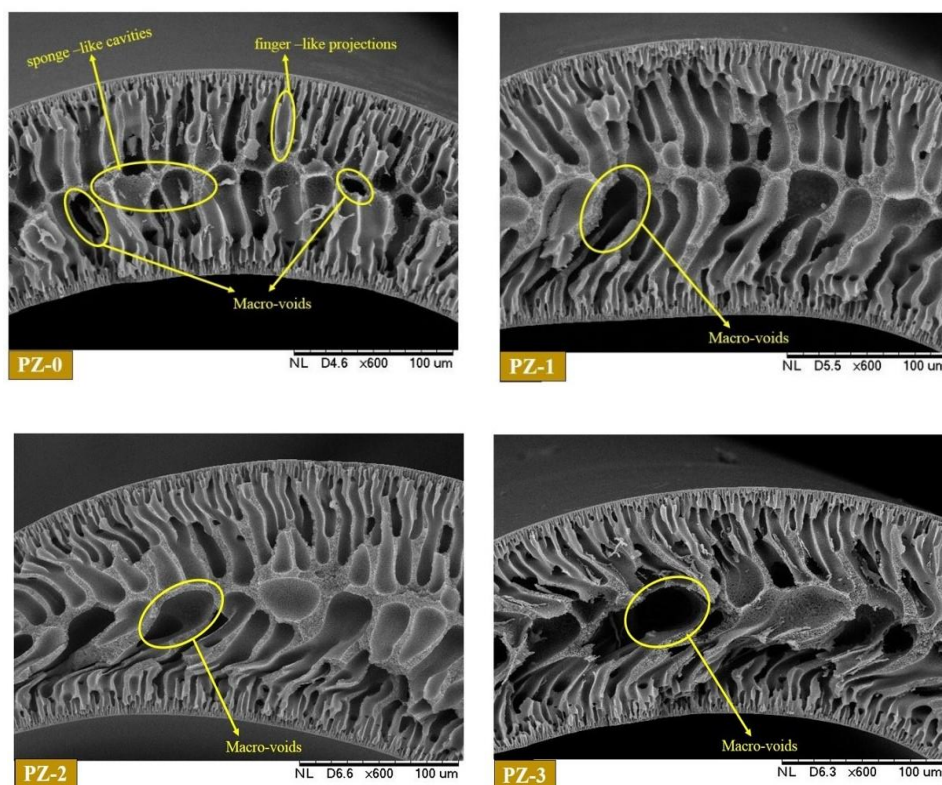


**Figure 3.14** (a) SEM cross-sectional outlook image of HF membrane, and remain are magnified SEM images of PZ-0, PZ-1, PZ-2, and PZ-3 membranes

The existence of Al, Si and other elements on PZ-3 membrane was identified by SEM-EDS analysis (Figure 3.15 b). In results observed, a large amount of sulfur element, this is because of the addition of excess PPSU polymer.

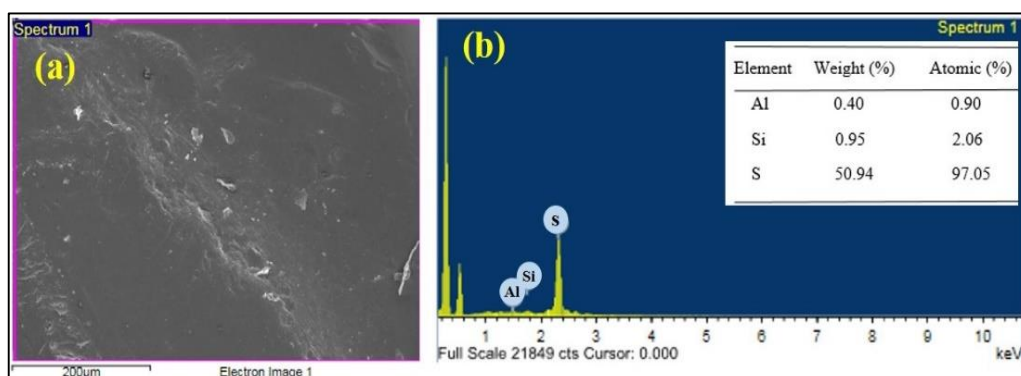


**Figure 3.15** (a) FESEM surface image, (b) EDS analysis of PZ-3 membrane



### 3.3.3 Pure water flux (PWF)

The additive contained membranes exhibited the enhanced permeability properties than pristine membrane (Adoor *et al.* 2008). The added additive ZSM-5 is acting as a good hydrophilic agent, and it can impact the pore morphologies of membranes. Hence, the water permeability was improved from 26.21 L/m<sup>2</sup> h to 113.98 L/m<sup>2</sup> h, and the flux values were stated in Table 3.4. The enhanced pore morphological changes of membranes were observed from SEM analysis (Figure 3.14). With the PZ-3 membrane, the obtained water flux was four times greater than the PZ-0 membrane (Figure 3.16), this is because of the ZSM-5 and PVP additives effect.

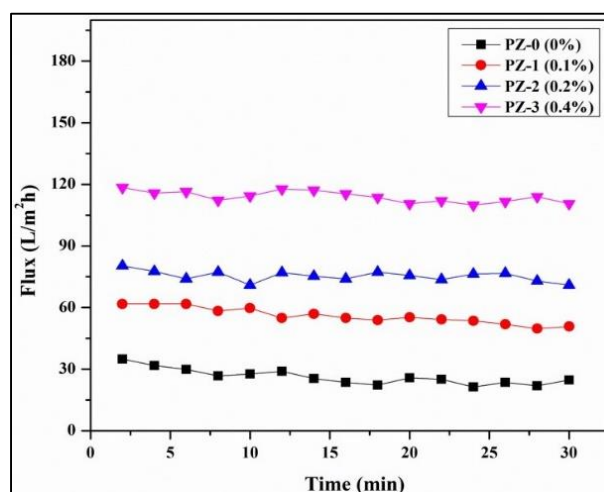


**Figure 3.16** Time-dependent PWF performance of membranes

### 3.3.4 Antifouling analysis

Initially, the water permeability was examined with all membranes. Later, time-bounded BSA proteins flux was performed to determine the antifouling behavior of membranes. While doing BSA flux, the less flux was originated than water flux, due to the larger sizes of BSA molecules. Compare with normal water molecules the BSA molecules size was very large, so in permeation test, the BSA molecules can deposit on membrane pores due to the ZSM-5 effect. Due to the pores blockage phenomena, with BSA less flux observed with membranes. Even, the BSA flux was improved from 5.25 L/m<sup>2</sup> h to 34.65 L/m<sup>2</sup> h, due to the adsorbing additive ZSM-5 effect. After the BSA

flux, membranes properly cleaned with water under continuous tap flow and repeated the water permeability test (Figure 3.17 a). In conclusions, the PZ-3 membrane exhibited better antifouling results. The antifouling conductance of membranes was intended with FRR (flux recovery ratio), and the FRR values were stated in Table 3.5.

**Table 3.4** Membrane permeability study

Membrane code	Permeate flux ( $L/m^2 h$ )			Fouling performance (%)			
	$J_{w1}$	$J_p$	$J_{w2}$	FRR	$R_t$	$R_r$	$R_{ir}$
PZ-0	26.21	5.25	19.14	73.02	79.96	52.99	26.97
PZ-1	55.96	12.24	36.56	65.33	78.12	43.45	34.66
PZ-2	75.34	25.53	51.95	68.95	66.11	35.06	31.04
PZ-3	113.98	34.65	78.36	68.74	69.59	38.35	31.25

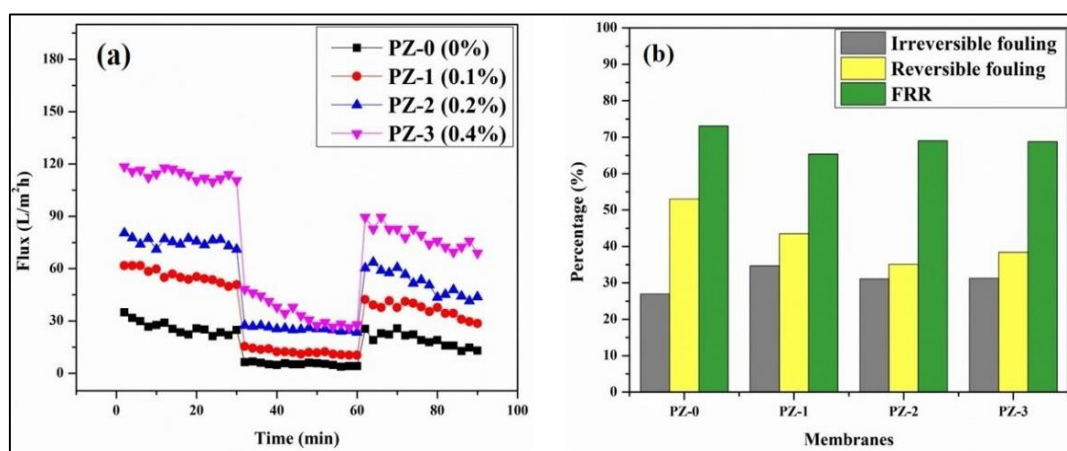


**Figure 3.17** (a) Flux V/s time for membranes at 0.3 MPa under three conditions: water flux; BSA Protein flux; and water flux after carefully wash with water, (b) FRR and antifouling outcomes of membranes

### 3.3.5 Water uptake and porosity studies

The added ZSM-5 can influence the pore sizes of membranes, so the membranes showed a good affinity towards water. With porosity and water uptake tests, a

noticeable enhancement was observed from PZ-0 to PZ-3 membrane, due to the hydrophilic ZSM-5 additive effect (Figure 3.18).

**Table 3.5** Membrane possessions

Membranes	Water uptake (%)	Porosity (%)	Contact angle ( $^{\circ}$ ) $\pm$ sdv
PZ-0	49.48	12.63	$74.05 \pm 1.47^{\circ}$
PZ-1	55.46	18.33	$72.16 \pm 0.76^{\circ}$
PZ-2	58.08	26.94	$70.93 \pm 1.23^{\circ}$
PZ-3	66.48	35.60	$69.06 \pm 1.60^{\circ}$

Sdv= standard deviation

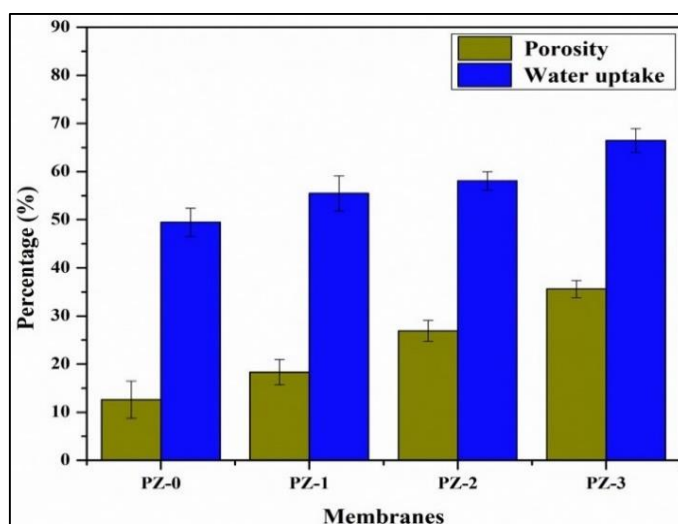


**Figure 3.18** water uptake and porosity outcomes of membranes

### 3.3.6 Rejection efficiency of membranes

#### 3.3.6.1 Proteins removal

The protein rejection experiment conducted with selective proteins such as BSA and EA. While performing the proteins removal study, protein solutions pH should be maintained constant, otherwise, the rejection results will vary (Brinck *et al.* 2000). Sieving mechanism was involved in current research. Accordingly to this mechanism, the larger size molecules can retain on the membrane surface and only the smaller molecules can move through the membranes. Here, the BSA molecules size (66 KDa) was larger than the EA (44 kDa). So, the BSA molecules cannot easily pass through the

membrane pores, and will be a deposit on membrane surface itself, so 100 % rejection results observed with BSA molecules. With EA, the rejection was 95 %, it's slightly lesser than the BSA rejection, due to the size variations of molecules (Figure 3.19). PZ-3 membrane revealed the best results than other membranes.

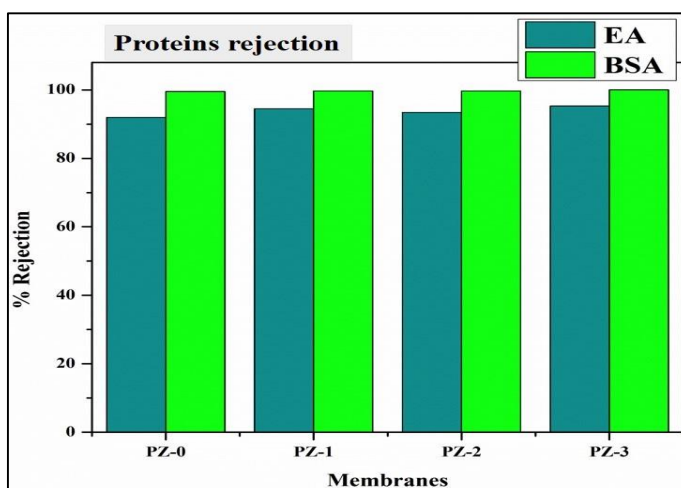


**Figure 3.19** Proteins rejection results of membranes

### 3.3.6.2 Dye removal

The fabricated HFMs preserved for the rejection of selective dyes such as RB-5 and RO-16 from aqueous media. The incorporated additive ZSM-5 can advance the hydrophilicity of membranes and acts as good adsorbing agent (Erdem Senatalar *et al.* 2004) towards removal of dyes from aqueous media. Figure 3.20(a) reveals the dye removal efficiency of membranes. With increasing the ZSM-5 wt. % in the polymer matrix, the dye removal ability of membranes also enhanced continuously from PZ-0 to PZ-3 membranes, due to the larger adsorptive nature of additive ZSM-5. The larger molecular weight contained RB-5 (MW 990 g/mol) exhibited good rejection performance than RO-16 dye (MW 617 g/mol). In conclusions, the PZ-3 membrane exhibited better rejection efficiency, above 90 % for RB-5 and above 82 % for RO-16 dyes, respectively (Figure 3.20 a). Time-bounded dye permeability test performed with PZ-3 membrane (Figure 3.20 b), and the dye flux reached 43.70 L/m<sup>2</sup> h for RO-16 and 38 L/m<sup>2</sup> h for RB-5. Figure 3.21 reveals the digital proof results of HF membranes after dye removal experiment.

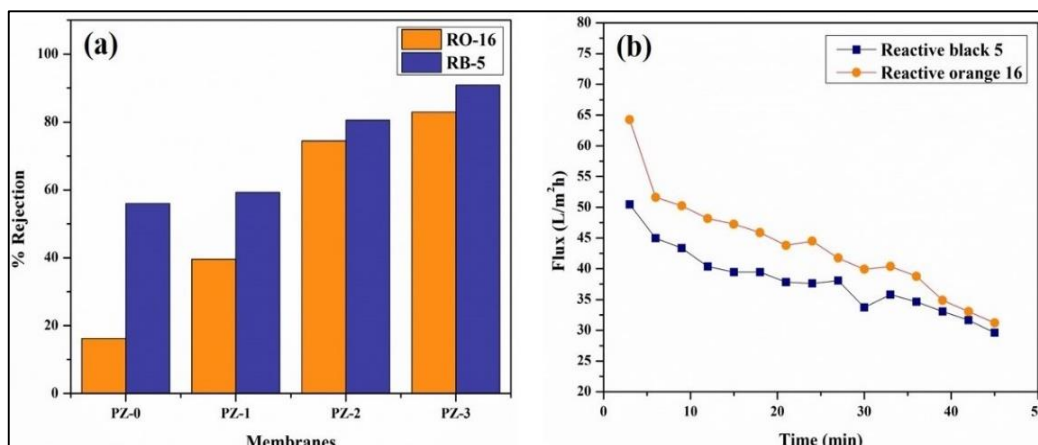


**Figure 3.20** (a) Dyes removal conductance of membranes, (b) time bounded dye flux analysis of PZ-3 membrane

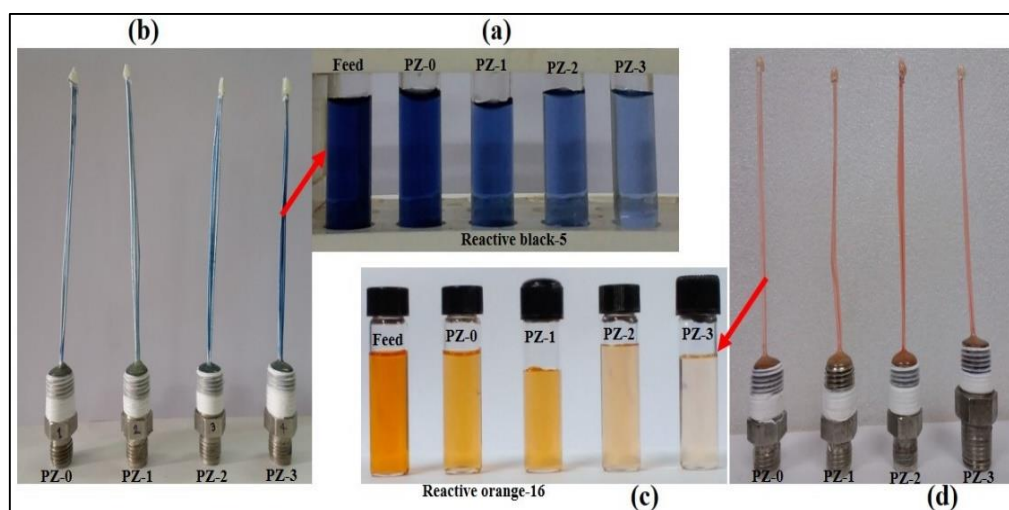


**Figure 3.21** the digital pictures of (a) RB-5, (c) RO-16 dyes removal results with membranes and (b & d) are the outlook images of membrane adaptors after rejection experiment

### 3.4 CONCLUSIONS

PPSU/ ZSM-5/ PVP mixed hollow fiber membranes fabricated via the dry/wet spinning process. The main object of current work is to examine the rejection efficacy of BSA, EA proteins and RB-5, RRO-16 dyes from aqueous media by cross-flow filter unit. The HF membranes were characterized by FESEM, water uptake, porosity, etc. ZSM-5 was acted as good adsorbing agent towards removal of proteins and dyes from

aqueous media. In conclusions, the permeability ability of membranes enhanced from PZ-0 to PZ-3 membranes. With PZ-3 membrane, rejection results reached 100 % for BSA, 95.23 % for EA proteins and with reactive dyes 90.81 % for RB-5 and 82.84 % for RO-16.

## **CHAPTER 4**

# **EFFECTS OF MULTIWALLED CARBON NANOTUBE ON NOVEL POLYPHENYLSULFONE COMPOSITE ULTRAFILTRATION MEMBRANES FOR THE EFFECTIVE REMOVAL OF LEAD, MERCURY AND CADMIUM FROM THE AQUEOUS SOLUTIONS**





**Abstract**

*In the current study, multiwalled carbon nanotubes (MWCNTs) were added directly to the polyphenylsulfone (PPSU)/N-methyl-2-pyrrolidone (NMP) solution to fabricate the ultrafiltration flat-sheet membranes via phase inversion technique. Membrane morphology and elemental mapping studies were assessed by scanning electron microscope (SEM) and energy dispersive spectroscopy (EDS). The characteristics of the prepared membranes were assessed by contact angle study, water uptake, porosity and permeability enactment of the membranes assessed with pure water flux (PWF) and antifouling measurements. Investigational reports displayed that, the rejection rate of metal ions increases with increasing the MWCNTs wt. % on PPSU polymer. In conclusions, the PCNT-3 membrane showed heavy metal ions removal efficiency of 98.13 % for  $Pb^{2+}$  ions, 76.12 % for  $Hg^{2+}$  ions and 72.92 % for  $Cd^{2+}$  ions respectively.*

**4.1 INTRODUCTION**

Due to the increased industrial activities, huge quantities of heavy metal wastages are discharging into the environs and contaminating our surroundings. These pollutants are mainly released by leather, textile, paint, wood processing, pigment, dyes, and petroleum refining industries by various processes i.e., electroplating, surface treatment process and other chemical treatments. These heavy metals cause harmful effect on the environment and may cause physical discomfort, illness and irreversible damage to vital body system of human beings (Malik *et al.* 2004, Aziz *et al.* 2005). Few of the heavy metal separation methods from wastewater are developed by researchers i.e., precipitation, ion exchange method, reverse osmosis, oxidation, reduction, electrodialysis, and adsorption methods.

In earlier reports, researchers reported the subtraction of heavy metals from wastewater by various nano adsorbents such as,  $TiO_2$  (Engates *et al.* 2011),  $MnO_2$  (Pakarinen *et al.* 2010),  $CeO_2$  (Cao *et al.* 2010),  $Al_2O_3$  (Tarasevich *et al.* 2001),  $Fe_2O_3$  (Chen *et al.* 2010),  $ZnO$  (Ma *et al.* 2010) etc. Cellulose acetate based mixed matrix membranes (Liu *et al.* 2006), nano-silver infused PSf membranes showed the enhanced antifouling and biofouling efficacy. In few of the reports, investigators conveyed the

importance of biomass wastes for example, sunflower leaves (Benaissa *et al.* 2007), sawdust (Kalavathy *et al.* 2010, Si *et al.* 2012), sugarcane bagasse (Khoramzadeh *et al.* 2013), guava leaf (Ponnusami *et al.* 2008), egg shells (Podstawczyk *et al.* 2014), green algae (Bakatula *et al.* 2014), etc., to separate the dyes, heavy metals and other organic pollutants from water.

Membrane filtration together with CNT can make better water desalination and decontamination approaches more effectual and cost-effective (Elimelech *et al.* 2011). Polymeric membranes were mechanized for diverse industrial applications (Lonsdale *et al.* 1982, Pusch *et al.* 1982, Mulder *et al.* 1992). Nowadays, CNT based nanomaterials are frequently using in wastewater treatments due to its huge availability and lesser manufacture cost compare with other nanomaterials (Thines *et al.* 2017). In particular, there are enormous amounts of studies have been performed by the researchers as regards to the rejection of heavy metals from the polluted water.

Weng *et al.* (2009) fabricated various flat-sheet membranes by the addition of various amounts of multi-walled carbon nanotube (MWCNTs) (1 %, 2.5 %, 5 %, 10 % and 15 %) to the organic polymer Poly(bisphenol A-co-4-nitrophthalic anhydride-co-1,3-phenylenediamine) (PBNPI) via solution casting method, to determine the H<sub>2</sub>/CO<sub>2</sub>/CH<sub>4</sub> gas permeability properties of membranes. Membrane characterization performed with various methods such as SEM, FTIR, TGA, XRD, etc. The gas permeability competency of membranes increased continuously with the continuous increment of MWCNTs wt. % in the polymer matrix. In results, continuous gas permeability enhancement was observed from 0 to 15 % membranes (Weng *et al.* 2009).

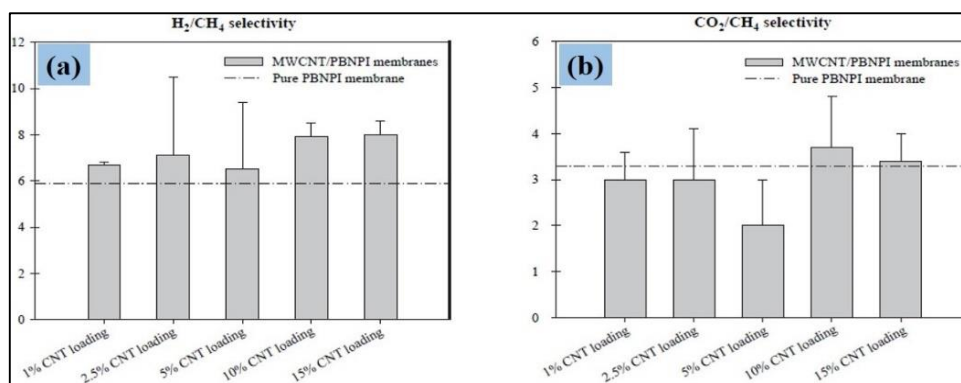


**Figure 4.1** Comparisons of H<sub>2</sub>/CH<sub>4</sub> (a), CO<sub>2</sub>/CH<sub>4</sub> (b) selectivity of PBNPI doped membranes earlier and afterward the addition of MWCNTs/PBNPI (Weng *et al.* 2009)

Pristine MWCNTs and 8-hydroxyquinoline modified MWCNTs (8-HQ-MWCNTs) was used as novel adsorbents to treat the selected metals Cu(II), Pb(II), Cd(II) and Zn(II), from the local plant collected wastewater and red sea water samples. Normally, MWCNTs exhibits good adsorption ability towards deletion of metal contaminants from wastewater. The 8-HQ-MWCNTs showed better rejection efficiency than pristine MWCNTs, due to the observable higher surface area on 8-HQ-MWCNTs (Kosa *et al.* 2012).

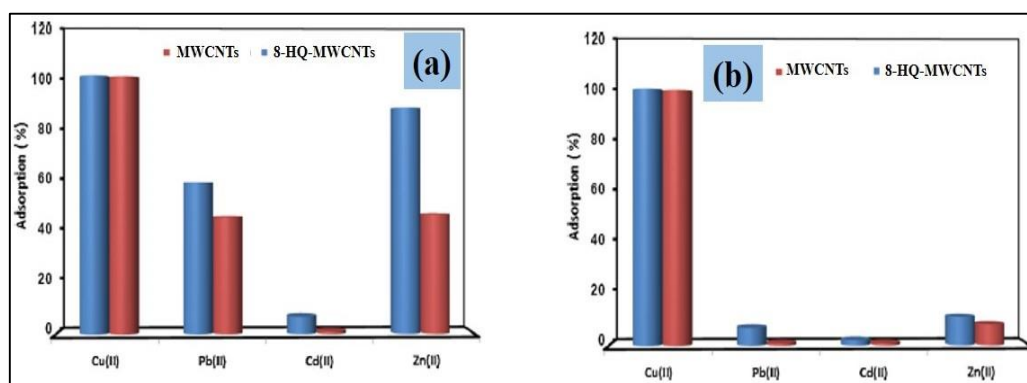


**Figure 4.2** Adsorption performance of selected metal ions, (a) wastewater and (b) Red Sea water (Kosa *et al.* 2012)

Carboxyl, amide, azide functionalized MWCNTs with different wt. % were mixed with polysulfone (PSf) polymer and fabricated flat-sheet membranes by casting process. Here N, N dimethylformamide (DMF) is solvent and water/ isopropanol mixture was as non-solvent for phase separation. The adopted functional groups can form the –H bonds with –SO<sub>2</sub> groups of PSf polymer, so the water contact nature on membrane surface enhanced and, due to that porosity, permeability properties also affected. In results, amide group functionalized MWCNT/PSf membranes exhibited superior performance towards heavy metals adsorption, above 94 % for Cr (VI) and above 78.2 % for Cd (II) ions (Shah *et al.* 2013).

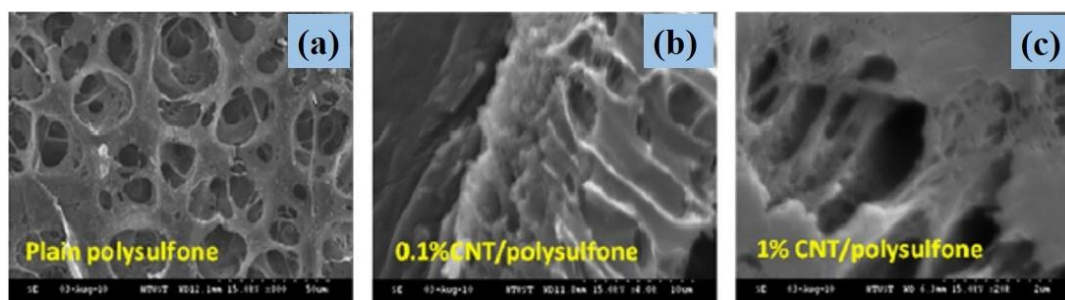


**Figure 4.3** FESEM micrographs of CNT/PSf composite membranes (Shah *et al.* 2013)

Principally, multiwalled carbon nanotubes (MWCNTs) can be chemically modified with thorium oxide ( $\text{ThO}_2$ ) (MWCNTs/ $\text{ThO}_2$ ) and characterized by various instruments such as SEM, TEM, XRD, and with FTIR. The batch adsorption experiment was conducted with MWCNTs/ $\text{ThO}_2$ , to detect the Pb (II) ions from aqueous solution. Atomic absorption spectroscopy (AAS) was used to examine the experimental results (Mittal *et al.* 2016).

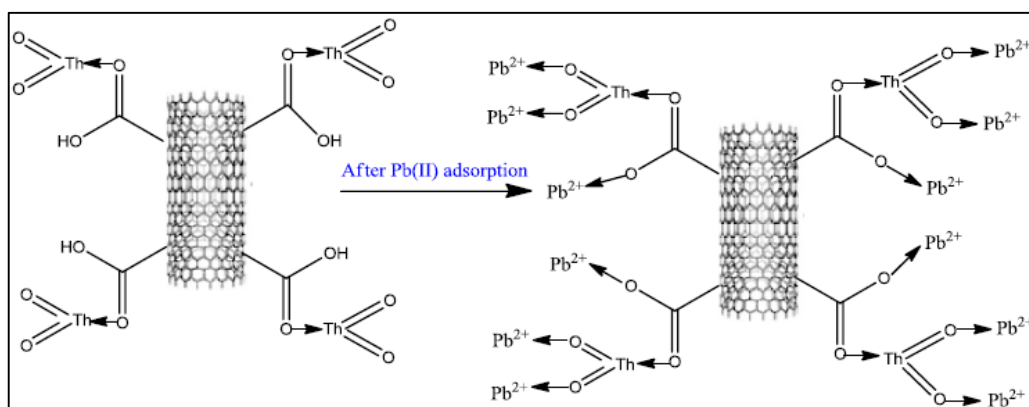


**Figure 4.4** Adsorption of Pb (II) onto MWCNTs/ $\text{ThO}_2$  nanocomposite (Mittal *et al.* 2016)

Moideen and group members fabricated Polysulfone (PSF) and polyphenylsulfone (PPSU) blend flat-sheet membranes by maintaining the different concentrations of PSF, PPSU polymers, to study the polyethyleneimine (PEI) complexed heavy metals rejection efficacy from aqueous media. Poly (ethylene glycol) 1,000 (PEG) was used as a hydrophilic additive to improve the flux ability of membranes. Here the rejection is followed based on size exclusion principle. In results

Observed 99.48 % and 95.5 % with  $\text{Pb}^{2+}$  and  $\text{Cd}^{2+}$  ions, respectively (Moideen *et al.* 2016).

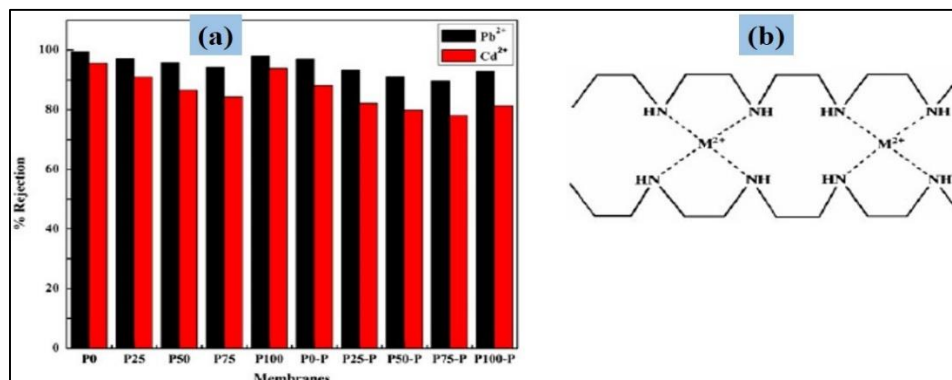
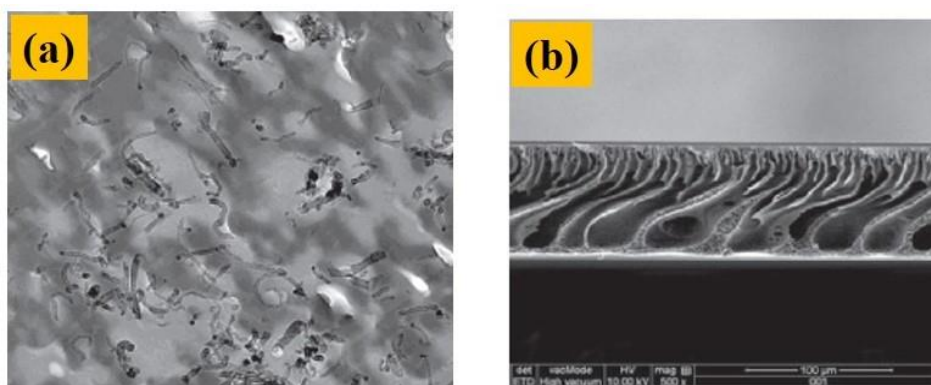


**Figure 4.5** (a) Heavy metals removal efficiency of membranes, (b) Schematic illustration of PEI complexation mechanism with the metal ion (Moideen *et al.* 2016)

Lead (II)-imprinted MWCNTs were synthesized by ion-imprinted technology to enhance the heavy metals adsorption efficiency from aqueous media. Mixed matrix membranes (MMMs) fabricated by the addition of Lead (II)-imprinted MWCNTs to the polyethersulfone (PES) polymeric matrix. The surface wettability and antifouling nature of the membranes were enhanced by increasing the nano additive concentration in the polymer matrix. The heavy metal solution contained with diverse metals  $\text{Pb}^{2+}$ ,  $\text{Zn}^{2+}$ ,  $\text{Co}^{2+}$ , and  $\text{Ca}^{2+}$ . In conclusion, membranes exhibited the heavy metals rejection order as follows:  $\text{Pb}^{2+} > \text{Zn}^{2+} > \text{Co}^{2+} > \text{Ca}^{2+}$  (Sun *et al.* 2017).









surface morphological changes, pure water ultrafiltration performance, fouling ability and polyethyleneimine (PEI) complexed heavy metals removal ability of membranes were systematically studied.

## 4.2 EXPERIMENTAL

### 4.2.1 Materials

PPSU (Radel R-5000) (MW~50,000 g/mol<sup>-1</sup>) was delivered through Solvay Advanced Polymer, Belgium. N-methyl-2-pyrrolidone (NMP) was obtained from Merck India, Ltd. Bovine Serum Albumin (BSA) (MW~69 KDa) procured since CDH Chemicals, India. MWCNTs (>98%), polyvinylpyrrolidone (PVP), lead (II) nitrate (≥99.0 %), cadmium nitrate tetrahydrate (98 %), and mercury (II) chloride (≥99.5%) were procured from Sigma-Aldrich Company. Polyethyleneimine (PEI) ~M.N. 60,000, 50 wt % aqueous solution acquired from New Jersey, USA.

### 4.2.2 PPSU/MWCNT membrane compositions

PPSU/MWCNT membranes fabricated through phase separation process (Shenvi *et al.* 2014). The concentration of MWCNTs in polymer matrix diverse as 0 wt. %, 0.1 wt. %, 0.2 wt. %, 0.3 wt. % and the membranes were categorized as PCNT-0, PCNT-1, PCNT-2, and PCNT-3, respectively (Table 4.1). Then, dispersed in an appropriate volume of NMP solvent and sonicated for 30 min. Further, added 18 g of PPSU polymer, 2 wt. % of PVP and kept for stirring at 60 °C up to 18 h to get a homogeneous solution. Afterward, the dope solution was poured on a glass plate and cast using K-202 control coater instrument. Then immediately glass plate dipped in the water bath for phase inversion (Kumar *et al.* 2013, Pereira *et al.* 2016).

**Table 4.1** Membrane configurations

Membranes	PPSU (g)	NMP (g)	PVP (g)	MWCNT (wt. %)	MWCNT (g)
PCNT-0	18	80	2	0	0
PCNT-1	18	79.982	2	0.1	0.018
PCNT-2	18	79.964	2	0.2	0.036
PCNT-3	18	79.946	2	0.3	0.054



### 4.2.3 Characterization techniques

#### 4.2.3.1 Scanning electron microscope (SEM)

Membrane cross-sectional studies were assessed using the SEM JEOL JSM-6380LA Instrument. The samples for SEM analysis were prepared as explained earlier in section 2.2.4.2 of CHAPTER 2.

#### 4.2.3.2 Atomic force microscope (AFM)

To evaluate the surface topography of membranes, Innova SPM atomic force microscope was used. Dry membrane samples were used, operated in tapping mode and the scan area was  $3 \mu\text{m}^2$ . The surface roughness of membranes stated in terms of average roughness (Ra), root mean square roughness (Rq) and roughness range (Rz) was measured.

To measure the Surface hydrophilic character of prepared membranes was evaluated by following the procedure mentioned in section 2.2.4.3 of CHAPTER 2.

Water uptake and porosity studies of fabricated membranes were done by following the method mentioned in sections 2.2.4.6 and 2.2.4.7 of CHAPTER 2.

The PWF and antifouling capability of the prepared membranes were tested by calculating the flux, FRR values as described in section 2.2.4.4 and 2.2.4.5 of CHAPTER 2. The PWF and BSA flux was measured at 0.3 MPa TMP and performed time-dependent studies maintained two min time interval and continued up to 1 h.

### 4.2.4 Rejection study of toxic heavy metal ions

The lab scale dead-end filter system (Figure 4.9) was used to check the heavy metal ions rejection ability through membranes. The procedure was followed as per the literature (Hebbar *et al.* 2016). A proper amount of aqueous solutions of lead nitrate, mercuric chloride, and cadmium nitrate were prepared in the manifestation of 1 wt. % of PEI. In current study, prepared 500 ppm aqueous solutions of lead nitrate, cadmium nitrate, and 50 ppm of mercuric chloride for the rejection studies. The pH of the resulting prepared solutions was balanced to  $6 \pm 0.2$  with 0.1 M HCl or 0.1 M NaOH solution. These aqueous solutions were stirred up to 5 days at room temperature to take

the complete proper interactions among the metal ions and complexing agent PEI. The 5 cm<sup>2</sup> area membrane samples were fixed in the membrane module cell, after which the aqueous solution was transferred in feed tank and filtered through the membranes. After the permeation study, the permeated samples were assessed by atomic absorption spectrometer. Throughout the study maintained 0.3 MPa TMP, and 40 min time duration was maintained to every membrane sample (PCNT-0 to PCNT-3).

$$\% R = \left(1 - \frac{C_p}{C_f}\right) \times 100 \quad \text{Eq. (4.1)}$$

Where ' $C_p$ ' and ' $C_f$ ' is the heavy metal concentrations of permeate and feed.

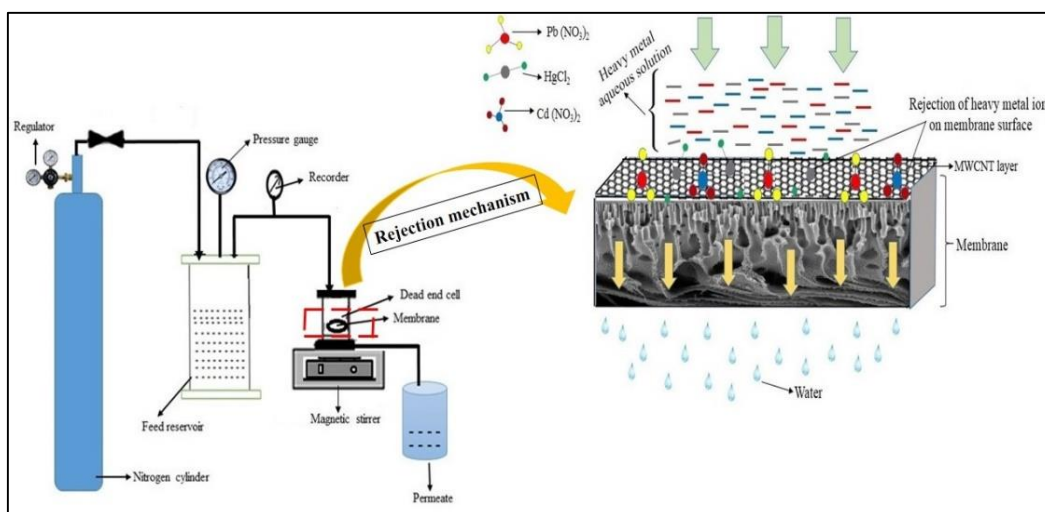


**Figure 4.9** Graphical illustration of heavy metal ions rejection by lab scale dead-end filter setup

After rejection experiment, the dried membrane sample surface was analyzed by SEM, coupled with EDS to identify the elemental mapping analysis of heavy metals on the membrane surface.

## 4.3. RESULTS AND DISCUSSION

### 4.3.1 Contact angle (CA)

Hydrophilic nature of the membranes was assessed by contact angle instrument. In general, the contact angle value is less, hydrophilicity will be more. The neat PCNT-0 membrane exhibited 65.73<sup>0</sup> CA because of the hydrophobic behavior of PPSU. With

increasing the MWCNTs wt. % in the polymer matrix, the continuous decrement in CA found from PCNT-0 to PCNT-3 and reported in Table 4.2. MWCNTs can impact the pore sizes of membranes. The contact angle results arising from PCNT-0 to PCNT-3 due to the fact that, during the phase inversion, the MWCNTs will move to the membrane/liquid partition, thereby decreases the interfacial energy.

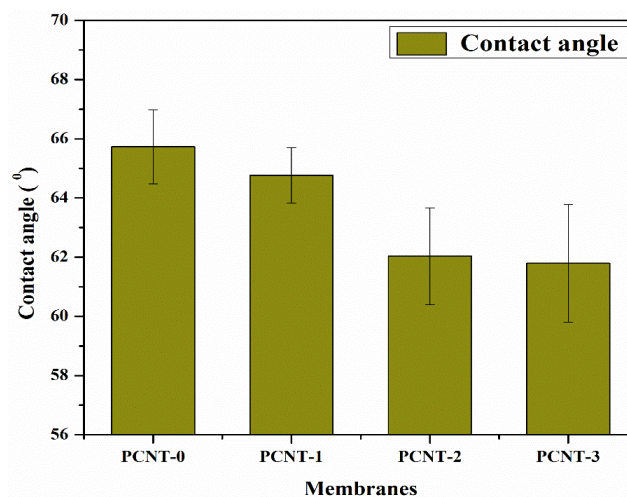


**Figure 4.10** Contact angle results of membranes

**Table 4.2** Membrane possessions

Membranes	Water uptake (%)	Porosity (%)	Contact angle (°)
PCNT-0	66.03± 1.02	41.17± 0.92	65.73 ± 1.25
PCNT-1	68.18± 0.65	37.03± 1.26	64.76 ± 0.94
PCNT-2	70.16± 0.32	46.77± 0.54	62.03 ± 1.63
PCNT-3	70.32± 0.72	50.93± 0.69	61.79 ± 1.98

#### 4.3.2 Porosity and water uptake

Water uptake study is one of the significant variables to define the wettability property of membranes. In results, continuous enhancement was found with water uptake test from PCNT-0 to PCNT-3 membrane (Figure 4.11). Water uptake ability of the membranes be determined by SEM results i.e. the attendance of macro-voids, pores in sub-layer (Ganesh *et al.* 2013). Initially, the water uptake capacity of PCNT-0 membrane was about 66.03 % and it was improved up to 70.32 % by growing the MWCNTs wt. % on PPSU polymer (Table 4.2).

In porosity results, PCNT-1 membrane porosity was decreased, while for PCNT-2 and PCNT-3 membranes porosity increased (Figure 4.11). This is because of the fact that the increase in the additive concentration of MWCNTs in the PPSU polymer matrix, the viscosity of the polymer solution tend to increases. Due to which diffusion of solvent is more favored than in diffusion of non-solvent, leading to decreased porosity. The porosity was increased progressively due to the observable developed finger-like projections and the macrovoids in membranes, which could be observed from Figure 4.13 SEM cross-sectional images. Also, the percentage of PVP drain out during the solvent-nonsolvent exchange process, so the membrane porosity is increasing (Zhao *et al.* 2012).

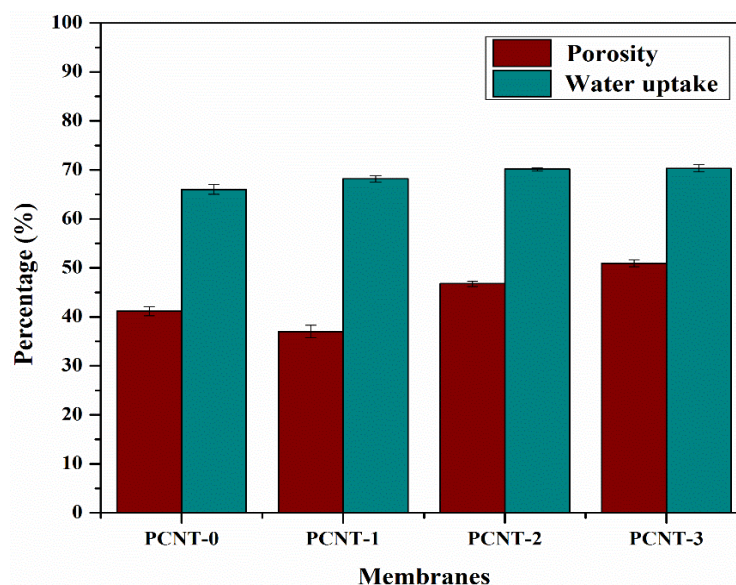


**Figure 4.11** Porosity and water uptake outcomes of membranes

### 4.3.3 Membrane morphology

#### 4.3.3.1 Scanning electron microscopy analysis

The structural changes of fabricated membranes were assessed with SEM analysis. Figure 4.12 displays the images of MWCNTs outlook image and magnified SEM images. MWCNTs with diameters between 96.0 nm and 97.7 nm (Figure 4.12 (B)). The cross-sectional SEM results of fabricated membranes showed asymmetric structures consist with dense skin layer on top and a porous supporting sublayer. With increasing the MWCNTs wt. % percentage in the polymer matrix, the sublayer effectively gets

modified. PCNT-0 membrane contains mainly sponge-like structures and few pear-like small pores as shown in Figure 4.13 (a). With the addition of MWCNTs to the membranes, the asymmetric structure consisting of a dense skin layer on top and a thick porous layer with finger-like pores and macrovoids at the bottom was affected. With increasing the MWCNTs wt. % in PPSU membranes the finger-like channels, macrovoids are increasing gradually and the spongy portion decreased significantly. In membranes containing additives (Figure 4.13 b-d), the presence of few of the horizontal channels, which can progress the water permeability of membranes (Zinadini *et al.* 2014; Wang *et al.* 2012). The added water-soluble additive PVP can affect the pore structures of membranes (Morihamma *et al.* 2014, Nayak *et al.* 2017).

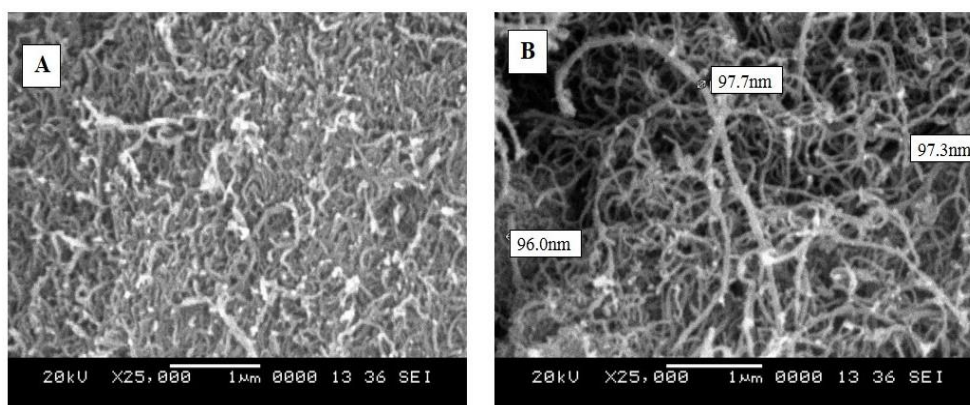


**Figure 4.12** SEM outlook (A), and magnified images of MWCNTs (B)



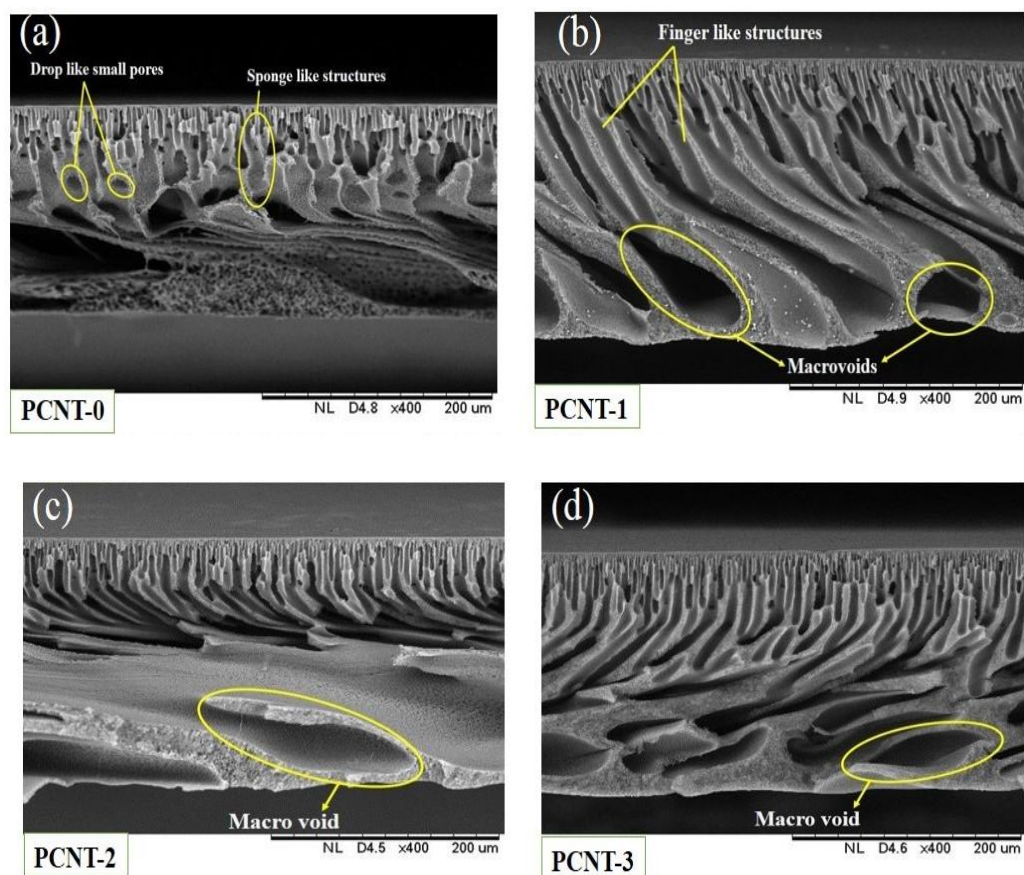


**Figure 4.13** Cross-sectional SEM images of PPSU/MWCNT membranes

#### 4.3.3.2 Atomic force microscopic results

AFM was employed to characterize the surface roughness of polymeric membranes. Table 4.3 represents the obtained surface roughness values of membranes. Figure 4.14 displays the 3-D scanned AFM images of membranes after the analysis. In results, the obtained surface roughness values of composite membranes were clearly greater than the virgin (PCNT-0) membrane. PCNT-3 membrane expressed higher Ra, Rq, and Rz values (21.7 nm, 27.7, nm and 334 nm). The surface roughness of polymeric membranes remarkably and conceptually explains the fouling performance of membranes, which directed to increase the pure water flux eventually (Yu *et al.* 2015).

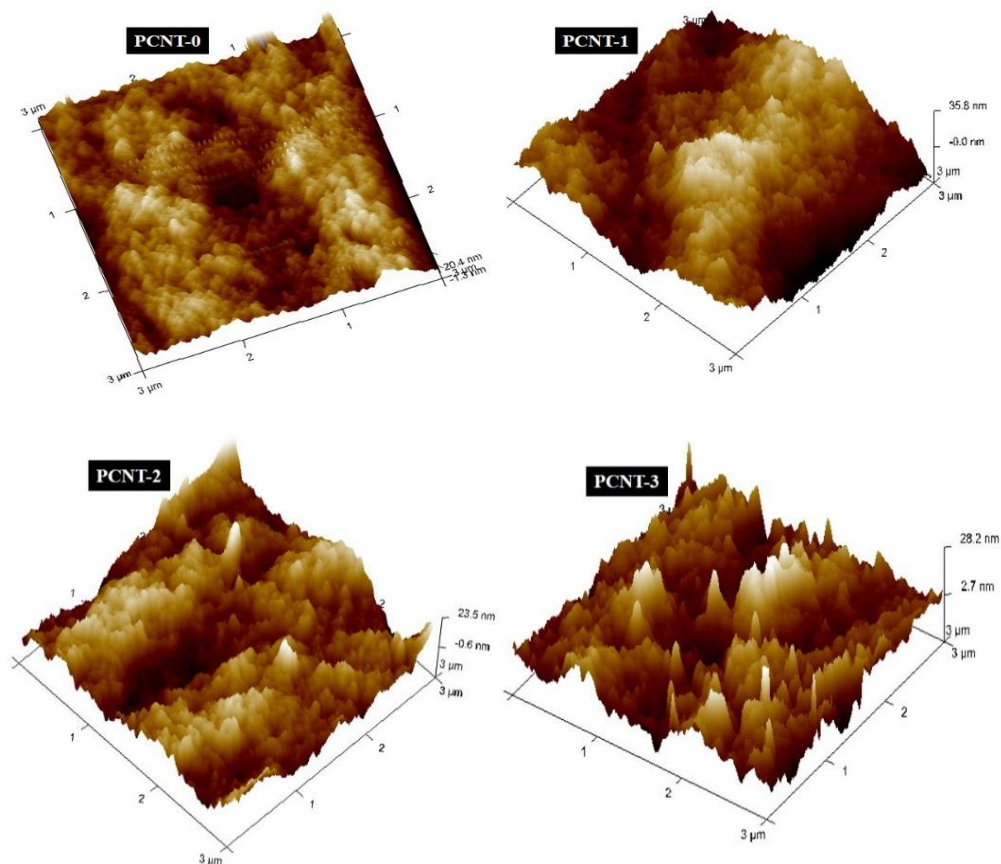


**Figure 4.14** 3D AFM analysis images of membranes

**Table 4.3** Surface roughness limits of membranes

Membrane	Roughness			Surface area ( $\mu\text{m}^2$ )
	$R_a$ (nm)	$R_q$ (nm)	$R_z$ (nm)	
PCNT-0	10.3	13.2	84.3	9.03
PCNT-1	12.7	17.4	146	9.12
PCNT-2	14.8	20.0	204	9.25
PCNT-3	21.7	27.7	334	27.2

#### 4.3.4 Pure water flux

With increasing the MWCNTs wt. % on PPSU, the water permeability also improved from PCNT-0 to PCNT-3 membranes continuously. With PCNT-3 membrane observed enhanced water flux, increased 4 times better than the neat membrane (PCNT-0) (Figure 4.15 (B)). It concludes, the added MWCNTs can impact

the pore sizes of polymeric membranes. PVP was added as a hydrophilic additive to the polymer matrix to increase the pore size of membranes, so there was growth in flux was observed. The morphological changes in membranes were observed in SEM.

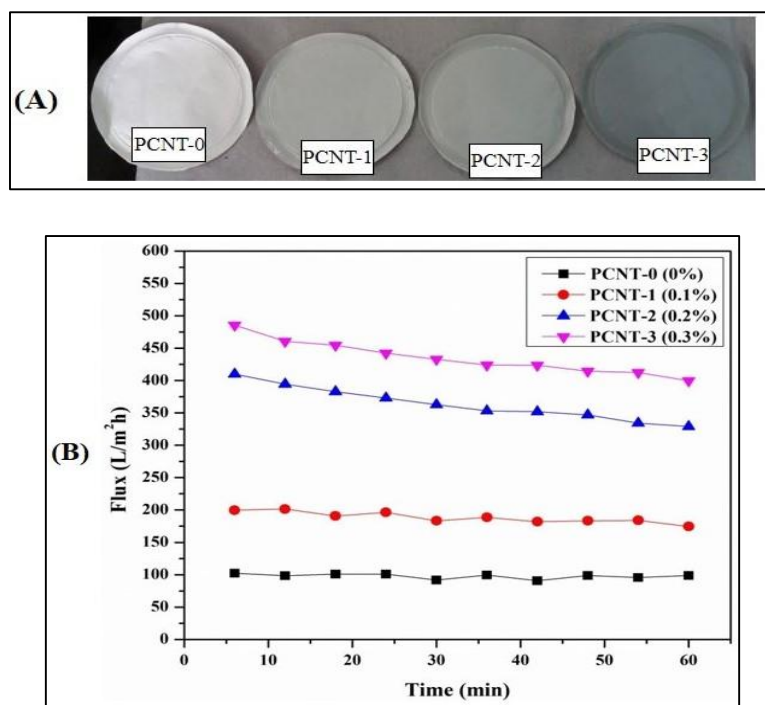


**Figure 4.15** (A) Top surface digital photograph of prepared membranes, (B) PWF outcomes of membranes

#### 4.3.5 Antifouling results

The antifouling performance of membranes was checked with BSA protein flux. After which, the membranes wash away systematically under continuous tap water flow and again repeated PWF study (Figure 4.16 a). With BSA filtration observed less flux compare with PWF, this is because of the larger size effect of BSA molecules. The BSA molecules cannot pass easily through the membrane pores, and deposit on the membrane surface causes the fouling effect. The PCNT-3 membrane exhibited enhanced antifouling outcomes than other membranes due to the authentic membrane fabrication. The higher antifouling ability of membranes was caused by the greater hydrophilic nature of membranes. To inspect the antifouling ability of membranes, the FRR,  $R_t$ ,  $R_r$ ,  $R_{ir}$  results (Figure 4.16 b) of membranes were detailed in Table 4.4.



**Table 4.4** Membrane permeability studies

Membrane code	Permeate flux ( $L/m^2 h$ )			Fouling performance (%)			
	$J_{w1}$	$J_p$	$J_{w2}$	FRR	$R_t$	$R_r$	$R_{ir}$
PCNT-0	41.69	6.80	16.96	40.68	83.68	24.37	59.31
PCNT-1	80.64	8.76	31.68	39.28	89.13	28.42	60.71
PCNT-2	155.98	9.13	58.24	37.33	94.13	31.48	62.66
PCNT-3	185.84	9.52	69	37.12	94.87	32	62.87

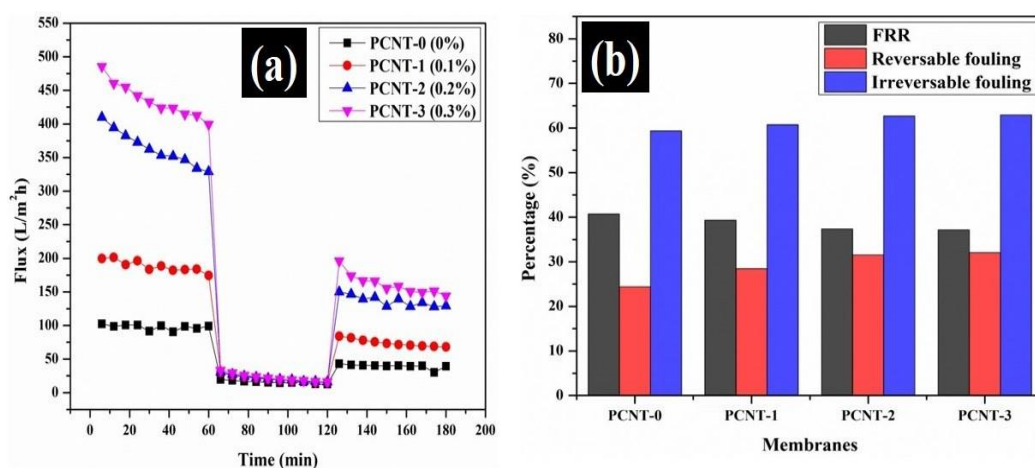


**Figure 4.16** (a) Flux V/s time for membranes at 0.3 MPa under three conditions: PWF; BSA flux; and PWF after systematically wash with water, (b) FRR and antifouling behavior of membranes

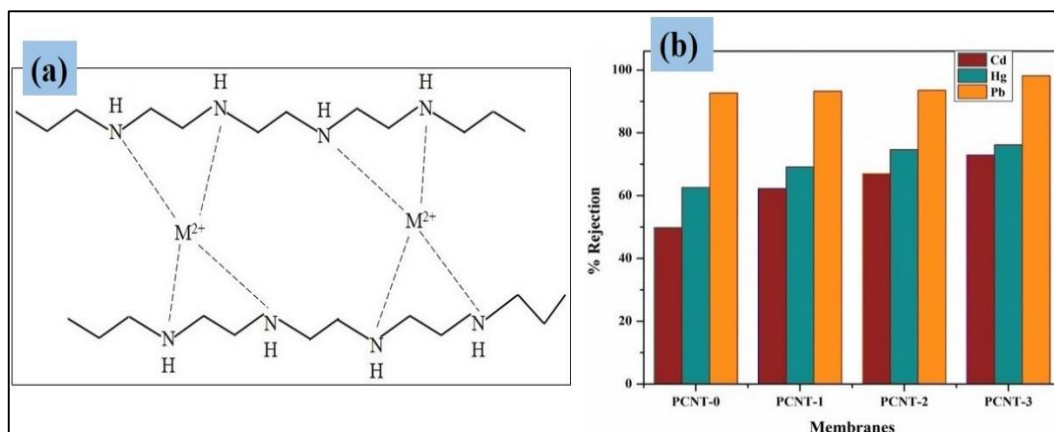
#### 4.3.6 Heavy metal ions rejection results

Heavy metals are highly toxic and can cause serious environmental problems (Zou *et al.* 2009). In the present study, polymer enhanced UF technique was employed to analyze the rejection behavior of selected heavy metal ions such as lead, cadmium, and mercury from laboratory prepared aqueous solution. Added PEI as a strong heavy metal complexing agent (Bolto *et al.* 1995). The heavy metal rejection enhancement was resulted due to the complexation, forms the strong interactions between PEI and heavy metals. After the addition of a complexing agent, obviously, the size of the metal ions will enhance than the membrane pore size. So, the metal ions are retained and

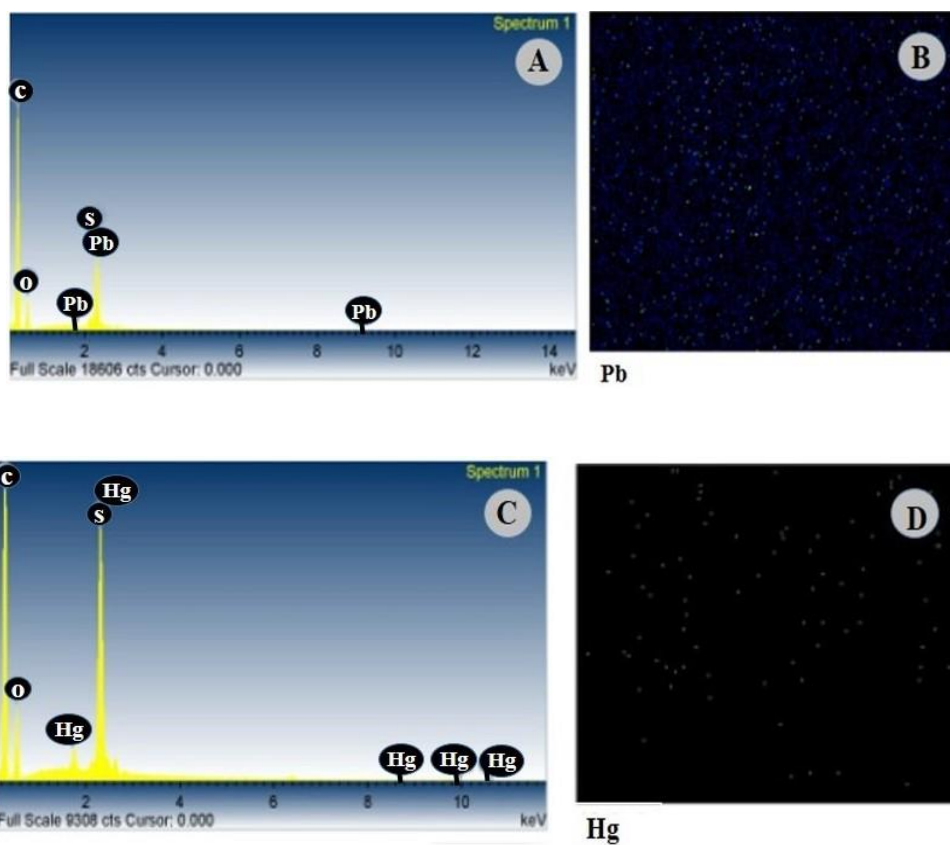
adsorbed on the membrane surface. Here, the sieving mechanism can be proposed (Schaep *et al.* 1998). The heavy metal rejection enhancement observed during the rejection studies could be mainly due to the sieving mechanism.

Throughout the study used double distilled water to prepare the aqueous solution, and pH of the heavy metal solutions fixed at  $6 \pm 0.2$  (acidic medium). The investigational results displayed that, the removal efficacies of metal ions improved progressively with cumulative quantities of MWCNTs on PPSU polymer. The best rejection results were acquired with PCNT-3 membrane, and showed 98.13 % for  $\text{Pb}^{2+}$  ions, 76.12 % for  $\text{Hg}^{2+}$  ions and 72.92 % for  $\text{Cd}^{2+}$  ions respectively (Figure 4.17 b).

Takagishi *et al.* (1985) proposed a complexation mechanism between various divalent metal cations and polyethyleneimine (PEI). The complexation mechanism between the PEI and metal ions expressed in Figure 4.17 (a). In results, the rejection percentage of  $\text{Pb}^{2+}$  ions is more as compared with  $\text{Cd}^{2+}$  ions, because the  $\text{Pb}^{2+}$  ions form larger complexes with PEI molecules as compare with  $\text{Cd}^{2+}$  ions (Liang *et al.* 2012). For  $\text{Hg}^{2+}$  ions rejection study, 50 ppm aqueous solution was used. Because, only at lower concentrations, mercury forms favorable sites with PEI. As the mercury concentration increases, then all the available sites gets the bind and fill with the mercury ions, this results in less rejection (Uludag *et al.* 1997). The increasing order of heavy metal ion rejection % of all membranes to  $\text{Pb}^{2+}$ ,  $\text{Hg}^{2+}$  and  $\text{Cd}^{2+}$  ions: PCNT-0 < PCNT-1 < PCNT-2 < PCNT-3. Figure 4.18 describes the information about SEM-EDS analysis results (A, C and E) and elemental mapping results (B, D, and F) of PCNT-3 membrane after the rejection of  $\text{Pb}^{2+}$ ,  $\text{Hg}^{2+}$  and  $\text{Cd}^{2+}$  ions.



**Figure 4.17** Graphical representation of heavy metal complexation with PEI (a), heavy metal ions rejection results of membranes (b)



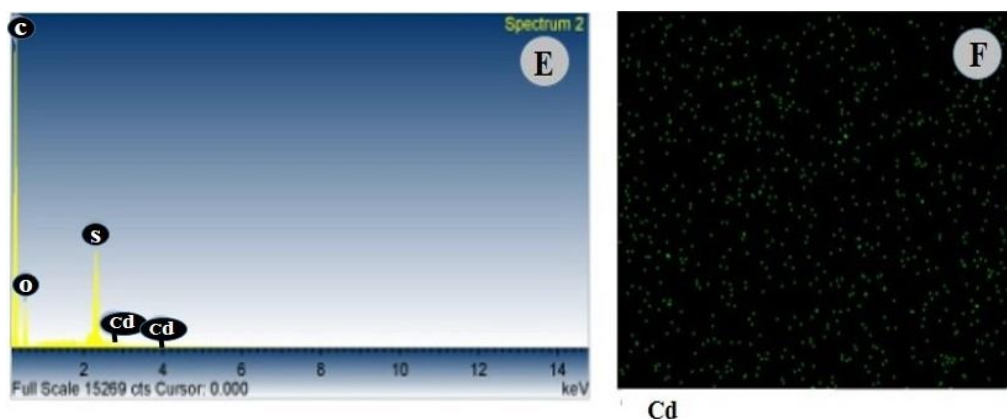


**Figure 4.18** A, C and E are the SEM-EDS analysis results of PCNT-3 membranes and B, D and F are the elemental mapping descriptions of  $\text{Pb}^{2+}$ ,  $\text{Hg}^{2+}$  and  $\text{Cd}^{2+}$  ions

#### 4.4 CONCLUSIONS

In summary, the PPSU/MWCNT/PVP membranes were prepared by the phase separation method. Experimental results showed enhanced permeability and good rejection ability with increasing the MWCNTs concentration on PPSU polymer. The added MWCNTs can impact the pore sizes of membranes. The PWF, antifouling property, hydrophilicity, porosity, water uptake and morphology of membranes were investigated. The PCNT-3 membrane showed PEI complexed heavy metal ions rejection performance of 98.13 %, 76.12% and 72.92 % for  $\text{Pb}^{2+}$ ,  $\text{Hg}^{2+}$ , and  $\text{Cd}^{2+}$  ions, respectively. In heavy metals rejection process sieving mechanism was involved, and in result observed the metal formed the larger complex with PEI exhibited greater rejection performance. Due to the greater complex formation nature, the rejection percentage of  $\text{Pb}^{2+}$  ions is higher than  $\text{Hg}^{2+}$  and  $\text{Cd}^{2+}$  metal ions.

## **CHAPTER 5**

# **NOVEL PPSU/ NANO TIN OXIDE MIXED MATRIX ULTRAFILTRATION HOLLOW FIBER MEMBRANES WITH ENHANCED ANTIFOULING PROPERTY AND TOXIC DYES REMOVAL**



## **Abstract**

*Novel Polyphenylsulfone (PPSU)/nano Tin oxide (SnO<sub>2</sub>) mixed matrix hollow fiber membranes were fabricated by dry-wet spinning via phase separation process for the removal of toxic reactive dyes such as Reactive black-5 (RB-5) and Reactive orange-16 (RO-16) from aqueous media. Different techniques were engaged to characterize the membranes such as Scanning Electron Microscopy (SEM), Energy Dispersive Spectroscopy (EDS), Atomic Force Microscopy (AFM), contact angle, water uptake, and porosity, etc. The cross-flow filter unit was engaged to conduct the permeability and dye separation studies. Membranes showed better water permeability, antifouling, and enhanced dye removal results by increasing the of SnO<sub>2</sub> NPs wt. % in PPSU polymer. PS-3 membrane exhibited high potential for dyes rejection application, of about 94.44 % for RB-5, and 73.09 % for RO-16 dye.*

## **5.1 INTRODUCTION**

Nowadays, a large amount of different types of dyes are used in different industrial applications, such as paper, textile, plastic, rubber, cosmetic, etc. in various processes (Grag *et al.* 2004). Normally such industries require a large amount of fresh water, particularly in textile industries. The released dye wastages and wastewater from the above industries are directly entering into the atmosphere and causing several environmental difficulties. These dyes have specific characteristics towards heat, light and biologically non-degradable. In earlier, several developments are defined towards dye removal from wastewater, such as sedimentation, adsorption (Rekha *et al.* 2015), liquid–liquid abstraction (Gharehbaghi *et al.* 2012), membrane filtration (Daas *et al.* 2010, Salleh *et al.* 2011), electrochemical oxidation and biological treatments (Dasgupta *et al.* 2015), etc.

Currently, membrane technology is considerable, superior in comparison with other techniques due to its specific characteristics such as cost-effectiveness, low energy consumption, easily scalable, simple and high efficacy, and non-chemical involvement ability (Baker *et al.* 2004). Membranes possess better rejection efficacy at low osmotic pressure. Different types of polymeric membrane materials, such as polysulfone (PSf) (Koseoglu-Imer *et al.* 2013), poly (vinylidene difluoride) (PVDF) (Liu

*et al.* 2011), polyethersulfone (PES) (Ouyang *et al.* 2015), cellulose acetate (CA) (Idris *et al.* 2006), polyacrylonitrile (PAN) (Li *et al.* 2014), and polyphenylsulfone (PPSU) (Nayak *et al.* 2017) have been practically used in various membrane separation processes.

Tin oxide ( $\text{SnO}_2$ ) is a good semiconductor photocatalyst, and attentively active in gas sensing applications (Korotcenkov *et al.* 2003), solar cells (Mao *et al.* 2016), photo catalytical devices (Pan *et al.* 2015), and in electrode materials (Kim *et al.* 2014) due to its better optical and electrical properties.

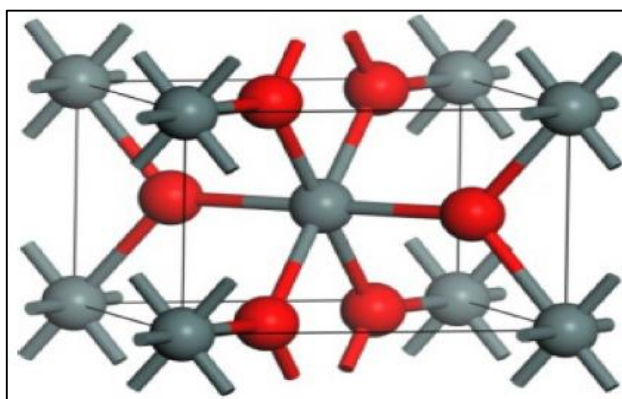


**Figure 5.1**  $\text{SnO}_2$  unit cell structure

(<https://en.wikipedia.org/wiki/Rutile#/media/File:Rutile-unit-cell-3D-balls.png>)

Tin oxide ( $\text{SnO}_2$ ) reinforced UF membranes fabricated by a sol-gel casting method, to evaluate the permeability properties of membranes with various salt solutions such as  $\text{NaCl}$ ,  $\text{CaCl}_2$ ,  $\text{Na}_2\text{SO}_4$ , and  $\text{CaSO}_4$  etc. at different pH levels. The cross-flow filter unit was applied to examine the salts permeability performance. Ionic exchange chromatography was employed to determine the salt solutions feed and permeate concentrations. The selectivity enactment increment order of membranes as follows as:  $\text{CaCl}_2 > \text{NaCl} > \text{CaSO}_4 > \text{Na}_2\text{SO}_4$  (Santos *et al.* 2001).



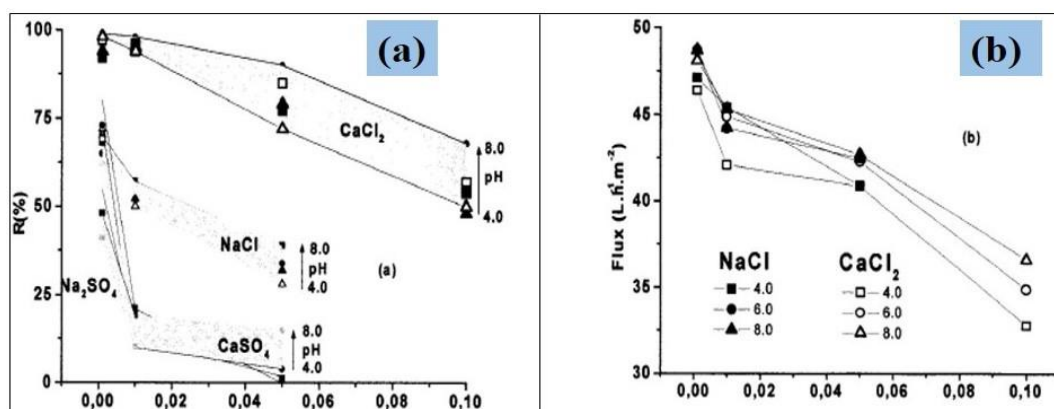


**Figure 5.2** Retention coefficient (a), permeate flux (b) of the different salts solutions (Santos *et al.* 2001)

Tin oxide nanoparticles (SnO<sub>2</sub> NPs) synthesized via a sol-gel method and modified with different wt. % of Tiron (OH)<sub>2</sub>C<sub>6</sub>H<sub>2</sub>(SO<sub>3</sub>Na)<sub>2</sub> (1-20 wt. %) to improve the membrane presentation. The main reason behind the modification is to fabricate the SnO<sub>2</sub> crack-free ceramic membranes. Tiron grafted on SnO<sub>2</sub> NPs and characterized with X-ray powder diffraction (XRPD), extended X-ray absorption fine structure (EXAFS), quasi-elastic light scattering and electrophoretic mobility tests, etc. In conclusion, Tiron grafted SnO<sub>2</sub> ceramic membranes influence the morphology, pore sizes of ceramic membranes (Belin *et al.* 2003).

Tin oxide doped Titania (TDT) nanofibers prepared by controlled hydrolysis method, to study the dye degradation efficacy of nanofibers. TDT nanofibers characterized by FESEM, powder XRD, TEM and with BET surface analyzer. The purpose of adding SnO<sub>2</sub> to TiO<sub>2</sub> was to improve the molecular sieve channels and the surface pore sizes. In results, TDT nanofibers exhibited effective dye degradation performance than TiO<sub>2</sub> nanofibers (Xiong *et al.* 2007).

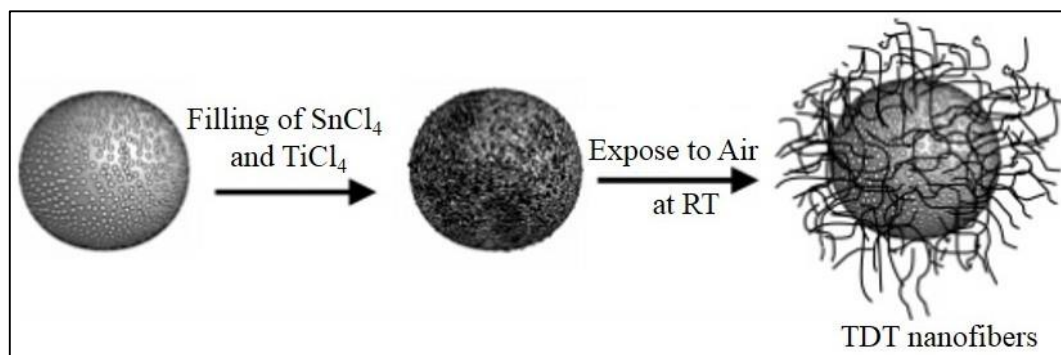


**Figure 5.3** Formation Process of TNT nanofibers from Mesoporous Silica (Xiong *et al.* 2007)

Zhu *et al.* (2011) demonstrated the preparation of tin oxide (SnO<sub>2</sub>)/ zinc oxide (ZnO) Quantum dots (QDs) (5 nm diameter), and immobilized on cross-linked chitosan films (SnO<sub>2</sub>/ZnO/chitosan films) by the solution casting method. Various techniques such as XRD, SEM, and HRTEM employed to characterize the SnO<sub>2</sub>/ZnO/chitosan films. Photocatalytic decolorization experimentations accompanied by initial methyl orange (MO) concentration of 10 mg L<sup>-1</sup> with 0.7 g L<sup>-1</sup> SnO<sub>2</sub>/ZnO/chitosan films, within 210 min of reaction. In conclusion, kinetic study results indicated that, by pseudo-first-order model SnO<sub>2</sub>/ZnO/chitosan films exhibited above 99 % of MO dye decolorization (Zhu *et al.* 2011).

Tin oxide nanoparticles (SnO<sub>2</sub> NPs) doped on reduced graphene oxide sheets (RGO-SnO<sub>2</sub>), to enhance the photocatalytic activity of organic dye methylene blue (MB) in aqueous solutions. The uniform distribution of SnO<sub>2</sub> NPs on GO surface was detected with SEM, HRTEM and found the average size of SnO<sub>2</sub> NPs 3-5 nm. In conclusion, RGO-SnO<sub>2</sub> presented good photocatalytic results compare with bare SnO<sub>2</sub> NPs under sunlight irradiation (Seema *et al.* 2012)

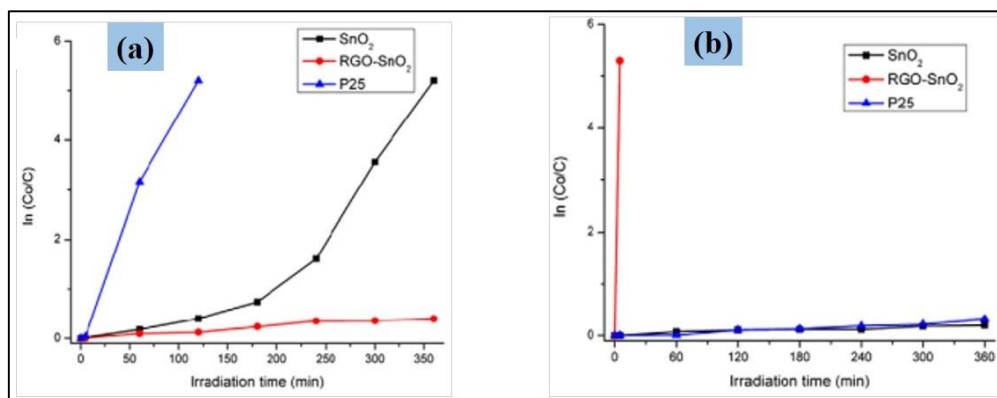


**Figure 5.4** MB photodegradation by SnO<sub>2</sub>, RGO–SnO<sub>2</sub> and P25 under UV irradiation (a), under sunlight (b) (Seema *et al.* 2012)

Stannic oxide (SnO<sub>2</sub>) NPs developed by Gram-negative bacteria *Erwinia herbicola* via green bio-synthesis process and characterized through dynamic light scattering (DLS) particle size analyzer, TEM, SEM-EDS, and XRD techniques. Afterward, the bio SnO<sub>2</sub> NPs photocatalytic ability was observed with various industrial dyes such as methylene blue, methyl orange, and erichrome black T (EBT) degradation experimentations. Degradation results were found to 93.3 % for methylene blue, 97.8 % for erichrome black T and 94 % for methyl orange (Srivastava *et al.* 2014).

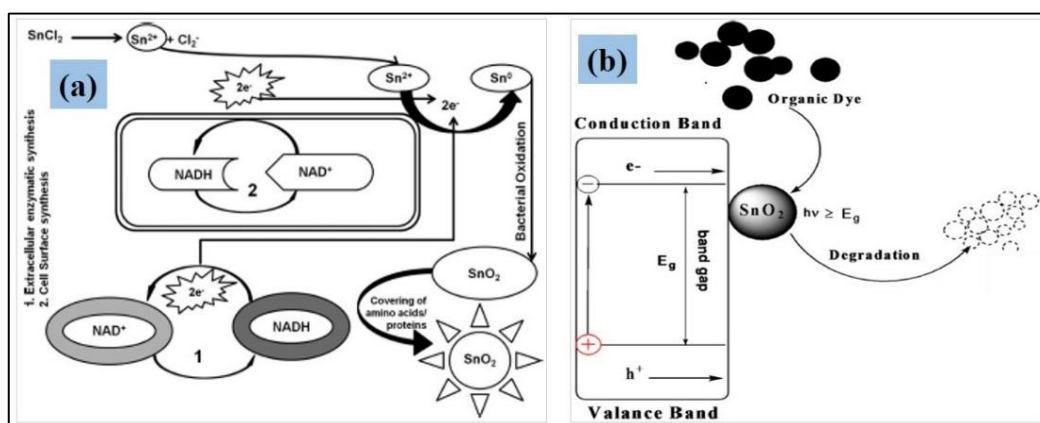


**Figure 5.5** (a) Biosynthesis of SnO<sub>2</sub> nanoparticles (b) photocatalytic degradation procedure of dyes by SnO<sub>2</sub> NPs (Srivastava *et al.* 2014)

Novel green adsorbents such as activated carbon synthesized from wood tree *Pistacia Atlantica* (AC-PAW) and SnO<sub>2</sub> NPs loaded activated carbon (SnO<sub>2</sub>-NP-AC) were synthesized, to study the methyl orange (MO) adsorption capability from aqueous

solutions. Least squares support vector regression (LSSVR) and multiple linear regressions (MLR) models were engaged for adsorption tests. The purpose of loading of SnO<sub>2</sub>-NPs on the activated carbon is to increase the adsorption efficiency on the surface. The LSSVR model showed better results as compared with MLR methods towards dye removal applications (Ghaedi *et al.* 2016).

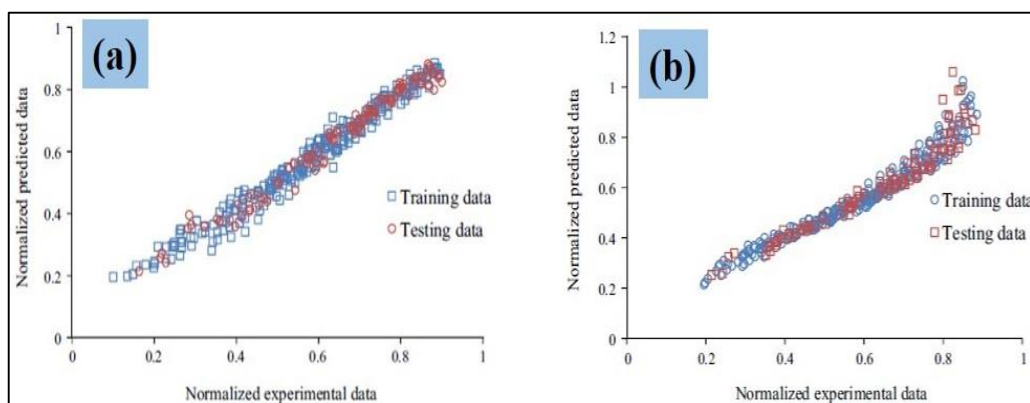


**Figure 5.6** Investigational data v/s expected data MLR (a), LSSVR (b) (Ghaedi *et al.* 2016)

Green tin oxide nanoparticles (SnO<sub>2</sub> NPs) were synthesized by microwave heating process and used as an effective catalyst to study the photocatalytic degradation of organic dyes such as methyl violet 6B (MV6B) and methylene blue (MB) from aqueous solution. SnO<sub>2</sub> NPs were characterized by FTIR, XRD, TEM (average size 13-17 nm) instruments, and the dyes photocatalytic degradation results were examined by Liquid chromatography–mass spectrometry (LC-MS) study (Bhattacharjee *et al.* 2016).

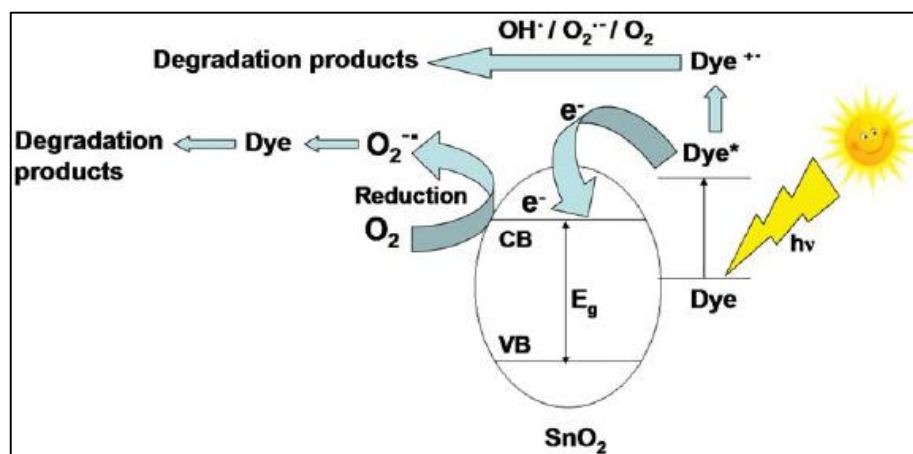


**Figure 5.7** Possible mechanism of dye degradation under SnO<sub>2</sub> photocatalyst (Bhattacharjee *et al.* 2016)

Natural SnO<sub>2</sub> NPs prepared by guava (*Psidium Guajava*) leaf extraction via simple cost-effective method to study the photocatalytic behavior of SnO<sub>2</sub> NPs under sunlight. SnO<sub>2</sub> NPs were characterized by SEM-EDS, TEM, and XRD. 40 ppm concentrated textile dye reactive yellow 186 (RY 186) was chosen as a dye material and UV visible spectroscopy was employed to analyze the dye degradation results. In conclusion, the SnO<sub>2</sub> NPs showed effective photocatalytic results, above 90 % degradation under sunlight (Kumar *et al.* 2018).

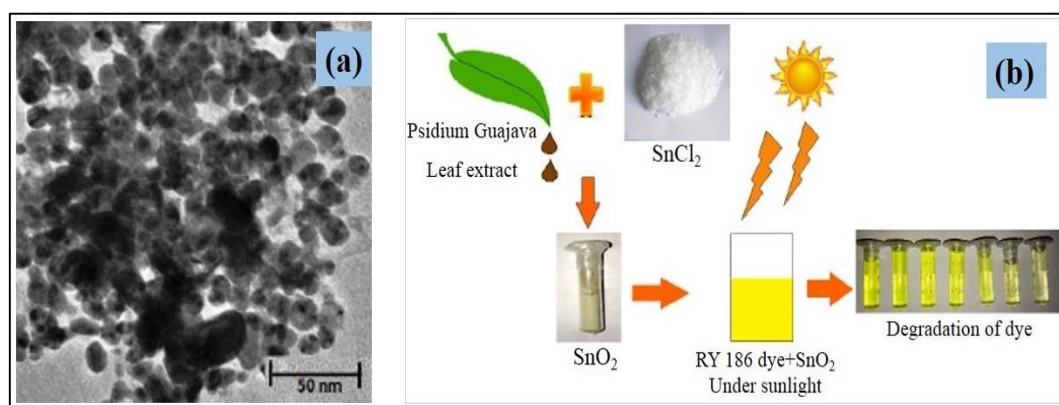


**Figure 5.8** (a) TEM image of SnO<sub>2</sub> NPs (8-10 nm) and (b) dye degradation mechanism (Kumar *et al.* 2018)

Poly (vinyl alcohol) (PVA) based thin film composite (TFC) membranes fabricated with the incorporation of SnO<sub>2</sub> NPs with different wt. % in PVA polymer, over poly (ether sulfone) (PES) as a base layer on TFC membranes. Afterward, membranes characterization was performed with FESEM, SEM-EDS, TGA, AFM, contact angle and check the permeability with PWF and the fouling behavior with humic acid flux. The main objective of the current study was to determine the acid and reactive dyes rejection capability through the membranes. The SnO<sub>2</sub> NPs contained membranes exhibited superior dye rejection performance as well as the enhanced flux recovery ratio (Babu *et al.* 2018).

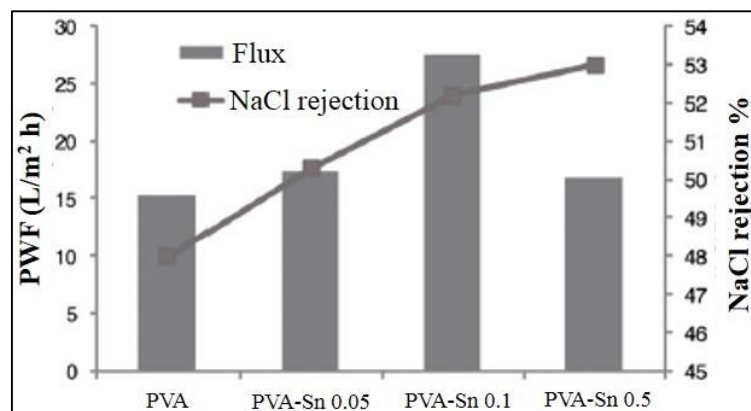


**Figure 5.9** Flux and rejection performance of the membranes (Babu *et al.* 2018)

In cotton industries, there is frequent use of reactive dyes to color the cellulosic fibers via the dyeing process. However, these reactive dyes are the reasons to cause serious ecological problems (Jiraratananon *et al.* 2000). Wastewater contained Reactive Black 5 dye mostly released from textile industries and causing several health issues. Reactive orange 16 dye is another good dyeing agent in textile units (Carneiro *et al.* 2004). These dyes are hazardous to wildlife and showed high resistance towards wastewater management, cause ecological difficulties, and degradation of these dyes is one of the main disadvantage (Chatterjee *et al.* 2010).

The above literature survey concludes that most of the researchers used SnO<sub>2</sub> NPs and modified SnO<sub>2</sub> NPs as a good adsorbing agent towards photocatalytic degradation, removal of dyes and other contaminants from wastewater. Till today the usage of SnO<sub>2</sub> NPs in membrane technology is very much limited. Keeping in view of the importance of the SnO<sub>2</sub> NPs and requirements of efficient and economical separation membranes, it was planned to fabricate nano SnO<sub>2</sub>/ PPSU/ PVP mixed matrix hollow fiber membranes. In the current research, Polyphenylsulfone (PPSU) was used as a principle polymeric membrane material due to its specific characteristics such as chemical stability, solvent-resistance ability, and better mechanical properties, hydrophobicity, high-temperature resistance, etc. (Darvishmanesh *et al.* 2011). In the present investigation, PPSU/nano SnO<sub>2</sub>/ PVP mixed matrix HFMs fabricated and employed to investigate the dye removal efficacy from wastewater. SEM, AFM, contact angle, MWCO, water uptake, and porosity studies were employed to characterize the

fabricated membranes. The cross-flow filter cell engaged to examine the HFMs permeability properties as well as the dye rejection ability.

## 5.2 EXPERIMENTAL

### 5.2.1 Materials

The key polymer PPSU (MW~50,000 g/mol) was delivered through Solvay Advanced Polymer, Belgium. Tin oxide nanoparticles (SnO<sub>2</sub>-NPs) (< 100 nm), Bovine Serum Albumin (BSA) (MW~66 KDa), polyvinylpyrrolidone (PVP) (~MW 36,000), dyes RO-16 and RB-5 were obtained from Sigma-Aldrich Co., USA. N-methyl-2-pyrrolidone (NMP) was procured from Merck Ltd. Germany. Polyethylene glycol (PEG) 6000 Da, PEG 10000 Da and PEG 20000 Da were procured from Merck, India Ltd.

### 5.2.2 Fabrication of PPSU/SnO<sub>2</sub> mixed matrix hollow fiber membranes

The extreme amount of SnO<sub>2</sub> and PVP was added to the principle polymer PPSU, so as to get the superior flux and rejection results. The PPSU/nano SnO<sub>2</sub> mixed matrix HFMs were fabricated by a dry-wet spinning, phase separation method, and the temperature maintained at 26 °C ± 1. The chosen amounts of SnO<sub>2</sub> NPs with 0 wt. %, 0.1 wt. %, 0.2 wt. %, and 0.4 wt. % was added to the NMP solvent, followed by sonication up to 40 min for the proper dispersion of nanoparticles. Moreover added 16 g of PPSU, 4 g of PVP and then kept for stirring at 65 °C followed by 24 h to get a homogeneous solution. The obtained dope solution was degassed in the sonicator. The membrane compositions were drafted in Table 5.1.

The above-obtained dope compositions were moved through the spinneret under constant nitrogen pressure, as explained in the Chapter-3, Figure 3.10 HFMs fabrication unit schematic representation and used deionized water as a bore fluid. The detailed spinneret parameters were given in Table 5.2. Maintained 6 cm air gap between the spinneret and the treatment bath (water). Both dope solutions and bore fluids were arisen extreme head on the spinneret and pass through on it, after enters into the treatment baths. Because of the phase inversion process immediately fibers will form, then the attained hollow fibers collect together at collecting drum. The obtained HFMs



kept in water for 24 h, and again membranes were placed in 10 % aqueous glycerol solution for post-treatment about 24 h. Afterward, the HFMs fully dry at normal room temperature and used for further studies (Nayak *et al.* 2017). The fabricated membranes were labeled as PS-0, PS-1, PS-2, and PS-3.

**Table 5.1** Membrane configurations

Membranes	PPSU (g)	NMP (g)	PVP (g)	SnO <sub>2</sub> (wt. %)	SnO <sub>2</sub> (g)
PS-0	16	80	4	0	0
PS-1	16	79.984	4	0.1	0.016
PS-2	16	79.968	4	0.2	0.032
PS-3	16	79.936	4	0.4	0.064

**Table 5.2** Spinning parameters of HFMs

Parameter	Condition
Spinneret (mm)	1.1 (OD)/0.55 (ID)
Dope solution	PPSU/SnO <sub>2</sub> /PVP/NMP
Bore flow rate (mL/min)	2.5
Bore fluid	Distilled water
Air gap (cm)	6
Treatment bath	Distilled Water
Washing bath temp.	26 °C

### 5.2.3 CHARACTERIZATION

To investigate the structural and surface morphological properties of SnO<sub>2</sub> NPs and fabricated HFMs used Zeiss Sigma Field Emission scanning electron microscopy (FESEM) instrument (Model: EVO MA18), and the incorporated SnO<sub>2</sub> NPs in membrane matrix was documented by SEM-EDS. The samples for SEM analysis were prepared as explained earlier in section 2.2.4.2 of CHAPTER 2.

The surface morphologies of laboratory-fabricated membranes were analyzed by using Innova SPM atomic force microscope (AFM). The scan area was maintained



3  $\mu\text{m} \times 3 \mu\text{m}$ . The HFM samples analysis procedure was explained earlier in section 4.2.3.2 of CHAPTER 4.

To measure the surface wettability character of prepared HFMs was evaluated by following the procedure mentioned in section 2.2.4.3 of CHAPTER 2.

To examine the water uptake and porosity studies of fabricated HFMs were done by following the method mentioned in sections 3.2.3.3 of CHAPTER 3 and 2.2.4.7 of CHAPTER 2.

The PWF and the antifouling ability of the prepared membranes were tested by calculating the flux, FRR values as described in sections 3.2.3.5 of CHAPTER 3 and 2.2.4.5 of CHAPTER 2. The PWF and BSA flux were measured at 0.2 MPa TMP and performed time-dependent studies maintained two min time interim for each of the membrane sample and continued up to 40 min.

#### **5.2.3.1 Molecular weight cut-off (MWCO) experiment**

To study the fabricated HFMs MWCO study, polyethylene glycol (PEG) with different molecular weights 6000, 10000 and 20000 Da were used to propose the type of membrane. In PEG filtration experiment, 500 ppm concentrated solution was preferred and did at 0.2 MPa TMP, and the results analyzed by the Eq. 5.1. The rejection with above 90 % can agree with the MWCO of the membrane. Usually, ultrafiltration membranes show the MWCO range between 1000–100000 Da (Ng *et al.* 2013). PS-3 membrane was used in filtration test, and different PEG solutions feed and permeate concentrations were examined using total organic carbon (TOC) (Model: TOC-L SHIMADZU TOC analyzer) instrument.

#### **5.2.4 Dyes rejection experimental methodology**

The laboratory prepared PPSU/SnO<sub>2</sub> HFMs dye rejection ability was examined by using cross flow filter unit (Figure 5.10). In the present work, dyes engaged in the rejection experiment were RO-16, RB-5 dye aqueous solutions with 50 ppm concentration. The pH was well-preserved at  $6.6 \pm 0.2$ . The dye rejection experimental conditions were maintained as stated in the PWF study, up to 40 min. After which the feed solution and collected permeates dye concentrations were evaluated by HACH,

DR/5000 UV-visible spectroscopy instrument (Zhong *et al.* 2003), at a wavelength of 596.89 nm to RB-5 and 493.64 nm to RO-16 dye. The equilibrium dye flux was determined by assessing the volume of permeates collected in a 2 min time interval. In dye rejection experiment, three trials were performed with each sample and reported the average data standard deviation reports. Eq. 5.1 employed to determine the rejection % of membranes,

$$\% R = \left(1 - \frac{C_p}{C_f}\right) \times 100 \quad \text{Eq. (5.1)}$$

Where ' $C_p$ ' and ' $C_f$ ' are the dye concentrations in permeate feed.

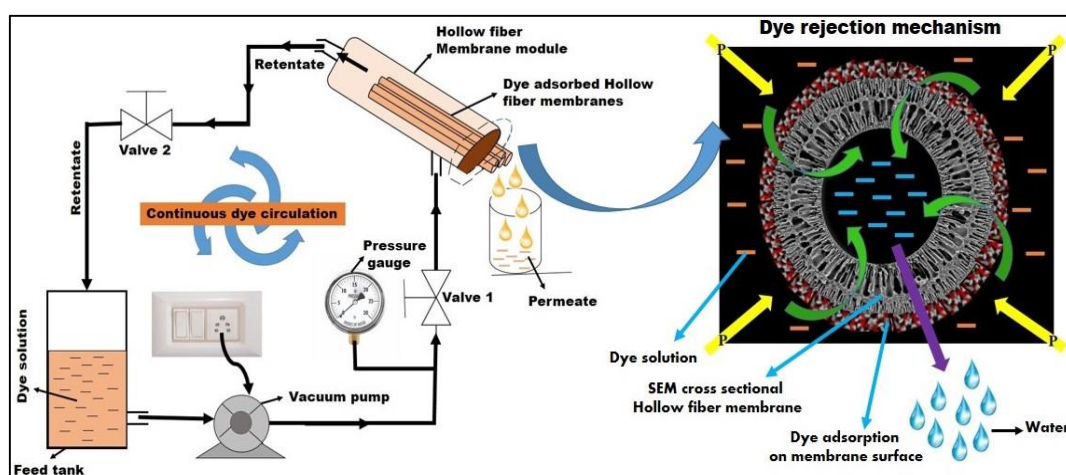


**Figure 5.10** Lab scale cross-flow filter unit and graphical representation of dye rejection mechanism

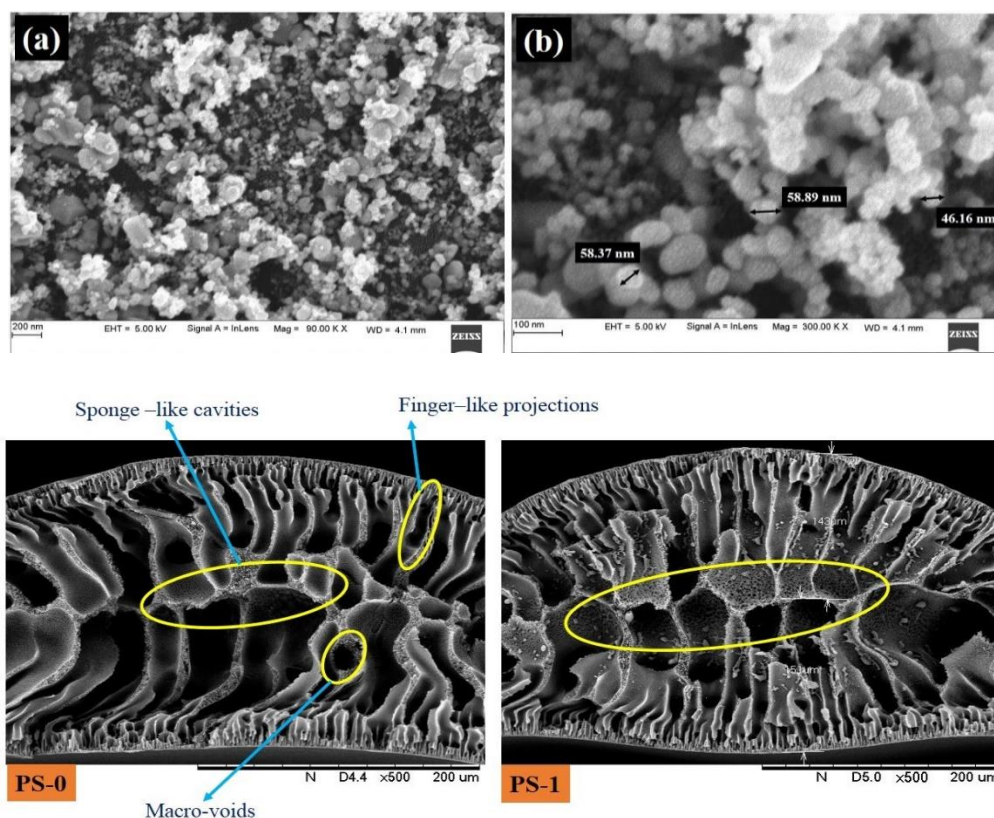
## 5.3 RESULTS AND DISCUSSION

### 5.3.1 Membrane morphological results

#### 5.3.1.1 SEM morphology

The surface morphological properties of SnO<sub>2</sub> NPs (Figure 5.11 a&b) and invented HFMs cross-sectional, structural properties were examined by using FESEM. From the obtained results, the SnO<sub>2</sub> NPs thickness obtained was close to the range between 46.16 nm and 58.89 nm (Figure 5.11 b). Figure 5.11 (PS-0 to PS-3) reveals the information regarding HFMs SEM cross-sectional morphological characteristics. It can be observed that the HFMs exhibited typically asymmetric structures with relatively

dense top skin layer and porous sublayers. In sub layers observed, few of the specific characteristics i.e. finger-like, sponge-like projections with closed ends and macro-voids (Chen *et al.* 2015 and Verma *et al.* 2015). These morphological changes in plane and blend membranes elucidated by the phase inversion method. Throughout the phase inversion stage, the polymer precipitation progression is usually precise by kinetic and thermodynamic assets, and that can impact the morphology of the membrane (Neill *et al.* 2000). By increasing the additive SnO<sub>2</sub> NPs wt. % in membranes, the appreciable changes noticed in porous sublayer. The finger-like, sponge-like projections and macro-voids are mounting continuously from PS-0 to PS-3 membranes. In few membranes (PS-1 to PS-3) several horizontal networks were observed. These channels effect the permeability property that means increases the flux behavior (Wang *et al.* 2012). Surprisingly, in the PS-3 membrane (Figure 5.11) observed the closed ends of sponge-like cavities are explored, it will affect the permeability property. This is also one of the reasons to raise the flux of PS-3 membrane. Water-soluble PVP will influence the hydrophilicity and pore morphologies of membranes (Morihamma *et al.* 2014).



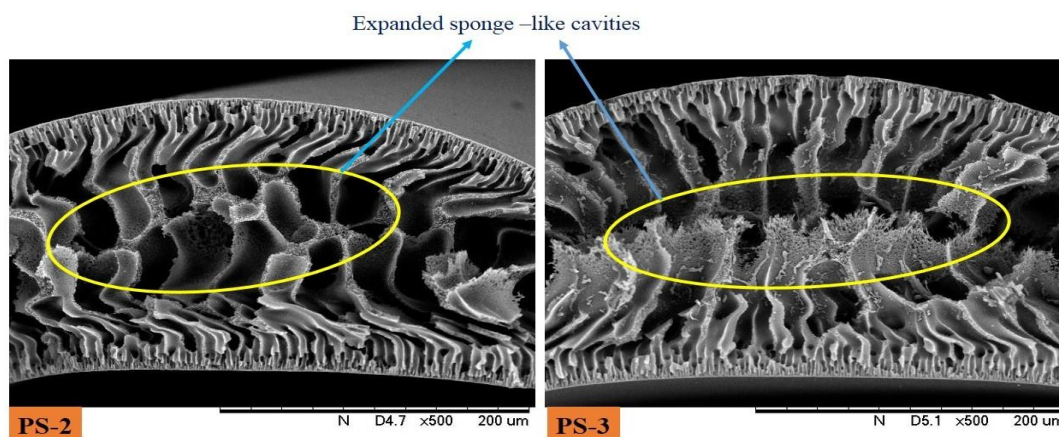


**Figure 5.11** SEM outlook image (a), magnified image of SnO<sub>2</sub> NPs (b), and PS-0, PS-1, PS-2 and PS-3 are the SEM cross-sectional images of HFMs

In the PS-3 membrane, the presence of additives tin and other elements was detected through FESEM-EDS analysis (Figure 5.12).

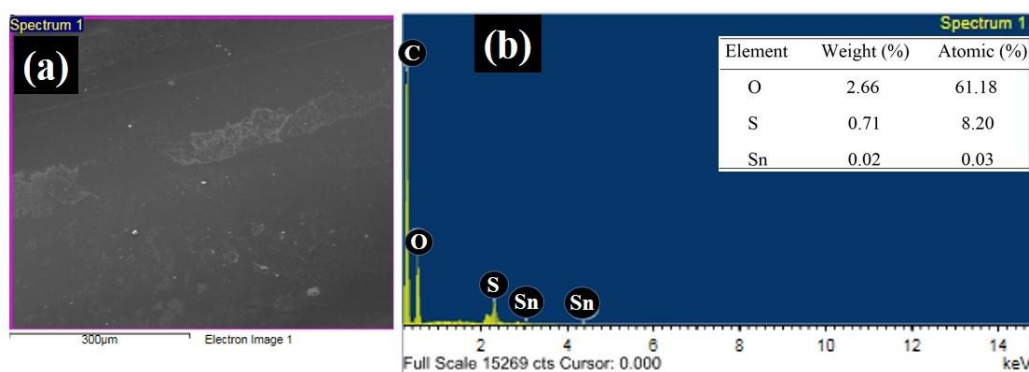


**Figure 5.12** PS-3 membrane FESEM surface outlook (a), EDS analysis result (b)

### 5.3.1.2 Atomic force microscopy results

AFM was utilized to illustrate the surface topography characteristics of the membranes. Figure 5.13 reveals the information regarding three dimensional AFM images of fabricated membranes. Surface roughness concept explains the permeability property of membranes. It means, ultimately the permeability of membranes will increase (Chen *et al.* 2015). From PS-0 to PS-3, by increasing the SnO<sub>2</sub> NPs wt. % in membranes, the continuous surface roughness enhancement has occurred, and values



are stated in Table 5.3. The higher additive membrane (PS-3) expressed higher Ra, Rq, and Rz values (24.1 nm, 38.2, nm and 372 nm).

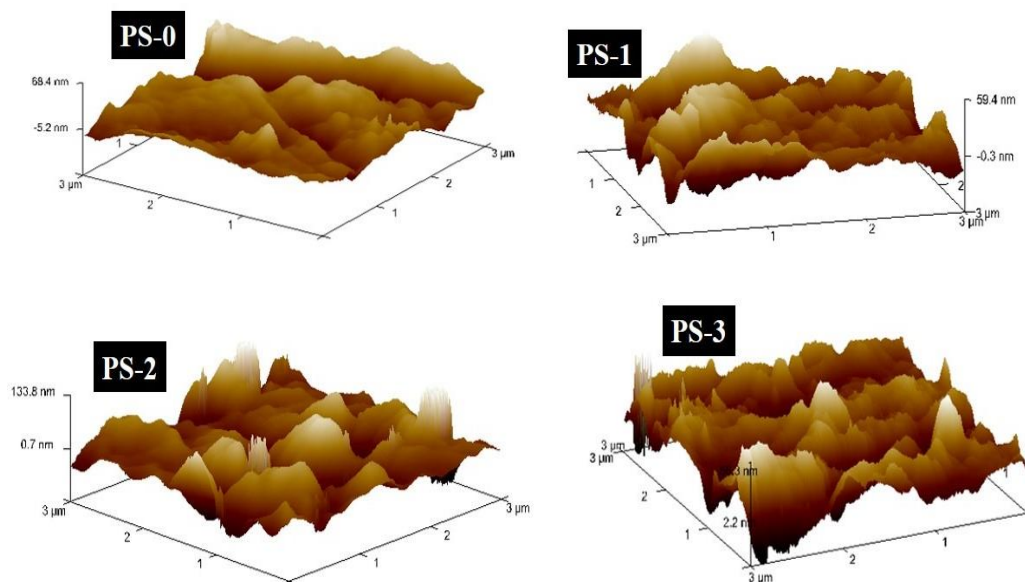


**Figure 5.13** AFM 3-D images of membranes

**Table 5.3** Surface roughness variables of membranes

Membrane	Roughness			Surface area ( $\mu\text{m}^2$ )
	R <sub>a</sub> (nm)	R <sub>q</sub> (nm)	R <sub>Z</sub> (nm)	
PS-0	13.8	19.0	135	9.16
PS-1	15.3	19.2	157	9.35
PS-2	22.0	28.9	235	9.53
PS-3	24.1	38.2	372	10.2

### 5.3.2 Contact angle

The prepared virgin and blend membranes surface wettability nature was assessed by contact angle measurement studies. The virgin membrane (PS-0) showed the highest CA value  $74.55 \pm 0.3^\circ$ , corresponds low affinity towards hydrophilicity. After the continuous addition of SnO<sub>2</sub> NPs to the membranes, the CA values tend to decrease (Figure 5.14). That means the significant enhancement was observed in hydrophilicity of membranes. CA values are decreased from  $74.55 \pm 0.3^\circ$  to  $63.77 \pm 4.4^\circ$ , due to the SnO<sub>2</sub> NPs effect and reported in Table 5.4. The reducing order of CA:

PS-0 < PS-1 < PS-2 < PS-3. It concludes that the added nano additive SnO<sub>2</sub> was acted as a hydrophilic agent and improved the hydrophilic property of membranes. The higher hydrophilic nature of the membrane showed a higher affinity towards permeability properties (Liao *et al.* 2010).

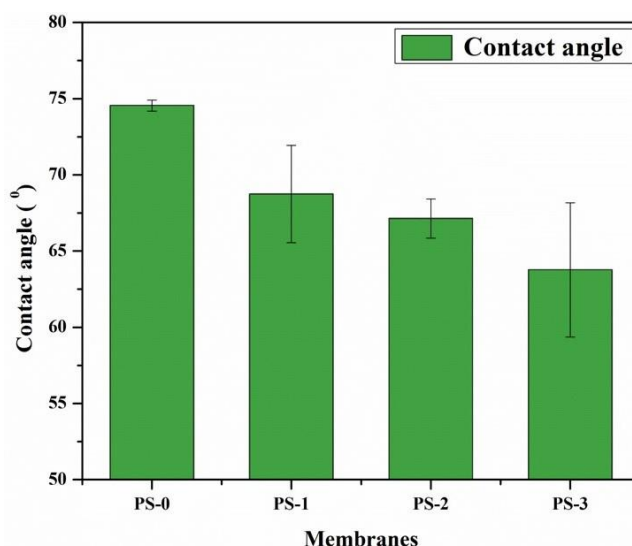


**Figure 5.14** Contact angle results of membranes

### 5.3.3 Water uptake and porosity

Water uptake study is a unique and major parameter to describe the hydrophilic property of the membranes. With increasing the SnO<sub>2</sub> NPs wt. % in membranes, the significant development was observed in water uptake and porosity results (Figure 5.15). The same has been depicted in Table 5.4. The porosity was improved progressively due to the noticeable developed finger-like projections and the macrovoids in membranes, which could be observed from Figure 5.11. The added pore forming additive PVP was also one of the reasons to enhance the porosity of membranes (Wang *et al.* 2012).

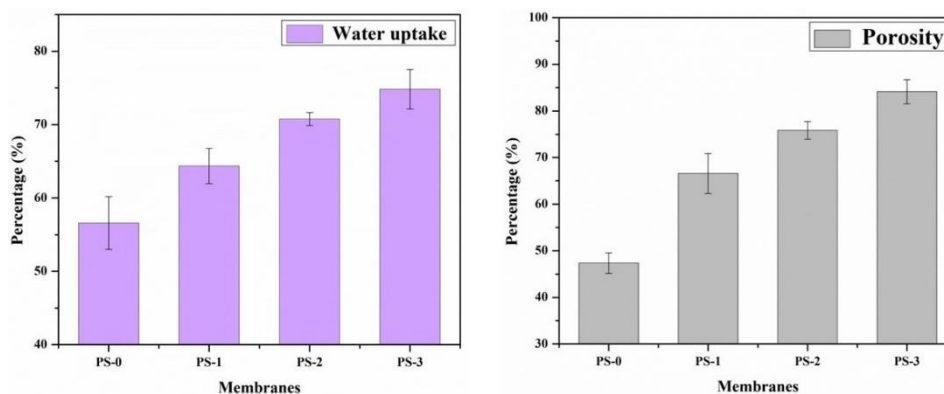


**Figure 5.15** Water uptake and porosity outcomes of membranes

**Table 5.4** Membrane properties

Membranes	Water uptake (%)	Porosity (%)	Contact angle (°)
PS-0	56.57 ± 3.6	47.34 ± 2.2	74.55 ± 0.3
PS-1	64.35 ± 2.4	66.59 ± 4.3	68.74 ± 3.1
PS-2	70.75 ± 0.9	75.83 ± 1.9	67.14 ± 1.2
PS-3	74.82 ± 2.7	84.13 ± 2.6	63.77 ± 4.4

### 5.3.4 Molecular weight cut-off (MWCO) results

MWCO results of membranes were evaluated with total organic carbon (TOC) analyzer instrument. Figure 5.16 stated the information regarding MWCO studies of higher additive (PS-3) membrane. From the results, the further increment was observed in rejection percentages with increasing the PEG concentrations. PEG with 20000 Da showed above 90 % rejection. The obtained results can conclude that the fabricated membranes belong to ultrafiltration category.

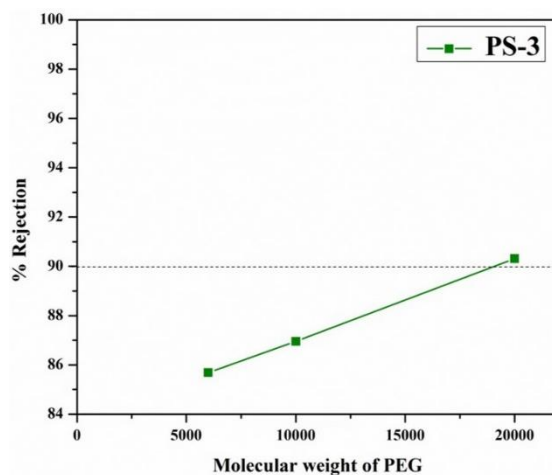


**Figure 5.16** MWCO results of PS-3 membrane

### 5.3.5 Pure water flux

Time resultant PWF study was performed with all the membranes (Figure 5.17). The fabricated HFMs showed best results with pure water. The PWF of membranes improved rapidly with enhancing the additive SnO<sub>2</sub> NPs wt. % in the polymer matrix. Especially with additive 0.2 wt. % and 0.4 wt. %, the PWF of membranes increased four times and six times better than the pristine membrane (PS-0) respectively. The permeability reached from 62.70 L/m<sup>2</sup> h (PS-0) to 362.91 L/m<sup>2</sup> h (PS-3). Sometimes membrane morphology will also affect the PWF, the changes observed with SEM cross-sectional study. Added additive PVP can affect the morphological characteristics of membranes, hence observed enhanced PWF results.

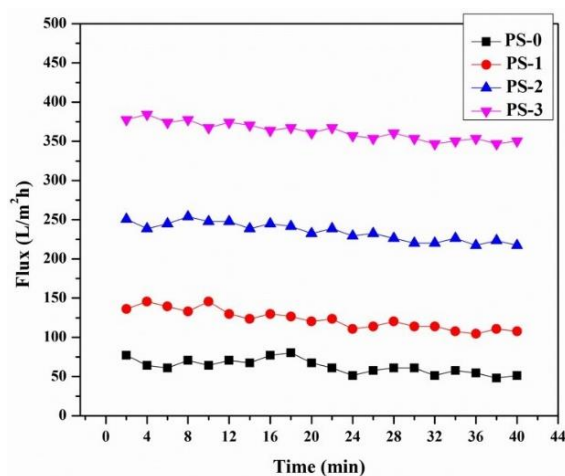


**Figure 5.17** Time-dependent PWF result of membranes



### 5.3.6 Antifouling study

The HFMs time dependent fouling resistance and long-standing stability was observed with BSA protein flux study (Figure 5.18 a). While performing the antifouling study, the flux was observed very less as compared to PWF study due to the surface pore blockage phenomena. In general, the BSA protein size is very large in comparison with water molecules, and these BSA molecules had the affinity towards hydrophilic surfaces, so proteins will effortlessly adsorb on the membrane surface. Hence, less flux observed compared with PWF. Continuous enhancement in BSA flux noticed from 22.56 L/m<sup>2</sup> h (PS-0) to 106.44 L/m<sup>2</sup> h (PS-3), this is due to the effect of hydrophilic additive PVP and the continuous enhancement of SnO<sub>2</sub> NPs wt. % in membranes (PS-0 to PS-3). The fouling resistance of membranes was intended with flux recovery ratio (FRR), and the obtained higher FRR values proposes the membranes better antifouling properties (Figure 5.18 b), and reported in Table 5.5.

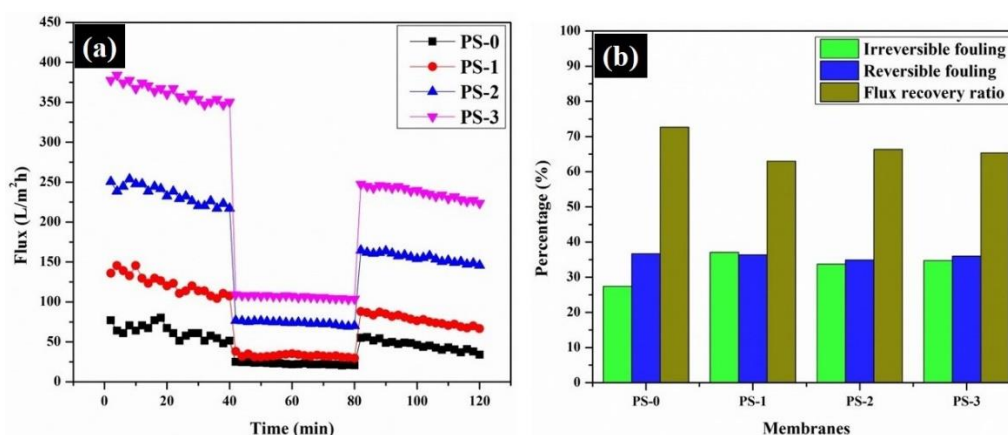


**Figure 5.18** (a) Flux v/s time for membranes at 0.2 MPa under three environments: water flux; BSA flux; and again water flux (b) FRR and antifouling outcomes of membranes

**Table 5.5** Membrane permeability studies

Membrane code	Permeate flux (L/m <sup>2</sup> h)			FRR	Fouling performance (%)		
	J <sub>w1</sub>	J <sub>p</sub>	J <sub>w2</sub>		R <sub>t</sub>	R <sub>r</sub>	R <sub>ir</sub>
PS-0	62.70	22.56	45.54	72.63	64.01	36.65	27.36
PS-1	122.79	32.70	77.31	62.96	73.36	36.33	37.03
PS-2	234.58	73.70	155.55	66.31	68.58	34.89	33.68
PS-3	362.91	106.44	237.01	65.30	70.67	35.97	34.69

### 5.3.7 Dye rejection and dye flux performance of membranes

The selected hazardous reactive dyes RB-5 and RO-16 with 50 ppm aqueous solution rejection experiments were performed with the cross-flow filter system. SnO<sub>2</sub> NPs was used as a good adsorbing agent towards removal of textile dyes, chromium, and other contaminants from aqueous solutions (Foletto *et al.* 2011 and Han *et al.* 2017). Throughout the study double distilled water was used to make the aqueous solutions, and the experiment performed at lab temperature 25 °C ± 1. The experimental results showed that, with increasing the additive SnO<sub>2</sub> NPs wt. % on PPSU polymer, the dye rejection efficacy also increasing progressively. Figure 5.19, A & B reveals the information regarding dye removal competence of membranes. From Figure 5.19, C1 & C2 clearly it can be able to find, the permeated solutions were nearly going to reach colorless. In the present study, the reactive dyes rejection execution mainly related to the molecular weights of dyes, it means the dye with high molecular weight express superior performance towards dye rejection (Ahmad *et al.* 2006). The molecular weight of RB-5 dye is 991.82 g/mol, and RO-16 dye is 617.54 g/mol. From the above information, it can conclude that the RB-5 dye rejection will be more compared with RO-16 dye. In outcome, the PS-3 membrane performed well and resulted in dye rejection 94.44 % for RB-5, and 73.09 % for RO-16 dye. The fabricated PPSU/nano SnO<sub>2</sub> based HFMs dye flux observed with the higher additive membrane (PS-3), results found with a decrease in dye flux. The PS-3 membrane showed average dye flux of 169.06 L/m<sup>2</sup> h for RO-16 and 109.77 L/m<sup>2</sup> h for RB-5 and reported in Figure 5.19, D. While performing the dye filtration study, the flux conditions maintained as similar to PWF study.

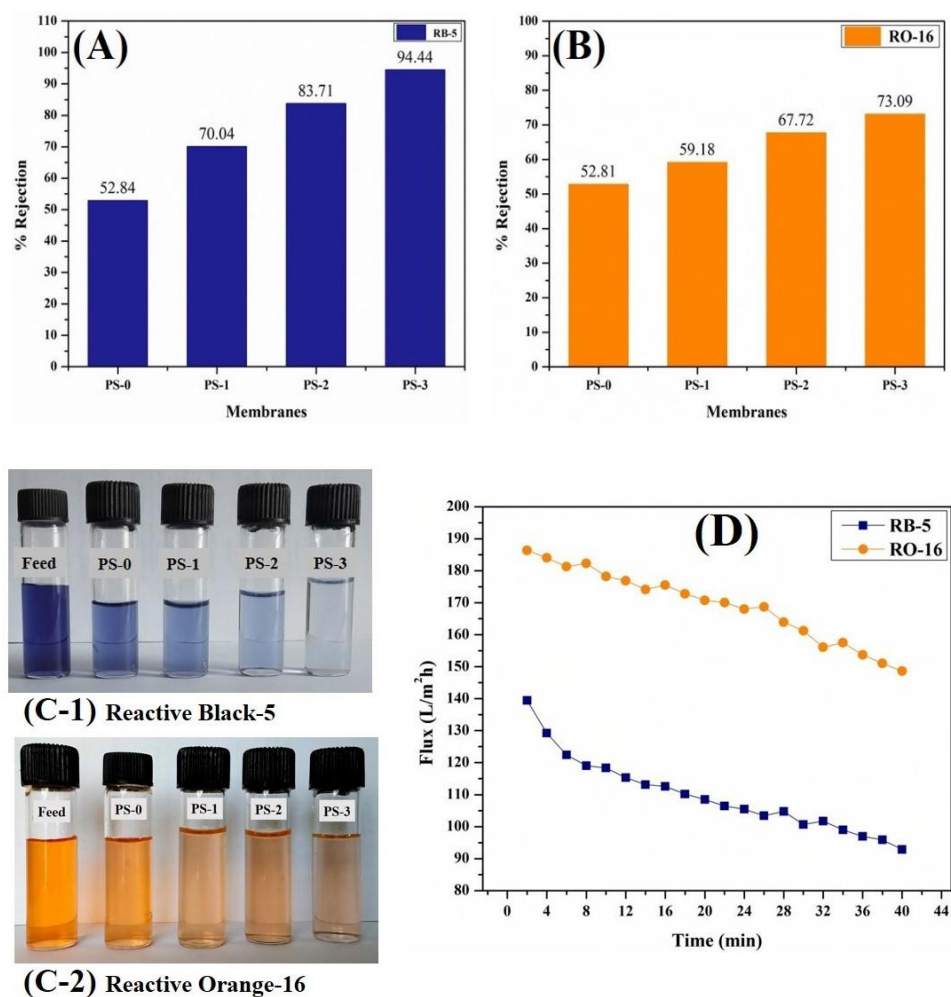


**Figure 5.19** A & B are the dye rejection results of membranes, C-1 & C-2 are the outlook images of dye permeates, D is the time-dependent dye flux of PS-3 membrane,

## 5.4 CONCLUSIONS

The present research is focused on the fabrication of novel PPSU/nano SnO<sub>2</sub> mixed matrix hollow fiber membranes by dry-wet spinning via phase inversion method for the rejection of selective toxic dyes RB-5 and RO-16 from aqueous solutions. By increasing the SnO<sub>2</sub> NPs wt. % in membranes, PS-0 to PS-3 showed enhanced results with various approaches, such as contact angle, scanning electron microscope, atomic force microscope, water uptake, and porosity, PWF, and BSA flux. Cross-flow filter cell was applied to perform the PWF, BSA protein flux and dye rejection study. The higher additive membrane (PS-3) revealed the best performance towards dyes rejection experiment and exhibited 94.44 % for RB-5, and 73.09 % for RO-16 dye.



## **CHAPTER 6**

**NOVEL PPSU/ NANO ALUMINIUM TRIOXIDE DOPED  
ACID TREATED ACTIVATED CHARCOAL  
INCORPORATED MIXED MATRIX MEMBRANES FOR  
EFFICIENT REMOVAL OF PROTEINS, HEAVY  
METALS, AND OIL/WATER EMULSION SEPARATION**



**Abstract**

*Polyphenylsulfone (PPSU)/ nano aluminium trioxide doped acid treated activated charcoal (Al<sub>2</sub>O<sub>3</sub>-AAC) incorporated mixed matrix UF membranes were fabricated by nonsolvent induced phase inversion process (NIPS). These membranes were used for the removal of proteins, heavy metals from aqueous media and for oil/water emulsion separation. The purpose of acid treatment of activated charcoal is to increase the micropores and adsorption capacity on the activated charcoal surface. The doped hydrophilic alumina improved the membranes hydrophilic characteristic as well as surface adsorption ability. Dead-end filtration unit was employed to revise the permeability properties of membranes. In conclusions, PA-3 membrane exhibited above 90 % rejection with BSA and egg albumin (EA) proteins, above 80 % and 70 % rejection with Pb<sup>2+</sup> and Cd<sup>2+</sup> heavy metal ions, and in oil/water separation showed above 94 % and 87 % rejection with bio-diesel and kerosene oils, respectively.*

**6.1 INTRODUCTION**

Nowadays, all over the world water scarcity and water pollution is becoming one of the major thoughtful problematic things due to the rapid development of population and growth of the economy (Kim *et al.* 2010, Elliott *et al.* 2013). This water problem can cause contrary effects not only to the human beings and to the ecosystem (Li *et al.* 2014, Okoye *et al.* 2014). The polluted water contaminated with biologically non-degradable dyes (Dogan *et al.* 2007), oil/water emulsions (Maguire *et al.* 2011), and these wastes mainly releasing from printing, textile, cosmetic industries, oil refinery, petrochemical, food processing units, and cause ecological side-effects (Omoriegbe *et al.* 1997). In recent years, with great deal of efforts several techniques were specified towards water distillation proficiently, such as sedimentation, adsorption (Rekha *et al.* 2015), crystallization, centrifugation, electrophoresis (Casey *et al.* 2011, Li *et al.* 2016), chemical treatment, evaporation, biological methods (Zhang *et al.* 2011) and membrane separation systems (Daas *et al.* 2010) etc.

In recent years, the rapid growth was observed in membrane technology and several membrane separation processes were developed to treat the industrial wastewater, by nanofiltration, microfiltration, ultrafiltration, and reverse osmosis.

Among all these membrane separation processes, ultrafiltration and microfiltration methods are favorable for conservative industrial separation methods due to the several benefits, such as low pressure driven operational conditions, economically feasible and fast operation, high selectivity, easy for separation, and low investment.

Symmetric and asymmetric  $\alpha$ -alumina supported zirconia ( $\text{ZrO}_2/\alpha\text{-Al}_2\text{O}_3$ ) microfiltration membranes fabricated by dip-coating mode. The rejection efficacy of fabricated membranes assessed by 5 ppm concentrated vegetable oil or mineral oil-water emulsion separation via cross-flow filtration setup, and the results were analyzed with Oil Concentration Analyzer. In results, the  $\text{ZrO}_2/\alpha\text{-Al}_2\text{O}_3$  membranes displayed more superior performance results with water permeability, as well as with oil separations tests (Yang *et al.* 1998).

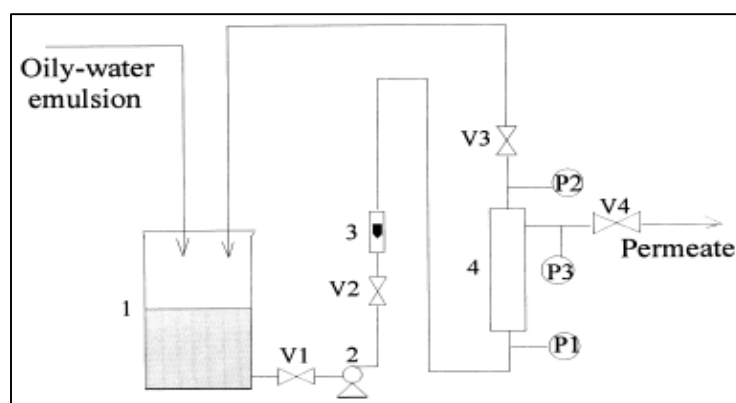


**Figure 6.1** Schematic scheme of oil-water filtration: 1 storage tank; 2 centrifugal pump; 3 flow-meter; 4 membrane module; V1, V2, V3, V4, control valve; P1, P2, P3 pressure gauge (Yang *et al.* 1998)

The  $\gamma$ -alumina membranes fabricated by the support of  $\alpha$ -alumina mesoporous layer, to study the separation ability of hexane and toluene through alumina membranes with dissimilar pore diameters. The alumina membranes solvent permeability investigations performed with cross-flow separation unit. The permeability ability of hexane and toluene is influenced by the pore sizes of alumina membranes and the present water content in organic liquids and observed different permeabilities. Hexane with less polar attained less flux compared to toluene. It concludes that, if the membrane pores smaller than the permeable solvent particle sizes, then the pore blocking chances



are more, so in results able to found the changes with permeability (Roy Chowdhury *et al.* 2004).

Various amounts of inorganic alumina nanoparticles ( $\text{Al}_2\text{O}_3$  NPs) discrete in poly (vinylidene difluoride) (PVDF) polymer, and fabricated flat-sheet membranes via phase inversion process. The fabricated ultrafiltration membranes were examined with several characterization techniques such as SEM, TEM, contact angle, porosity, molecular weight cut-off study, and tensile tests. Permeability ability was checked with water flux and fouling ability examined with oil/wastewater flux via dead-end filtration setup. The experimental results revealed that the additive contained membranes displayed good fouling behavior as compared with plane membranes (Yan *et al.* 2005).

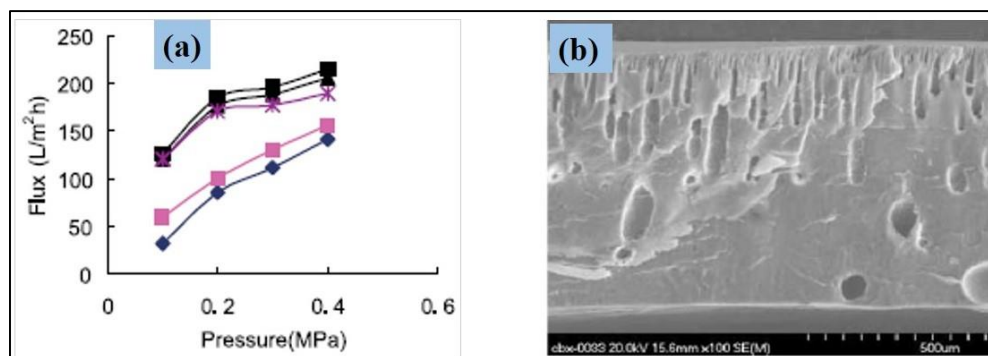


**Figure 6.2** Water flux results (a), SEM cross-sectional micrograph (b) of membranes (Yan *et al.* 2005)

Synthetic ceramic tubular membranes were used to examine the kerosene oil/water emulsion separation via microfiltration process. No other surfactants are added to the kerosene to stabilize the oil/water emulsion. Different oil concentrations of 400 ppm, 800 ppm, 1200 ppm, and 1600 ppm were applied to study the permeability properties of membranes through pressure dependent study. The feed and permeate solution's oil concentrations were analyzed with UV-visible spectrometry. Flux decline behavior of membranes increased by the continuous enhancement of oil concentration in water. So, in result, less flux observed with higher oil concentrations due to the pore blockage phenomena (Lue *et al.* 2009).

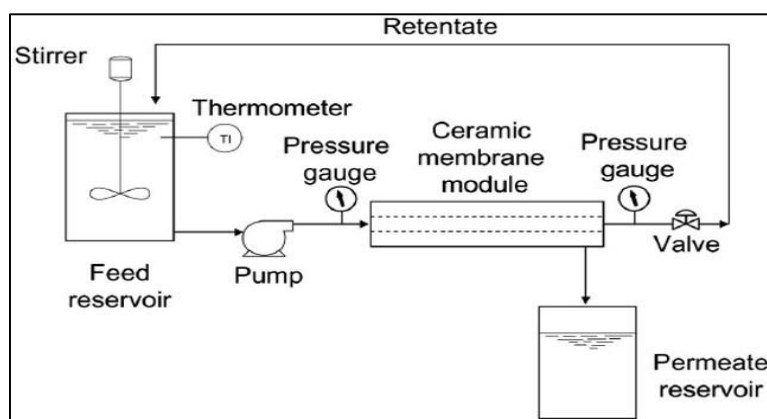


**Figure 6.3** Lab-scale oil-water microfiltration experimental setup (Lue *et al.* 2009)

Nontoxic, non-flammable, and highly flexible polydimethylsiloxane (PDMS) sponge material selected and this sponge replicated with sugar cubes, followed by an environmentally green process. The main objectives of the current research were to describe the selective oils absorption on PDMS sponge with following both hydrophobic and oleophilic properties. The absorption capability depends on the type of sugar replicating with PDMS sponge. The results displayed PDMS sponge replicated with various commercial granular sugar showed enhanced results towards absorption of oils, porosity improvement as well as eliminating the organic impurities from wastewater. The oil and organic solvents absorbed on PDMS sponge are removed by squeezing and reusability can possible (Choi *et al.* 2011).

Polymethylmethacrylate (PMMA) based nanofibrous membranes were fabricated via electrospinning method with the addition of different wt. % of Rhodanine to the PMMA polymer used 1,1,1,3,3,3-hexafluoro-2-propanol (HFIP) as a solvent. The obtained nanofibrous membranes size range was observed between 840 nm to 1440 nm, with SEM instrument. The main objective of the current study was to examine the adsorption capability of selected heavy metals such as Ag (I) and Pb (II) from aqueous solutions. Finally observed, the heavy metal ions adsorption efficacy of membranes enhanced with the continuous enhancement of rhodanine wt. % in membranes (Lee *et al.* 2013).

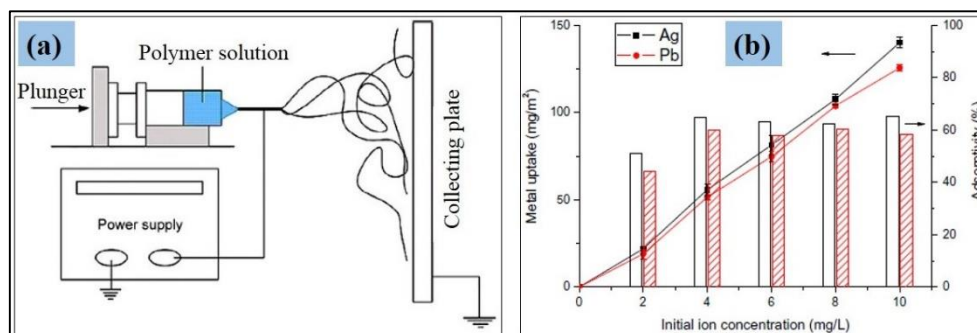


**Figure 6.4** (a) Electrospinning unit (b) Effect of initial ion concentrations on nanofibrous membranes (Lee *et al.* 2013)

Metal-organic framework (MOF) membranes were fabricated with the support of tubular alumina by a provision of cobalt salts such as cobalt butyrate and cobalt valerate, to study the selective  $\text{CO}_2/\text{CH}_4$  gas separation capability of bio-MOF-1, bio-MOF-13, and bio-MOF-14 membranes. Here, the gas separation performance of membranes was elucidated by membrane thickness and number of layers occurrences. By increasing the number of layers in membranes, the  $\text{CO}_2$  adsorption capacity declined due to the enlarged membrane thickness. The final results conclude, in separation assessment under same operational conditions the bio-MOF-13 and bio-MOF-14 membranes exhibited better performance than bio-MOF-1 type membrane (Xie *et al.* 2014).

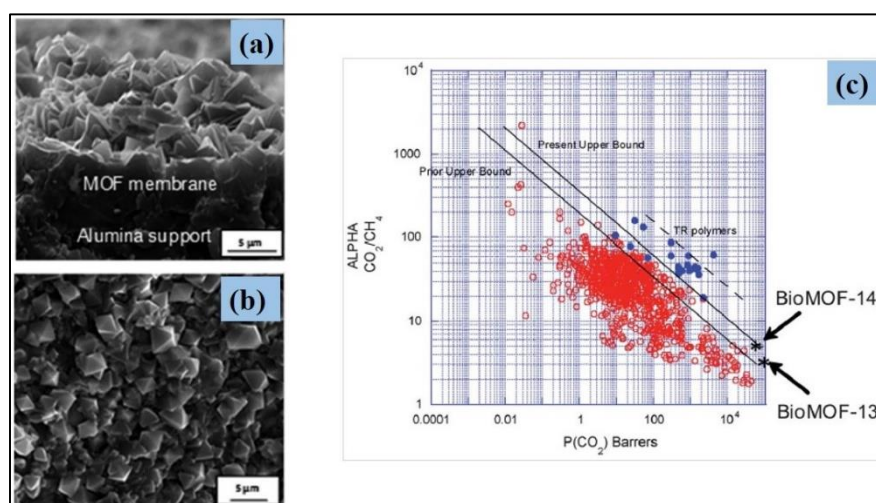


**Figure 6.5** SEM images of membranes (a) cross-sectional, (b) top view image, and (c) Revisited Robeson plot for  $\text{CO}_2/\text{CH}_4$  mixtures (Xie *et al.* 2014)

Ceramic hollow fiber membranes (HFMs) practically applied to examine the oil/water separation performance through cross-flow filter technique with recirculation mode and concentration modes. These ceramic HFMs with double layer, the active layer contains  $\text{Al}_2\text{O}_3$ , supportive layer with  $\text{SiC}/\text{Al}_2\text{O}_3$ . Oil concentrations were maintained up to 5000 ppm, and the results analyzed with total organic carbon analyzer, after that the filtration concentrations decreased up to 1 ppm. From experimental results, ceramic UF HFMs displayed improved flux presentations as well as effective superior oil/water emulsion separations (Schutz *et al.* 2015).

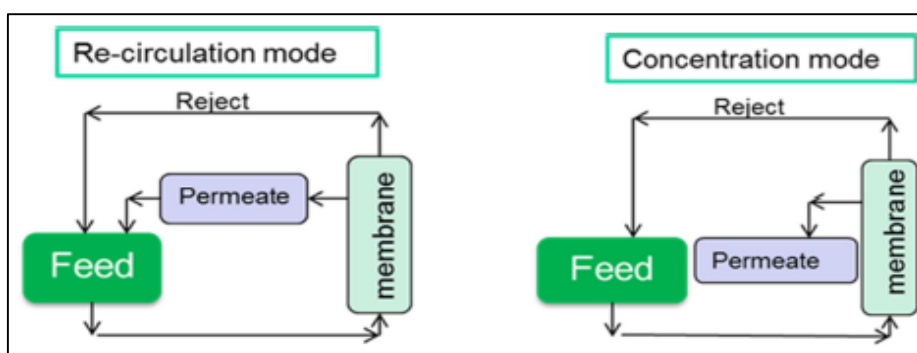


**Figure 6.6** Schematic illustrations of recirculation and concentrate mode operations (Schutz *et al.* 2015)

Shashikala and team members developed alumina concealed carbon as a low-cost adsorbent via precipitation deposition technique to detect the fluoride ions from crushed water. Excess of fluorides containing water can seriously affect to the human life. In the current research, the water samples collected from Nalgonda district of Telangana state, India and conducted fluoride ions removal experiment with the help of National Environmental Engineering Research Institute (CSIR-NEERI). In this research, the alumina surface was covered with various amounts of carbons such as 5, 10, 15, 20, 25 and 50 wt. %. In conclusions, continues enhancement of fluoride ions removal was observed by the continuous increment of additive to the solution (Shashikala *et al.* 2016).

Carbon nanotube (CNT) surface infused with various amounts of Aluminum oxide ( $\text{Al}_2\text{O}_3$ ) nanoparticles, and synthesized aluminium oxide-infused carbon nanotube (CNT- $\text{Al}_2\text{O}_3$ ) membranes to examine the cadmium (II) ions removal efficacy

from aqueous media via continuous filtration unit. Due to the nano additive effect of the membranes hydrophilicity, permeability, as well as adsorption properties were enhanced from the pristine membrane to higher additive membrane. The higher additive membrane (20 %) showed above 80 % rejection results for cadmium (II) ions (Ihsanullah *et al.* 2017).

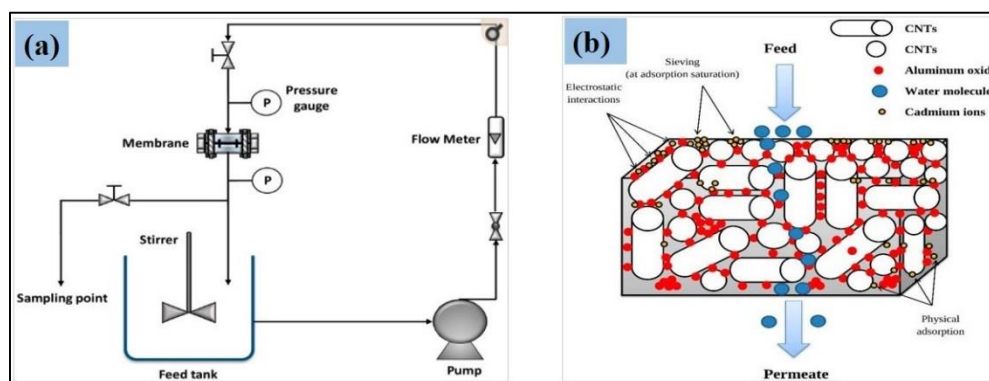


**Figure 6.7** (a) Flow loop system, (b) Cd (II) ion interactions with the CNT-Al<sub>2</sub>O<sub>3</sub> membrane (Ihsanullah *et al.* 2017)

Biodegradable activated carbon membranes (ACMs) synthesized by the dispersion of reduced graphene oxide (rGO) on activated carbon, to study the pollutants removal efficacy from wastewater via a separation process. Various types of ACMs fabricated by the addition of various amounts of activated carbon and rGO together. Due to the nano additive effect, the surface wettability and adsorption competence characteristics were enhanced continuously from plane membrane to higher additive membrane. Sieving mechanism involved in the separation process. In separation results observed, above 95 % for silica and silver particles, above 98 % for *Chlorella*, *Escherichia coli* (*E. coli*) bacteria's (Yang *et al.* 2017).

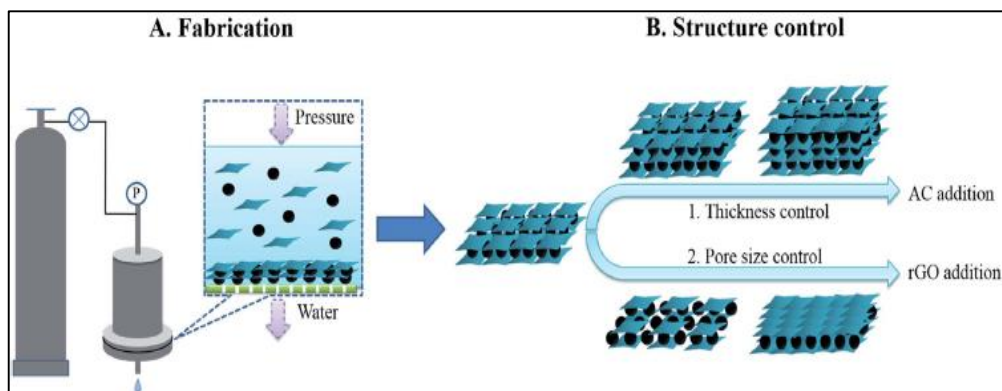


**Figure 6.8** Schematic illustration of ACM fabrication (A), membrane thickness and pore size were controlled by the addition of AC and rGO (B) (Yang *et al.* 2017)

A basic method applied to fabricate the polymer@CNT nanohybrid membranes to study the antifouling properties and oil/water separation ability of membranes. In the current research, several polymeric materials such as polyethyleneimine (PEI), chitosan (CS), polyacrylamide (PAM), polyvinyl alcohol (PVA), sodium alginate (SA) and polyacrylic acid (PAA) were chosen to coat on CNT surface and fabricated the membranes. To get the polymer@CNT nanohybrid membranes, primarily synthesized polymer@CNT nanohybrid films dipped in dimethylacetamide (DMAC), and afterward preserved in water. The oil/water separation test executed with three types of 1000 ppm concentrated soybean oil mixed oil/water samples. These oil samples stabilized with different surfactants such as hexadecyl trimethyl ammonium chloride (HTAC), Tween 80 and sodium dodecyl sulfate (SDS). The separation results analyzed with UV-spectrophotometer. The attained results determine, CNT based membrane materials revealed higher permeability, good antifouling properties and extraordinary separation efficacy (Liu *et al.* 2017).



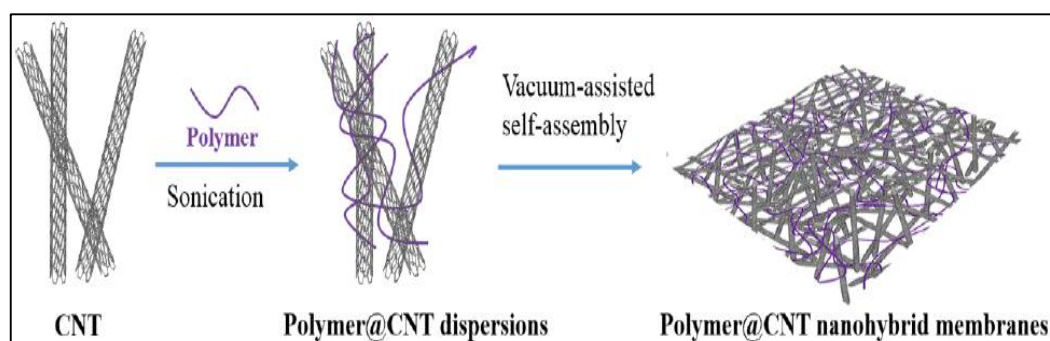


**Figure 6.9** Fabrication procedure of the polymer@CNT nano hybrid membranes (Liu *et al.* 2017)

Superhydrophobic and superoleophilic alumina doped flat-sheet membranes were fabricated via simple method by thermal decomposition of polytetrafluoroethylene (PTFE) polymer on alumina membranes surface. The main objective was to determine the volume of water in oil/water mixture, then feed and permeate samples were analyzed by Karl Fischer coulometric method. In contact angle analysis, the membranes displayed superhydrophobic ( $155^{\circ}$ ) and superoleophilic ( $0^{\circ}$ ). The modified alumina membranes showed above 90 % water separation from the oil-water mixture (Tang *et al.* 2018).

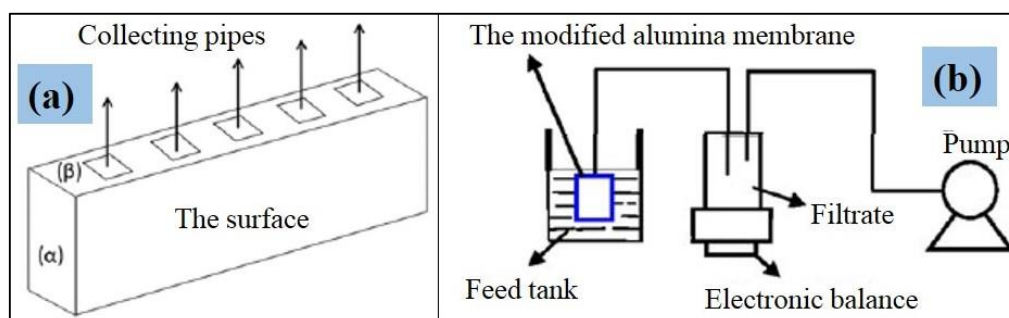


**Figure 6.10** (a) Schematic image of alumina membrane, (b) Oil/water separation experimental setup (Tang *et al.* 2018)

Alumina ( $\text{Al}_2\text{O}_3$ ) is a most well-known metal-oxide (Patel *et al.* 2011), and widely used in membrane filtration processes due to its specific characteristics, such as large surface area, good adsorption efficacy, high density, oppose to organic solvents, well particle size distributions and low production cost (Sarkar *et al.* 2012). Generally, alumina coated/ doped membranes show better separation efficacy towards proteins,

heavy metals removal from aqueous media due to the realistic hydrophilic characteristic of alumina particles. PVP was added to the key polymer as a pore forming additive to advance the pore size distributions in membranes. In the current research, PPSU was used as a principle polymer to prepare the flat-sheet ultrafiltration membranes to study the rejection efficiency, because of its good mechanical, good dimensional stability, chemical resistance properties and have high resistance from hydrolysis process.

Various types of nano-additives were loaded/ doped on activated charcoal to improve the surface activity of activated charcoal, and used in several purification processes to decontaminate the water. Among few of the reports, such as titanium dioxide loaded onto activated carbon for the removal of pollutants from water (Puma *et al.* 2008), zinc oxide loaded activated charcoal for the detection of Orange G and Rhodamine B dyes from water (Saini *et al.* 2017). Nickel (II) nitrate doped on activated charcoal for the elimination of arsenic from water (Dobrowolski *et al.* 2013) and cadmium hydroxide nanowire loaded on activated charcoal for the effective abstraction of bromocresol green from aqueous media (Ghaedi *et al.* 2012). Titanate nanotube reinforced activated carbon for the removal of lead ions from water (Ma *et al.* 2017), etc. Previously, few of the researchers reported that the oil-water mixture separation processes performed using various nano additives and materials, such as superhydrophilic graphene oxide membranes (Liu *et al.* 2015), superhydrophobic TiO<sub>2</sub> fabrics (Huang *et al.* 2015), superhydrophobic copper foam membranes (Rong *et al.* 2018), polydopamine nanocluster adorned nanofibrous membranes (Wang *et al.* 2018). Carbon nanotube nanohybrid membranes (Liu *et al.* 2017), superhydrophilic poly (p-phenylene sulfide) membrane (Gao *et al.* 2018), graphene oxide coated cellulose nanofibers (Ao *et al.* 2017), polysulfone/ hydrous aluminium oxide ultrafiltration membranes (Gohari *et al.* 2015), etc.

From the literature review reports, it can be determined that the activated charcoal was doped with different nano additives and can be used as a good adsorbing agent towards the removal of various contaminants from water. The removal of proteins, heavy metal ions and in oil/water emulsion separations using PPSU polymeric membrane so far has not been reported. In view of these observations, in the current research, fabricated the novel flat-sheet ultrafiltration membranes by the addition of



different loadings of additive  $\text{Al}_2\text{O}_3$ -AAC to the PPSU polymer, via the phase inversion method. The effect of incorporated additive  $\text{Al}_2\text{O}_3$ -AAC on membrane morphology and surface topography were inspected by SEM and AFM analysis. The water permeability, antifouling behavior, contact angle, porosity, and water uptake characteristics were investigated in detail. The main objective of the current study was to investigate the fabricated membranes removal efficacy of BSA and EA proteins, lead and cadmium heavy metals from aqueous systems and for bio-diesel, kerosene oil-water emulsion separations. Dead-end filtration cell was employed to quantify the permeability and rejection performance of membranes.

## 6.2 EXPERIMENTAL

### 6.2.1 Materials

The basic polymer PPSU (MW~50,000 g/mol) was delivered over Solvay Advanced Polymer, Belgium. Aluminium trioxide nanoparticles ( $\text{Al}_2\text{O}_3$  NPs) (< 50 nm, TEM), Bovine Serum Albumin (BSA) (MW~66 KDa), Egg Albumin (MW~44 KDa), polyvinylpyrrolidone (PVP) (MW~36,000), were obtained from Sigma-Aldrich Co., Missouri, USA. N-methyl-2-pyrrolidone (NMP) was bought from Merck Ltd., Germany. Sulphuric acid ( $\text{H}_2\text{SO}_4$ ) 98 % extra pure was obtained from Loba Chemie, India. Ethanol was procured from Changshu yangyuan chemicals, China. Polyethylene glycol (PEG) 6000 Da, PEG 10000 Da and PEG 20000 Da were acquired from Merck, India Ltd.

### 6.2.2 $\text{Al}_2\text{O}_3$ -AAC mixture preparation

#### 6.2.2.1 Acid treatment of activated charcoal (AAC)

A mixture of 10 wt. % of sulphuric acid and 10 g of activated charcoal was stirred (280 rpm) at room temperature for 12 h. After that, the solution filtered under vacuum pump and maintained constant pH. Afterward, the obtained charcoal kept for dry at 100 °C for 30 h (Pak *et al.* 2016). The purpose of acid treatment of activated charcoal is to increase the micropores and surface area of charcoal, due to this, the adsorption conduct on the charcoal surface will increase.

### 6.2.2.2 Doping process of Al<sub>2</sub>O<sub>3</sub> NPs on AAC

In one of the beaker, 6 g of acid treated activated charcoal (AAC) was taken and added 60 ml of water, and in another beaker, 0.5 g of Al<sub>2</sub>O<sub>3</sub> NPs was added. To this added 40 ml of deionized water. Afterward, both of the above solutions were mixed together and performed sonication process up to 2 hr, for the proper dispersion of Al<sub>2</sub>O<sub>3</sub> NPs on AAC. Later, the mixture was kept constantly overnight. Next day, the mix was filtered with water and ethanol. The purpose of washing with ethanol is to remove the complete water from the particles. In final, the obtained mixture was kept for calcination in a tubular furnace at 400 °C for 6 h. Further, it was stored in a sample container for future work.

### 6.2.3 Fabrication of PPSU/ Al<sub>2</sub>O<sub>3</sub>-AAC mixed matrix membranes

The PPSU/ Al<sub>2</sub>O<sub>3</sub>-AAC mixed matrix ultrafiltration membranes fabricated via phase separation method (Kumar *et al.* 2013). Table 6.1 lists the compositions of the dope solutions for membrane fabrication. First, a definite amount of Al<sub>2</sub>O<sub>3</sub>-AAC was dispersed in NMP solvent and sonication (Model: Ultrasonic cleaner, USC-100) performed up to 30 min for the proper dispersion of Al<sub>2</sub>O<sub>3</sub>-AAC in NMP solvent. Further added 16 g of PPSU, 4 g of PVP and then kept for stirring at 60 °C followed by 24 h to become a uniform clear solution. The obtained dope solution was degassed in a sonicator, and cast on a glass plate using a *K-202 control coater* instrument. Then immediately glass plate was placed in a water bath for phase inversion process. The membranes placed in water for 24 h to remove the excess of NMP solvent (Rashmi *et al.* 2016).

**Table 6.1** Membrane dope solutions compositions

Membranes	PPSU (g)	NMP (g)	PVP (g)	Al <sub>2</sub> O <sub>3</sub> -AC (wt. %)	Al <sub>2</sub> O <sub>3</sub> -AC (g)
PA-0	16	80	4	0	0
PA-1	16	79.968	4	0.2	0.032
PA-2	16	79.92	4	0.5	0.08
PA-3	16	79.84	4	1	0.16

## 6.2.4 CHARACTERIZATION

To distinguish the surface morphology of Al<sub>2</sub>O<sub>3</sub> NPs and the fabricated flat-sheet membranes cross-sectional morphology was captured with Field Emission scanning electron microscopy (FESEM, Zeiss Sigma). The samples for SEM analysis were prepared as explained earlier in section 2.2.4.2 of CHAPTER 2.

To investigate the surface roughness parameters of membranes, used Nanodrive Innova SPM atomic force microscope (AFM). The scan area was maintained 3 μm × 3 μm. The sample analysis procedure was explained earlier in section 4.2.3.2 of CHAPTER 4.

The contact angle measurements of membranes were evaluated by following the procedure mentioned in section 2.2.4.3 of CHAPTER 2.

The water uptake and porosity studies of membranes were done by following the method mentioned in sections 2.2.4.6 and 2.2.4.7 of CHAPTER 2.

The PWF and antifouling capability of the prepared membranes were tested by calculating the flux, FRR values as described in sections 2.2.4.4 and 2.2.4.5 of CHAPTER 2. The PWF and BSA flux were measured at 0.2 MPa TMP and performed time-dependent studies maintained two min time interim for every membrane sample and continued up to 40 min.

To study the Molecular weight cut-off (MWCO) membranes were tested by following the method mentioned in section 5.2.3.1 of CHAPTER 5.

## 6.2.5 Membranes rejection experimentations

### 6.2.5.1 Protein rejection study

A dead-end filter unit (Figure 6.11) was employed to analyze the fabricated membranes proteins rejection efficiency, such as BSA and EA respectively. Al<sub>2</sub>O<sub>3</sub> incorporated polymeric membranes are extensively familiarized in protein separation and purification studies (Treccani *et al.* 2013). In current work, 800 mg/L concentrated BSA and EA protein solutions were equipped for the rejection study. The pH of the

protein solutions adjusted at  $6.6 \pm 0.2$ , then solution shifted into the feed tank and continued the rejection study at 0.2 MPa TMP and performed time bounded study up to 45 min. Further, the feed and collected protein solutions concentrations were analyzed by UV-visible spectroscopy (Zhong *et al.* 2003). The maximum absorbance of the prepared membranes was recorded at 278 nm for both BSA and EA proteins. The results of permeated protein concentrations were examined using Eq. (6.1).

$$\% R = \left(1 - \frac{C_p}{C_f}\right) \times 100 \quad \text{Eq. (6.1)}$$

Where ' $C_p$ ' and ' $C_f$ ' are the protein concentrations in permeate and feed.

### 6.2.5.2 Heavy metals rejection study

To analyze the  $Pb^{2+}$  and  $Cd^{2+}$  heavy metals rejection efficacy of fabricated UF membranes, employed dead-end stirred filter cell (Figure 6.11). In the present work, 50 mg/L lead nitrate and cadmium nitrate aqueous solutions were prepared, and pH of the solutions maintained stable at  $5.8 \pm 0.2$  with 0.1 M NaOH solution. Further, added 0.5 wt. % of polyethyleneimine (PEI) as a complexing agent, and then the solutions stirred up to five working days under  $25^\circ C$  to have good contacts between the complexing agent and metal ions. Afterward, the heavy metal solutions were poured in feed tank and performed the filtration experiment using  $5\text{ cm}^2$  membrane area, at 0.2 MPa TMP. The feed and collected permeate samples were further evaluated using atomic absorption spectrometer (AAS). The rejection % of membranes measured by Eq. 6.1. During the filtration study maintained 2 min time interval, 40 min time duration. After the rejection study, the surface of the dried membrane was employed with SEM-EDS to study the adsorbed heavy metal elemental mapping analysis.

### 6.2.5.3 Oil/water emulsion separation study

The oil samples, *Pongamia Pinnata* (Local name: *Karanja*) plant extracted bio-diesel collected from Karnataka state bio-energy development board, India and the kerosene was obtained from outside the local market. 100 mg/L oil/water mixtures were developed individually by adding oil in water and preserved for sonication up to 10 h at  $30^\circ C$ . No, any other surfactants were added to stabilize the oil/water mixtures. A

dead-end filtration unit (Figure 6.11) was applied to investigate the prepared membranes oil/water separation efficacy. The oil/water mixture poured into the feed tank and passed through the membranes. The rejection results of feed and permeate (oil concentrations in feed and permeate) samples were analyzed using Eq. 6.1, by total organic carbon (TOC) (Model: TOC-L SHIMADZU TOC analyzer) instrument.

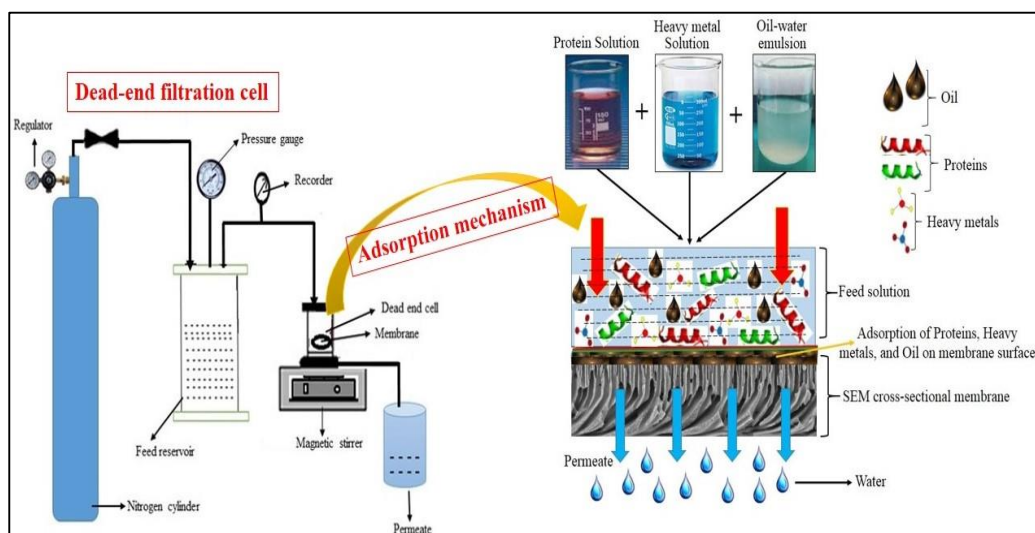


**Figure 6.11** Schematic image of lab scale dead-end filter unit for separation

## 6.3 RESULTS AND DISCUSSION

### 6.3.1 Morphological results

#### 6.3.1.1 FESEM results of $\text{Al}_2\text{O}_3$ NPs and EDS elemental mapping analysis of $\text{Al}_2\text{O}_3$ -AAC

FESEM was examined to study the shape and size distribution of  $\text{Al}_2\text{O}_3$  NPs. In results, the  $\text{Al}_2\text{O}_3$  NPs thickness obtained close to the range between 53.74 nm to 66.41 nm (Figure 6.12 (A)). After the completion of the doping process, the particles were viewed with SEM. Figure 6.12 (B) reveals the information as regards  $\text{Al}_2\text{O}_3$ -AAC SEM outlook. The  $\text{Al}_2\text{O}_3$ -AAC again examined with SEM-EDS analysis. The obtained results (Figure 6.12 (D)) can conclude that the  $\text{Al}_2\text{O}_3$  NPs distribution on activated charcoal is proper and noticeably found the elements aluminium, carbon, and oxygen. Figure 6.12 (E) reveals the elemental mapping results of the  $\text{Al}_2\text{O}_3$ -AAC.

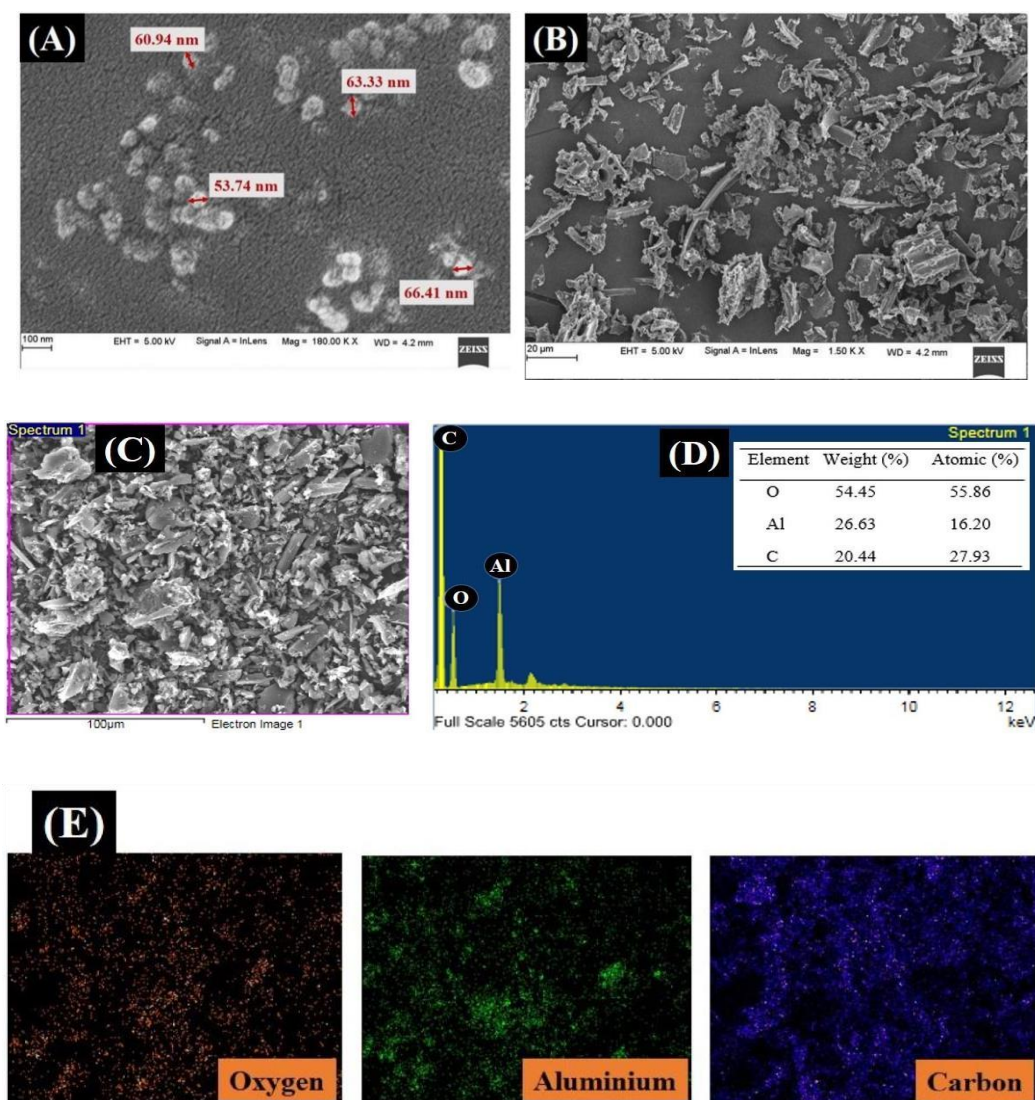


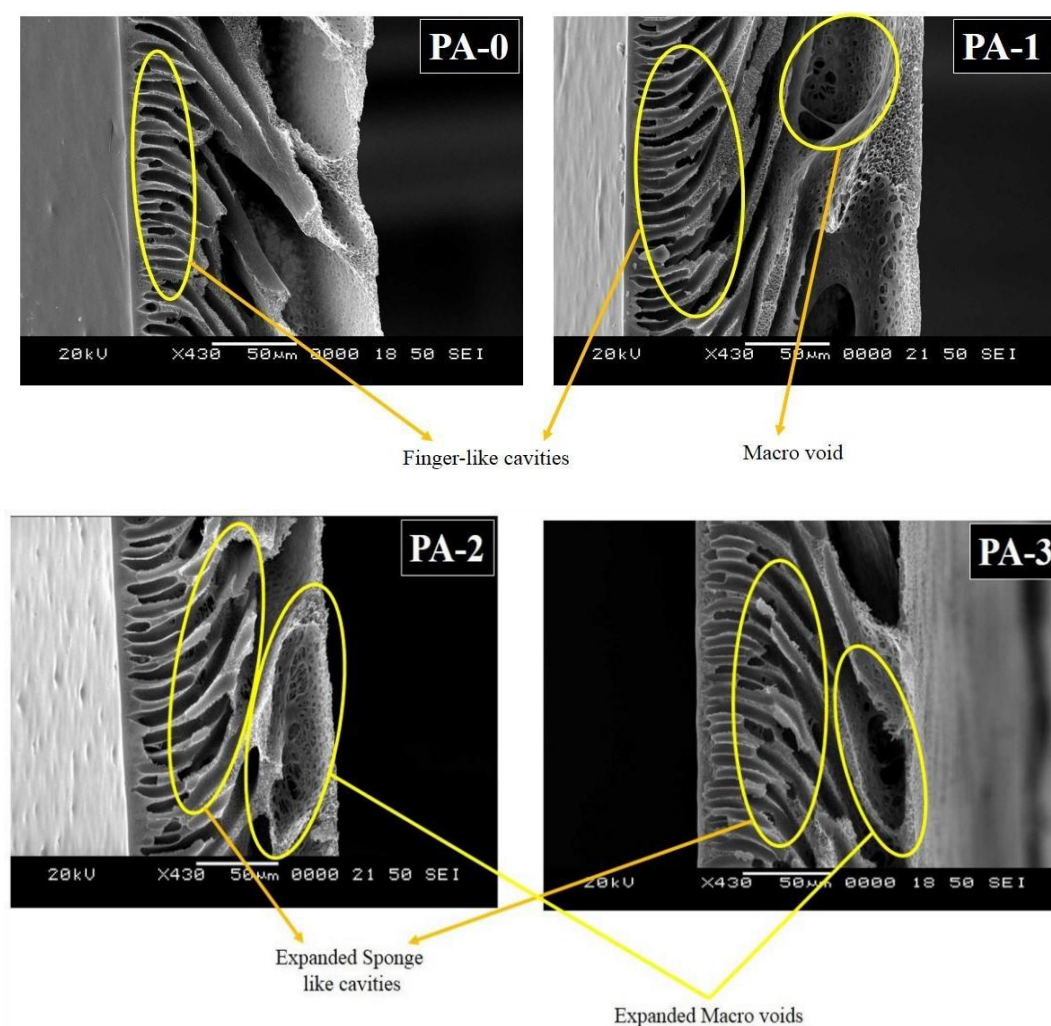
**Figure 6.12** (A) Magnified FESEM image of Al<sub>2</sub>O<sub>3</sub>-NPs, (B) Outlook FESEM image of Al<sub>2</sub>O<sub>3</sub> doped AAC, (C) FESEM surface appearance Al<sub>2</sub>O<sub>3</sub>-AAC, (D) EDS result and (E) elemental mapping results of Al<sub>2</sub>O<sub>3</sub>-AAC

### 6.3.1.2 SEM results of the Al<sub>2</sub>O<sub>3</sub>-AAC incorporated PPSU membranes

The membranes cross-sectional morphological features were supervised by SEM. Figure 6.13 discloses the information concerning fabricated UF membranes SEM morphological changes. The membranes exhibited asymmetric structures with active skin layer and porous sublayer. In the sublayer one can observe the various channels, such as finger-like, sponge-like projections and macrovoids (Young *et al.* 1995). This is because of the solvent non-solvent exchange, phase inversion process (Hinke *et al.*



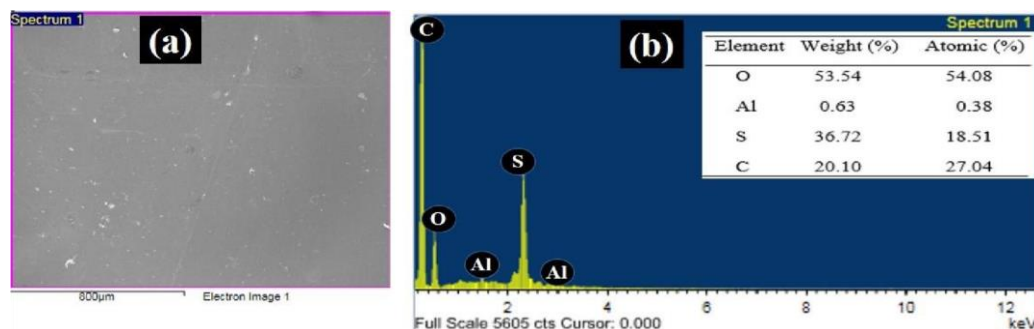
1991). These channels performed a remarkable role in transportation properties. From the obtained results the finger-like, sponge-like projections and macro voids are noticeably increased from PA-0 to PA-3 with increasing the  $\text{Al}_2\text{O}_3$ -AAC concentration in the membranes.  $\text{Al}_2\text{O}_3$  NPs might affect the pore size of membranes. The added PVP is extremely water soluble, increases the hydrophilicity and further acts as a pore-forming agent, so that pore morphology will effect. From PA-0 to PA-3 the vertical channels are slowly converting into the horizontal forms, these horizontal channels can increase the permeability, rejection properties of membranes (Morihaman *et al.* 2014). From the above observations, it can be concluded that the added additives  $\text{Al}_2\text{O}_3$ -AAC and PVP were impressively changed the morphology properties of membranes.



**Figure 6.13** SEM cross-sectional results of membranes

### 6.3.1.3 SEM-EDS analysis of PA-3 membrane

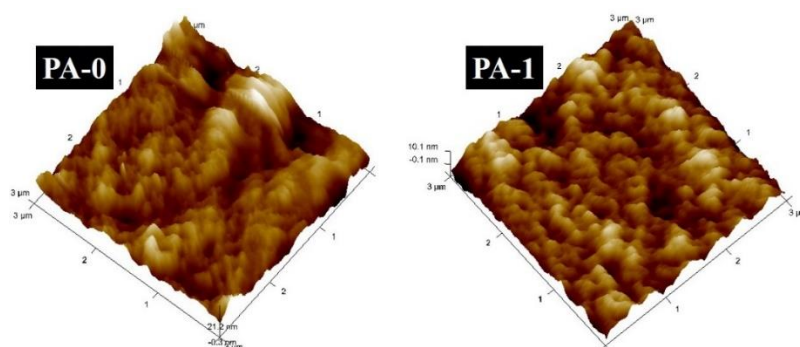
In SEM-EDS analysis, the PA-3 membrane top surface was examined by SEM-EDS, and in the observed results observed the Al and O elements, reported in Figure 6.14 (b). It means the  $\text{Al}_2\text{O}_3$ -AAC additive is properly dispersed in the membrane matrix.



**Figure 6.14** (a) FESEM surface appearance and (b) EDS result of PA-3 membrane

### 6.3.1.4 AFM analysis

Top surface morphological changes of the fabricated membranes, roughness characteristics were observed by AFM with tapping mode, and the attained parameters results were reported in Table 6.2. Figure 6.15 reveals the 3-D AFM images of membranes. The added additive  $\text{Al}_2\text{O}_3$ -AAC makes the surface rough, hence surface roughness parameters  $R_a$ ,  $R_q$ , and  $R_z$  were continuously increased from PA-0 to PA-3 membrane with increasing the  $\text{Al}_2\text{O}_3$ -AAC weight percentage in membranes. The surface roughness perception will affect the wettability and permeability characteristics of membranes, which directed to improve the permeability assets of membranes (Yu *et al.* 2015).





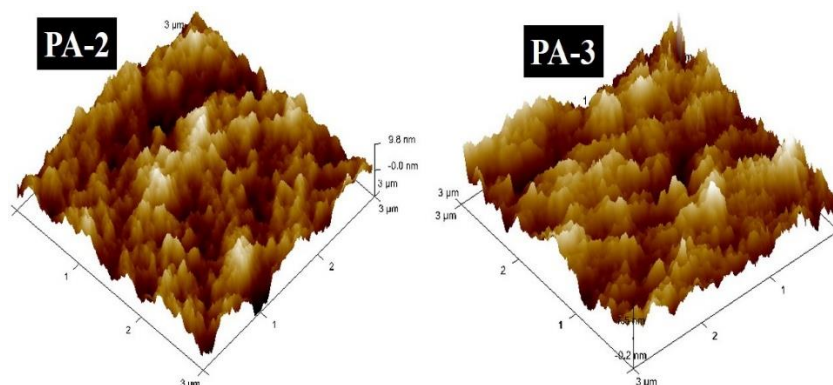


**Figure 6.15** AFM surface roughness results of membranes

**Table 6.2** Surface roughness variables of membranes

Membrane	Roughness			Surface area ( $\mu\text{m}^2$ )
	$R_a$ (nm)	$R_q$ (nm)	$R_z$ (nm)	
PA-0	2.15	2.76	18.9	9.00
PA-1	2.47	3.10	24.0	9.02
PA-2	2.89	3.67	27.4	9.03
PA-3	3.31	4.19	28.1	9.01

### 6.3.2 Contact angle (CA) results

The membranes physical characteristics such as surface wettability, hydrophilic efficacy were analyzed by CA experiment. Figure 6.16 (a) discloses the information regarding plane (PA-0) and blend membranes (PA-1 to PA-3) CA values. In results, the continuous decrease in CA values was observed from  $79.79^0$  to  $67.95^0$  by increasing the additive  $\text{Al}_2\text{O}_3$ -AAC wt. % in membranes (Table 6.3). The reducing order of CA is as follows: PA- 0 < PA-1 < PA-2 < PA-3. This directs that the surface hydrophilic capacity of the membranes increased due to the doped hydrophilic  $\text{Al}_2\text{O}_3$  NPs (Mehrnia *et al.* 2015) and as well as these  $\text{Al}_2\text{O}_3$  NPs can impact the pore sizes of membranes. Due to this the pure water permeability even the fouling also affected.

### 6.3.3 Membrane water uptake and porosity results

Water uptake capacity and porosity are the foremost characteristics to illustrate the membrane wettability nature. The outstanding results are attained in water uptake

and porosity tests (Figure 6.16 (b)) by the continual increment of  $\text{Al}_2\text{O}_3$ -AAC wt. % in membranes, and embodied in Table 6.3. The enhancement of water uptake and porosity due to the observable changes in finger-like, sponge-like cavities and macrovoids in membranes (Figure 6.13). The additives PVP and hydrophilic  $\text{Al}_2\text{O}_3$  were played the main role to advance the pore morphology of the membranes (Zhao *et al.* 2012). The increasing order of water uptake and porosity is as follows: PA- 0 < PA-1 < PA-2 < PA-3.

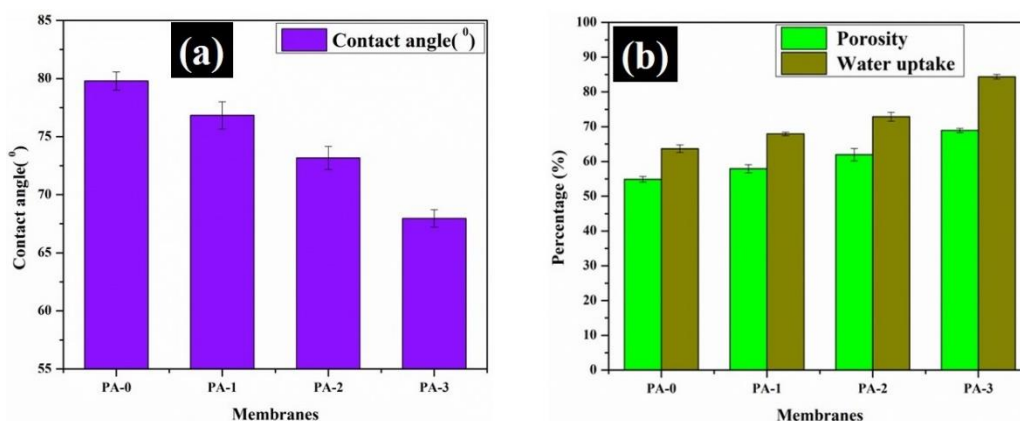


**Figure 6.16** (a) Contact angle, (b) porosity and water uptake results of membranes

**Table 6.3** Membrane properties

Membranes	Water uptake (%)	Porosity (%)	Contact angle (°)	Membrane thickness ( $\mu\text{m}$ )
PA-0	63.70 ± 1.1	54.88 ± 0.8	79.79 ± 0.79	157
PA-1	67.93 ± 0.5	57.90 ± 1.2	76.83 ± 1.18	154
PA-2	72.86 ± 1.3	61.96 ± 1.8	73.16 ± 1.0	152
PA-3	84.39 ± 0.7	68.92 ± 0.6	67.95 ± 0.75	173

### 6.3.4 MWCO results

Figure 6.17 reveals the information regarding MWCO results of membrane. In results, with PA-3 membrane noticeable % R increment was observed, it is as > 70 % with PEG 6 kDa, > 88 % with PEG 10 kDa, and > 90 % with PEG 20 kDa, respectively. However, the rejection reached > 90 % with PEG 20 kDa. It can conclude that, the prepared membranes were belongs to ultrafiltration type.

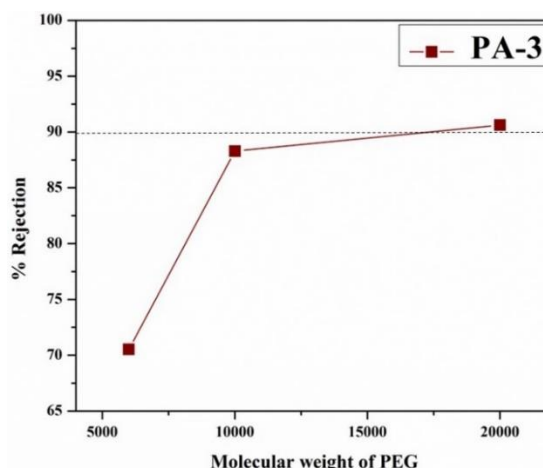


**Figure 6.17** Molecular weight cut-off result of PA-3 membrane

### 6.3.5 Water permeability results of membranes

Primarily, the PWF study was conducted to notice the stability and porosity nature of the fabricated membranes. Time-dependent water permeation tests were accompanied in the present study. Figure 6.18 conveys the information regarding PWF of fabricated membranes with diverse additive concentrations. The water permeability amount was increased from 160.12 L/m<sup>2</sup> h to 223.52 L/m<sup>2</sup> h by increasing the additive Al<sub>2</sub>O<sub>3</sub>-AAC concentration in membranes. Based on PWF results, it can be concluded that the doped hydrophilic additive Al<sub>2</sub>O<sub>3</sub> and pore forming agent PVP were improved the pore sizes and pore morphology in membranes, it can be supported by the SEM results (Figure 6.13).

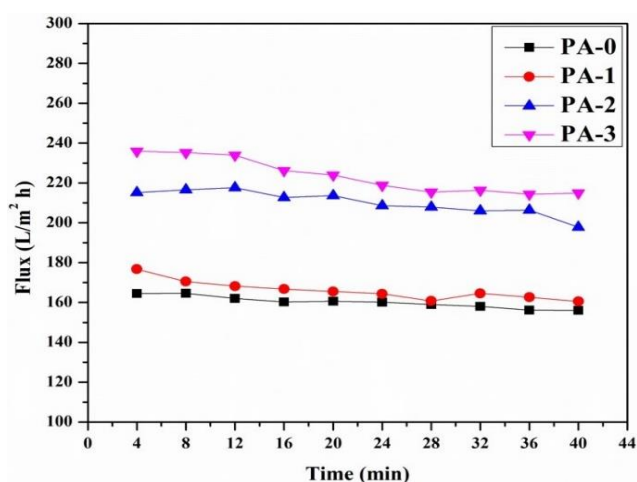


**Figure 6.18** Water permeability results of membranes

### 6.3.6 Antifouling performance of membranes

After the PWF study, fouling ability of the membranes was examined with BSA protein 800 mg/L concentrated aqueous solution. Figure 6.19 (a) reveals the information regarding the antifouling performance of membranes. From the obtained results, it was observed that BSA flux ( $J_p$ ) was increased from 9.29 L/m<sup>2</sup> h to 20.10 L/m<sup>2</sup> h. The obtained BSA flux was very less compared with PWF, this is because of the larger size effects of BSA molecules (Kang *et al.* 2012) and terminated on the membrane surface. Further, due to the blockage of the pores, BSA molecules cannot pass easily through the membrane pores, hence very less flux was obtained. After the BSA flux, membranes kept under continuous water flow for cleaning up to 20 min, again performed PWF study ( $J_{w2}$ ). Among all PA-3 membrane showed better performance. The fouling resistance capacity of membranes was intended by flux recovery ratio (FRR), and the irreversible fouling, reversible fouling and total fouling (Figure 6.19 (b)), are reported in Table 6.4. Moreover, in results, the reversible fouling is increased and irreversible fouling is decreased, this may be due to the hydrophobic BSA confront with the hydrophilic membrane surface.

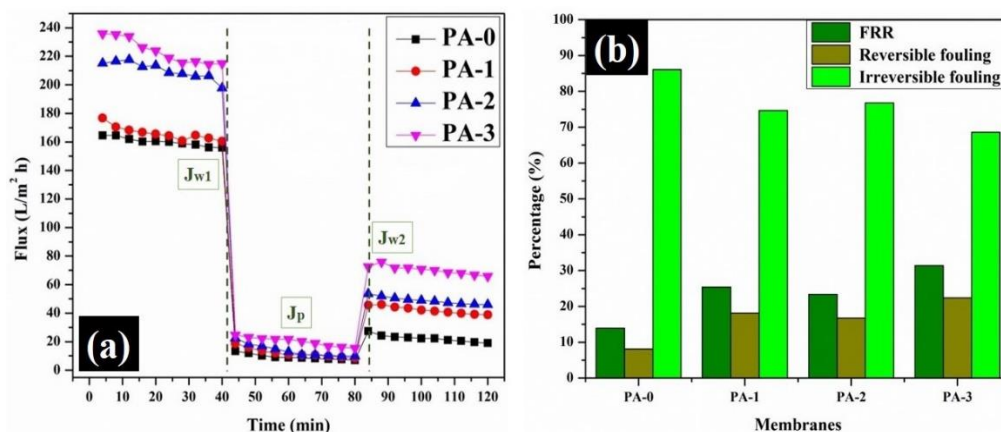


**Figure 6.19** (a) Flux V/s time for membranes at 0.2 MPa under three conditions:  $J_{w1}$ ;  $J_p$ ; and  $J_{w2}$ , (b) FRR and antifouling effects of membranes

**Table 6.4** Membrane permeability results

Membrane code	Permeate flux (L/m <sup>2</sup> h)			FRR	Fouling performance (%)		
	J <sub>w1</sub>	J <sub>p</sub>	J <sub>w2</sub>		R <sub>t</sub>	R <sub>r</sub>	R <sub>ir</sub>
PA-0	160.12	9.29	22.30	13.92	94.19	8.12	86.07
PA-1	166.05	12.03	42.16	25.38	92.75	18.14	74.61
PA-2	210.23	13.72	48.93	23.37	93.47	16.74	76.72
PA-3	223.52	20.10	70.16	31.38	91	22.39	68.61

### 6.3.7 Rejection results

#### 6.3.7.1 Proteins rejection performance of membranes

The separation efficiency of the membranes was assessed with two model proteins BSA and EA. Even though performing the rejection study, the protein solutions pH values preserved continually. If any changes in the pH value, can affect the fouling performance of the membranes (Brinck *et al.* 2000). From the results, it was found that, higher rejection percentages with BSA comparable with EA. This is due to the size effect of proteins. Here, the rejection is based on size exclusion principle. According to this principle, the larger size proteins will retain on the membrane surface and cannot move freely through the membrane pores. Here another reason, protein with high molecular weight express the superior protein separation performance. The rejection percentage of BSA (MW~66 kDa) is high due to the high molecular weight compared with EA (MW~44 kDa) protein. Antifouling stuff is one of the main characteristics and it will play the main role in proteins rejection study. Though, hydrophilic nature on membrane surface increased due to the hydrophilic Al<sub>2</sub>O<sub>3</sub> NPs. It can concluded that, the Al<sub>2</sub>O<sub>3</sub> NPs are most preferable for proteins serration study. The protein rejection results increased with increasing the additive Al<sub>2</sub>O<sub>3</sub>-AAC concentration in membranes (Figure 6.20 (a)). Time-bound protein flux results reported in Figure 6.20 (b). The continuous decrease was observed in proteins flux. With PA-3 membrane, proteins average flux obtained 20.10 L/m<sup>2</sup> h and 42.65 L/m<sup>2</sup> h for BSA and EA, respectively.

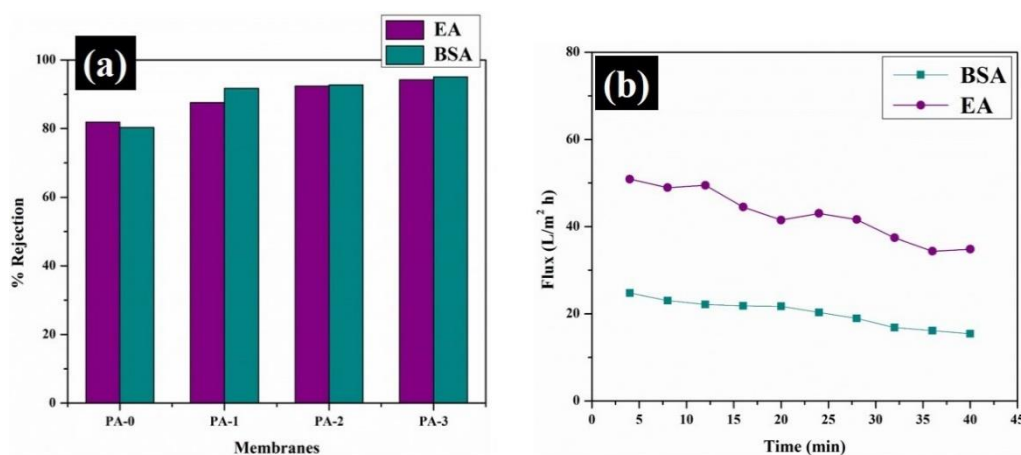


**Figure 6.20** Proteins rejection (a), and time-dependent protein flux of PA-3 membrane (b)

### 6.3.7.2 Heavy metals rejection performance

Polymer enhanced ultrafiltration process was employed to examine the  $\text{Pb}^{2+}$  and  $\text{Cd}^{2+}$  heavy metals rejection efficiency through membranes. The membranes exhibited better rejection of heavy metals such as lead and cadmium. Takagishi and group members projected a complexation mechanism among various divalent metal cations and polyetherimide (PEI) (Takagishi *et al.* 1985). In results, better rejection was achieved to  $\text{Pb}^{2+}$  as compared with  $\text{Cd}^{2+}$  ions, this is due to the size and complexation effect. Normally, lead nitrate (MW: 331.21 g/mol) forms larger complexation compare with cadmium nitrate (MW: 308.48 g/mol) (Liang *et al.* 2012). In general, membrane separation performances can be explained by the theories size exclusion and electrostatic repulsions on the membrane surface. In the present work, it can be concluded that the heavy metal rejection phenomena was engaged with size exclusion principle (Schaepe *et al.* 1998, Wei *et al.* 2013). After adding the complexing agent, the lead nitrate will forms larger complexes compared with cadmium nitrate and in filtration test, these metal complexes cannot pass easily through the membrane pores and metal ions can adsorb on the membrane surface. After the doping of alumina to activated charcoal, the adsorption efficacy on the activated charcoal surface will improve. So that, the heavy metals can adsorb strongly on the membrane surface. In conclusion, high rejection above 80 % was achieved with  $\text{Pb}^{2+}$  ions. The PA-3 membrane displayed rejection 80.90 % for  $\text{Pb}^{2+}$ , and 70.11 % for  $\text{Cd}^{2+}$ , respectively

(Figure 6.21 (a)). The increasing order of heavy metal ion rejection % of all membranes to  $\text{Pb}^{2+}$  and  $\text{Cd}^{2+}$  ions:  $\text{PA-0} < \text{PA-1} < \text{PA-2} < \text{PA-3}$ . In Figure 6.21 (c1&d1) were reveals the information regarding the SEM-EDS elemental mapping analysis results of heavy metals  $\text{Pb}^{2+}$  and  $\text{Cd}^{2+}$ . Heavy metal average flux was observed at  $25.24 \text{ L/m}^2 \text{ h}$  and  $29.97 \text{ L/m}^2 \text{ h}$  for  $\text{Pb}^{2+}$  and  $\text{Cd}^{2+}$ , respectively (Figure 6.21 (b)).

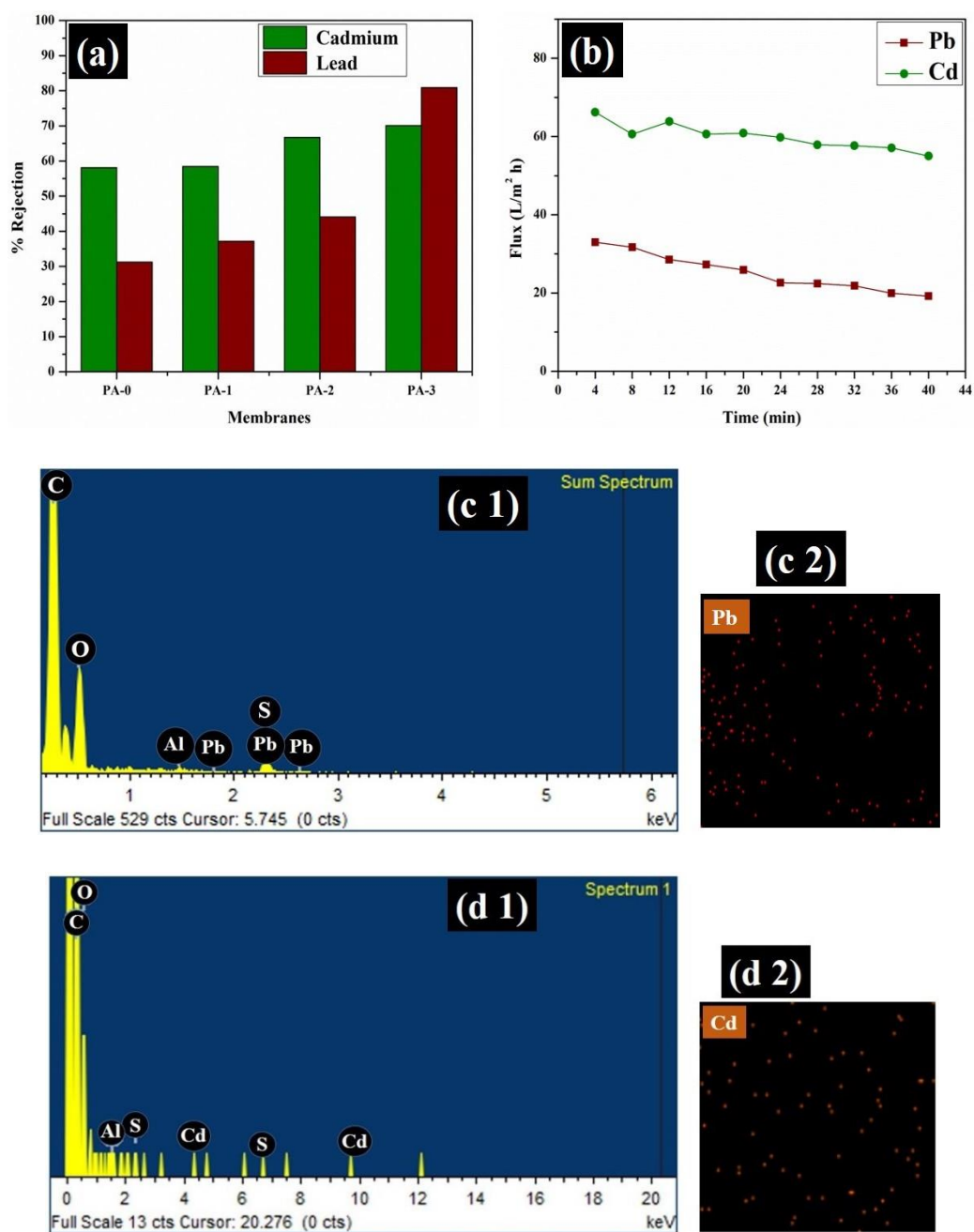
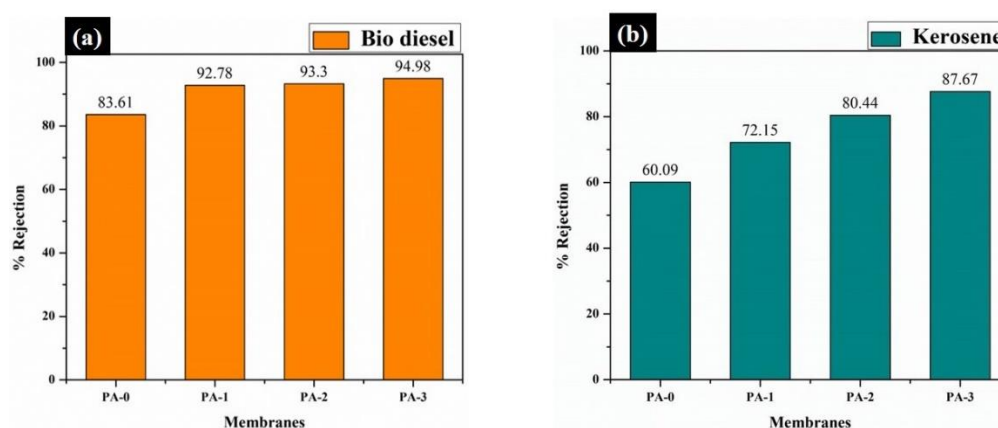


**Figure 6.21** Heavy metals rejection (a), and heavy metal flux of PA-3 membrane (b), elemental mapping results of  $\text{Pb}^{2+}$  ions (c1 & c2) and  $\text{Cd}^{2+}$  ions (d1 & d2)



### 6.3.7.3 Oil/water separation studies

The prepared membranes exhibited better oil/water separation results by enhancing the additive  $\text{Al}_2\text{O}_3$ -AAC percentages in membranes. Figure 6.22 reveals the information regarding bio-diesel and kerosene oil/water mixtures separation efficiency through membranes. The added additives, pore forming agent PVP and the  $\text{Al}_2\text{O}_3$ -AAC both have influenced the pore morphologies of membranes, and the morphological changes can be observed from PA-0 to PA-3 membranes in Figure 6.13. Usually, activated charcoal acts as a tapping agent and having good adsorption competence because of its pore structural morphology on the surface. With enhancing the activated charcoal wt. % to the polymer matrix, obviously the adsorption capacity on membrane surface will improve. Additionally, in the present research, the  $\text{Al}_2\text{O}_3$  NPs loaded on AAC as an adsorbent to increase the surface adsorption capability of AAC. Due to this effect, while performing the oil/water separation experimental study through the membranes, the oil drops were adsorbed on the membrane surface strongly and only the water can permit through membrane pores, and in results get oil-free water. In conclusions, the continuous oil rejection enhancement was observed from PA-0 to PA-3 membranes. The PA-3 membrane exhibited 94.98 % and 87.67 % rejections for bio-diesel and kerosene, respectively.





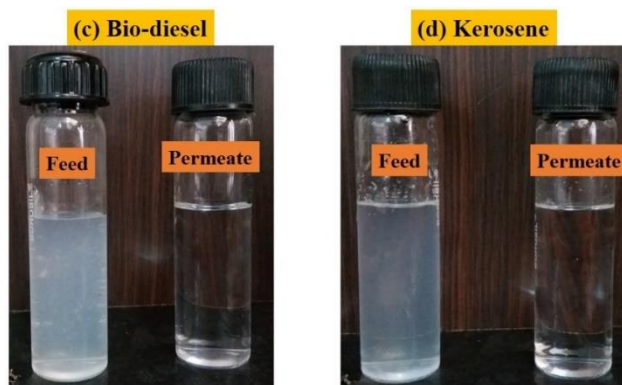


**Figure 6.22** Oil/water emulsions separation results (a) bio-diesel, and (b) kerosene, (c & d) are the feed and permeate samples outlook images

#### 6.4 CONCLUSIONS

The PPSU/ $\text{Al}_2\text{O}_3$ -AAC embedded mixed matrix membranes were fabricated successfully by non-solvent induced phase separation (NIPS) method. For the laboratory prepared membranes, filtration applications such as proteins, heavy metals rejection and for oil/water separation studies were carried out. Membrane surface and cross-sectional morphological changes were observed with a scanning electron microscope and atomic force microscope analysis. Due to the effects of hydrophilic additives  $\text{Al}_2\text{O}_3$  and polyvinylpyrrolidone, better-enhanced results observed with permeability studies. With all membranes in rejection studies, continuous enhancement was observed with increasing the  $\text{Al}_2\text{O}_3$ -AAC wt. % on PPSU polymer. Among all, type PA-3 membrane exhibited best results towards proteins, heavy metals rejection and in oil/water separation processes.



## **CHAPTER 7**

### **SUMMARY AND CONCLUSIONS**



**Abstract**

*This chapter summarizes the entire work in brief and draws a comparison between in house synthesized membranes in terms of their properties and performance. It also lists the major conclusions drawn from the work.*

**7.1 SUMMARY**

- In the current research, totally twenty membranes (5 series) with different nano additives were prepared.
- Among the twenty membranes, twelve were flat-sheet membranes and eight were hollow fiber membranes.
- Different types of nano additives such as BiOCl-AC, ZSM-5, MWCNTs, SnO<sub>2</sub> NPs, and Al<sub>2</sub>O<sub>3</sub>-AAC were used as additives and incorporated into the membrane matrix.
- Both flat-sheet and hollow fiber membranes were fabricated by phase inversion method using NMP as solvent and water as non-solvent.
- Scanning electron microscopy and Atomic force microscopy instruments were employed to analyze the morphological changes and the surface topography of membranes.
- The surface wettability ability of membranes was evaluated with water contact angle study.
- The permeability ability of membranes evaluated by pure water flux, BSA flux, water uptake, and porosity measurements.
- The fabricated membranes separation performance was determined with proteins, dyes rejection, toxic heavy metals removal from aqueous solutions and with various oil-water emulsion separation study.

**Table 7.1** Membrane series

Membrane series	Membrane codes	Nanoadditive	Type of membrane
MS-1	M-0, M-1, M-2, M-3	BiOCl-AC	UF-FS
MS-2	PZ-0, PZ-1, PZ-2, PZ-3	ZSM-5	UF-HFM
MS-3	PCNT-0, PCNT-1, PCNT-2, PCNT-3	MWCNTs	UF-FS
MS-4	PS-0, PS-1, PS-2, PS-3	SnO <sub>2</sub> NPs	UF-HFM
MS-5	PA-0, PA-1, PA-2, PA-3	Al <sub>2</sub> O <sub>3</sub> -AAC	UF-FS

(UF-Ultrafiltration, FS-Flat-sheet, HFM-Hallow fiber membrane)

Following major findings were acquired from the experimental investigations.

- i. In MS-1 series, M-3 membrane with BiOCl-AC nano additive (2 wt. %) showed higher PWF results of 465.35 L/m<sup>2</sup> h, displayed improved FRR of above 53 % with BSA protein and with oil/water separation test exhibited above 80 % rejection for Diesel fuel and above 90 % rejection for Crude oil, respectively.
- ii. In MS-2 series, PZ-3 membrane with ZSM-5 additive (0.4 wt. %) revealed good Contact angle of 69.06<sup>0</sup> with water and with rejection experiments revealed above 95 % for proteins and above 83 % for dyes, respectively.
- iii. In MS-3 series, PCNT-3 membrane with MWCNTs (0.3 wt. %) displayed PEI complexed heavy metal ions removal efficiency of above 98 % for Pb<sup>2+</sup> ions, above 76 % for Hg<sup>2+</sup> ions and above 72 % for Cd<sup>2+</sup> ions, respectively.
- iv. In MS-4 series, PS-3 membrane with SnO<sub>2</sub> NPs (0.4 wt. %) showed good Contact angle of 63.77<sup>0</sup> with water and observed enhanced PWF of 362.91 L/m<sup>2</sup> h, and exhibited high potential for dyes removal application, of above 94 % for RB-5, and above 73 % for RO-16 dye, respectively.
- v. In MS-5 series, PA-3 membrane with Al<sub>2</sub>O<sub>3</sub>-AAC NPs (1 wt. %) shown improved FRR of above 31 % with BSA protein and exhibited above 90% rejection with BSA and egg albumin (EA) proteins, above 80 % and 70 % with PEI complexed Pb<sup>2+</sup> and Cd<sup>2+</sup> heavy metal ions, and with oil-water separation exhibited above 94 % and 87 % rejection for bio-diesel and kerosene oils, respectively.

In the present research, totally fabricated, three categories of FS membranes (MS-1, MS-3, and MS-5) and two categories of HFMs (MS-2 and MS-4). The performance of all the prepared membranes in terms of PWF, contact angle and antifouling ability (% FRR) are compared and discussed below.

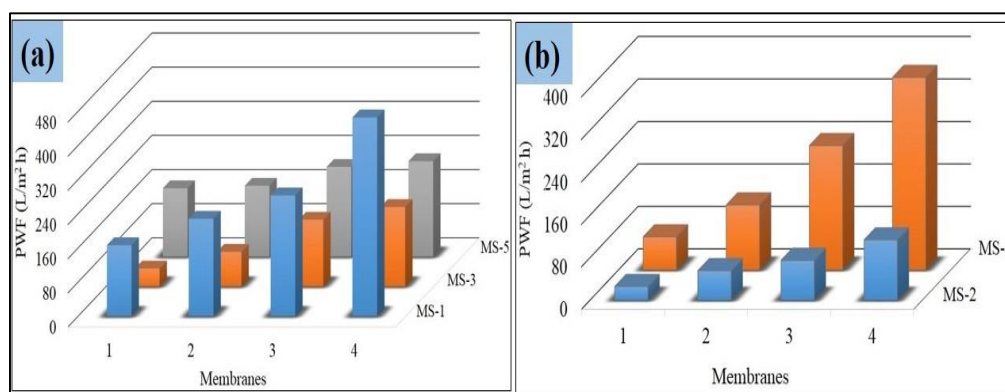


**Figure 7.1** PWF comparison results of fabricated (a) Flat-sheet and (b) HFMs

Figure 7.1 reveals the information regarding PWF of fabricated various membrane series of flat-sheet (Figure 7.1 a) and HFMs (Figure 7.1 b). From the experimental investigations, it was observed that flat-sheet membranes with BiOCl-AC additive contained membranes (MS-1) exhibited greater PWF results compare with MS-3 (MWCNTs) and MS-5 (AAC-Al<sub>2</sub>O<sub>3</sub>) series membranes. This was due to the effect of added BiOCl NPs. The loaded BiOCl NPs enhance the charcoal surface roughness and acted as good adsorbing agents towards oil/water separation studies. So that the permeability belongings of membranes increased continuously with the continuous enhancement of BiOCl-AC wt. % in membranes. Here, the added pore forming agent PVP also one of the main cause to enhance the PWF of membranes.

In HFMs, MS-4 series membranes exhibited higher PWF performance than MS-2. This is due to the effect of added SnO<sub>2</sub> NPs. These hydrophilic SnO<sub>2</sub> NPs can impact the pore size of membranes, so with PWF, the continuous improvement was observed. In MS-2 series incorporated hydrophilic ZSM-5 additives, but in size ZSM-5 is in micro level. Here, another reason is different operational pressure. In PWF study, MS-4 series membranes operated at 0.2 MPa and MS-2 series membranes operated at 0.3 MPa.

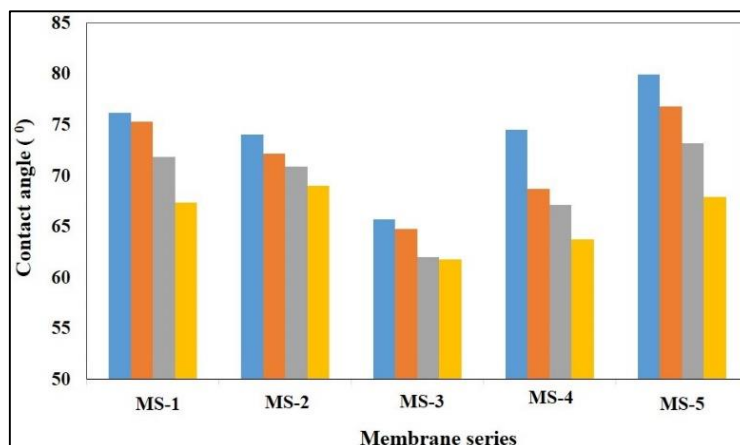


**Figure 7.2** Contact angle results of fabricated membranes

Figure 7.2 reveals information regarding the fabricated flat-sheet and hollow fiber membranes water contact angle (WCA) investigations. In membranes, this WCA characteristic will play a major role in permeability and performance. Here, to all series of membranes added various inorganic nanoparticles with different wt. %. Due to these nano additives effect in all membranes the WCA results are decreasing gradually, it concludes that the hydrophilic behavior of membranes increased. So in results observed enhanced permeability performance with membranes. Among all membranes, MS-4 series membranes exhibited better contact angle outcomes, due to the effect of hydrophilic SnO<sub>2</sub> NPs.

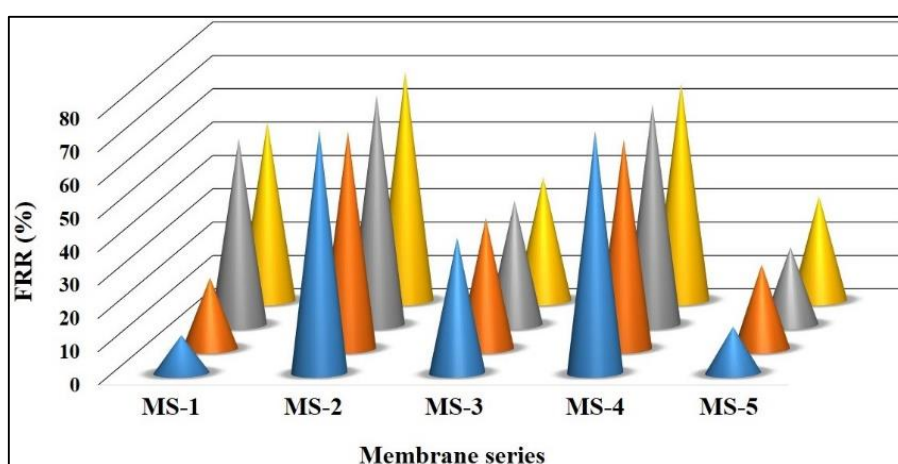


**Figure 7.3** FRR results of fabricated membranes



The antifouling performance of membranes was studied by measuring the FRR (%) values for the membranes. Figure 7.3 reveals the FRR behavior of various fabricated membrane series. All membrane series displayed an increasing trend in the % FRR values due to the effect of incorporated various nano additives. Among all, in MS-2 series PCNT-3 membrane with 0.3 wt. % of MWCNTs exhibited maximum FRR of above 68 %.

## 7.2 CONCLUSIONS

The PPSU based membranes were modified with different nano additives to expand the flux property and hydrophilicity. The ability of membranes to selectively reject proteins, dyes, and heavy metals were displayed with a judicial selection of modification techniques.

*The major conclusions of the present research work are listed below*

- ✓ The addition of BiOCl NPs and MWCNTs are considerably enhanced the antifouling and heavy metal ions removal properties.
- ✓ The addition of hydrophilic inorganic additives ZSM-5, SnO<sub>2</sub> NPs, and Al<sub>2</sub>O<sub>3</sub> NPs preferably extend the hydrophilicity, porosity, water uptake, pure water permeability and antifouling properties of membranes.
- ✓ Variation in coagulation bath compositions during phase separation process affects the morphological and permeability properties of membranes. In flat-sheet membrane series, MS-1 series membranes revealed best permeability outcomes as well as enhanced morphology results than MS-3 and MS-5 series. In hollow fibers MS-4 series revealed better performance than MS-2 series membranes.
- ✓ The change in spinning parameters during hollow fiber membranes fabrication like air gap maintenance and fiber collecting drum speed changes affects the morphology and performance of membranes. Due to the air gap maintenance variation, MS-4 series hollow fibers exhibited better outcomes, greater water permeability than MS-2 series membranes.
- ✓ The well-performed membranes in present research work used for removal of proteins, toxic heavy metal ions, and hazardous dyes from aqueous solutions

and for different oil/water emulsions separation under suitable conditions and obtained better outcomes with all series of membranes.

In future, the fabricated nanoadditive incorporated flat-sheet and hollow fiber membranes of current research can be extended to further applications such as, various toxic metals, few other dyes, and various oil/water emulsion separations, anti-biofouling, drug filtration and for hemodialysis applications. Also, the different nanomaterials synthesized in current research can assist as a guiding path for fabrication of new membranes with novel applications.

## **REFERENCES**



- Adoor, S. G., Manjeshwar, L. S., Bhat, S. D., & Aminabhavi, T. M. (2008). "Aluminum-rich zeolite beta incorporated sodium alginate mixed matrix membranes for pervaporation dehydration and esterification of ethanol and acetic acid." *J. Membr. Sci.*, 318(1-2), 233-246.
- Ahmad, A. L., Puasa, S. W., & Zulkali, M. M. D. (2006). "Micellar-enhanced ultrafiltration for removal of reactive dyes from an aqueous solution." *Desalination*, 191(13), 153-161.
- Anonymous. "Design guide for Radel polymers." Solvay Advanced Polymers. Alpharetta, GA, USA, 2009.
- Ao, C., Yuan, W., Zhao, J., He, X., Zhang, X., Li, Q., ... & Lu, C. (2017). "Superhydrophilic graphene oxide@ electrospun cellulose nanofiber hybrid membrane for high-efficiency oil/water separation." *Carbohydr. Polym.*, 175, 216-222.
- Argauer, Robert J., and Landolt, George R. (1972). "Crystalline zeolite zsm-5 and method of preparing the same". *U.S. Patent 3,702,886*.
- Arockiasamy, D. L., Alam, J., & Alhoshan, M. (2013). "Carbon nanotubes-blended poly (phenylene sulfone) membranes for ultrafiltration applications." *Appl. Water Sci.*, 3(1), 93-103.
- Aziz, H. A., Adlan, M. N., Hui, C. S., Zahari, M. S. M., & Hameed, B. H. (2005). "Removal of Ni, Cd, Pb, Zn and colour from aqueous solution using potential low cost adsorbent." *Indian J. eng. Mater. Sci.*, 12, 248-258.
- Babu, J., & Murthy, Z. V. P. (2018). "Synthesis of Nanocomposite Poly (vinyl alcohol) -Tin Oxide Mixed-Matrix Membranes for Textile Effluent Treatment." *Chem. Eng. Technol.*, 41(2), 294-302.
- Bakatula, E. N., Cukrowska, E. M., Weiersbye, I. M., Mihaly-Cozmuta, L., Peter, A., & Tutu, H. (2014). "Biosorption of trace elements from aqueous systems in gold mining sites by the filamentous green algae (*Oedogonium* sp.)." *J. Geochem. Explor.*, 144, 492-503.

- Baker, R. W. (2004). "Overview of membrane science and technology." *Membrane Technology and Applications, Second Edition*, John Wiley & Sons Ltd., England, 1-14.
- Baker, R. W. (2004). Pervaporation. "Membrane Technology and Applications," Second Edition, 355-392.
- Begon, M., Townsend, C. R., and Harper, J. L. (2006). *Ecology: from individuals to ecosystems*, Wiley-Blackwell, UK.
- Belin, S., Santos, L. R. B., Briois, V., Lusvardi, A., Santilli, C. V., Pulcinelli, S. H., ... & Larbot, A. (2003). "Preparation of ceramic membranes from surface modified tin oxide nanoparticles." *Colloids Surf. A: Physicochem. Eng. Aspects*, 216(1-3), 195-206.
- Benaissa, H., & Elouchdi, M. A. (2007). "Removal of copper ions from aqueous solutions by dried sunflower leaves." *Chem. Eng. Process. : Process intensification*, 46(7), 614-622.
- Benito, J., Ríos, G., Ortea, E., Fernández, E., Cambiella, A., Pazos, C., & Coca, J. (2002). "Design and construction of a modular pilot plant for the treatment of oil-containing wastewaters." *Desalination*, 147(1-3), 5-10.
- Bhattacharjee, A., Ahmaruzzaman, M., Devi, T. B., & Nath, J. (2016). "Photo degradation of methyl violet 6B and methylene blue using tin-oxide nanoparticles (synthesized via a green route)." *J. Photochem. Photobiol. A: Chem.*, 325, 116-124.
- Bodzek, M., & Konieczny, K. (1992). "The use of ultrafiltration membranes made of various polymers in the treatment of oil-emulsion wastewaters." *Waste manag. Res.*, 12(1), 75-84.
- Bolto, B. A. (1995). "Soluble polymers in water purification." *Prog. Polym.*, 20(6), 987-1041.
- Bowry, S. K., Gatti, E., and Vienken, J. (2011). "Contribution of polysulfone membranes to the success of convective dialysis therapies." *In High-Performance Membrane Dialyzers, Karger, Basel*, 173, 110-118.

- Brinck, J., Jönsson, A. S., Jönsson, B., & Lindau, J. (2000). "Influence of pH on the adsorptive fouling of ultrafiltration membranes by fatty acid." *J. Membr. Sci.*, 164(1-2), 187-194.
- Cao, C. Y., Cui, Z. M., Chen, C. Q., Song, W. G., & Cai, W. (2010). "Ceria hollow nanospheres produced by a template-free microwave-assisted hydrothermal method for heavy metal ion removal and catalysis." *J. Phys. Chem. C*, 114(21), 9865-9870.
- Carneiro, P. A., Osugi, M. E., Sene, J. J., Anderson, M. A., & Zanoni, M. V. B. (2004). "Evaluation of color removal and degradation of a reactive textile azo dye on nanoporous TiO<sub>2</sub> thin-film electrodes." *Electrochim. Acta*, 49(22-23), 3807-3820.
- Casey, C., Gallos, T., Alekseev, Y., Ayturk, E., & Pearl, S. (2011). "Protein concentration with single-pass tangential flow filtration (SPTFF)." *J. Membr. Sci.*, 384(1-2), 82-88.
- Chakrabarty, B., Ghoshal, A. K., & Purkait, M. K. (2008). "Ultrafiltration of stable oil-in-water emulsion by polysulfone membrane." *J. Membr. Sci.*, 325(1), 427-437.
- Chatterjee, S., Lim, S. R., & Woo, S. H. (2010). "Removal of Reactive Black 5 by zero-valent iron modified with various surfactants." *Chem. Eng. J.*, 160(1), 27-32.
- Chen, Y. H., & Li, F. A. (2010). "Kinetic study on removal of copper (II) using goethite and hematite nano-photocatalysts." *J. Colloid Interface Sci.*, 347(2), 277-281.
- Chen, Y., Hu, X., Hu, X., Zhang, S., & Zhang, Y. (2015). "Polymeric hollow fiber membranes prepared by dual pore formation mechanism." *Mater. Lett.*, 143, 315-318.
- Choi, S. J., Kwon, T. H., Im, H., Moon, D. I., Baek, D. J., Seol, M. L., ... & Choi, Y. K. (2011). "A polydimethylsiloxane (PDMS) sponge for the selective absorption of oil from water." *ACS Appl. Mater. & interfaces*, 3(12), 4552-4556.

- Christian maletzko, nina herz. Ludwigshafen, Germany. *Kunststoffe international* 10/2011, 12-17.
- Daas, A., & Hamdaoui, O. (2010). "Extraction of anionic dye from aqueous solutions by emulsion liquid membrane." *J. Hazard. Mater.*, 178(1-3), 973-981.
- Darvishmanesh, S., Jansen, J. C., Tasselli, F., Tocci, E., Luis, P., Degrève, J., Drioli, E., and Van der Bruggen, B. (2011). "Novel polyphenylsulfone membrane for potential use in solvent nanofiltration." *J. Membr. Sci.*, 379(1-2), 60-68.
- Darvishmanesh, S., Tasselli, F., Jansen, J. C., Tocci, E., Bazzarelli, F., Bernardo, P., Luis, P., Degrève, J., Drioli, E., and Van der Bruggen, B. (2011). "Preparation of solvent stable polyphenylsulfone hollow fiber nanofiltration membranes." *J. Membr. Sci.*, 384(1), 89-96.
- Dasgupta, J., Sikder, J., Chakraborty, S., Curcio, S., & Drioli, E. (2015). "Remediation of textile effluents by membrane based treatment techniques: a state of the art review." *J. Environ. Manage.*, 147, 55-72.
- Deng, S., Sourirajan, S., Chan, K., Farnand, B., Okada, T., & Matsuura, T. (1991). "Dehydration of oil-water emulsion by pervaporation using porous hydrophilic membranes." *J. Colloid Interface Sci.*, 141(1), 218-225.
- Di Vona, M. L., Sgreccia, E., Tamilvanan, M., Khadhraoui, M., Chassigneux, C., & Knauth, P. (2010). "High ionic exchange capacity polyphenylsulfone (SPPSU) and polyethersulfone (SPES) cross-linked by annealing treatment: Thermal stability, hydration level and mechanical properties." *J. Membr. Sci.*, 354(1-2), 134-141.
- Diez-Pascual, A. M., & Diez-Vicente, A. L. (2014). "Effect of TiO<sub>2</sub> nanoparticles on the performance of polyphenylsulfone biomaterial for orthopedic implants." *J. Mater. Chem. B.*, 2(43), 7502-7514.
- Dobrowolski, R., & Otto, M. (2013). "Preparation and evaluation of Ni-loaded activated carbon for enrichment of arsenic for analytical and environmental purposes." *Microporous and Mesoporous Mater.*, 179, 1-9.



- Dogan, M., Ozdemir, Y., & Alkan, M. (2007). "Adsorption kinetics and mechanism of cationic methyl violet and methylene blue dyes onto sepiolite." *Dyes Pigm.*, 75(3), 701-713.
- Donnan, F. G. (1911). "Theorie der Membran gleichgewichte und Membran potentiale bei Vorhandensein von nicht dialysierenden Elektrolyten. Ein Beitrag zur physikalisch chemischen Physiologie." *Berichte der Bunsengesellschaft für physikalische Chemie.*, 17(14), 572-581.
- Doraisammy, V., Lai, G. S., Kartohardjono, S., Lau, W. J., Chong, K. C., Lai, S. O., ... & Ismail, A. F. (2018). "Synthesis and characterization of mixed matrix membranes incorporated with hydrous manganese oxide nanoparticles for highly concentrated oily solution treatment." *Can. J. Chem. Eng.*, 96(7), 1612-1619.
- Dorosti, F., Omidkhah, M. R., Pedram, M. Z., & Moghadam, F. (2011). "Fabrication and characterization of polysulfone/polyimide-zeolite mixed matrix membrane for gas separation." *Chem. Eng. J.*, 171(3), 1469-1476.
- Economics of Zeolites. (1988). "Reports on metals & minerals." ISBN-13:978-0862149727. *Roskill Information Services Ltd.*
- Elimelech, M., & Phillip, W. A. (2011). "The future of seawater desalination: energy, technology, and the environment." *Sci.*, 333(6043), 712-717.
- Elliott, J. E., & Elliott, K. H. (2013). "Tracking marine pollution." *Sci.*, 340(6132), 556-558.
- Engates, K. E., & Shipley, H. J. (2011). "Adsorption of Pb, Cd, Cu, Zn, and Ni to titanium dioxide nanoparticles: effect of particle size, solid concentration, and exhaustion." *Environ. Sci. Pollut. Res.*, 18(3), 386-395.
- Erdem-Şenatalar, A., Bergendahl, J. A., Giaya, A., & Thompson, R. W. (2004). "Adsorption of methyl tertiary butyl ether on hydrophobic molecular sieves." *Environ. Eng. Sci.*, 21(6), 722-729.
- Fick, A. (1855). "Ueber Diffusion." *Annalen der Physik*, 170, 59-86.

- Foletto, E. L., Collazzo, G. C., Mazutti, M. A., & Jahn, S. L. (2011). "Adsorption of textile dye on zinc stannate oxide: equilibrium, kinetic and thermodynamics studies." *Sep. Sci. Technol.*, 46(16), 2510-2516.
- Fritsch, D., & Bengtson, G. (2006). "Development of catalytically reactive porous membranes for the selective hydrogenation of sunflower oil." *Catal. Today*, 118(1-2), 121-127.
- Fritzsche, A. K., Cruse, C. A., Murphy, M. K., & Kesting, R. E. (1990). "Polyethersulfone and polyphenylsulfone hollow fiber tri-layer membranes spun from Lewis acid: base complexes Structure determination by SEM, DSC, and oxygen plasma ablation." *J. Membr. Sci.*, 54(1-2), 29-50.
- Ganesh, B. M., Isloor, A. M., & Ismail, A. F. (2013). "Enhanced hydrophilicity and salt rejection study of graphene oxide-polysulfone mixed matrix membrane." *Desalination*, 313, 199-207.
- Gao, F., Zeng, D., Huang, Q., Tian, S., & Xie, C. (2012). "Chemically bonded graphene/BiOCl nanocomposites as high-performance photocatalysts." *Phys. Chem. Chem. Phys.*, 14(30), 10572-10578.
- Gao, Y., Li, Z., Cheng, B., & Su, K. (2018). "Superhydrophilic poly (p-phenylene sulfide) membrane preparation with acid/alkali solution resistance and its usage in oil/water separation." *Sep. Purif. Technol.*, 192, 262-270.
- Garg, V. K., Kumar, R., & Gupta, R. (2004). "Removal of malachite green dye from aqueous solution by adsorption using agro-industry waste: a case study of *Prosopis cineraria*." *Dyes Pigm.*, 62(1), 1-10.
- Ghaedi, M., Heidarpour, S., Kokhdan, S. N., Sahraie, R., Daneshfar, A., & Brazesh, B. (2012). "Comparison of silver and palladium nanoparticles loaded on activated carbon for efficient removal of Methylene blue: Kinetic and isotherm study of removal process." *Powder Technol.*, 228, 18-25.

Ghaedi, M., Khajesharifi, H., Yadkuri, A. H., Roosta, M., Sahraei, R., & Daneshfar, A. (2012). "Cadmium hydroxide nanowire loaded on activated carbon as efficient adsorbent for removal of Bromocresol Green." *Spectrochim. Acta A Mol. Biomol. Spectrosc.*, 86, 62-68.

Ghaedi, M., reza Rahimi, M., Ghaedi, A. M., Tyagi, I., Agarwal, S., & Gupta, V. K. (2016). "Application of least squares support vector regression and linear multiple regression for modeling removal of methyl orange onto tin oxide nanoparticles loaded on activated carbon and activated carbon prepared from Pistacia atlantica wood." *J. Colloid Interface Sci.*, 461, 425-434.

Gharehbaghi, M., & Shemirani, F. (2012). "A Novel Method for Dye Removal: Ionic Liquid-Based Dispersive Liquid-Liquid Extraction (IL-DLLE)." *CLEAN-Soil, Air, Water.*, 40(3), 290-297.

Gohari, R. J., Korminouri, F., Lau, W. J., Ismail, A. F., Matsuura, T., Chowdhury, M. N. K., ... & Gohari, M. J. (2015). "A novel super-hydrophilic PSf/HAO nanocomposite ultrafiltration membrane for efficient separation of oil/water emulsion." *Sep. Purif. Technol.*, 150, 13-20.

Graham, T. (1866). "LV. On the absorption and dialytic separation of gases by colloid septa." *The London, Edinburgh, and Dublin Philosophical Magazine, J. of Sci.*, 32(218), 401-420.

Gryta, M., & Karakulski, K. (1999). "The application of membrane distillation for the concentration of oil-water emulsions." *Desalination*, 121(1), 23-29.

Guo, H., Jiao, T., Zhang, Q., Guo, W., Peng, Q., & Yan, X. (2015). "Preparation of graphene oxide-based hydrogels as efficient dye adsorbents for wastewater treatment." *Nanoscale Res. Lett.*, 10(1), 272.

Gupta, V. K. (2009). "Application of low-cost adsorbents for dye removal—A review." *J. Environ Manage.*, 90(8), 2313-2342.

Hammed, A. K., Dewayanto, N., Du, D., Ab Rahim, M. H., & Nordin, M. R. (2016). "Novel modified ZSM-5 as an efficient adsorbent for methylene blue removal." *J. Environ. Chem. Eng.*, 4(3), 2607-2616.

- Han, L., Mao, D., Huang, Y., Zheng, L., Yuan, Y., Su, Y., ... & Fang, D. (2017). "Fabrication of unique Tin (IV) Sulfide/Graphene Oxide for photocatalytically treating chromium (VI)-containing wastewater." *J. Clean. Prod.*, 168, 519-525.
- Harold, B., Tanh Jeazet, Claudia, S., and Christoph Janiak. (2012). "Metal–organic frameworks in mixed-matrix membranes for gas separation". *Dalton Trans.*, 41, 14003-14027.
- Hebbar, R. S., Isloor, A. M., Ananda, K., & Ismail, A. F. (2016). "Fabrication of polydopamine functionalized halloysite nanotube/polyetherimide membranes for heavy metal removal." *J. Mater. Chem. A.*, 4(3), 764-774.
- Hebbar, R. S., Isloor, A. M., Zulhairun, A. K., Abdullah, M. S., & Ismail, A. F. (2017). "Efficient treatment of hazardous reactive dye effluents through antifouling polyetherimide hollow fiber membrane embedded with functionalized halloysite nanotubes." *J. Taiwan Inst. Chem. Eng.*, 72, 244-252.
- Hegde, R. R., Sharma, P., Raj, P., Keny, R. V., Bhide, P. J., Kumar, S., ... & Chakraborty, P. (2016). "Factors affecting emissions from diesel fuel and water-in-diesel emulsion." *Energy Sources, Part A: Recovery, Util. and Environ. Eff.*, 38(12), 1771-1778.
- Hinke, E., & Staude, E. (1991). "Streaming potential of microporous membranes made from homogeneously functionalized polysulfone." *J. Appl. Polym. Sci.*, 42(11), 2951-2958.
- Hong, Z., Sun, F., Chen, D., Zhang, C., Gu, X., & Xu, N. (2013). "Improvement of hydrogen-separating performance by on-stream catalytic cracking of silane over hollow fiber MFI zeolite membrane." *Int. J. Hydrogen Energy*, 38(20), 8409-8414.
- Hsieh, H. (1996). "Inorganic membranes for separation and reaction." Elsevier, Vol. 3.
- Huang, J. Y., Li, S. H., Ge, M. Z., Wang, L. N., Xing, T. L., Chen, G. Q., ... & Lai, Y. K. (2015). "Robust superhydrophobic TiO<sub>2</sub> fabrics for UV shielding, self-cleaning and oil–water separation." *J. Mater. Chem. A*, 3(6), 2825-2832.

- Hudaib, B., Gomes, V., Shi, J., Zhou, C., & Liu, Z. (2018). "Poly (vinylidene fluoride)/ polyaniline/MWCNT nanocomposite ultrafiltration membrane for natural organic matter removal." *Sep. Purif. Technol.*, 190, 143-155.
- Huotari, H. M., Huisman, I. H., & Tragardh, G. (1999). "Electrically enhanced crossflow membrane filtration of oily waste water using the membrane as a cathode." *J. Membr. Sci.*, 156(1), 49-60.
- Hwang, L. L., Tseng, H. H., & Chen, J. C. (2011). "Fabrication of polyphenylsulfone/ polyetherimide blend membranes for ultrafiltration applications: The effects of blending ratio on membrane properties and humic acid removal performance." *J. Membr. Sci.*, 384(1-2), 72-81.
- Idris, A., & Yet, L. K. (2006). "The effect of different molecular weight PEG additives on cellulose acetate asymmetric dialysis membrane performance." *J. Membr. Sci.*, 280(1-2), 920-927.
- Ihsanullah, Faheemuddin P., Majeda K., Muataz Ali A., & Tahar L. (2017). "Novel Aluminum Oxide-Impregnated Carbon Nanotube Membrane for the Removal of Cadmium from Aqueous Solution." *Materials*, 10(10), 1144.
- Jansen, R. H. S., De Rijk, J. W., Zwijnenburg, A., Mulder, M. H. V., & Wessling, M. (2005). "Hollow fiber membrane contactors—A means to study the reaction kinetics of humic substance ozonation." *J. Membr. Sci.*, 257(1-2), 48-59.
- Jha, B., & Singh, D. N. (2016). "Basics of Zeolites. In Fly Ash Zeolites." *Springer*, Singapore, 5-31.
- Jin, X., Jiang, M. Q., Shan, X. Q., Pei, Z. G., & Chen, Z. (2008). "Adsorption of methylene blue and orange II onto unmodified and surfactant-modified zeolite." *J. Colloid. Interface Sci.*, 328(2), 243-247.
- Jiraratananon, R., Sungpet, A., & Luangsowan, P. (2000). "Performance evaluation of nanofiltration membranes for treatment of effluents containing reactive dye and salt." *Desalination*, 130(2), 177-183.

- Kalavathy, M. H., & Miranda, L. R. (2010). "Comparison of copper adsorption from aqueous solution using modified and unmodified *Hevea brasiliensis* saw dust." *Desalination*, 255(1-3), 165-174.
- Kandah, M. I., & Meunier, J. L. (2007). "Removal of nickel ions from water by multi-walled carbon nanotubes." *J. Hazard. Mater.*, 146(1-2), 283-288.
- Kang, G. D., & Cao, Y. M. (2012). "Development of antifouling reverse osmosis membranes for water treatment: a review." *Water res.*, 46(3), 584-600.
- Kauss, P. B., & Hutchinson, T. C. (1975). "The effects of water-soluble petroleum components on the growth of *Chlorella vulgaris* Beijerinck." *Environ. Pollut.*, 9(3), 157-174.
- Khoramzadeh, E., Nasernejad, B., & Halladj, R. (2013). "Mercury biosorption from aqueous solutions by sugarcane bagasse." *J. Taiwan Inst. Chem. Eng.*, 44(2), 266-269.
- Khulbe, K. C., Feng, C. Y., Matsuura, T., Mosqueada-Jimenez, D. C., Rafat, M., Kingston, D., & Khayet, M. (2007). "Characterization of surface-modified hollow fiber polyethersulfone membranes prepared at different air gaps." *J. Appl. Polym. Sci.*, 104(2), 710-721.
- Kiani, S., Mousavi, S. M., Shahtahmassebi, N., & Saljoughi, E. (2015). "Hydrophilicity improvement in polyphenylsulfone nanofibrous filtration membranes through addition of polyethylene glycol." *Appl. Surf. Sci.*, 359, 252-258.
- Kim, J. C., & Kim, D. W. (2014). "Synthesis of multiphase SnSb nanoparticles-on-SnO<sub>2</sub>/Sn/C nanofibers for use in Li and Na ion battery electrodes." *Electrochem. Commun.*, 46, 124-127.
- Kim, J., and Bruggenb, B. V. D. (2010). "The use of nanoparticles in polymeric and ceramic membrane structures: Review of manufacturing procedures and performance improvement for water treatment." *Environ. Pollut.*, 158, 2335-2349.

- Kim, S. J., Ko, S. H., Kang, K. H., & Han, J. (2010). "Direct seawater desalination by ion concentration polarization." *Nat. Nanotechnol.*, 5(4), 297-301.
- Kolff, W., Berk, H., Welle, N. M., Ley, A., Dijk, E., and Noordwijk, J. (1944). "The artificial kidney: a dialyser with a great area." *Acta Med. Scand.*, 117(2), 121-134.
- Korotcenkov, G., Brinzari, V., Boris, Y., Ivanov, M., Schwank, J., & Morante, J. (2003). "Influence of surface Pd doping on gas sensing characteristics of SnO<sub>2</sub> thin films deposited by spray pyrolysis." *Thin Solid Films*, 436(1), 119-126.
- Kosa, S. A., Al-Zhrani, G., & Salam, M. A. (2012). "Removal of heavy metals from aqueous solutions by multi-walled carbon nanotubes modified with 8-hydroxyquinoline." *Chem. Eng. J.*, 181, 159-168.
- Koseoglu-Imer, D. Y., Kose, B., Altinbas, M., & Koyuncu, I. (2013). "The production of polysulfone (PS) membrane with silver nanoparticles (AgNP): physical properties, filtration performances, and biofouling resistances of membranes." *J. Membr. Sci.*, 428, 620-628.
- Kumar, M., Mehta, A., Mishra, A., Singh, J., Rawat, M., & Basu, S. (2018). "Biosynthesis of tin oxide nanoparticles using Psidium Guajava leave extract for photocatalytic dye degradation under sunlight." *Mater. Lett.*, 215, 121-124.
- Kumar, R., Isloor, A. M., Ismail, A. F., and Matsuura, T. (2013). "Synthesis and characterization of novel water soluble derivative of Chitosan as an additive for polysulfone ultrafiltration membrane." *J. Membr. Sci.*, 440, 140-147.
- Kumar, R., Isloor, A. M., Ismail, A. F., Rashid, S. A., and Matsuura, T. (2013). "Polysulfone–Chitosan blend ultrafiltration membranes: preparation, characterization, permeation and antifouling properties." *RSC Adv.*, 3(21), 7855-7861.
- Kumar, R., Isloor, A. M., Ismail, A., Rashid, S. A., and Ahmed, A. A. (2013). "Permeation, antifouling and desalination performance of TiO<sub>2</sub> nanotube incorporated PSf/CS blend membranes." *Desalination*, 316, 76-84.

- Kumar, R., Ismail, A., Kassim, M., and Isloor, A. M. (2013). "Modification of PSf/PIAM membrane for improved desalination applications using Chitosan coagulation media." *Desalination*, 317, 108-115.
- Kurbus, T., Le Marechal, A. M., & Vončina, D. B. (2003). "Comparison of H<sub>2</sub>O<sub>2</sub>/UV, H<sub>2</sub>O<sub>2</sub>/O<sub>3</sub> and H<sub>2</sub>O<sub>2</sub>/Fe<sup>2+</sup> processes for the decolorisation of vinylsulphone reactive dyes." *Dyes Pigm.*, 58(3), 245-252.
- Lalia, B. S., Kochkodan, V., Hashaikheh, R., and Hilal, N. (2013). "A review on membrane fabrication: Structure, properties and performance relationship." *Desalination*, 326, 77-95.
- Larous, S., & Meniai, A. H. (2012). "Removal of copper (II) from aqueous solution by agricultural by-products-sawdust." *Energy procedia*, 18, 915-923.
- Lee, C. H., Chiang, C. L., & Liu, S. J. (2013). "Electrospun nanofibrous rhodanine/polymethylmethacrylate membranes for the removal of heavy metal ions." *Sep. Purif. Tech.*, 118, 737-743.
- Li, B., Wu, L., Li, L., Seeger, S., Zhang, J., & Wang, A. (2014). "Superwetting double-layer polyester materials for effective removal of both insoluble oils and soluble dyes in water." *ACS Appl. Mater. Interfaces*, 6(14), 11581-11588.
- Li, B., Zhang, J., Gao, Z., & Wei, Q. (2016). "Semi-transparent superoleophobic coatings with low sliding angles for hot liquids based on silica nanotubes." *J. Mater. Chem. A.*, 4(3), 953-960.
- Li, D., & Wang, H. (2010). "Recent developments in reverse osmosis desalination membranes." *J. Mater. Chem. A.*, 20(22), 4551-4566.
- Li, D., Yao, J., Sun, H., Liu, B., van Agtmaal, S., & Feng, C. (2018). "Recycling of phenol from aqueous solutions by pervaporation with ZSM-5/PDMS/PVDF hollow fiber composite membrane." *Appl. Surf. Sci.*, 427, 288-297.
- Li, W., Yang, Z., Meng, Q., Shen, C., & Zhang, G. (2014). "Thermally stable and solvent resistant self-cross-linked TiO<sub>2</sub>/PAN hybrid hollow fiber membrane fabricated by mutual supporting method." *J. Membr. Sci.*, 467, 253-261.



- Liang, X., Su, Y., Yang, Y., & Qin, W. (2012). "Separation and recovery of lead from a low concentration solution of lead (II) and zinc (II) using the hydrolysis production of poly styrene-co-maleic anhydride." *J. Hazard. Mater.*, 203, 183-187.
- Liao, C., Zhao, J., Yu, P., Tong, H., & Luo, Y. (2010). "Synthesis and characterization of SBA-15/poly (vinylidene fluoride) (PVDF) hybrid membrane." *Desalination*, 260(1-3), 147-152.
- Lin, S. H., & Lan, W. J. (1998). "Treatment of waste oil/water emulsion by ultrafiltration and ion exchange." *Water Res.*, 32(9), 2680-2688.
- Liu, C., & Bai, R. (2006). "Adsorptive removal of copper ions with highly porous chitosan/cellulose acetate blend hollow fiber membranes." *J. Memb. Sci.*, 284(1-2), 313-322.
- Liu, F., Hashim, N. A., Liu, Y., Abed, M. M., & Li, K. (2011). "Progress in the production and modification of PVDF membranes." *J. Membr. Sci.*, 375(1-2), 1-27.
- Liu, J., Lu, X. L., & Wu, C. R. (2013). "Effect of annealing conditions on crystallization behavior and mechanical properties of NIPS poly (vinylidene fluoride) hollow fiber membranes." *J. Appl. Polym. Sci.*, 129(3), 1417-1425.
- Liu, J., Zhong, Z., Ma, R., Zhang, W., & Li, J. (2016). "Development of High-Antifouling PPSU Ultrafiltration Membrane by Using Compound Additives: Preparation, Morphologies, and Filtration Resistant Properties." *Membranes*, 6(2), 35.
- Liu, N., Zhang, M., Zhang, W., Cao, Y., Chen, Y., Lin, X., ... & Wei, Y. (2015). "Ultralight free-standing reduced graphene oxide membranes for oil-in-water emulsion separation." *J. Mater. Chem. A*, 3(40), 20113-20117.
- Liu, Y., Su, Y., Cao, J., Guan, J., Zhang, R., He, M., ... & Jiang, Z. (2017). "Antifouling, high-flux oil/water separation carbon nanotube membranes by polymer-mediated surface charging and hydrophilization." *J. Membr. Sci.*, 542, 254-263.

- Liu, Y., Su, Y., Cao, J., Guan, J., Zhang, R., He, M., ... & Jiang, Z. (2017). "Antifouling, high-flux oil/water separation carbon nanotube membranes by polymer-mediated surface charging and hydrophilization." *J. Memb. Sci.*, 542, 254-263.
- Liu, Y., Yue, X., Zhang, S., Ren, J., Yang, L., Wang, Q., & Wang, G. (2012). "Synthesis of sulfonated polyphenylsulfone as candidates for antifouling ultrafiltration membrane." *Sep. Purif. Technol.*, 98, 298-307.
- Lloyd, A. C., & Cackette, T. A. (2001). "Diesel engines: environmental impact and control." *J. Air Waste Manag. Assoc.*, 51(6), 809-847.
- Lonsdale, H. K. (1982). "The growth of membrane technology." *J. Membr. Sci.*, 10(2-3), 81-181.
- Lue, S. J., Chow, J., Chien, C., & Chen, H. (2009). "Cross-Flow microfiltration of oily water using a ceramic membrane: flux decline and oil adsorption." *Sep. Sci. Technol.*, 44(14), 3435-3454.
- Luo, L., Han, G., Chung, T. S., Weber, M., Staudt, C., & Maletzko, C. (2015). "Oil/water separation via ultrafiltration by novel triangle-shape tri-bore hollow fiber membranes from sulfonated polyphenylenesulfone." *J. Membr. Sci.*, 476, 162-170.
- Ma, J., Li, F., Qian, T., Liu, H., Liu, W., & Zhao, D. (2017). "Natural organic matter resistant powder activated charcoal supported titanate nanotubes for adsorption of Pb (II)." *Chem. Eng. J.*, 315, 191-200.
- Ma, X., Wang, Y., Gao, M., Xu, H., & Li, G. (2010). "A novel strategy to prepare ZnO/PbS hetero-structured functional nanocomposite utilizing the surface adsorption property of ZnO nanosheets." *Catal. Today*, 158(3-4), 459-463.
- Maguire-Boyle, S. J., & Barron, A. R. (2011). "A new functionalization strategy for oil/water separation membranes." *J. Membr. Sci.*, 382(1-2), 107-115.

- Mahdavi, M. R., Delnavaz, M., & Vatanpour, V. (2017). "Fabrication and water desalination performance of piperazine–polyamide nanocomposite nanofiltration membranes embedded with raw and oxidized MWCNTs." *J. Taiwan Inst. Chem. Eng.*, 75, 189-198.
- Malik, A. (2004). "Metal bioremediation through growing cells." *Environ. int.*, 30(2), 261-278.
- Mall, I. D., Srivastava, V. C., & Agarwal, N. K. (2006). "Removal of Orange-G and Methyl Violet dyes by adsorption onto bagasse fly ash—kinetic study and equilibrium isotherm analyses." *Dyes Pigm.*, 69(3), 210-223.
- Mao, X., Zhou, R., Zhang, S., Ding, L., Wan, L., Qin, S., ... & Miao, S. (2016). "High efficiency dye-sensitized solar cells constructed with composites of TiO<sub>2</sub> and the hot-bubbling synthesized ultra-small SnO<sub>2</sub> nanocrystals." *Sci. Rep.*, 6, 19390.
- Mehrnia, M. R., Mojtahedi, Y. M., & Homayoonfal, M. (2015). "What is the concentration threshold of nanoparticles within the membrane structure? A case study of Al<sub>2</sub>O<sub>3</sub>/PSf nanocomposite membrane." *Desalination*, 372, 75-88.
- Mittal, A., Naushad, M., Sharma, G., AlLothman, Z. A., Wabaidur, S. M., & Alam, M. (2016). "Fabrication of MWCNTs/ThO<sub>2</sub> nanocomposite and its adsorption behavior for the removal of Pb (II) metal from aqueous medium." *Desalin. Water Treat.*, 57(46), 21863-21869.
- Mohammadi, T., Kazemimoghadam, M., & Saadabadi, M. (2003). "Modeling of membrane fouling and flux decline in reverse osmosis during separation of oil in water emulsions." *Desalination*, 157(1-3), 369-375.
- Moideen K, I., Isloor, A. M., Ismail, A. F., Obaid, A., & Fun, H. K. (2016). "Fabrication and characterization of new PSF/PPSU UF blend membrane for heavy metal rejection." *Desalin. Water Treat.*, 57(42), 19810-19819.
- Morihama, A. C. D., & Mierzwa, J. C. (2014). "Clay nanoparticles effects on performance and morphology of poly (vinylidene fluoride) membranes." *Braz. J. Chem. Eng.*, 31(1), 79-93.

- Moslehyani, A., Ismail, A. F., Othman, M. H. D., & Matsuura, T. (2015). "Design and performance study of hybrid photocatalytic reactor-PVDF/MWCNT nanocomposite membrane system for treatment of petroleum refinery wastewater." *Desalination*, 363, 99-111.
- Mueller, J., Cen, Y., & Davis, R. H. (1997). "Crossflow microfiltration of oily water." *J. Membr. Sci.*, 129(2), 221-235.
- Mulder, M. (1992). "Basic Principles of Membrane Technology." Kluwer Academic, Dordrecht. The Netherlands.
- Mulder, M. (1996). "Membrane Processes." *Basic Principles of Membrane Technology Second Edition*, Kluwer Academic Publishers, Netherlands, 280-412.
- Nayak, M. C., Isloor, A. M., Moslehyani, A., & Ismail, A. F. (2017). "Preparation and characterization of PPSU membranes with BiOCl nanowafers loaded on activated charcoal for oil in water separation." *J. Taiwan Inst. Chem. Eng.*, 77, 293-301.
- Nayak, M. C., Isloor, A. M., Moslehyani, A., Ismail, N., & Ismail, A. F. (2018). Fabrication of novel PPSU/ZSM-5 ultrafiltration hollow fiber membranes for separation of proteins and hazardous reactive dyes. *J. Taiwan Inst. Chem. Eng.*, 82, 342-350.
- Neill, J., & Karasz, F. (2000). "Miscibility of some polycarbonates with polyvinyl chloride and chlorinated polyvinyl chloride." *J Therm Anal Calorim.*, 59(1-2), 33-58.
- Nekouei, F., & Nekouei, S. (2017). "Comparative evaluation of BiOCl-NPIs-AC composite performance for methylene blue dye removal from solution in the presence/absence of UV irradiation: kinetic and isotherm studies." *J. Alloys. Compd.*, 701, 950-966.
- Ng, L. Y., Mohammad, A. W., Leo, C. P., & Hilal, N. (2013). "Polymeric membranes incorporated with metal/metal oxide nanoparticles: a comprehensive review." *Desalination*, 308, 15-33.

- Ng, L. Y., Mohammad, A. W., Leo, C. P., and Hilal, N. (2013). "Polymeric membranes incorporated with metal/metal oxide nanoparticles: A comprehensive review." *Desalination*, 308, 15-33.
- Nollet, J. A. (1995). "Investigations on the causes for the ebullition of liquids." *J. Membr. Sci.*, 100(1), 1-3.
- Ohya, H., Kim, J. J., Chinen, A., Aihara, M., Semenova, S. I., Negishi, Y., ... & Yasuda, M. (1998). "Effects of pore size on separation mechanisms of microfiltration of oily water, using porous glass tubular membrane." *J. Membr. Sci.*, 145(1), 1-14.
- Okoye, C. O., & Okunrobo, L. A. (2014). "Impact of oil spill on land and water and its health implications in odu-gboro community, sagamu, ogun state, nigeria." *World J. Environ. Sci. Eng.*, 1(1), 1-21.
- Omoriegie, E., Ufodike, E. B. C., & Onwuliri, C. O. E. (1997). "Effects of water soluble fractions of crude oil on carbohydrate reserves of *Oreochromis niloticus* (L)." *J. Aquat. Sci.*, 12, 1-7.
- Onwurah, I. N. E., Ogugua, V. N., Onyike, N. B., Ochonogor, A. E., & Otitoju, O. F. (2007). "Crude oil spills in the environment, effects and some innovative clean-up biotechnologies." *Int. J. Envir. Res.*, 4, 307-320.
- Othman, I., Mohamed, R. M., Ibrahim, I. A., & Mohamed, M. M. (2006). "Synthesis and modification of ZSM-5 with manganese and lanthanum and their effects on decolorization of indigo carmine dye." *Appl. Catal. A: General*, 299, 95-102.
- Ouyang, G., Hussain, A., Li, J., & Li, D. (2015). "Remarkable permeability enhancement of polyethersulfone (PES) ultrafiltration membrane by blending cobalt oxide/graphene oxide nanocomposites." *RSC Adv.*, 5(86), 70448-70460.
- Pagga, U., & Brown, D. (1986). "The degradation of dyestuffs: Part II Behavior of dyestuffs in aerobic biodegradation tests." *Chemosphere*, 15(4), 479-491.

- Pak, S. H., Jeon, M. J., & Jeon, Y. W. (2016). "Study of sulfuric acid treatment of activated carbon used to enhance mixed VOC removal." *Int. Biodeterioration & Biodegradation*, 113, 195-200.
- Pakarinen, J., Koivula, R., Laatikainen, M., Laatikainen, K., Paatero, E., & Harjula, R. (2010). "Nanoporous manganese oxides as environmental protective materials—Effect of Ca and Mg on metals sorption." *J. Hazard. Mater.*, 180(1-3), 234-240.
- Pan, X., & Yi, Z. (2015). "Graphene oxide regulated tin oxide nanostructures: Engineering composition, morphology, band structure, and photocatalytic properties." *ACS Appl. Mater. & interfaces*, 7(49), 27167-27175.
- Parceró, E., Herrera, R., & Nunes, S. P. (2006). "Phosphonated and sulfonated polyphenylsulfone membranes for fuel cell application." *J. Membr. Sci.*, 285(1-2), 206-213.
- Patel, F., Baig, M. A., & Laoui, T. (2011). "Processing of porous alumina substrate for multilayered ceramic filter." *Desalin. Water Treat.*, 35(1-3), 33-38.
- Pereira, V. R., Isloor, A. M., Zuhairun, A. K., Subramaniam, M. N., Lau, W. J., & Ismail, A. F. (2016). "Preparation of polysulfone-based PANI–TiO<sub>2</sub> nanocomposite hollow fiber membranes for industrial dye rejection applications." *RSC Adv.*, 6(102), 99764-99773.
- Petkowicz, D. I., Pergher, S. B., Da Silva, C. D. S., Da Rocha, Z. N., & Dos Santos, J. H. (2010). "Catalytic photo degradation of dyes by in situ zeolite-supported titania." *Chem. Eng. J.*, 158(3), 505-512.
- Podstawczyk, D., Witek-Krowiak, A., Chojnacka, K., & Sadowski, Z. (2014). "Biosorption of malachite green by eggshells: mechanism identification and process optimization." *Bioresour. Technol.*, 160, 161-165.
- Ponnusami, V., Vikram, S., & Srivastava, S. N. (2008). "Guava (*Psidium guajava*) leaf powder: novel adsorbent for removal of methylene blue from aqueous solutions." *J. Hazard. Mater.*, 152(1), 276-286.

- Prince, J. A., Bhuvana, S., Anbharasi, V., Ayyanar, N., Boodhoo, K. V. K., & Singh, G. (2016). "Ultra-wetting graphene-based PES ultrafiltration membrane—A novel approach for successful oil-water separation." *Water res.*, 103, 311-318.
- Puma, G. L., Bono, A., Krishnaiah, D., & Collin, J. G. (2008). "Preparation of titanium dioxide photocatalyst loaded onto activated carbon support using chemical vapour deposition: a review paper." *J. Hazard. Mater.*, 157(2-3), 209-219.
- Pusch, W., & Walch, A. (1982). "Synthetic membranes—preparation, structure, and application." *Angew. Chem. Int. Ed.*, 21(9), 660-685.
- Rajak, V. K., Kumar, S., Thombre, N. V., & Mandal, A. (2018). "Synthesis of activated charcoal from saw-dust and characterization for adsorptive separation of oil from oil-in-water emulsion." *Chem. Eng. Commun.*, 205(7), 897-913.
- Rajesh, S., Ismail, A. F., & Mohan, D. R. (2012). "Structure-property interplay of poly (amide-imide) and TiO<sub>2</sub> nanoparticles impregnated poly (ether-sulfone) asymmetric nanofiltration membranes." *RSC Adv.*, 2(17), 6854-6870.
- Ratledge, C. (1992). "Biodegradation and biotransformations of oils and fats introduction." *J. Chem. Technol. Biotechnol.*, 55(4), 397-398.
- Refaai, W., Van Aert, M., El-Aal, A. A., Behery, A. E., & Opsomer, G. (2013). "Infectious diseases causing lameness in cattle with a main emphasis on digital dermatitis (Mortellaro disease)." *Livest. Sci.*, 156(1), 53-63.
- Rekha, P., Muhammad, R., & Mohanty, P. (2015). "Sonochemical synthesis of cyclophosphazene bridged mesoporous organosilicas and their application in methyl orange, congo red and Cr (VI) removal." *RSC Adv.*, 5(83), 67690-67699.
- Rong, J., Zhang, T., Qiu, F., Xu, J., Zhu, Y., Yang, D., & Dai, Y. (2018). "Design and preparation of efficient, stable and superhydrophobic copper foam membrane for selective oil absorption and consecutive oil–water separation." *Mater. Des.*, 142, 83-92.

- Roy Chowdhury, S., Keizer, K., ten Elshof, J. E., & Blank, D. H. (2004). "Effect of trace amounts of water on organic solvent transport through  $\gamma$ -alumina membranes with varying pore sizes." *Langmuir*, 20(11), 4548-4552.
- Saadati, J., & Pakizeh, M. (2017). "Separation of oil/water emulsion using a new PSf/pebax/F-MWCNT nanocomposite membrane." *J. Taiwan Inst. Chem. Eng.*, 71, 265-276.
- Sabarish, R., & Unnikrishnan, G. (2018). "PVA/PDADMAC/ZSM-5 zeolite hybrid matrix membranes for dye adsorption: Fabrication, characterization, adsorption, kinetics and antimicrobial properties." *J. Environ. Chem. Eng.*
- Saini, J., Garg, V. K., Gupta, R. K., & Kataria, N. (2017). "Removal of Orange G and Rhodamine B dyes from aqueous system using hydrothermally synthesized zinc oxide loaded activated carbon (ZnO-AC)." *J. Environ. Chem. Eng.*, 5(1), 884-892.
- Salleh, M. A. M., Mahmoud, D. K., Karim, W. A. W. A., & Idris, A. (2011). "Cationic and anionic dye adsorption by agricultural solid wastes: A comprehensive review." *Desalination*, 280(1-3), 1-13.
- Santos, L. R. B., Santilli, C. V., Larbot, A., Persin, M., & Pulcinelli, S. H. (2001). "Influence of membrane-solution interface on the selectivity of SnO<sub>2</sub> ultrafiltration membranes." *Sep. Purif. Technol.*, 22, 17-22.
- Sardari-Mamaghani, M., Aroon, M. A., Sadjadi, S., Matsuura, T., & Nouri, A. (2018). "Effect of MWCNTs on the Performance of Mixed-Matrix Membranes in Removing Cerium Ions from Aqueous Feed Solutions." *J. Environ. Eng.*, 144(3), 04018005.
- Sarkar, S., Bandyopadhyay, S., Larbot, A., & Cerneaux, S. (2012). "New clay–alumina porous capillary supports for filtration application." *J. Membr. Sci.*, 392, 130-136.
- Sarwan, B., Pare, B., Acharya, A. D., & Jonnalagadda, S. B. (2012). "Mineralization and toxicity reduction of textile dye neutral red in aqueous phase using BiOCl photo-catalysis." *J. Photochem. Photobiol. B.*, 116, 48-55.



Schaep, J., Van der Bruggen, B., Vandecasteele, C., & Wilms, D. (1998). "Influence of ion size and charge in nanofiltration." *Sep. Purif. Technol.*, 14(1-3), 155-162.

Schütz, S., Ehlen, F., Unger, I., Kariveti, S., Wang, C., Ebrahimi, M., ... & Czermak, P. (2015). "Ceramic Hollow Fiber Membranes As New Filter Media And Their Application In Oil/Water Separation Processes." In *FILTECH 2015*. Cologne, Germany.

Seema, H., Kemp, K. C., Chandra, V., & Kim, K. S. (2012). "Graphene-SnO<sub>2</sub> composites for highly efficient photocatalytic degradation of methylene blue under sunlight." *Nanotech.*, 23(35), 355705.

Selim, M. M., & El-Maksoud, I. H. A. (2004). "Hydrogenation of edible oil over zeolite prepared from local kaolin." *Microporous and Mesoporous Materials*, 74(1-3), 79-85.

Setiawan, L., Wang, R., Li, K., & Fane, A. G. (2011). "Fabrication of novel poly (amide-imide) forward osmosis hollow fiber membranes with a positively charged nanofiltration-like selective layer." *J. Memb. Sci.*, 369(1-2), 196-205.

Setthaya, N., Chindaprasirt, P., Yin, S., & Pimraksa, K. (2017). "TiO<sub>2</sub>-zeolite photocatalysts made of metakaolin and rice husk ash for removal of methylene blue dye." *Powder Technol.*, 313, 417-426.

Shah, P., & Murthy, C. N. (2013). "Studies on the porosity control of MWCNT/polysulfone composite membrane and its effect on metal removal." *J. Membr. Sci.*, 437, 90-98.

Shannon, M. A., Bohn, P. W., Elimelech, M., Georgiadis, J. G., Marinas, B. J., and Mayes, A. M. (2008). "Science and technology for water purification in the coming decades." *Nature*, 452, 301-310.

Shao, L., Wang, Z. X., Zhang, Y. L., Jiang, Z. X., & Liu, Y. Y. (2014). "A facile strategy to enhance PVDF ultrafiltration membrane performance via self-polymerized polydopamine followed by hydrolysis of ammonium fluotitanate." *J. Membr. Sci.*, 461, 10-21.

- Shashikala V, Raju B D and Rao KSR. (2016). "Application of Adsorbents - A Viable technology for the Removal of Fluoride ion in Ground Water." *Science Spectrum*, 1, 76-83.
- Shenvi, S. S., Isloor, A. M., Ismail, A. F., Shilton, S. J., & Al Ahmed, A. (2015). "Humic acid based biopolymeric membrane for effective removal of methylene blue and rhodamine B." *Ind. Eng. Chem. Res.*, 54(18), 4965-4975.
- Shenvi, S., Ismail, A. F., & Isloor, A. M. (2014). "Enhanced permeation performance of cellulose acetate ultrafiltration membranes by incorporation of sulfonated poly (1, 4-phenylene ether ether sulfone) and poly (styrene-co-maleic anhydride)." *Ind. Eng. Chem. Res.*, 53(35), 13820-13827.
- Shukla, A. K., Alam, J., Alhoshan, M., Dass, L. A., & Muthumareeswaran, M. R. (2017). "Development of a nanocomposite ultrafiltration membrane based on polyphenylsulfone blended with graphene oxide." *Sci. Rep.*, 7, 41976.
- Smith, S. P. J., Linkov, V. M., Sanderson, R. D., Petrik, L. F., O'connor, C. T., & Keiser, K. (1995). "Preparation of hollow-fibre composite carbon-zeolite membranes." *Microporous mater.*, 4(5), 385-390.
- Solvay Company, Radel (PPSU), Veradel (PES), Acudel (PSf). PPSU-design guide. [www.solvay.com](http://www.solvay.com).
- Son, L. T., & Takaomi, K. (2011). "Hollow-fiber membrane absorbents embedded molecularly imprinted polymeric spheres for bisphenol A target." *J. Memb. Sci.*, 384(1-2), 117-125.
- Spillman, R. W. (1989). "Economics of gas separation membranes." *Chem. Eng. Prog.*, 85(1), 41-62.
- Srivastava, N., & Mukhopadhyay, M. (2014). "Biosynthesis of SnO<sub>2</sub> nanoparticles using bacterium *Erwinia herbicola* and their photocatalytic activity for degradation of dyes." *Ind. Eng. Chem. Res.*, 53(36), 13971-13979.

- Sukitpaneent, P., & Chung, T. S. (2012). "High performance thin-film composite forward osmosis hollow fiber membranes with macro void-free and highly porous structure for sustainable water production." *Environ. Sci. Technol.*, 46(13), 7358-7365.
- Sun, H., Sur, G. S., & Mark, J. E. (2002). "Microcellular foams from polyethersulfone and polyphenylsulfone: preparation and mechanical properties." *Eur. Polym. J.*, 38(12), 2373-2381.
- Sun, H., Venkata subramanian, N., Houtz, M. D., Mark, J. E., Tan, S. C., Arnold, F. E., & Lee, C. Y. (2004). "Molecular composites by incorporation of a rod-like polymer into a functionalized high-performance polymer, and their conversion into microcellular foams." *Colloid Polym. Sci.*, 282(5), 502-510.
- Sun, J., Wu, L., & Li, Y. (2017). "Removal of lead ions from polyether sulfone/Pb (II)-imprinted multi-walled carbon nanotubes mixed matrix membrane." *J. Taiwan Inst. Chem. Eng.*, 78, 219-229.
- Takagishi, T., Okuda, S., Kuroki, N., & Kozuka, H. (1985). "Binding of metal ions by polyethylenimine and its derivatives." *J. Polym. Sci. Part A: Polym. Chem.*, 23(8), 2109-2116.
- Tang, H., Hao, L., Chen, J., Wang, F., Zhang, H., & Guo, Y. (2018). "Surface modification to fabricate superhydrophobic and superoleophilic alumina membranes for oil/water separation." *Energy & Fuels*, 32(3), 3627-3636.
- Tarasevich, Y. I., & Klimova, G. M. (2001). "Complex-forming adsorbents based on kaolinite, aluminium oxide and polyphosphates for the extraction and concentration of heavy metal ions from water solutions." *Appl. Clay Sci.*, 19(1-6), 95-101.
- The Yang C., Zhang G., Xu N., Shi J. (1998). "Preparation and application in oil/water separation of ZrO<sub>2</sub>/  $\alpha$ -Al<sub>2</sub>O<sub>3</sub> MF membrane." *J. Membr. Sci.*, 142, 235-243.

- Traube, M. (1867). "Physiologie und wissenschaftliche Medizin." *Arch. An. Physiol*, 87.
- Treccani, L., Klein, T. Y., Meder, F., Pardun, K., & Rezwani, K. (2013). "Functionalized ceramics for biomedical, biotechnological and environmental applications." *Acta biomater.*, 9(7), 7115-7150.
- Tylkowski, B., & Tsibranska, I. (2015). "Overview of main techniques used for membrane characterization." *J. Chem. Tech. & Metallurgy*, 50(1), 3-12.
- Uludag, Y., Ozbelge, H. O., & Yilmaz, L. (1997). "Removal of mercury from aqueous solutions via polymer-enhanced ultrafiltration." *J. Membr. Sci.*, 129(1), 93-99.
- Um, M. J., Yoon, S. H., Lee, C. H., Chung, K. Y., & Kim, J. J. (2001). "Flux enhancement with gas injection in crossflow ultrafiltration of oily wastewater." *Water res.*, 35(17), 4095-4101.
- Van de Witte, P., Dijkstra, P. J., Van den Berg, J. W. A., & Feijen, J. (1996). "Phase separation processes in polymer solutions in relation to membrane formation." *J. Membr. Sci.*, 117(1-2), 1-31.
- Verissimo, S., Peinemann, K. V., & Bordado, J. (2005). "Thin-film composite hollow fiber membranes: an optimized manufacturing method." *J. Membr. Sci.*, 264(1-2), 48-55.
- Verma, S. K., Kar, P., Yang, D. J., & Choudhury, A. (2015). "Poly (m-aminophenol)/functionalized multi-walled carbon nanotube nanocomposite based alcohol sensors." *Sens. Actuators B Chem.*, 219, 199-208.
- Vilakati, G. D., Hoek, E. M., and Mamba, B. B. (2014). "Probing the mechanical and thermal properties of polysulfone membranes modified with synthetic and natural polymer additives." *Polym. Test.*, 34, 202-210.
- Voncina, D. B., & Majcen-Le-Marechal, A. (2003). "Reactive dye decolorization using combined ultrasound/H<sub>2</sub>O<sub>2</sub>." *Dyes Pigm.*, 59(2), 173-179.

- Wang, D., Teo, W. K., & Li, K. (2002). "Preparation and characterization of high-flux polysulfone hollow fibre gas separation membranes." *J. Memb. Sci.*, 204(1-2), 247-256.
- Wang, J., Hou, L. A., Yan, K., Zhang, L., & Yu, Q. J. (2018). "Polydopamine nanocluster decorated electrospun nanofibrous membrane for separation of oil/water emulsions." *J. Memb. Sci.*, 547, 156-162.
- Wang, Z., Yu, H., Xia, J., Zhang, F., Li, F., Xia, Y., & Li, Y. (2012). "Novel GO-blended PVDF ultrafiltration membranes." *Desalination*, 299, 50-54.
- Wei, X., Kong, X., Sun, C., & Chen, J. (2013). "Characterization and application of a thin-film composite nanofiltration hollow fiber membrane for dye desalination and concentration." *Chem. Eng. J.*, 223, 172-182.
- Weng, T. H., Tseng, H. H., & Wey, M. Y. (2008). "Preparation and characterization of PPSU/PBNPI blend membrane for hydrogen separation." *Int. J. Hydrogen Energy*, 33(15), 4178-4182.
- Weng, T. H., Tseng, H. H., & Wey, M. Y. (2009). "Preparation and characterization of multi-walled carbon nanotube/PBNPI nanocomposite membrane for H<sub>2</sub>/CH<sub>4</sub> separation." *Int. J. Hydrogen Energy*, 34(20), 8707-8715.
- Xie, Z., Li, T., Rosi, N. L., & Carreon, M. A. (2014). "Alumina-supported cobalt-adeninate MOF membranes for CO<sub>2</sub>/CH<sub>4</sub> separation." *J. Mater. Chem. A.*, 2(5), 1239-1241.
- Xing, R., Wang, W., Jiao, T., Ma, K., Zhang, Q., Hong, W., ... & Peng, Q. (2017). "Bioinspired polydopamine sheathed nanofibers containing carboxylate graphene oxide nanosheets for high-efficient dyes scavenger." *ACS Sustain. Chem. Eng.*, 5(6), 4948-4956.
- Xiong, C., & Balkus, K. J. (2007). "Mesoporous molecular sieve derived TiO<sub>2</sub> nanofibers doped with SnO<sub>2</sub>." *J. Phys. Chem. C*, 111(28), 10359-10367.

- Xu, Y. C., Tang, Y. P., Liu, L. F., Guo, Z. H., & Shao, L. (2017). "Nanocomposite organic solvent nanofiltration membranes by a highly-efficient mussel-inspired co-deposition strategy." *J. Membr. Sci.*, 526, 32-42.
- Yamashita, A. C., and Sakurai, K. (2015). "Dialysis Membranes—Physicochemical Structures and Features." In Updates in Hemodialysis. *In Tech.*, 1-26.
- Yan L, Lib S Y, Xiang B. C. (2005). "Preparation of poly (vinylidene fluoride) ultrafiltration membrane modified by nano-sized alumina (Al<sub>2</sub>O<sub>3</sub>) and its antifouling research." *Polymer*, 46, 7701–7706.
- Yang, K., Zhu, X., & Chen, B. (2017). "Facile fabrication of freestanding all-carbon activated carbon membranes for high-performance and universal pollutant management." *J. Mater. Chem. A.*, 5(38), 20316-20326.
- Young, T. H., & Chen, L. W. (1995). "Pore formation mechanism of membranes from phase inversion process." *Desalination*, 103(3), 233-247.
- Yu, Z., Zeng, G., Pan, Y., Lv, L., Min, H., Zhang, L., & He, Y. (2015). "Effect of functionalized multi-walled carbon nanotubes on the microstructure and performances of PVDF membranes." *RSC Adv.*, 5(93), 75998-76006.
- Yuan, X., Li, W., Zhu, Z., Han, N., & Zhang, X. (2017). "Thermo-responsive PVDF/PSMA composite membranes with micro/nanoscale hierarchical structures for oil/water emulsion separation." *Colloids Surf. A Physicochem. Eng. Aspects*, 516, 305-316.
- Yusoff, A., & Murray, B. S. (2011). "Modified starch granules as particle-stabilizers of oil-in-water emulsions." *Food Hydrocoll.*, 25(1), 42-55.
- Zhang, G., Lu, S., Zhang, L., Meng, Q., Shen, C., & Zhang, J. (2013). "Novel polysulfone hybrid ultrafiltration membrane prepared with TiO<sub>2</sub>-g-HEMA and its antifouling characteristics." *J. Membr. Sci.*, 436, 163-173.
- Zhang, J., & Seeger, S. (2011). "Polyester materials with super-wetting silicone nano filaments for oil/water separation and selective oil absorption." *Adv. Funct. Mater.*, 21(24), 4699-4704.

- Zhang, J., Shao, Y., Hsieh, C. T., Chen, Y. F., Su, T. C., Hsu, J. P., & Juang, R. S. (2017). "Synthesis of magnetic iron oxide nanoparticles onto fluorinated carbon fabrics for contaminant removal and oil-water separation." *Sep. Purif. Technol.*, 174, 312-319.
- Zhao, S., Wang, Z., Wei, X., Zhao, B., Wang, J., Yang, S., & Wang, S. (2012). "Performance improvement of polysulfone ultrafiltration membrane using well-dispersed polyaniline–poly (vinylpyrrolidone) nanocomposite as the additive." *Ind. Eng. Chem. Res.*, 51(12), 4661-4672.
- Zhong, J., Sun, X., & Wang, C. (2003). "Treatment of oily wastewater produced from refinery processes using flocculation and ceramic membrane filtration." *Sep. Purif. Tech.*, 32(1-3), 93-98.
- Zhu, H. Y., Xiao, L., Jiang, R., Zeng, G. M., & Liu, L. (2011). "Efficient decolorization of azo dye solution by visible light-induced photocatalytic process using SnO<sub>2</sub>/ZnO heterojunction immobilized in chitosan matrix." *Chem. Eng. J.*, 172(2-3), 746-753.
- Zinadini, S., Zinatizadeh, A. A., Rahimi, M., Vatanpour, V., & Zangeneh, H. (2014). "Preparation of a novel antifouling mixed matrix PES membrane by embedding graphene oxide nanoplates." *J. Membr. Sci.*, 453, 292-301.
- Zodrow, K., Brunet, L., Mahendra, S., Li, D., Zhang, A., Li, Q., & Alvarez, P. J. (2009). "Polysulfone ultrafiltration membranes impregnated with silver nanoparticles show improved biofouling resistance and virus removal." *Water Res.*, 43(3), 715-723.
- Zou, X., Zhu, G., Guo, H., Jing, X., Xu, D., & Qiu, S. (2009). "Effective heavy metal removal through porous stainless-steel-net supported low siliceous zeolite ZSM-5 membrane." *Microporous and Mesoporous Materials*, 124(1-3), 70-75.





**LIST OF PUBLICATIONS**

1. **Chandrashekhhar Nayak, M.,** Arun M. Isloor, Moslehyani, and Ismail. (2017). “Preparation and characterization of PPSU membranes with BiOCl nanowafers loaded on activated charcoal for oil in water separation.” *J. Taiwan Inst. Chem. Eng.*, 77, 293-301, Impact factor-3.849.
2. **Chandrashekhhar Nayak, M.,** Arun M. Isloor, Moslehyani, and Ismail. (2018). “Fabrication of novel PPSU/ZSM-5 ultrafiltration hollow fiber membranes for separation of proteins and hazardous reactive dyes.” *J. Taiwan Inst. of Chem. Eng.*, 82, 342–350, Impact factor-3.849.
3. **Chandrashekhhar Nayak, M.,** Arun M. Isloor and Ismail. “Effects of multiwalled carbon nanotube on novel polyphenylsulfone composite ultrafiltration membranes for the effective removal of lead, mercury and cadmium from the aqueous solutions.” *Manuscript communicated to J. Ind. Eng. Chem.-Elsevier, December-2018, and Under Review.*
4. **Chandrashekhhar Nayak, M.,** Arun M. Isloor, and Ismail. “Novel PPSU/SnO<sub>2</sub> mixed matrix ultrafiltration hollow fiber membranes with enhanced antifouling property and toxic dyes removal.” *Manuscript communicated to Reactive and Functional Polymers, December-2018, came for minor revision on 24-01-2018.*
5. **Chandrashekhhar Nayak, M.,** Arun M. Isloor, and Ismail. “Novel PPSU/Al<sub>2</sub>O<sub>3</sub>-AAC incorporated mixed matrix membranes for efficient removal of proteins, heavy metals, and oil-water separation.” *Manuscript under preparation.*



**LIST OF CONFERENCES ATTENDED**

1. Presented **Poster** presentation on a research paper titled “Antifouling and performance enhancement of Polyphenylsulphone ultrafiltration membranes using Carbonnanotubes” at International conference on recent advances in Material and chemical sciences-2016, March 25, 2016, Department of chemistry, Bundelkhand University, Jhansi, U.P., India.
2. Presented **Poster** presentation on a research paper titled “Preparation and characterization of PPSU membranes with BiOCl nanowafers loaded on activated charcoal for oil in water separation” at International Symposium for Research Scholars on Metallurgy, Materials Science and Engineering (ISRS)-2016, December 21-23, Department of Metallurgical and Materials Engineering, Indian Institute of Technology Madras, Chennai.
3. Presented **Oral** presentation on a research paper titled “Preparation of PPSU/MWCNT composite membranes for the effective removal of heavy metals lead and cadmium from aqueous system” at National Conference on Advances in Materials Research-2017, 18-19 August, Ramaiah University, Bangalore.
4. Presented **Poster** presentation on a research paper titled “Removal of lead and mercury from wastewater using Polyphenylsulfone/ multiwalled carbon nanotube composite ultrafiltration membranes” at International Conference on Emerging Trends in Chemical Sciences-2017, 14-16 September, 2017, Department of Chemistry, Manipal Institute of Technology, Manipal.
5. Presented **Poster** presentation on a research paper titled “Preparation and characterization of novel PPSU/ZSM-5 zeolite mixed matrix hollow fiber membranes for dye removal application” at 9<sup>th</sup> BENGALURU INDIA NANO-2017 International conference, 7-9 December, 2017, Bangalore.
6. Presented **Poster** presentation on a research paper titled “Toxic Reactive Black-5 dye removal from wastewater using novel PPSU/nano SnO<sub>2</sub> mixed matrix ultrafiltration hollow fiber membranes” at International Conference on Material Science and Technology-2018, 10-13 October, 2018, Indian Institute of Space Science and Technology, Dept. of Chemistry, Thiruvananthapuram.

7. Presented **Oral** presentation on a research paper titled “Novel PPSU/nano SnO<sub>2</sub> mixed matrix ultrafiltration hollow fiber membranes with enhanced antifouling and RO-16 toxic dye removal properties” at International Conference on Advances in Material Science-2018, 24-25 October, Sree Sankara College, Dept. of Chemistry, Kalady, Ernakulum (Dist.), Kerala.
8. Presented **Oral** presentation on a research paper titled “Fabrication and characterization of polyphenylsulfone/tin oxide mixed matrix hollow fiber membranes for Reactive Black-5 dye removal application from wastewater” at Telangana State Science Congress-2018, 22-24 December, 2018, NIT Warangal, Telangana state.

## BIO DATA

### M Chandra Shekhar Nayak

Technical Assistant (Instruments)-A,

Division of Polymeric Medical Devices,

SCTIMST, BMT wing, Poojappura,

Thiruvananthapuram, Kerala-695012.

Email: nayaknitk@gmail.com,

mcsnayak@sctimst.ac.in,

Contact No.: +91 9490335563.

---

### EDUCATIONAL QUALIFICATIONS

- B.Sc. (B.Z.C) from Osmania University, Telangana state (2005-2008).
- M.Sc. (Organic Chemistry) from Jawaharlal Nehru Technological University Anantapur, Andhra Pradesh (2008-2010).
- B.Ed. (Biological Sciences) from Acharya Nagarjuna University, Andhra Pradesh (2012-2013).
- M.Ed. (General Education) from Regional Institute of Education (NCERT) Mysore, Karnataka (2014-2015).
- Ph.D. (Chemistry) from National Institute of Technology, Karnataka (January-2019).

### EXPERIENCE

- ❖ Worked as Research Trainee at CSIR-Indian Institute of Chemical Technology, Hyderabad (2010)
- ❖ Worked as Junior Lecturer at Rao's Junior college, Wanaparthy Dist. Telangana state (2011-2012)
- ❖ Worked as a research student intern for three months at Advanced Membrane Technology Research Centre (AMTEC), Universiti Teknologi Malaysia, Skudai, Johor, Malaysia (June 2016, January 2017 and July 2017)
- ❖ Conducted laboratory practical classes for B.Tech. & M.Sc. students at NITK Surathkal (2015-2018)
- ❖ April-2018 to Present: Technical Assistant-A (Instruments), Division of Polymeric Medical Devices, Sree Chitra Tirunal Institute for Medical Sciences and Technology (DST, Govt. of India), Thiruvananthapuram, Kerala, India

**ACHIEVEMENTS:** Received NCERT-Delhi merit scholarship in M.Ed. (2014-2015).

**RESEARCH INTERESTS:**

1. Polymers
2. Membrane Technology
3. Nanoscience and Technology

**RESEARCH JOURNAL PUBLICATIONS:**

1. Chandrashekhhar Nayak, M., Arun M. Isloor, Moslehyani, and Ismail. (2017). "Preparation and characterization of PPSU membranes with BiOCl nanowafers loaded on activated charcoal for oil in water separation." *J. Taiwan Inst. Chem. Eng.*, 77, 293-301.
2. Chandrashekhhar Nayak, M., Arun M. Isloor, Moslehyani, and Ismail. (2018). "Fabrication of novel PPSU/ZSM-5 ultrafiltration hollow fiber membranes for separation of proteins and hazardous reactive dyes." *J. Taiwan Inst. of Chem. Eng.*, 82, 342–350.
3. Chandrashekhhar Nayak, M., Arun M. Isloor and Ismail. "Effects of multiwalled carbon nanotube on novel polyphenylsulfone composite ultrafiltration membranes for the effective removal of lead, mercury and cadmium from the aqueous solutions." Manuscript communicated to *J. Ind. eng. chem.*, under review-December 2018.
4. Chandrashekhhar Nayak, M., Arun M. Isloor, and Ismail. "Novel PPSU/SnO<sub>2</sub> mixed matrix ultrafiltration hollow fiber membranes with enhanced antifouling property and toxic dyes removal." *Reactive and Functional Polymers Journal-Elsevier*, came for minor revision on 24-01-2018.

**LIST OF CONFERENCES ATTENDED:**

1. Presented *Poster* presentation on a research paper titled "Antifouling and performance enhancement of Polyphenylsulphone ultrafiltration membranes using Carbonnanotubes" at International conference on recent advances in Material and chemical sciences-2016, March 25, 2016, Department of chemistry, Bundelkhand University, Jhansi, Uttar Pradesh, India.

2. Presented **Poster** presentation on a research paper titled “Preparation and characterization of PPSU membranes with BiOCl nanowafers loaded on activated charcoal for oil in water separation” at International Symposium for Research Scholars on Metallurgy, Materials Science and Engineering (ISRS)-2016, December 21-23, Department of Metallurgical and Materials Engineering, Indian Institute of Technology Madras, Chennai, Tamilnadu.
3. Presented **Oral** presentation on a research paper titled “Preparation of PPSU/MWCNT composite membranes for the effective removal of heavy metals lead and cadmium from aqueous system” at National Conference on Advances in Materials Research-2017, 18-19 August, Ramaiah University, Bangalore, Karnataka.
4. Presented **Poster** presentation on a research paper titled “Removal of lead and mercury from wastewater using Polyphenylsulfone/ multiwalled carbon nanotube composite ultrafiltration membranes” at International Conference on Emerging Trends in Chemical Sciences-2017, 14-16 September, 2017, Department of Chemistry, Manipal Institute of Technology, Manipal, Udupi, Dakshina Kannada.
5. Presented **Poster** presentation on a research paper titled “Preparation and characterization of novel PPSU/ZSM-5 zeolite mixed matrix hollow fiber membranes for dye removal application” at 9<sup>th</sup> BENGALURU INDIA NANO-2017 International conference, 7-9 December, 2017, Bangalore, Karnataka.
6. Presented **Poster** presentation on a research paper titled “Toxic Reactive Black-5 dye removal from wastewater using novel PPSU/nano SnO<sub>2</sub> mixed matrix ultrafiltration hollow fiber membranes” at International Conference on Material Science and Technology-2018, 10-13 October, 2018, Indian Institute of Space Science and Technology, Dept. of Chemistry, Thiruvananthapuram.
7. Presented **Oral** presentation on a research paper titled “Novel PPSU/nano SnO<sub>2</sub> mixed matrix ultrafiltration hollow fiber membranes with enhanced antifouling and RO-16 toxic dye removal properties” at International Conference on Advances in Material Science-2018, 24-25 October, Sree Sankara College, Dept. of Chemistry, Kalady, Ernakulum (Dist.), Kerala.

8. Presented *Oral* presentation on a research paper titled “Fabrication and characterization of polyphenylsulfone/tin oxide mixed matrix hollow fiber membranes for Reactive Black-5 dye removal application from wastewater” at Telangana State Science Congress-2018, 22-24 December, 2018, NIT Warangal, Telangana state.

#### **TECHNICAL SKILLS:**

- Polymeric membranes fabrication,
- Membrane characterization with several instruments such as FTIR, Contact angle, Zeta potential analyzer, Scanning electron microscopy, UV-visible spectrometer, Universal testing machine.

---

#### **PERSONAL DETAILS**

Name	:	M Chandra Shekhar Nayak
Date of Birth	:	15-08-1988
Sex	:	Male
Nationality	:	Indian
Languages known	:	Telugu, English, Hindi
Permanent Address	:	1-25, Maddelabanda Thanda (Vil. & Post), Maldakal Mandal-509132, Jogulamba Gadwal (Dist.), Telangana state, India.

---

#### **REFERENCES**

##### **1. Dr. Arun M. Isloor**

Professor  
Dept. of Chemistry,  
NITK-Surathkal, Mangalore,  
Phone no: +91-9448523990,  
Email: isloor@yahoo.com.

##### **2. Prof. Dr. Ahmad Fauzi Ismail**

Deputy vice chancellor-Research  
Advanced Membrane Technology Centre,  
AMTEC, Universiti Teknologi Malaysia,  
Phone no: +60-97775545/ +60-75535807,  
Email: afauzi@utm.my.